A STUDY OF THE PERFORMANCE OF A CYCLIC SOLID-LIQUID REACTOR

Thesis submitted for the Degree of Doctor in Philosophy
in the
Faculty of Chemical Engineering
in the
University of London

by

ROMAN GOMEZ VAILLARD

Department of Chemical Engineering and Chemical Technology
Imperial College of Science and Technology
London SW7

May 1976

ABSTRACT

An experimental and theoretical study was performed on the Cloete-Streat stage-wise semicontinuous solid-liquid contactor in which counter-current flow of solids and liquid is achieved by periodic transfer of solids from stage to stage. The reacting system investigated was the neutralization of NaOH with a cationic ion-exchange resin. The range of operating conditions studied included the region where the rate of mass transfer is film diffusion controlled and the region where it is intraparticle diffusion controlled.

The effect of cycling on the performance of the contactor was studied by varying certain system parameters (the length of the cycle and the fraction of solids periodically transferred) while keeping all other parameters constant. This maintained the mean residence times of both phases constant.

The experimental results show that for the range of operating conditions investigated, the system performance improved monotonically with higher values of fractional transfer and that improvements of up to 8 per cent are achieved when increasing the fractional transfer from 0.4 to 0.8. Low values of fractional transfer correspond to short cycle times and, in the limit, to a continuous contactor; accordingly, an improvement over the continuous steady state system is observed.

A population-based model was used for simulation purposes. This model considered the solids conversion distribution and its evolution with time. The method of characteristics and the method of leading moments of the distribution were used to solve the system equations numerically. A good agreement between predicted and theoretical results (less than 9 per cent difference) was obtained for most of the simulation runs when using literature values of the transport parameters.

ACKNOWLEDGEMENTS

I wish to express my sincerest appreciation to Dr. L. Kershenbaum for his guidance, supervision and friendship. I also thank Dr. M. Streat for many valuable suggestions, and for providing the experimental facilities to carry out this work.

I dedicate this thesis to my wife, my son and my daughter, and thank my parents for their continuous support.

The financial support of the Banco de Mexico and the Consejo Nacional de Ciencia y Tecnologia is also gratefully acknowledged.

TABLE OF CONTENTS

NOTATION

a	External surface area per unit volume of solid	(m^{-1})
$\bar{c}$	Concentration of fixed ion groups (true capacity)	$(keq\ m^{-3})$
$C\bar{a}p^{f}$	Exit solid capacity (experimental)	$(keq\ m^{-3})$
$C\bar{a}p^{o}$	Initial solid capacity (experimental)	$(keq\ m^{-3})$
C_f	Exit liquid concentration (average)	$(keq\ m^{-3})$
C_j	Concentration of solution in stage j	$(keq\ m^{-3})$
C_0	Initial liquid concentration	$(keq\ m^{-3})$
d	Fractional transfer	
$\bar{d}$	Average fractional transfer	
d_p	Particle diameter	(m)
$\hat{d}_p$	Average (surface) particle diameter	(m)
D	Effective diffusivity	$(m^2 s^{-1})$
E	Mass balance error	
$\underline{f}(\underline{x},\underline{u})$	Vector function of state and control variables	
$f(x,t)$	Continuous distribution (density) function of x and t	
$f_s^0(x,t)$	Density function for old resin in stage s	
$f_s^N(x,t)$	Density function for new resin in stage s	
$F(t)$	Fractional attainment of equilibrium	
$F(x_n,j)$	Cumulative distribution function	
$g(t)$	Residence time distribution	
G	Net generation term in integral balance	
$G(t)$	Cumulative residence time distribution	
H	Total resin hold up (absolute volume of resin)	(m^3)
k_D	Rate constant in the simplified rate expression	(s^{-1})
k_L	Liquid film mass transfer coefficient	$(m\ s^{-1})$
k_θ	Rate constant in the simplified rate expression	
L	Liquid forward flow rate	$(m^3 s^{-1})$
L_{av}	Liquid average flow rate	$(m^3 s^{-1})$
n	Number of characteristics	
$P(x,j)$	Discrete probability distribution for stage j	

$Q_A(t)$	Amount of component A left in Ion-exchanger at t	
Q_A^o	Amount of component A initially present	
Q_A^∞	Amount of component A left in Ion-exchanger at equilibrium	
r''	Dimensionless rate of reaction	
$r(x,C_j)$	Rate of reaction per unit vol of solid at conversion x and Liquid at C_j	(keq $m^{-3}s^{-1}$)
r_p	Radius of particle	(m)
$\Re$	Region in the (m+4) dimensional space	
R_j	Rate of reaction per unit vol of solid at all conversions and liquid at C_j	(keq $m^{-3}s^{-1}$)
R_s^0	Rate of reaction for old resin	(keq $m^{-3}s^{-1}$)
R_s^N	Rate of reaction for new resin	(keq $m^{-3}s^{-1}$)
s	Number of stages in the contactor	
S	Resin flow rate in terms of absolute volume of resin	(m^3s^{-1})
S'	Resin flow rate in terms of freely settled resin	(m^3s^{-1})
t	Time	(s)
t_F	Forward flow period time	(s)
T	Total cycle time	(s)
u	Superficial velocity	($m\ s^{-1}$)
$\underline{u}$	Vector of control variables	
V	Volume of stage	(m^3)
X	Experimentally measured conversion	
x	Conversion	
$\underline{x}$	Vector of state variables	
x_f	Conversion of feed resin	
X_L	Liquid conversion	
x_o	Initial conversion of resin	
X_S	solid conversion	
Z_i	Cartesian coordinates	

δ	Film thickness	(m)
$\delta(t)$	Time interval	(s)
ε	Stage voidage	
ε_B	Voidage of the freely settled bed	
ε_b	Voidage of the fluidized bed	
$\bar{\varepsilon}$	Average stage voidage	
$\bar{\varepsilon}_b$	Average fluidized bed voidage	
ε'	Fraction of solids added to top stage during $\delta(t)$	
ε_o	Voidage of top stage at beginning of cycle ($t = 0$)	
$\varepsilon_s(t_F)$	Voidage of top stage at end of forward flow	
θ	Dimensionless time	
μ	Viscosity of solution	(kg $m^{-1}s^{-1}$)
$\mathcal{l}$	$\mathcal{l}^{th}$ moment of a distribution	
ξ	Property of entities	
ρ	Density of solution	(kg m^{-3})
τ	Liquid residence time per stage	(s)
τ_L	Liquid residence time	(s)
τ_S	Solid residence time	(s)
ψ	Distribtuion function	
ϕ	Coefficient of mass the transfer correlation	
Φ	Term of Equation (4.1)	

Subscripts

i	Discrete value of conversion
j	General stage j
k	k^{th} time step

Dimensionless Groups

Re	Particle Reynolds number
Sc	Schmidt number for the liquid
Sh	Sherwood number

CHAPTER 1

1.1 Introduction

The need for a continuous solid-liquid contactor has long been recognised. With the advent of high capacity synthetic resins, the ion-exchange industry has been particularly interested in the development of such a contactor which would overcome some of the disadvantages of fixed bed columns.

Over the years, many designs have appeared; most of these consist of adaptations of a moving fixed bed column. More recently, several designs have incorporated a cascade of fluidized beds. The development of this type of contactor has been prompted by the potential application of ion-exchange processes to the recovery of metals from unclarified solutions. Briefly, continuous fluidized bed contactors consist of a series of stages in which the solids are periodically transferred countercurrent to liquid flow.

In recent years, numerous publications have established both theoretically and experimentally that the periodic operation of processes can be superior to the conventional steady state. The concept of controlled cycling has been applied to a number of mass transfer operations. In these, the flow of the phases is alternated in a cyclic manner. Robinson and Engel (31) experimentally and Horn (48) theoretically have shown that a periodically operated distillation column in which a fraction of the liquid hold up in each stage, is allowed to drop to the stage below, can exhibit improvements in overall efficiency of up to 100%.

The Cloete-Streat solid-liquid contactor is a multi-stage fluidized bed process whose operation is similar to the operation of the distillation column described above. In this case, the solids are transferred from stage to stage by periodic reversals of flow. In view of the results of the periodic operation of analogous processes, it is reasonable to suggest that this configuration may show similar improvements over a steady-state continuous contactor.

1.2 Objectives

The present study was carried out in a vertical version of the Cloete-Streat solid-liquid contactor. An extensive experimental plan was devised to study the behaviour of the system under a wide range of operating conditions.

The reaction system studied was the neutralization of sodium hydroxide with a hydrogen form strong-cation ion-exchange resin. The reaction in this case, can be said to be controlled by the rate of diffusion either within the resin or in a film around it. The operating conditions were chosen so that both cases could be studied. The experimental data gathered were later used to assess the mathematical model and the methods for the solution of the resulting equations.

This thesis is divided into seven chapters. The first of which is this short introduction. A review of the related literature is presented in chapter two. The aim there, is to situate this work into the perspective of both periodically operated processes and continuous solid-liquid contactors. In chapter three the mathematical models are developed. This is followed by a chapter on the solution methods of the resulting equations. Chapter five describes the experimental set up and the design of experiments. The results are discussed in chapter six. The last chapter contains the conclusions reached and some recommendations for future work are included.

CHAPTER 2

REVIEW OF THE RELATED LITERATURE

For ease of presentation, this review is divided into an introductory historical overview and two main sections. In the first section, the development of continuous and semi-continuous solid-liquid contactors is considered. The second section is dedicated to a survey of the most relevant contributions to the area of periodic operation of chemical processes.

Historical Overview

The development of continuous solid-liquid contactors and periodic processes have followed parallel, albeit quite separate, lines of research. It was in 1926 when the first design of a continuous ion-exchange system appeared in the literature (1). A few years later Van Dijck (2), first applied the concept of periodic operation by the invention of a pulsed liquid-liquid extractor. Later, the decade of 1950 saw the invention of numerous devices for liquid-solid contacting, culminating in the development of rather sophisticated staged, counter-current fluidized bed contactors. At about the same time, Cannon (23) published his initial investigations of cyclic mass transfer equipment (extraction and distillation). The concept of periodic operation was quickly extended to almost all other chemical engineering fields, and a number of papers established, both theoretically and experimentally, that periodic operation can be superior to the conventional steady-state operation. It is in the development of the latest types of solid-liquid contactors where both lines of research meet. These contactors are periodic in their operation and are particularly interesting in view of the results of other cyclic processes.

2.1 Development of Continuous and Semicontinuous Ion-Exchange Processes

Ion-exchange is one aspect of the more general problem of solid-liquid contacting and many of the designs are applicable for use in ion-exchange and other solid-liquid operations. Therefore, this review is mainly concerned with those designs particularly significant to ion-exchange applications.

Ion-exchange is a typical solid-liquid reaction which has numerous applications. The ion-exchange properties of certain rocks and sands have been used for the purification of water for many centuries. With the advent

of high capacity synthetic ion-exchange resins, the full potential of this method of separation was realized and began to be exploited.

To date, it is possible to regard ion-exchange as a unit operation by itself with an ever widening field of application. Its main use is still for the purification and demineralization of water. However, it has been successfully applied in the nuclear, metallurgical, food and fine-chemicals industries. It is therefore, not surprising that, a considerable amount of effort has been dedicated in the improvement of the technology for solid-liquid contacting. For many years however, most of the advances were confined to the development of better ion-exchange resins, while the basic contacting technique remained fundamentally unchanged. The batch wise, packed-bed column, although relatively simple to operate presents a number of disadvantages. The resin loading step is inefficient because only a small section of the bed is used at any one time, as the reaction band moves down through the column. Prior to regeneration, the bed has to be carefully back washed to remove suspended matter and resin debris which could have settled on the bed. The regeneration step, due to less favourable kinetics has to be carried out at low flow rates. This is done cocurrent to the loading step flow which leads to low chemical efficiency and hence, tends to be wasteful on chemical reagents. Furthermore, since the outlet end (bottom) of the bed is the least regenerated portion, high effluent leakage can occur in the following cycle. Finally, the bed has to be rinsed through to wash out regenerant residues and this also tends to be wasteful on water.

Consequently, many attempts have been made to overcome the mentioned draw backs. Many of these, have been towards the development of a continuous counter-current contactor. A continuous contactor could offer the following advantages:

a) lower resin inventory, since all resin performs an active role
b) counter-current regeneration and washing lead to economies in regenerants and water
c) physical size of equipment reduced.

All this, results in lower capital and operating costs over the corresponding batch operation. In addition, in the treatment of high concentration feeds, continuous processes stand alone, since the rapid exhaustion of resin, severely restricts the capacity of fixed bed installations. Designs based on a cascade of fluidized beds have the further advantage that turbid solutions can be treated. Also, low pressure drops are obtained in those contactors

and the need for expensive pressurised tanks is eliminated.

Some of these concepts can be generalised to other solid-liquid processes. For instance, selective adsorption is a separation method with important uses in the petroleum, sugar and fine-chemicals industries. An effective continuous or semicontinuous contactor would permit the exploitation of chemical wealth from such sources as fermentation liquors, sewage and other complex mixtures, since existing fractionation methods are uneconomical. In some cases adsorbents are expensive and fixed-bed contactors require large inventories. From this it is clear that the development of equipment for ion-exchange has analogies with other solid-liquid operations.

The main requirement for a continuous solid-liquid contactor is a method of continuously or semicontinuously introducing and removing the solids. Considerable ingenuity has been shown in the efforts to satisfy this requirement. The method used can serve as a classification criterion.

Mechanical Methods

Several initial designs intended to mechanically move the resin through the contactor. Cormack and Howard (3) used an endless tube of cloth filled with resin which moved in a flexible casing between three reservoirs. Loading, stripping and washing took place in each of these reservoirs. Hiester (4) introduced a rotating system in which the solution passed to an air agitated mixer for loading then to a reservoir and from there to another mixer stage. Meanwhile, the resin in the first stage is regenerated and so on. These and many other methods were really laboratory tools which never had any industrial potential. Some others, are reviewed in a paper by Clayton (5).

Moving Bed Methods

The simplest type of a continuously moving bed is that in which the solids flow as a continuous phase by gravity in a vertical column. Solids may be removed at the base with a variety of devices such as rotary metering valves or star valves. Designs based on this principle are reported by Johnson (6), and Hiester (7). This method has a number of drawbacks: since the liquid flows counter-current to the solid, its velocity has to be below the solids fluidizing velocity which restricts its industrial application. Also, some difficulty is encountered in balancing solids inlet flow and exit flow. In addition, the valves actuating on resin, tend to grind it.

These problems lead to intermittent removal of resin. Here, the liquid flow is briefly stopped to allow resin out of the column. Higher liquids velocities can be used since the resin is restrained during the liquid flow. However, other problems arise. As the bed diameter increases, the difficulty of evenly extracting the solids from the base without channeling also increases. There were many attempts devoted to alleviate this problem. Porter (8), used a secondary liquid to fluidize a zone of solids at the base of the bed and force the solids to flow out of the column. Resins can be easily moved by hydraulic transport (9) and this has been used to move the packed bed in several designs. To this type of intermittent moving bed, belong the two most commercially successful processes to date. The Asahi process, in which a fraction of the bed is periodically removed from the loading section and passed to a similar regenerating and washing section in a closed loop, by static or pressure head in the previous unit. There exist several industrial scale plants based on this design, mainly for water purification. The Higgins process (11) is similar to the above, the different units being enclosed in a loop round which the resin is moved by regular hydraulic pulses. The main drawback in large scale moving beds is that liquid channelling can occur and this reduces performance. This can be overcome by contacting the phases in a fluidized bed.

The use of fluidized beds for solid-liquid contacting has several advantages:

a) Unclarified liquids can be treated. This has important applications in hydrometallurgical installations.

b) Pressure drop across the column is significantly reduced.

c) Resin removal and feeding is less difficult.

To avoid axial mixing, the contactor is divided in zones, and thus becomes a stage-wise process. Liquid flows upwards through perforated or sieved plates and the solid movement is through downcomers similar to distillation columns (12). The main difficulty here is in preventing the liquid by-passing up the downcomers. Also, hydrodynamic stability has been a source of trouble.

Some of these problems can be solved by using rapid pulses of liquid. This is claimed to greatly improve stability and balancing of solids inflow and outflow. Grimmet (13), has reported a system based on this principle. It was originally devised for the separation of fission-products from solidified wastes. A similar design was used by Swinton and Weiss (14). In these contactors hydraulic pulses are used to periodically

fluidize the solids bed whilst solids and liquid are continuously metered into the top and the bottom of the column respectively. Solid movement between stages is also through overflowing downcomers. Grimment and Brown have studied the effect of pulse frequency on the flow pattern. They found that for frequencies between 300-630 pulses/min. the flow pattern is characterized by smooth fluidization and a definite solids-liquid interface. Operation at this frequency range is therefore, similar to the operation of the next type of contactor.

This type, can be classifed as semicontinuous multistage fluidized bed contactors and their development has been much more recent. Here, solids are transferred by means of periodic reversals of flow. The main difference between these and the pulsed contactors described above is that solids and liquid flow in an alternate manner. In most cases these contactors consist of a vertical column with perforated plates to separate the stages. In this case both solids and liquid flow through the same orifices on the plates and eliminated the need for downcomers, simplifying design. George et al. (16) and Javed (17) have described equipment used industrially for the extraction of uranium from waste leaching solutions. Full scale developments of the Cloete-Streat contactor (18) have been described by Stevenson (19) for the case of water softening and by Cloete et al. (20) for the recovery of zinc from pickling solutions.

This ends the list of the most important contactors. Here it was hoped to show how the idea of continuously contacting solids and liquids evolved from the early and rather crude mechanical methods to the latest fluidized bed contactors. Many other designs have been reported in the open and in the patent literature. On the main they consist of adaptations of the basic types described here. Slater (21), Horie (22) and Clayton (5) include a list of other designs.

2.2 Review of Periodic Processes

Traditionally chemical processes have been operated in either batch or steady state mode. However, in the last 25 years, the concept of periodic operation has received considerable attention in the literature and numerous papers have shown that it can be superior to conventional steady state operation.

Although the concept of cyclic operation was applied earlier (2), it was Cannon (23,24) who really introduced it to the chemical literature. Since then this idea has been tried in almost all other chemical engineering areas, in some instances with great success. Also, some inherently periodic processes, such as parametric pumping and heatless absorption have been developed.

One of the simplest classifications of periodic processes is in terms of whether the alteration variable is extensive or intensive in nature. This classification is used here for ease of presentation.

Extensive Alteration Variable

All initial studies correspond to the extensive type. In this case the alteration variable is the flow rate. Operation in this mode is commonly called 'controlled cycling' and is based on square wave variations of flow rate.

In early publications on experimental work, Cannon and coworkers (25,26,27) reported that cycling of a distillation column improved efficiency and capacity. The operating principle is simple: for a period of time, vapour flows up the column at sufficient velocity to maintain the liquid on the plates. After a time, the vapour flow is cut off and liquid is allowed to drop from each stage to the stage below; later the vapour flow is reinitiated. They found that for high ratio of vapour to liquid time periods, increases in the efficiency are obtained. If the ratio is reversed, high increases in capacity are obtained instead. This adds a degree of flexibility not possible in conventional operation. Also, these types of columns have the attraction of simplified design since simple perforated plates are used.

McWhirter and Lloyd (28) published, in 1963, the first theoretical study of controlled cycling applied to distillation and compared their theoretical results with further experimental work. They found that up

to three-fold increases in efficiency when compared with conventional steady-state, can be obtained. In using their theoretical model to ascertain the causes of the improvements, they concluded that the improvement resulted from the step-wise manner in which the reflux descends in the column. This, they remarked, produced higher (almost twice as large) driving forces in the stages. Because at the start of the vapour flow the driving force is high in all stages, a close approach to equilibrium is prevented by having relatively short vapour flow periods. Thus, a large concentration gradient develops across the column.

When applied to liquid-liquid extraction, the cycle consists of 4 parts: a light phase flow period followed by a pause for coalescence, then, a heavy phase flow period and another coalescing pause. Szabo et al. (29), in reporting their initial investigations, observed that significant improvement in capacity and efficiency are obtained with a cyclic extractor. They compared their column with several other industrial types of extractors and found that the efficiency they obtained was higher than all other types except for the rotatory disc contactors. Capacity however, was higher even than the latter contactor. Later, Belter and Speaker (30) published the first theoretical analysis of cyclic liquid-liquid extractors. In this paper it was shown that efficiency increased with the fraction of hold up transferred reaching a maximum when the entire hold up is transferred. In this last situation the column gave a separation equal to double the number of theoretical stages (200% efficiency).

Similar results were obtained by Robinson and Engel (13) and Sommerfeld et al. (32) for distillation columns. In the first study, a mathematical model was developed in terms of a time-varying concentration gradient and constituted an adaptation of a lateral concentration gradient model developed for a conventionally operated column by Lewis (33). In this paper the effect of point efficiency and the fraction of liquid hold up transferred on the overall column efficiency, was investigated. The maximum efficiency found, corresponded the fractional transfers of unity. Sommerfeld's paper was more general in scope. This is a long paper which studies, theoretically, the effect on the overall efficiency of a number of parameters such as fractional transfer, relative volatility, slope of the operation line on others. Their results were closely in accordance with those previously mentioned.

Semi-plant size experimental studies for distillation columns were performed by Schrodt et al. (34). In this investigation, it was found that

in columns of up to 10-12 stages, increased performance is observed when cycling. However, if more stages are added the operation becomes marginal. The reason for this was found to be existence of a transient pressure wave up the column, at the beginning of the liquid flow periods. This pulse interfered with the liquid flow so that the lower plates drained to dryness before the upper trays began to drain.

Other theoretical studies include Horn's(48) paper on staged vapour-liquid counter-current processes. He has analytically solved the difference-differential mass balance equation imposing the periodicty boundary conditions. These conditions simply say that the liquid concentration on each stage at the beginning of the vapour flow periods are the same for all cycles. The effect of fractional transfer and stage efficiency on the overall column efficiency was studied and the results were identical to those of Sommerfeld and Robinson et al.

The concept of controlled cycling has been successfully applied to other fields. For instance, in screening, it has been reported (35) that a three-fold increase in throughput is obtained by using an on-off blast of air to periodically fluidize the solids bed. This blast of air is used instead of other mechanical shaking methods with the advantage of simplicity it also helps to reduce blinding problems.

To end this section on cycling of an extensive variable, an example of sinusoidal variations of flow rate is considered. Most studies of this type of variation (sometimes called pulsed operation) are applied to chemical reactors and are reviewed later in a separate section. Ritter et al. (36) have studied theoretically the case of a steam-heated exchanger in which the coolant flow rate (velocity) is varied in this form. They found that although some improvement can be obtained by fluctuating the flow rate alone, if both the coolant velocity and the temperature of the condensate are varied sinusoidally a resonance effect can occur (depending on the phase angle between signals), and, still higher improvements are feasible. However since this is a linear system the improvement is small.

Intensive Alteration Variable

First, studies in which a pressure pulse has been used as the alteration variable are considered. In the field of heat transfer, Di Cicco and Schoenhels (37), in an experimental study, reported that periodic pressure pulses increased the heat transfer coefficient in the film boiling region. The magnitude of the increase depended upon the frequency but improvements

of up to 100% were obtained. Other studies by Lemlich (38) and Baird et al. (39) have claimed that increased heat transfer coefficients between a fixed surface and a flowing fluid are obtained by pulsing. The reasons for these improvements are unclear and are ascribed to a number of secondary effects such as cavitation and renewal of the boundary layer.

In the case of mass transfer, Krasuck and Smith (40) have studied a system in which mass transfer from a tube wall to a flowing fluid is considered. They found that pulsing can increase the value of the mass transfer coefficient. Both frequency and amptitude increases have beneficial effects on the coefficient, but only for the stream-line flow region. No effect is observed for Re > 11,000.

Pressure pulses have also been used in crystallization. McKay and Goard (41) have described a crystallizer in which a piston is used to periodically compress the crystal bed. The pressure applied has a beneficial effect on the melting point of the liquid-solid system, since it changes the equilibrium freezing temperature and contributes to a close approach of the crystals and mother liquor to equilibrium.

Finally, separation processes based on pressure and temperature cycles are considered briefly. The process called heatless adsorption or pressure swing adsorption was introduced by Skarstrom (42). Here, adsorption of a solute from a gas stream takes place at high pressures while the desorption step is done at low pressures. The benefit here is that at high pressure more solute is adsorbed than at lower pressures. A second type process has been studied by Kadlec (43). In this technique, a high pressure gas stream is intermittently fed into an adsorber. When the feed is off, the gas is exhausted at the feed end of the column while a second product stream is withdrawn continously from the other end.

They are two main separation systems based on cyclic temperature changes: parametric pumping and cycle zone adsoption. The first has received considerable attention in the recent years and has been reviewed and discussed in detail by Sweed (44). It was introduced to the Chemical Literature by Wilhelm et al. (40). He developed a process in which the liquid to be separated is driven up and down by a couple of pistons through the adsorbent bed. Heat exchangers are used to heat the liquid before it flows upwards and to cool it before it flows down through the bed. Since the adsorbent holds more solute when the liquid is cool, the solute is held by the adsorbent during the cold half of the cycle and released to

the liquid during the hot half. After a number of cycles a concentration gradient is established in the column and, in principle, it is possible to achieve total separation of binary mixtures.

Cycle zone adsorption was first developed by Pigford et al. (46) and is similar to parametric pumping but in this case the mixture to be separated flows in a single direction through a series of columns instead of up and down through a single bed. The columns are heated or cooled in a cyclic manner and are out of phase. In other words, during the first part of the cycle, when one column is hot, adjacent columns are cold, and during the second part the order is inverted. A more extensive list of references on cycle zone adsorption and parametric pumping is given by Wankat (47).

Chemical Reactors

The area of periodic operation of chemical reactors has received little experimental attention. However, numerous theoretical investigations have established that imposing fluctuations on the system can be advantageous.

Initial studies on a CSTR by Douglas and coworkers (51,52,53), investigated the effect of sinusoidal variations of the feed concentrations and developed approximate solutions by perturbation techniques. They found that average conversion for the periodic system was higher than the steady state operation and that the higher the non-linearity of the system the greater the possibility for improvement.

Horn (54) studied the effect of temperature variations on a CSTR for a complex reacting system (parallel reactions). This is a highly non-linear system and accordingly, it was determined that for high frequency disturbances the periodic process gives higher time-average yield than the corresponding optimal steady-state. Also, in this important paper the foundations of the theory of optimal periodic processes were first studied.

More recently, Bailey, Horn and Lee have published a series of papers in which the effect of a number of parameters on the performance of periodic reactors were studied. The effect of heat and mass transfer resistance was investigated (55). There it was found that when this resistance is included in the model, there exists an optimal cycle time. The area of

catalytic reactors is one in which the application of cycling may be particularly profitable. Bailey and Lee have shown in a number of papers (56,58) that selectivity can be improved by cycling the reactants compositions.

Other studies by Ray (61) indicated that cycling a polymerization reactor can yield significant different molecular weight distributions. This effect was further studied by Lee and Bailey (57). They studied the effect of mixing on a periodic polymerization reactor. The most important result of this investigation is that cycling can add controllability on the choice of molecular weight distributions. Stability and multiplicity of cyclic stirred tank reactors have been recently investigated by Ausikaitis and Engel (63). They proved, experimentally and theoretically the existence of multiplicity. More significantly, their results indicated that an unstable steady state operation can be stablized by cycling. Many other contributions are discussed in an extensive review of the field of periodic chemical reactors recently published by Bailey (64).

CHAPTER 3

THEORETICAL

3.1 Periodic Behaviour of Processes

3.1.1 Generalities

A process is said to be operated in a cyclic or periodic manner when a regular repetitive sequence of operations is established such that its time varying behaviour repeats itself every cycle. This (cyclic) behaviour could be caused by intentionally altering either the controls or the inputs to the process or by an intrinsic (natural) instability of the system (as in chemical oscillators) which causes the system to behave periodically even when inputs and controls are kept constant.

A unified theory for periodic processes has not yet been developed, mainly because of the wide variety of processes which fall into this category. A general classification is lacking for the same reason. The characteristic response time and the period or cycle time are two important properties, and have been used as a basis for classification (64). Other authors prefer to classify them according to the nature of the periodic alteration (47). In the following discussion, reference is made to processes in which the cyclic behaviour is caused by pre-determined variation of either the control or input variables.

Such a system can be described by

$$\dot{\underline{x}}\,(t) = f\,(\underline{x},\underline{y})\,, \qquad (3.1.1\text{-}1)$$

and the periodic operation or pseudo-steady-state (p.s.s.) condition is stated as

$$x_i(t + T) = x_i(t) \quad \text{for any } t \text{ in } 0 \leqslant t \leqslant T, \quad i = 1,2 \ldots m \qquad (3.1.1\text{-}2)$$

By denoting $\underline{u}'(t)$ the set of time varying inputs and controls, the following relation is observed

$$u'_\ell(t + T) = u'_\ell(t) \quad \text{for any } t \text{ in } 0 \leqslant t \leqslant T, \quad \ell = 1,2 \ldots q \qquad (3.1.1\text{-}3)$$

For certain processes, the initial state of a cycle, $\underline{x}(0)$, depends on the final state $\underline{x}(t_F)$ of the previous cycle, i.e.,

$$x_i(0) = g_i(\underline{x}(t_F)), \qquad (3.1.1\text{-}4)$$

where g_i represents the modification of the state variables, carried out between the end of a cycle and the beginning of the next. This function is called the state transformation.

Equations (3.1.1-4) and (3.1.1-1) represent the periodic operation of a process in which the continuous and discrete operations described by Equations (3.1.1-1) and (3.1.1-4) respectively are repeated in a cyclic manner.

For the calculation of the pseudo-steady-state, two approaches are generally available:

(i) Relaxation Method. Here the system Equations (3.1.1-1) are integrated forward in time until identical cycles are found. Usually a large number of cycles are required to achieve p.s.s. conditions.

(ii) Newton Raphson Iteration. An iterative method whereby Equations (3.1.1-1) are integrated using Equation (3.1.1-4) as a boundary condition has been developed by Lin (54). In this procedure, a good initial approximation of the end state $\underline{x}\ (t_F)$ is required in order to ensure convergence.

Usually method (ii) is applied in combination with method (i) which provides the initial estimate of $\underline{x}\ (t_F)$. By switching to method (ii) at a suitable point, a faster approach to p.s.s. is obtained.

Descriptions of the implementation of both methods are given in section 4.3.

3.1.2 The Cyclic Operation of the Cloete-Streat Contactor

The vertical version of the Cloete-Streat contactor studied in this work can be described as a semicontinuous solid liquid fluidized bed reactor with countercurrent flow of liquid and solids. A detailed description of the contactor and its operation is given in section 5.2. For the purpose here, only a brief description is necessary. The contactor consisted of a vertical arrangement of a number of stages, separated by perforated plates. Liquid flowed upwards fluidizing the solids in each stage, and periodically, particles were transferred downwards. The column was operated in a cyclic mode as described below.

The operation of the plant, consisted in the repetitive sequence of three operations. Every time operation 1 started a cycle had been completed. Each cycle is divided into two periods, the forward flow period, to which operation 1 corresponds, and the transfer or reversal of flow period, during which operations 2 and 3 take place. In the main, most of the cycle time was taken up by operation 1.

These operations consisted of the following:

Operation 1: Liquid fed at the bottom stage flows upwards through the column fluidizing the solids on each stage.

Operation 2: The liquid feed is stopped, a controlled volume of liquid is allowed to flow out from the bottom part of the column. The head of liquid in the system forces the solids downwards, transferring a specified volume of solids from each stage to the stage below. From the bottom stage, the solids leave the contactor.

Operation 3: The volume of solids transferred is controlled by the amplitude of the oscillation of a magnetic float between two reed switches. The liquid allowed out of the column during operation 2, pushes the float up; the float upon reaching the upper reed switch, is forced down. Hence, transfer of solids ceases as the displaced liquid is fed back to the contactor. Operation 3 refers to the repositioning of the float from the upper to the lower reed switch.

During all three operations resin is being fed into the top stage at a constant flow rate.

The cyclic behaviour of this process is caused by the periodic displacement of a fraction of solids from each stage while the liquid input is cut off.

Assuming for the moment that an important variable in the description of the process is the liquid concentration, pseudo-steady-state operation requires that

$$C_j(t) = C_j(t + T) \qquad j = 1,2 \ldots s$$

and similar relations for other state variables.

3.2 Modelling of Reactor

A dynamic model of the contactor assuming that its behaviour can be represented by the forward flow operation only, i.e., operations 2 and 3 are instantaneous, has been developed by Dodds et al. (49). Their derivation, is presented here with some additions and modifications.

3.2.1 Assumptions

The following assumptions are made with regard to the liquid and solid behaviour and the operation of the system:

(i) Resin beads are perfectly mixed on each stage

(ii) The liquid phase is also perfectly mixed

(iii) Reaction only takes place during the forward flow periods, that is to say that the reversal of flow and repositioning of the float are instantaneous operations

(iv) There is no transfer of liquid with the solids during reversal of flow

(v) Solid particles are of uniform density and size throughout the column.

An experimental study of the residence time distribution for particles in a horizontal version of the contactor has been performed by Bennett et al. (50). They reported that the behaviour of a stage corresponds closely to that of a perfectly mixed vessel as far as the solid is concerned. Therefore, assumption (i) is quite reasonable.

Assumption (ii) is taken as an approximation since in reality the movement of the liquid through a deep fluidized bed is rather complex lying between plug flow and perfect mixing.

If the cycle is long enough so that the forward flow periods are considerably longer than the time taken for operations two and three, assumption (iii) is valid.

During solids transfer there is some backmixing of liquid to the stage below. However, the volume of liquid transferred is very small when compared with the liquid hold up in the stage and its effect can be considered negligible.

Changes in particle size when converted from the H^+ to the Na^+ form depend on the degree of crosslinking of resin and are usually small. Density changes are significant only at high conversions of solids. Thus, assumption (v) is a good approximation when operating at low conversions.

For stable periodic operation of the contactor, it is required that the volume of solid transferred from each stage to the one below, be equal for all stages. Similarly, for modelling purposes, it was convenient that the solid hold ups in all stages were the same. Hence, the fraction of solids transferred per cycle is the same for all stages. In practice, the resin hold ups in stages were rarely equal. An average value for the fractional transfer has been used in such cases. If the hold ups are very different, the actual volume of resin transferred could be used as a system parameter instead of the fractional value. An alternative to this last formulation, is to introduce a vector of fractional transfers in which each element represents the fractional transfer from state j+1 to stage j.

By denoting the fraction of the total stage volume that is occupied by the liquid as ε, the stage voidage, the condition of equal resin hold ups can be stated as

$$(1-\varepsilon_j)\ V_j = \text{Constant} \quad j = 1,2, \ldots s-1 \qquad (3.2.1\text{-}1)$$

For the top stage the voidage varies with time and its value just before transfer must obey the relation

$$(1-\varepsilon_s(t_F))\ V_s = (1-\varepsilon_j)\ V_j \quad j = 1,2, \ldots s-1 \qquad (3.2.1\text{-}2)$$

where $\varepsilon_s(t_F)$ denotes the voidage of the top stage just before the solids transfer.

To avoid build up or depletion of solids in the contactor, the amount of resin fed to the top stage during the entire cycle must be equal to the volume of resin transferred at the end of the forward flow period of the cycle. This is stated by

$$ST = (1-\varepsilon_1)\ Vd\ , \qquad (3.2.1\text{-}3a)$$

where d is the fraction of the resin hold up transferred per cycle. In this work all stage volumes are equal hence $V_1 = V_2 = V_j = V$ and if Equation (3.2.1-1) holds

$$ST = (1-\varepsilon_j)\ Vd \qquad j = 1,2 \ldots s-1 \ . \qquad (3.2.1\text{-}3b)$$

3.2.2 Derivation of Equations

The system of equations that govern the process are obtained in the following manner:

Liquid Phase Mass Balance

In the case of an ion-exchange process in which the component B is transferred from the fluid to the resin phase, a mass balance for component B on the general stage j (Figure 3.2-1) gives

$$\frac{d}{dt}\ (\varepsilon_j V_j C_j) = L\ C_{j-1} - L\ C_j - (1-\varepsilon_j)\ V_j\ R_j \qquad (3.2.2\text{-}1)$$

(accumulation) = (input)-(output)-(consumption)

For constant ε_j and V_j

$$\frac{dC_j}{dt} = \frac{1}{\tau_j}\ (C_{j-1} - C_j) - \frac{1-\varepsilon_j}{\varepsilon_j}\ R_j \ . \qquad (3.2.2\text{-}2)$$

R_j is the rate of reaction per unit solid volume, between liquid of concentration C_j and resin which exists at resin conversions between 0 and 1 and is expressed by

$$R_j = \int_0^1 f_j\ (x,t)\ r\ (x,C_j) \qquad (3.2.2\text{-}3)$$

where $r(x,C_j)$ is the rate of reaction per unit solid volume between liquid of concentration C_j and resin at the particular conversion x, and $f(x,t)$ is the resin conversion distribution function.

Resin Phase Mass Balance

In problems in which it is desired to study how some characteristic (velocity, size, conversion) is distributed between a very large number of entities (particles, crystals) the population balance approach is used. The quantititive treatment of the collection of entities (population) is achieved by means of a distribution function such as

$$\psi\ (z_1,\ z_2,\ z_3,\ \xi_1,\ \xi_2,\ \ldots\ t)$$

where z_1, z_2 and z_3 are the three spatial coordinates, the ξ's represent some properties of the entity, and t is the time.

Physically, $\psi\ \Delta z_1\ \Delta z_2\ \Delta z_3\ \Delta\xi_1\Delta\xi_2\ \ldots$, represents the fraction of entities in the volume element $\Delta V = \Delta z_1\ \Delta z_2\ \Delta z_3$, that have property values in the range $\Delta\xi_1$, $\Delta\xi_2$ etc. Hence, a balance of entities can be performed in the element of volume ΔV, and a conservation expression obtained. Derivations of the general microscopic population balances are reported by Randolph (60) and Hulburt (81).

For the problem under consideration here, the continuous density function for the conversion x and time t, $f(x,t)$ is used. Hence, $f(x,t)\Delta x$ represents the fraction of particles with conversion in the interval $(x, x+\Delta x)$.

Since it has been assumed that the solid is perfectly mixed in each stage, the properties of the particles are position independent. Thus, the following balance can be performed.

Consider an interval of the conversion axis $(x,x+\Delta x)$ as shown in Figure (3.2-2); a mass balance over the fraction of particles in this conversion segment gives

$$f(x,t)\left.\frac{dx}{dt}\right|_x - f(x+\Delta x,t)\left.\frac{dx}{dt}\right|_{x+\Delta x} = \frac{d}{dt}\int_x^{x+\Delta x} f(z,t)\,dz\,. \qquad (3.2.2\text{-}4)$$

[rate at which particles enter the composition interval]	[rate at which particles leave the composition interval]	[rate of accumulation of particles within the composition interval]

After some transformations (see appendix A.1 for details),

$$\frac{\partial f}{\partial t}(x,t) = -\frac{\partial}{\partial x}\left[f(x,t)\left(\frac{dx}{dt}\right)\right] \qquad (3.2.2\text{-}5a)$$

or

$$\frac{\partial f}{\partial t}(x,t) + \frac{dx}{dt}\frac{\partial f(x,t)}{\partial x} = -f(x,t)\frac{\partial}{\partial x}\left(\frac{dx}{dt}\right) \qquad (3.2.2\text{-}5b)$$

Equation (3.2.2-5) could also have been derived from an integral mass balance as follows:

Considering again the general distribution function $\psi(z_1, z_2, z_3, \xi_1, \ldots \xi_m, t)$, it can be thought of as a function in

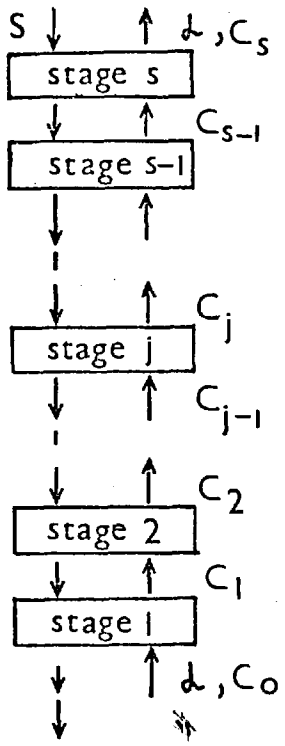

FIGURE 3.2-1 Schematic diagram of contactor.

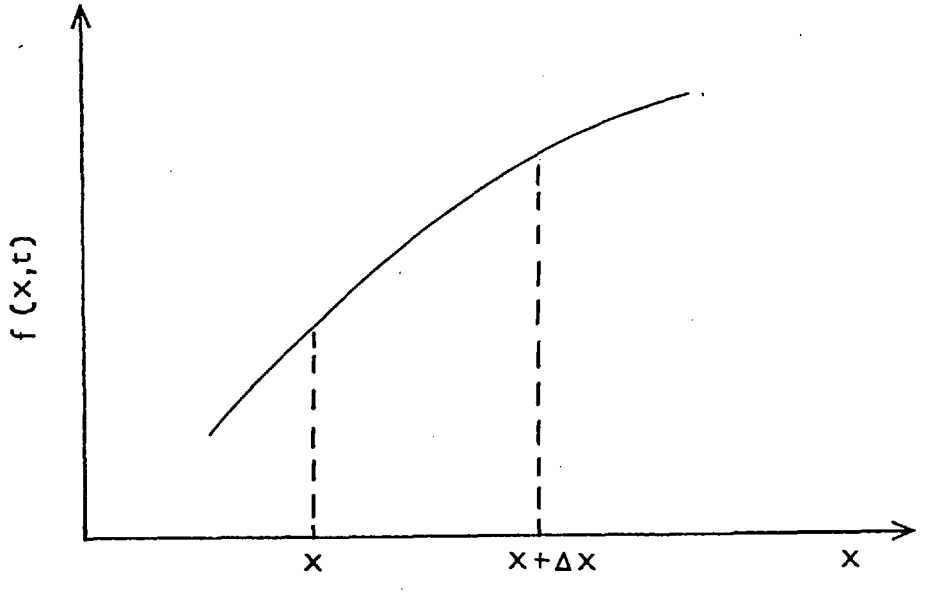

FIGURE 3.2-2 A section of the conversion distribution function.

a (m+4) dimensional space. A balance over a region $\Re$ of this space is given as

$$\frac{d}{dt}\int_{\Re} \psi \, d\Re = \int_{\Re} G \, d\Re$$

(Accumulation) (net generation)

G represents the net generation of entities. In our case, since there is neither creation or destruction of particles, this term is zero. Now, $d\Re$ is given by

$$d\Re = dz_1 \, dz_2 \, dz_3 \, d\xi_1 \, d\xi_2 \ \ldots \ d\xi_m \ .$$

However, by the assumption of perfectly mixed solid, and since, only one characteristic is treated, this expression reduces to

$$d\Re = dx \ .$$

Finally, by taking the derivative of the integral,

$$\int_x \frac{\partial \psi}{\partial t} + \frac{\partial}{\partial x}\left(\frac{dx}{dt} \cdot \psi\right) = 0$$

and for the integral to vanish

$$\frac{d\psi}{dt} + \frac{\partial}{\partial x}\left(\frac{dx}{dt} \ \psi\right) = 0$$

which is identical to Equation (3.2.2-5).

Now, the term dx/dt, the rate of change of the conversion, can be expressed in terms of the rate of reaction $r(x,C_j)$ by a mass balance on the transferring ions B.

The conversion x has been defined as

$$x = \frac{\bar{c} - \bar{c}_t}{\bar{c}}$$

where $\bar{c}$ and $\bar{c}_t$ are the initial and the current capacities of resin.

Considering a unit volume of solid at conversion x in contact with liquid at concentration C_j, it follows that

$$r(x,C_j) = \frac{d}{dt}(\bar{c}.x)$$

[rate of transfer of ions from the liquid to the solid phase] [accumulation of ions in the solid phase]

Hence,

$$\frac{dx}{dt} = \frac{1}{\bar{c}} \; r\,(x,C_j) \qquad (3.2.2\text{-}6)$$

By substitution of Equation (3.2.2-6) in Equation (3.2.2-5b),

$$\frac{\partial f_j(x,t)}{\partial t} + \frac{1}{\bar{c}}\, r(x,C_j)\, \frac{\partial f_j(x,t)}{\partial x} = \frac{-1}{\bar{c}}\, f_j(x,t)\, \frac{\partial r(x,C_j)}{\partial x} \qquad (3.2.2\text{-}7)$$

Equations (3.2.2-2) and (3.2.2-7) must be integrated simultaneously with the appropriate expression for r(x,C).

Solid Feed

Due to the continuous addition of solids, the top stage requires a different treatment. Two approaches can be taken. One is to consider a discretisation of the feed over a number of time steps. The other studies the residence time distribution of the new resin added since the beginning of the forward flow period of the cycle and derives the corresponding conversion distribution. Both methods are discussed in detail with the description of their implementation in Chapter 4.

Fractional Transfer

The solid transfer involves the mixing of the conversion distributions of stages j and j+1. The proportions of each are given by the fractional transfer value. Thus, the following expression is obtained.

$$f'_j\,(x,0) = (1\text{-}d)\; f_j\,(x,t_F) + df_{j+1}\,(x,t_F) \qquad (3.2.2\text{-}8)$$

where t_F is the time at the end of the forward flow period.

Mass Balance for the Top Stage

Consider the volume of solid present in the top stage at time t. This volume has been made up from the volume left on the stage after the last transfer plus the solids fed since the beginning of the cycle at t = 0. Under certain conditions, as will be seen in section 4.1.2, it is convenient to segregate the two portions and assume that the total rate of reaction R_s can be split into two

factors. These factors are: R^0_s which refers to the 'old' resin and R^N_s which represents the rate of reaction of the volume of resin fed since t = 0. Under these conditions, a mass balance on component B gives

$$L\,C_{s-1} - LC_s = \frac{d}{dt}(\varepsilon_s V_s C_s) + (1-\varepsilon_s(t_F))\,(1-d)\,V_j R^0_s + StR^N_s$$

and for constant V

$$\frac{d}{dt}(\varepsilon_s V_s C_s) = V\left(\varepsilon_s \frac{dC_s}{dt} + C\frac{d\varepsilon_s}{dt}\right) .$$

In section 4.1.1., Equation (4.1.1-14b), it is shown that

$$\varepsilon_s = \varepsilon_0 - \frac{St}{V}$$

and

$$\frac{d\varepsilon_s}{dt} = -\frac{S}{V}$$

Hence,

$$\frac{dC_s}{dt} = \frac{L}{\varepsilon_s V_s}(C_{s-1} - C_s) - \frac{(1-\varepsilon_s(t_F))(1-d)}{\varepsilon_s V_s} V_s R^0_s - \frac{StR^N_s}{\varepsilon_s V_s} - \frac{C_s S}{\varepsilon_s V_s}$$

Now, the term $\frac{C_s S}{V_s \varepsilon_s}$ represents the change in liquid concentration due to the diminished liquid hold up. In a step-wise procedure, changes of resin hold up during a time interval are small. Hence, for a given step ε_s can be considered constant and the term dropped.

$$\frac{dC_s}{dt} = \frac{1}{\tau_s}(C_{s-1} - C_s) - \frac{(1-\varepsilon(t_F))(1-d)}{\varepsilon_s} R^0_s - \frac{StR^N_s}{\varepsilon_s V_s} \qquad (3.2.2\text{-}9)$$

In integrating this last equation an adequate updated value of ε_s is used for each time step.

3.3. Kinetics of the Rate of Reaction

The reacting system studied in this work is in fact an ion-exchange process accompanied by a chemical reaction. Hence, the kinetics of the rate of reaction really refers to the kinetics of the ion-exchange which is the rate controlling factor.

It has been known since the early work by Boyd et al. (65), that the rate of an ion-exchange process is controlled by diffusion of counter-ions within the particle (ion-exchanger) or through an adherent stagnant film.

Rates of ion-exchange processes coupled with chemical reactions have been recently studied by Helfferich (66). In these situations, apart from the rare cases in which the chemical step itself becomes the controlling factor, the reaction can strongly affect the mechanism of ion-exchange. The mode and degree of the effect depends on the particular reacting system and on whether the process is intraparticle or film diffusion controlled.

In general, the chemical step will consume co-ions or counter-ions either inside or outside the particle. This can create or destroy concentration gradients and affect the rate. Also, the diffusion of a reacting co-ion could become an important factor in the mechanism of the process.

The reacting system studied in this work can be represented by the total equation

$$R^- H^+ + Na^+ OH^- \rightarrow R^- Na^+ + H_2O \qquad (3.3\text{-}1)$$

Here the counter-ion H^+, released from the ion-exchange resin, is consumed by the co-ion OH^- by neutralization. R^-, denotes the resin matrix; the one used here was the strong acid cation Zeo Karb 225, 8% DVB - a sulphonated styrene-divinyl benzene copolymer.

The effect of the neutralization reaction in this system depends on whether the process is film or particle diffusion controlled. Each case is now examined in turn.

3.3.1 Film Diffusion Controlled Case

Here, the chemical step strongly affects the ion-exchange process. Due to conditions of electroneutrality in the film, linked to the dissociation equilibrium for water, the concentration of H^+ can not exceed that of OH^-. Therefore, the released H^+ ions are consumed right at the particle surface. In this situation the diffusion of counter-ion Na^+ and co-ion OH^- becomes the rate controlling step rather than the diffusion of counter-ions as in ordinary ion-exchange. This reasoning also indicates that the concentration of Na^+ and OH^- at

the particle surface is negligible compared with the bulk concentrations. Thus, the boundary conditions are simplified and an analytical solution of the diffusion equation can be obtained (66).

The solution for conditions of ionic capacity of the liquid larger than the ionic capacity of the resin i.e., resin can be completely converted, is given as

$$F(t) = \frac{6\ DCt}{d_p\ \delta\ \bar{c}} \quad , \tag{3.3.1-1}$$

where F(t) is the fractional attainment of equilibrium and is defined as

$$F(t) = \frac{Q_A^o - Q_A(t)}{Q_A^o - Q_A^\infty} \tag{3.3.1-2}$$

and D, the effective diffusion or Nernst coefficient, is given as

$$D = \frac{2D_{Na}\ D_{OH}}{D_{Na}+D_{OH}} \quad . \tag{3.3.1-3}$$

The rate of ion exchange is obtained by differentiation of Equation (3.3.3-1), i.e.,

$$r = \bar{c}\ \frac{dF}{dt} = \frac{6}{d_p}\ \frac{D}{\delta}\ C \tag{3.3.1-4}$$

In mass transfer studies the film thickness δ is more conveniently represented by the Sherwood number

$$\delta = \frac{d_p}{2Sh} \quad . \tag{3.3.1-5}$$

By definition

$$Sh = \frac{k_L a}{D}$$

hence, (3.3.1-6)

$$r = k_L aC$$

where a is the area for unit volume of solids (6/dp) and k_L is a mass transfer coefficient which depends on the physical properties of the system and the conditions of operation. The mass transfer coefficient can be estimated by correlations of the type:

$$Sh = \frac{k_L\ D}{d_p} = \frac{\phi}{\epsilon_b}\ Re^{1/2}\ Sc^{1/3} \tag{3.3.1-7}$$

Correlations of this form, for liquid fluidized beds, have been studied by several authors. In Snowdon and Turner's paper (67), a value for ϕ of .81 is reported; whereas Rahman (75) obtained a value of ϕ = .86 as the best fit for his experiments.

An experimental verification of Equation (3.3.1-1) has been reported by Blickenstaff et al. (68). There, the reaction given by Equation (3.3-1) was investigated under conditions to ensure film diffusion control. An excellent agreement of experimental and theoretical results verified the validity of Equation (3.3.1-1).

Another experimental verification of the film diffusion model, this case in a small fluidized bed, but for a different reacting system, has been given by Turner and Snowdon (69). A good agreement with the theory was also found.

3.3.2 Intraparticle Diffusion Controlled Case

Numerical solutions for the intraparticle non-linear diffusion equation for ion exchange were given in a early paper by Helfferich (70). In subsequent publications (71,72), more precise and extensive results were reported.

The diffusion equation for the ion exchange process is given in spherical coordinates by

$$\frac{\partial C_B}{\partial t} = \frac{1}{\rho^2} \frac{\partial}{\partial \rho} \left(\rho^2 D_{AB} \frac{\partial C_B}{\partial \rho} \right)$$

The non-linearity in this equation arises in the concentration dependence of the diffusion coefficient D_{AB}. An expression for this coefficient is derived from the Nernst-Planck equations which give.

$$D_{AB} = \frac{D_A D_B (Z_A^2 C_A + Z_B^2 C_B)}{Z_A^2 C_A D_A + Z_B C_B D_B}$$

where Z_A and Z_B are the valences of ions A and B respectively (one in this case).

The necessary relation between C_A and C_B is obtained from the condition of electroneutrality within the particle. This condition requires that the total ionic equivalent concentration of counter ions remain constant and equal to the total concentration of fixed ion groups, i.e.,

$$C_A + C_B = \bar{c}$$

Here, C_A, C_B, D_A, D_B and D_{AB} are quantities inside the particle. In the references given above, the diffusion equation was integrated numerically with the following boundary conditions:

(i) @ $t = 0$ $\quad 0 \leq \rho \leq \rho_0$ $\quad C_B = C_B^0$

(ii) @ $\rho \geq \rho_0$ $\quad C_B(\rho,t) = 0$

Boundary condition (ii) refers to the case of infinite solution volume where the concentration of ion B in the solution is negligible and can be considered zero.

For the reacting system under consideration, the consumption of the H^+ ions does not affect the inter-diffusion of counter-ions within the particle since the co-ion OH^- is effectively excluded from the particle by the Donnan effect. Hence, only the boundary condition at the surface bead is affected. This situation, however, corresponds precisely to the ion-exchange case of infinite solution volume for which the numerical solutions referred to above were given. Thus, those solutions can be applied as they stand.

Results for different ionic diffusivity ratios were presented in a tabulated form (70,71,72). Also, an explicit expression for the fractional attainment of equilibrium was fitted to the numerical results and is of the form

$$F(\theta) = \{1-\exp(\pi^2(\gamma_1(\alpha)\theta + \gamma_2(\alpha)\theta^2 + \gamma_3(\alpha)\theta^3)\}^{\frac{1}{2}} \qquad (3.3.2\text{-}1)$$

where θ is the dimensionless time $D_A t/r_0^2$ and α is the ratio of diffusivity, D_A/D_B. In the case of counter-ions of the same valence the $\gamma(\alpha)$ functions are given by

$$\gamma_1(\alpha) = -1/(.570 + .430\ \alpha^{.775})$$

$$\gamma_2(\alpha) = 1/(.260 + .782\ \alpha)$$

$$\gamma_3(\alpha) = -1/(.165 + .117\ \alpha)$$

The rate of ion-exchange can then be obtained by differentiation of Equation (3.3.2-1) which gives the dimensionless expression

$$r'' = -\frac{dF}{d\theta} = \frac{\pi^2}{2}\left(\gamma_1(\alpha) + 2\gamma_2(\alpha)\theta + 3\gamma_3(\alpha)\theta^2\right)\left(\frac{1-F^2}{F}\right) \qquad (3.3.2\text{-}2)$$

A comparison of theoretical and experimental results for the case of intraparticle diffusion control illustrated by Equation (3.3-1) has been made by Blikenstaff et al. (73). There, a close agreement between theory and experiment was obtained as in the case of film diffusion.

3.3.3 Simplification of the Rate Expression

A complex expression as given by Equation (3.3.2-2) would be difficult to use in the solution of the system Equations (3.2.2-2) and (3.2.2-5). For this purpose, a simplified form may be obtained by neglecting the terms $2\gamma_2(\alpha)\theta$ and $3\gamma_3(\alpha)\theta^2$ from Equation (3.3.2-2). Hence,

$$r'' = -\frac{dF}{d\theta} \simeq \frac{\pi^2\gamma_1(\alpha)}{2}\left(\frac{1-F^2}{F}\right) \simeq -k_D'\ \frac{1-F^2}{F} \qquad (3.3.3\text{-}1)$$

is obtained. The validity of the simplification can be verified by plotting in linear coordinates $\frac{dF}{d\theta}$ VS $\frac{1-F^2}{F}$ as shown in figure (3.3-1). There, it is seen that in fact a linear relation is obtained for θ in the range $1 \times 10^{-3} \leq \theta \leq .50$, which corresponds to $0.02 \leq F \leq 0.95$. The best fit slope of the straight line provides a value for k_D'. A value of $\alpha = D_{H^+}/D_{Na^+} = 6.8$ was used here.

In the definition of F(t), Equation (3.3.1-2), it can be seen that if the factor Q_A^∞ is zero or negligible, the fractional attainment of equilibrium can be regarded as the solid conversion i.e.

$$x = \frac{Q_A^0 - Q_A(t)}{Q_A^0} \qquad (3.3.3\text{-}2)$$

In the reacting system described by Equation (3.3-1), Q_A^∞ would correspond to the amount of H^+ left in the resin when equilibrium is obtained, and is, in fact, zero.

Replacing θ and F with t and x, the rate of ion-exchange can be written as

$$\frac{dx}{dt} = k_D \frac{1-x^2}{x} \qquad (3.3.3\text{-}3)$$

where

$$k_D = \frac{D_A}{r_o^2} k'_D \quad . \qquad (3.3.3\text{-}4)$$

Here, D_A refers to the diffusivity of the ion initially present in the ion-exchanger.

An alternative simplified expression in which the residence time θ is the independent variable, can be obtained as follows:

From Equation (3.3.2-1),

$$1-F^2(\theta) = \exp\left(\pi^2(\gamma_1(\alpha)\theta + \gamma_2(\alpha)\theta^2 + \gamma_3(\alpha)\theta^3)\right)$$

neglecting the terms $\gamma_2(\alpha)\theta^2$ and $\gamma_3(\alpha)\theta^3$ one obtains,

$$1-F^2(\theta) \cong \exp\left(-k_\theta\theta\right),$$

where $k_\theta = -\pi^2\gamma_1(\alpha)$.

By differentiation of (3.3.3-1) with respect to the dimensionless time;

$$-2F(\theta)\frac{dF(\theta)}{d\theta} = -k_\theta \exp\left(-k_\theta\theta\right)$$

and

$$\frac{dF(\theta)}{d\theta} = \frac{k_\theta}{2}\frac{e^{-k_\theta\theta}}{F} = \frac{k_\theta}{2}\frac{e^{-k_\theta\theta}}{\left(1-e^{-k_\theta\theta}\right)^{\frac{1}{2}}} .$$

Expanding in Taylor's series the term $1-e^{-k_\theta\theta}$

$$1 - e^{-k_\theta\theta} = 1-(1-k_\theta\theta + \frac{k^2\theta^2}{2} + \ldots) = k_\theta\theta(1-\frac{k_\theta\theta}{2} + \ldots) \cong k_\theta\theta e^{-\frac{k_\theta\theta}{2}}$$

Substituting this result in the last equation gives

$$\frac{dF}{d\theta} \cong \frac{1}{2}\sqrt{k_\theta}\ \theta^{-\frac{1}{2}}\ e^{-3/4 k_\theta \theta} \qquad (3.3.3\text{-}5)$$

A plot of ln $(\frac{dF}{d\theta}\ \sqrt{\theta})$ VS θ will give an indication of the validity of the approximation. In Figure (3.3.-2) such a plot is presented. There it is seen that for the range $.01 \leq \theta \leq .4$ the approximation is justified. A best linear fit can be used to obtain the value of the parameter k_θ, which turns out to be almost identical to $-\pi^2\gamma_1(\alpha)$ as would be expected.

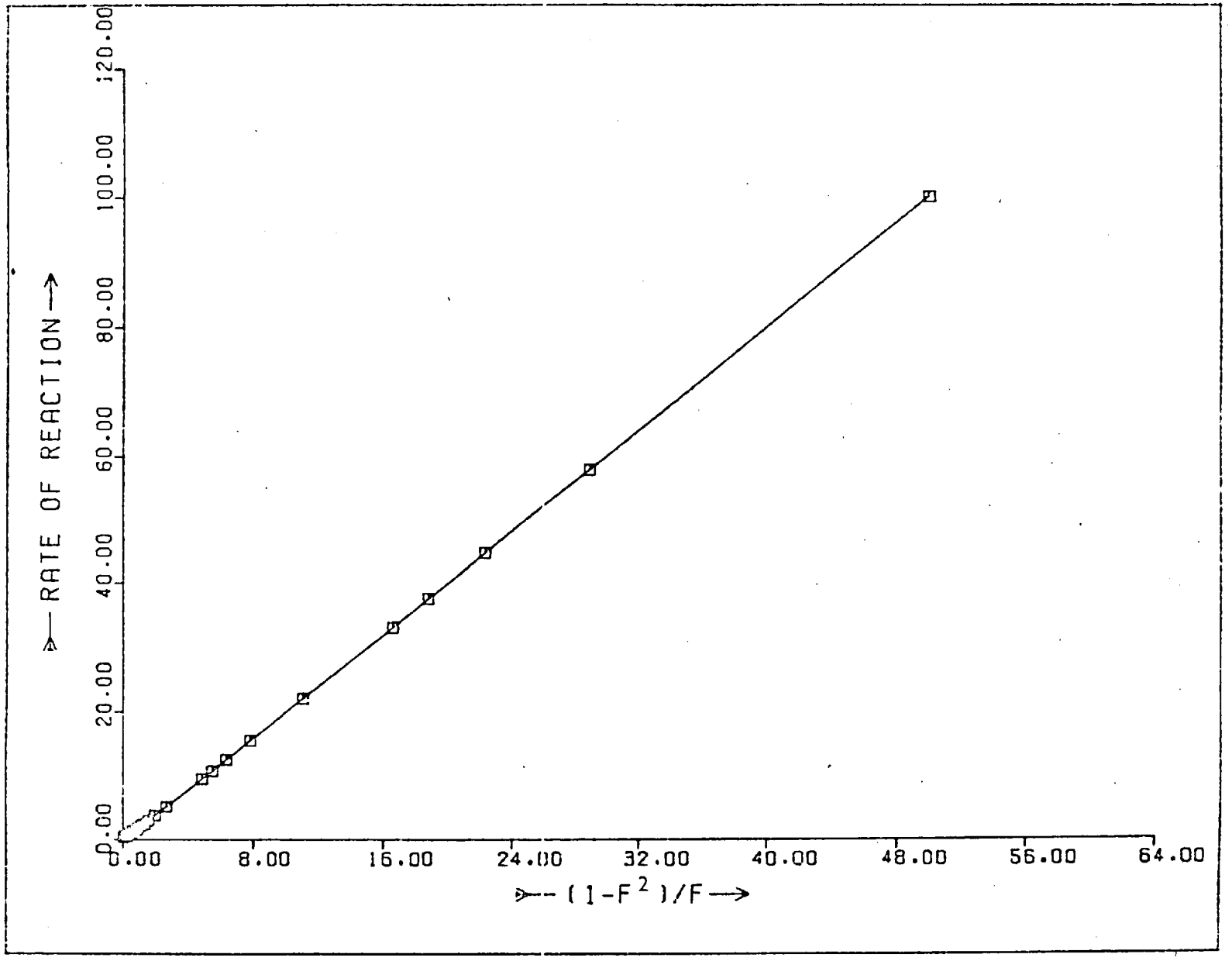

FIGURE 3.3-1 Plot of the simplified expression for the rate of reaction as a function of solid conversion

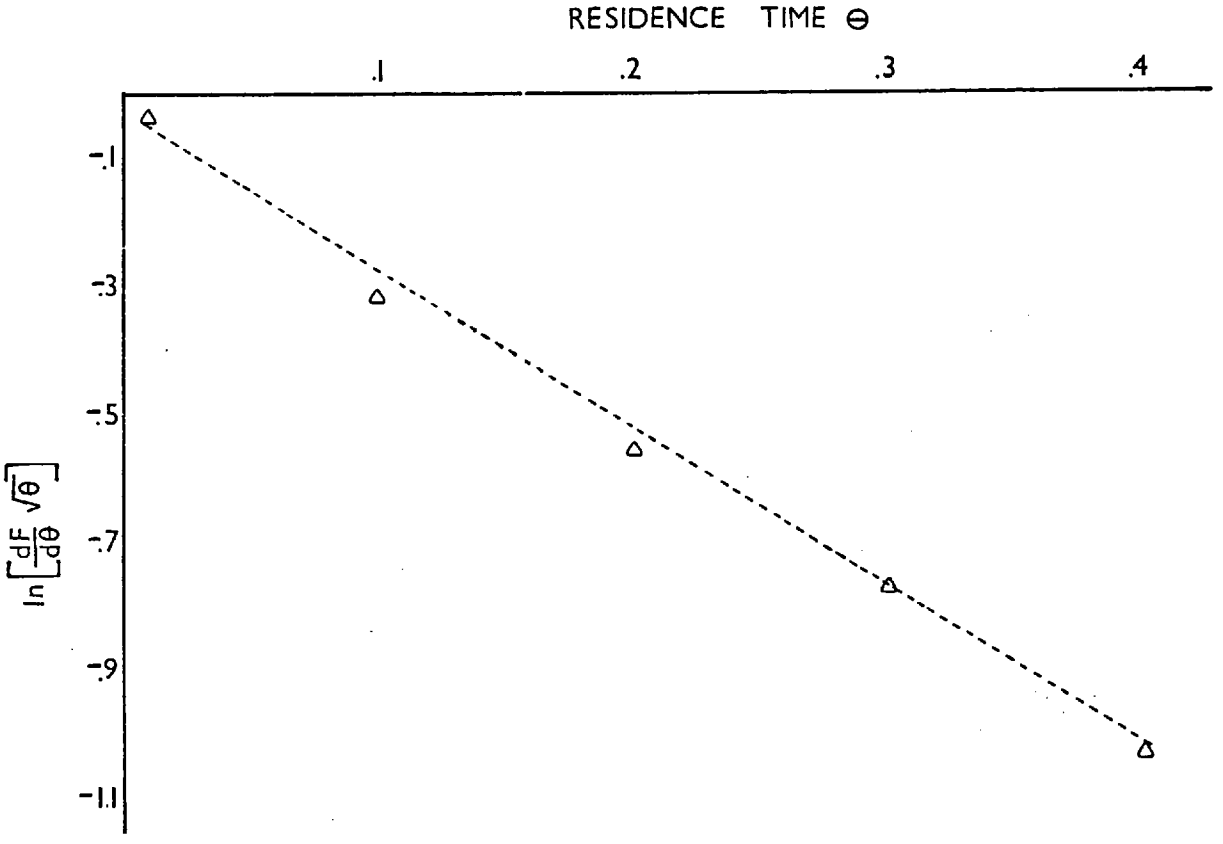

FIGURE 3.3-2 Verification of the approximation for the rate of reaction as a function of residence time.

CHAPTER 4

SOLUTION OF MODELS

In section 3.2 the equations describing the dynamic behaviour of the contactor were introduced. Equation (3.2.2-2) can also be written as

$$\frac{\partial C_j}{\partial t} + 0\,\frac{\partial C_j}{\partial x} = \Phi_j = \frac{1}{\tau_j}(C_{j-1} - C_j) - \frac{1-\epsilon_j}{\epsilon_j} R_j \qquad (4\text{-}1)$$

which with Equation (3.2.2-7)

$$\frac{\partial f_j}{\partial t}(x,t) + \frac{1}{c}\, r(x,C_j)\,\frac{\partial f_j}{\partial x}(x,t) = -\frac{1}{c}\, f_j(x,t)\,\frac{\partial}{\partial x}(r(x,C_j)) \qquad (4\text{-}2)$$

form a set of non-linear hyperbolic partial differential equations which must be solved simultaneously.

Several methods can be used for solving this system, including finite differences, the method of characteristics and (for unimodal density functions) an approximation using the leading moments of the distribution. The last two methods were used in this work and are now discussed.

4.1 Method of Characteristics

In the method of characteristics the problem of solving (4-1) and (4-2) is reduced to the easier task of solving a new set of two ordinary differential equations along two fixed trajectories (characteristics curves) in the x-t plane. The method of characteristics is now widely used in the numerical solution of hyperbolic differential equations. Acrivos (76) was among the first authors to use this method in the solution of chemical engineering problems; he applied it to heat and mass transfer problems in columns. A complete and detailed description of the method is found in books by Abbot (77), Ames (78), Gilbert and Courant (79).

The method mainly consists in finding the equation of the characteristics curves (directions) and the differential equations to be solved along them. The process is in this case straightforward and is presented in detail in Appendix A.2, where the following results are obtained:

The equation for the I-characteristics is

$$\left.\frac{dx}{dt}\right|_I = 0 \qquad (4.1\text{-}1)$$

along which it is needed to solve

$$\frac{dC_j}{dt} = \underline{\Phi}_j \qquad (4.1\text{-}2)$$

and the II-characteristic direction is

$$\left.\frac{dx}{dt}\right|_{II} = \frac{r(x,C)}{\bar{c}} \qquad (4.1\text{-}3)$$

and in that direction the equation to integrate is

$$\frac{df}{dx}(x,t) = -\frac{f(x,t)}{r(x,c)} \frac{\partial}{\partial x} r(x,C) \qquad (4.1\text{-}4)$$

In the actual calculation procedure a grid in the x-t plane is constructed step by step as the solution unfolds. Along the II-characteristics the density function is known continuously whereas the liquid concentration, C, is known along the I-characteristics. At the intersection points both values are known. To advance forward in time a logical time step length would be one that corresponds to the time needed to move from one point of intersection to the next along a II-characteristic; i.e. from x_i at t to x_{i+1} at $t+\Delta t$. However, since the gradients of the II-characteristic are in general functions of x and C, an iterative method is required to find the correct time step.

In this case due to the assumption of perfectly stirred liquid, there is no term $\partial C/\partial x$. Therefore, the directions of the I-characteristics are parallel to the t axis. On the other hand, the II-characteristics depend on the expression of the rate of reaction $r(x,C)$. Since two types of rate laws were used, detailed descriptions of the calculation procedures are left to the corresponding sections in which liquid film and particle diffusion control cases are studied.

Solid feed and fractional transfer are also treated differently in each case. Details of the approaches taken are also discussed in the appropriate sections.

4.1.1 Application to the film-controlled case

Here the method of characteristics is further simplified by the expression for the rate of reaction, which is resin conversion independent and a function only of the liquid concentration. Therefore, at a given time all n+1 II-characteristics (or their gradients) are parallel and the same time step is used for all of them.

As seen in section 3.3-1

$$r(x,C) = k_L aC \cdot \qquad (4.1.1\text{-}1)$$

Then the family of II-characteristics is given by

$$\left.\frac{dx}{dt}\right|_{II} = \frac{k_L aC}{\bar{c}} \qquad (4.1.1\text{-}2)$$

Now, since a numerical technique was being used, it was convenient to approximate the continuous density function f(x,t) by a discrete probability distribution (d.p.d) in which, $p(x_i,j)$, for $i = 1,2 \ldots n+1$ and $j = 1,2 \ldots s$ represents the probability of solid being at conversion x_i, in stage j. By definition this is the same as the fraction of solid at that conversion x_i.

Hence, (n+1) I-characteristics can be drawn equally separated by a distance $\frac{1}{n}$ across the conversion range (0,1) at conversion values $x_i = \frac{i-1}{n}$ $i = 1,2 \ldots (n+1)$, parallel to the t axis. The rate of reaction for the mixture of solids at stage j with conversions x_i and liquid concentration C_j is now given by

$$R_j = \sum_{i=1}^{n} p(x_i,j)\, k_L\, aC_j \cdot \qquad (4.1.1\text{-}3)$$

By using the definition of cumulative distribution function $F(x_n,j)$ one gets

$$R_j = k_L\, aF\,(x_n,j)\, C_j \cdot \qquad (4.1.1\text{-}4)$$

Here $F(x_n,j)$ represents the fraction of particles which are not exhausted.

The characteristic network is then constructed in the following manner:

At the initial conditions (t=0) the conversion distribution is given and this is equal to the fraction of particles at each conversion value. From time t=0, all I-characteristics will move from the departing points x_i for i = 1,2 ... (n+1), towards the direction of higher conversion, advancing in time until the next intersection at x_{i+1} is reached, thus requiring a time denoted by Δt. As mentioned earlier an iterative method is needed to find the correct Δt.

Figure (4.1-1) shows a section of a typical characteristics grid in the t-x plane; reference to it would be helpful in the description of the method. Since the same time step is needed for all I-characteristics, take any point x_i $i \neq (n+1)$, in the graph at t=0. An initial estimate of the time step size can be obtained by linear extrapolation from x_i using the gradient $(dt/dx)_{x_i}$ calculated from Equation (4.1-3):

$$\Delta t^0 = \left(\frac{dt}{dx}\right)_{x_i} \Delta x \qquad (4.1.1\text{-}5)$$

where

$$\Delta x = x_{i+1} - x_i = \frac{1}{n} \quad .$$

With this time step, it is now possible to integrate simultaneously Equations (4.1-2) and (4.1.1-2). Since they are uncoupled and during a time step the rate of reaction R_j is constant, it is possible to integrate them analytically over the time step. The solutions are

$$C(t) = (C_k - \frac{C_{j-1}}{b\tau_j})\, e^{-bt} + \frac{C_{j-1}}{b\tau_j}$$

and

$$x(t) = \frac{k_L a}{b\bar{c}} (C_k - \frac{C_{j-1}}{b\tau_j})(1 - e^{-bt}) + \frac{k_L a}{b\tau_j} \frac{C_{j-1}}{\tau_j} t$$

where

$$b = \frac{1}{\tau_j} - \frac{1-\varepsilon}{\varepsilon} k_L a\, F(x_n, j)$$

and C_k is the liquid concentration at the begining of the time-step.

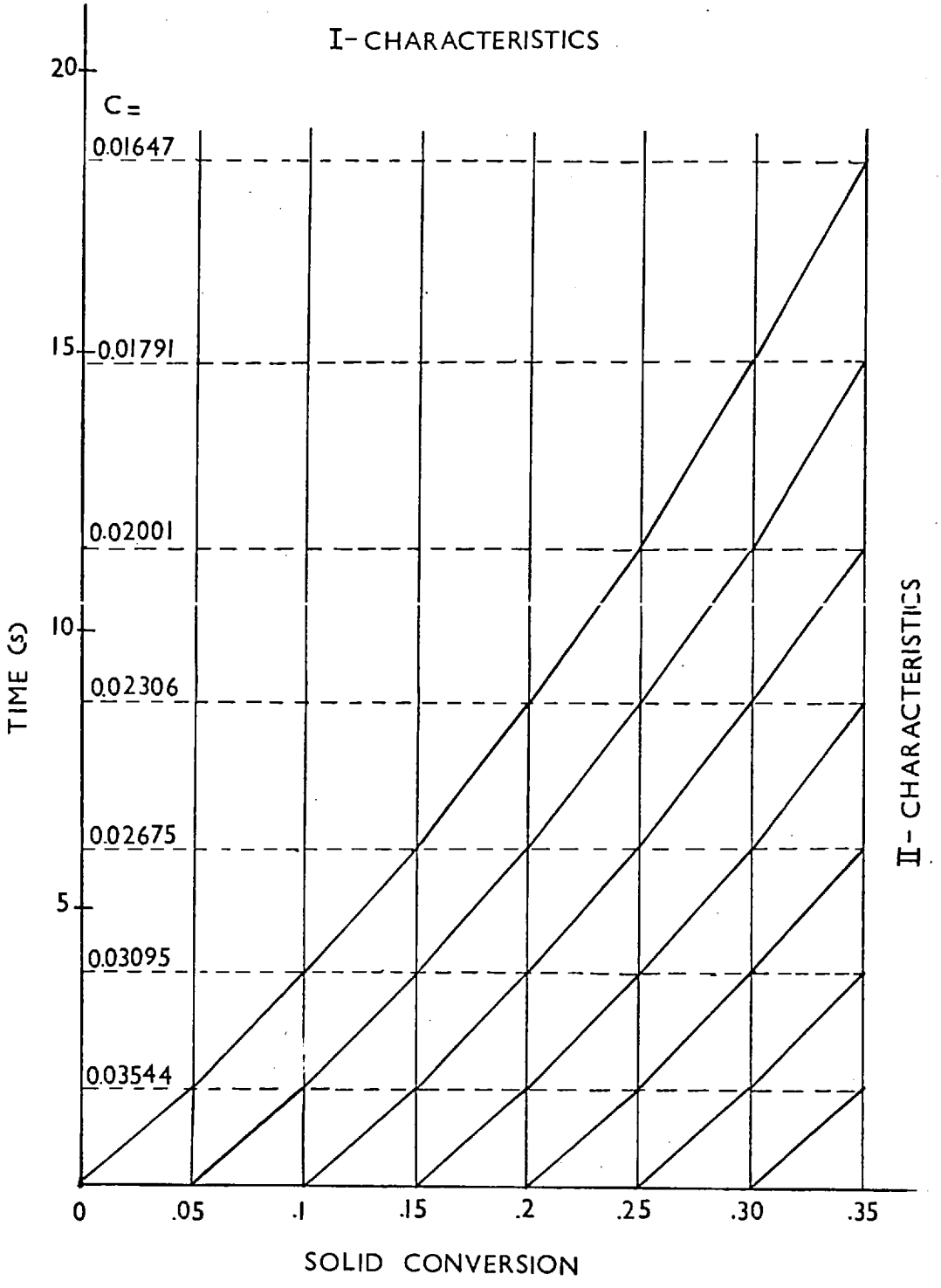

FIGURE 4.1-1 A typical characteristics grid for the liquid film controlled case.

A Newton-Raphson algorithm can then be used to update the time step size by comparing the values x_{i+1} and x* (from integration), i.e.

$$\Delta t^k = \Delta t^{k-1} + \left(\frac{dt}{dx}\right)_{x^*} (x_{i+1} - x^*) \qquad (4.1.1\text{-}6)$$

see Figure (4.1-2). Convergence of this procedure is almost assured since, unless too few characteristics are used, the conversion increment $(x_{i+1} - x_i)$ is small and the first guess at Δt is usually a good one. Furthermore, after the three initial time steps a quadratic extrapolation technique was used instead of Equation (4.1.1-5) to estimate the next time step. This gives a better first estimate of the time step.

From Equation (4.1.1-1) it is seen that since the rate expression is independent of resin conversion

$$\frac{\partial}{\partial x} r(x, C_j) = 0 \quad , \qquad (4.1.1\text{-}7)$$

and from Equation (4.1-4)

$$\frac{\partial f_j}{\partial t} = 0 \quad ; \qquad (4.1.1\text{-}8)$$

the density function is constant along the characteristics. The d.p.d. after each time step is given by

$$p'(x_{i+1}, j) = p(x_i, j) \qquad i = 1, 2 \ldots n-1$$

and (4.1.1-9)

$$p'(x_{n+1}, j) = p(x_{n+1}, j) + p(x_n, j)$$

where p' represents the d.p.d. after the time step and p, before the time step.

In this form the entire network is constructed and the movements of the liquid concentration and density function with time are obtained.

The column can then be solved stage-wise from the bottom upwards. Since during the forward flow period each stage is independent of the

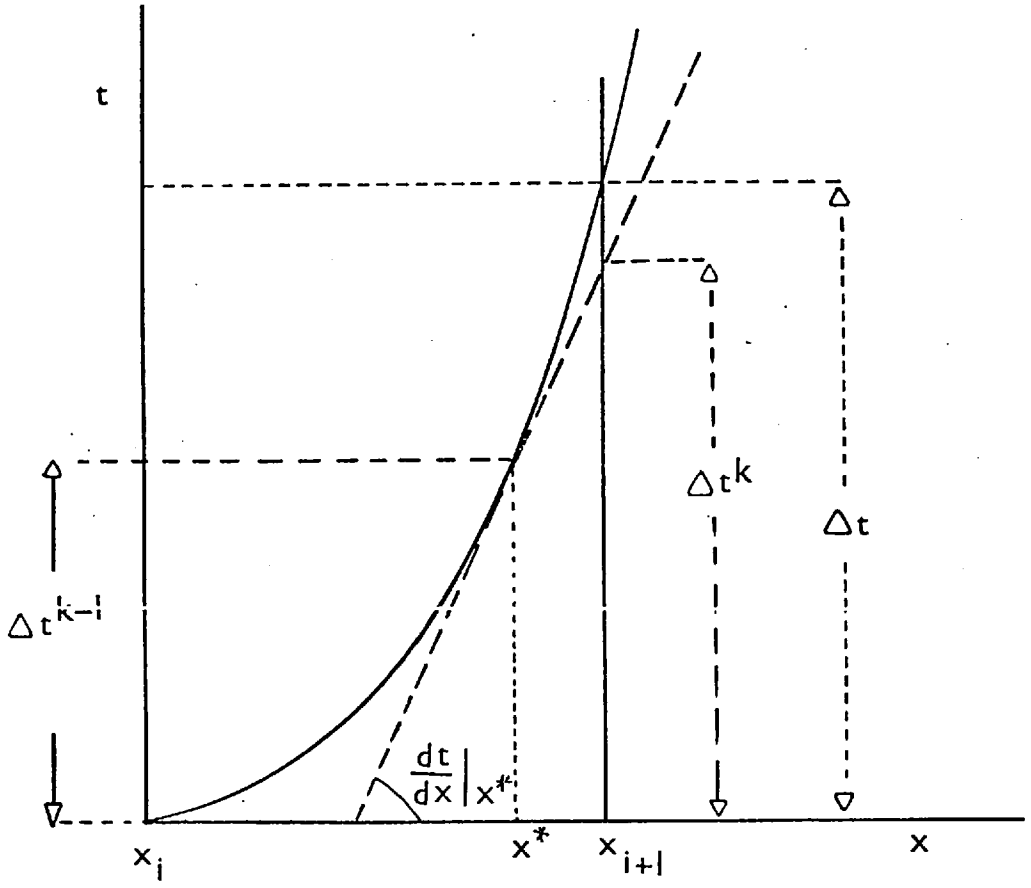

FIGURE 4.1-2 Use of the Newton-Raphson algorithm to evaluate the time step length

stages above, only the inlet liquid concentration as a function of time is needed to calculate the stage behaviour. It is then only required that the exit liquid concentration along the cycle is stored after the calculation of each stage for further use in calculating the stage above. Since the procedure described finds and uses time steps of different sizes, in the calculation of a stage other than the bottom one, the inlet liquid concentrations at the time required are evaluated by quadratic interpolation of the corresponding stored values. Analogously, it is very unlikely that the time at end of the last step, t_{k+1}, coincides with the end of the forward flow period t_F. Hence it is needed to decide whether the d.p.d takes the value it would have attained after the time step or remains at the previous value. The following criterium is used:

If $t_F - t_k < \frac{\Delta t}{2}$ the d.p.d remains unchanged.

If $t_F - t_k > \frac{\Delta t}{2}$ the d.p.d takes the value it would have reached at the end of the time step.

Here, t_k represents the time at the end of the $(k-1)^{th}$ step and $\Delta t = t_{k+1} - t_k$. For the same reason, the liquid concentration at t_F needs to be evaluated; this is done by a quadratic extrapolation using the concentration values at the last three time steps.

Treatment of solid transfer

Solid transfer is easily accounted for in this case. Since an equal number of characteristics are used for all stages, the conversion divisions are the same. Remembering assumption (v) in section (3.2.1), i.e., there are no appreciable changes in density or size of particles, it can be further assumed that the conversion distribution of the transferring solid particles is equal to that of the fluidized particles at the end of the forward flow. Therefore, the new distribution of resin on stage j is obtained by performing a solids mass balance which gives

$$(1-\varepsilon_j)\, V_j\, p'(x_i,j) = (1-\varepsilon_j)\, V_j\, p(x_i,j)(1-d) + (1-\varepsilon_{j+1})V_{j+1}\, p(x_i,j+1)d \qquad (4.1.1\text{-}10)$$

$$\begin{bmatrix}\text{volume of particles of conversion } x_i \text{ on stage j after transfer.}\end{bmatrix} = \begin{bmatrix}\text{volume of particles of conversion } x_i \text{ which remained on stage.}\end{bmatrix} + \begin{bmatrix}\text{volume of particles of conversion } x_i, \text{ transferred from stage j+1.}\end{bmatrix}$$

and since it was assumed (section 2.1), that all voidages and stage volumes are equal, one gets

$$p'(x_i,j) = p(x_i,j)(1-d) + p(x_i,j+1) \qquad \begin{matrix} i = 1,2 \ldots n+1 \\ j = 1,2 \ldots s-1 \end{matrix} \qquad (4.1.1\text{-}11)$$

Treatment of solid feed

A discretisation of the continuous solid feed was used here. It is considered that the solids are added at the end of each time step at the same rate as the continuous feed, and a volume $S\Delta t$ is fed after each time step. Consequently, the voidage changes (discretely) as the solid hold up is increased.

At the begining of the forward flow operation the volume of solid present on stage s is

$$V_s(1-\varepsilon_0) = V_s(1-\varepsilon_s(t_F)) - V_s(1-\varepsilon_s(t_F))d \qquad (4.1.1\text{-}12)$$

where $\varepsilon_s(t_F)$ and ε_0 denote the voidages at the end and at the begining of the forward flow.

After k time steps, the volume of solid in the top has been increased by $S.t_k$, that is,

$$V_s(1-\varepsilon_s) = V_s(1-\varepsilon_s(t_F))\,(1-d) + S.t_k \qquad (4.1.1\text{-}13)$$

ε_s denotes the actual value of the porosity during the k^{th} step, and can be calculated from (4.1.1-13)

$$\varepsilon_s = 1 - (1-\varepsilon_s(t_F))(1-d) - \frac{S.t_k}{V_s} \quad , \qquad (4.1.1\text{-}14a)$$

and from (4.1.1-12)

$$\varepsilon_s = \varepsilon_0 - \frac{S.t_k}{V_s} \qquad (4.1.1\text{-}14b)$$

At the end of the k^{th} time step a volume $S(t_{k+1} - t_k)$ at zero conversion is added to the stage s. During this step all solid initially present has moved one conversion division and at the end of the step no solid with x = 0 exists. Thus the modified d.p.d at the end of the k^{th} step can easily be found by adjusting the fractions of solid at each conversion division, that is,

$$p'(x_1,s) = \frac{S\,\Delta t}{V_s(1-\varepsilon_s) + S\Delta t} \qquad (4.1.1\text{-}15a)$$

(i.e., the fraction of solid at zero conversion), and for all other conversions

$$p'(x_i,s) = \frac{p(x_i,s)\,V_s\,(1-\varepsilon_s)}{V_s\,(1-\varepsilon_s) + S\,\Delta t}\ , \ i = 2,3 \ldots n+1 \qquad (4.1.1\text{-}15b)$$

Consider the k^{th} time step which encloses the end of the forward flow period, that is $t_k < t_F \leq t_{k+1}$. The solid added up to t_F in this step is $S(t_F - t_k)$. Here again is necessary to decide whether the d.p.d is changed during the step.

If $(t_F - t_k) > \Delta t/2$ it is assumed that the distribution has moved over, i.e., the solid has reached the next conversion division and thus, no solid exists at zero conversion. The adjustments of the d.p.d. are then as follows:

$$p'(x_1,s) = \frac{S(t_F - t_k)}{V_s(1-\varepsilon_s(t_F))} \qquad (4.1.1\text{-}16a)$$

and

$$p'(x_i,s) = \frac{p(x_i,s)(1-\varepsilon_s)}{(1-\varepsilon_s\,(t_F))} \qquad i = 2,3 \ldots n+1\,. \qquad (4.1.1\text{-}16b)$$

In the case where $(t_F - t_k) < \Delta t/2$, the assumption is that the d.p.d has not changed over the last step and material added during the previous time step has not reacted. Thus,

$$p'(x_1,s) = p(x_1,s)\ V_s(1-\varepsilon_s(t_F)) + S(t_F - t_k) \qquad (4.1.1\text{-}17a)$$

and

$$p'(x_i,s) = \frac{p(x_i,s)\ (1-\varepsilon_s(t_F))}{(1-\varepsilon_s(t_F))} \qquad i = 2,3 \ldots n+1 \qquad (4.1.1\text{-}17b)$$

In this treatment of the solid feed it has been assumed that the volume of resin fed during the forward flow period is equivalent to the volume fed during the total cycle time T. This assumption is valid if the duration of the reversal of flow period is very short. In other situations, to account for the solid feed during transfer two approaches can be taken:

a) The resin flow rate is modified so that the volume of resin fed during the forward flow equals that of the total cycle, i.e.,

$$ST = S_m t_F$$

and S_m the modified flow rate is simply

$$S_m = S\ T/t_F$$

b) A more strict approach considers the solids fed during the transfer period in the following manner:
During transfer a volume $S(T - t_F)$ of resin has been added to the top stage. Hence at the begining of the forward flow one has

$$V_s(1-\varepsilon_s) = V_s(1-\varepsilon_s(t_F)) - V_s(1-\varepsilon_s(t_F))\ d + S(T-t_F)$$

and at time t

$$\varepsilon_s = 1 - (1-\varepsilon_s(t_F))\ (1-d) - \frac{S.t}{V_s} - \frac{S(T-t_F)}{V_s} \qquad (4.1.1\text{-}18)$$

According to assumption (iii) in section (3.2.1), there is no mass transfer during reversal of flow. Therefore, the entire volume $S(T-t_F)$ can be considered to be at zero conversion and the adjustments to the d.p.d are easily performed as follows:

$$p'(x_1,s) = \frac{S\ (T-t_F)}{V_s\ (1-\varepsilon_s(t_F))(1-d) + S(T-t_F)} \qquad (4.1.1\text{-}19a)$$

and for all other resin

$$p'(x_i,s) = \frac{p(x_i,s)(1-\varepsilon(t_F))V_s(1-d)}{V_s(1-\varepsilon_s(t_F))(1-d) + S(T-t_F)} \quad . \qquad (4.1.1\text{-}19b)$$

This last approach has been used in this work.

4.1.2 Application to the intraparticle diffusion case

An expression for the rate of reaction applicable under conditions in which it is intraparticle diffusion controlled was obtained in section (3.3.3). Using Equation (3.2.2-6) the expression takes the form:

$$r(x,C_j) = k_D \bar{c} \frac{1-x^2}{x} \qquad (4.1.2\text{-}1)$$

Upon substitution in (4.1-3) the equation for the set of II-characteristics is obtained,

$$\left.\frac{dx}{dt}\right|_{II} = k_D \frac{1-x^2}{x} \qquad (4.1.2\text{-}2)$$

In that direction it is required to integrate

$$\frac{df}{dx}(x,t) = f(x,t) \frac{1+x^2}{x(1-x^2)} \qquad (4.1.2\text{-}3)$$

which is obtained after performing the derivative indicated in Equation (4.1-4).

The direction of the I-characteristics for this case is identical to that of the film controlled case. From Equation (4.1-1)

$$\left.\frac{dx}{dt}\right|_{I} = 0$$

and along it, one needs to solve as in the previous case

$$\left.\frac{dC_j}{dt}\right|_{I} = \frac{1}{\tau}(C_{j-1} - C_j) - \frac{1-\varepsilon_j}{\varepsilon_j} R_j(x) \quad . \qquad (4.1.2\text{-}4)$$

However, in this case

$$R_j = \bar{c} \int_0^1 f(x,t) \frac{(1-x^2)}{x} dx, \qquad (4.1.2\text{-}5)$$

is used. Here, it is more convenient not to approximate the continuous density function (c.d.f.) by a discrete probability distribution, and therefore, the integral form of (4.1.2-5) is used instead of the summation in (4.1.1-3).

As it is indicated by Equation (4.1.2-2), the II-characteristics are now liquid concentration independent, so they can be constructed immediately together with the I-characteristics. Integration of (4.1.2-2) gives an explicit expression of the conversion as a function of time; for n + 1 characteristics,

$$x_i = \left[1 - (1-x_{0_i}^2)\, e^{-2k_D t}\right]^{\frac{1}{2}} \qquad i = 1, 2 \ldots n+1 \qquad (4.1.2\text{-}6)$$

where x_{0_i} is the initial resin conversion at t = 0.

To construct the characteristics network (n+1) conversion values are chosen across the conversion range. Here the conversion range is somewhat different from the previous case. It is computationally convenient to avoid the zero conversion point, since at that value the predicted rate of reaction becomes infinite. This would also represent the practical situation where 100% regeneration of resin is difficult and not always obtained. Therefore, the conversion range in this case is $x_f \leq x \leq 1$, where x_f represents the composition of the solid feed.

Thus, $$x_i = x_f + \frac{(1-x_f)(1-i)}{n} \qquad i = 1, 2 \ldots n+1 \qquad (4.1.2\text{-}7)$$

Both sets of characteristics are constructed at the chosen conversion values, x_i. For the II-characteristics these points represent the initial conversion at t = 0, for the first cycle. Figure (4.1-3) shows a section of a typical characteristics grid in the t-x plane. A plot of the II-characteristics in a x-t plane gives a picture of how the rate of reaction varies with time, as seen in Figure (4.1-4).

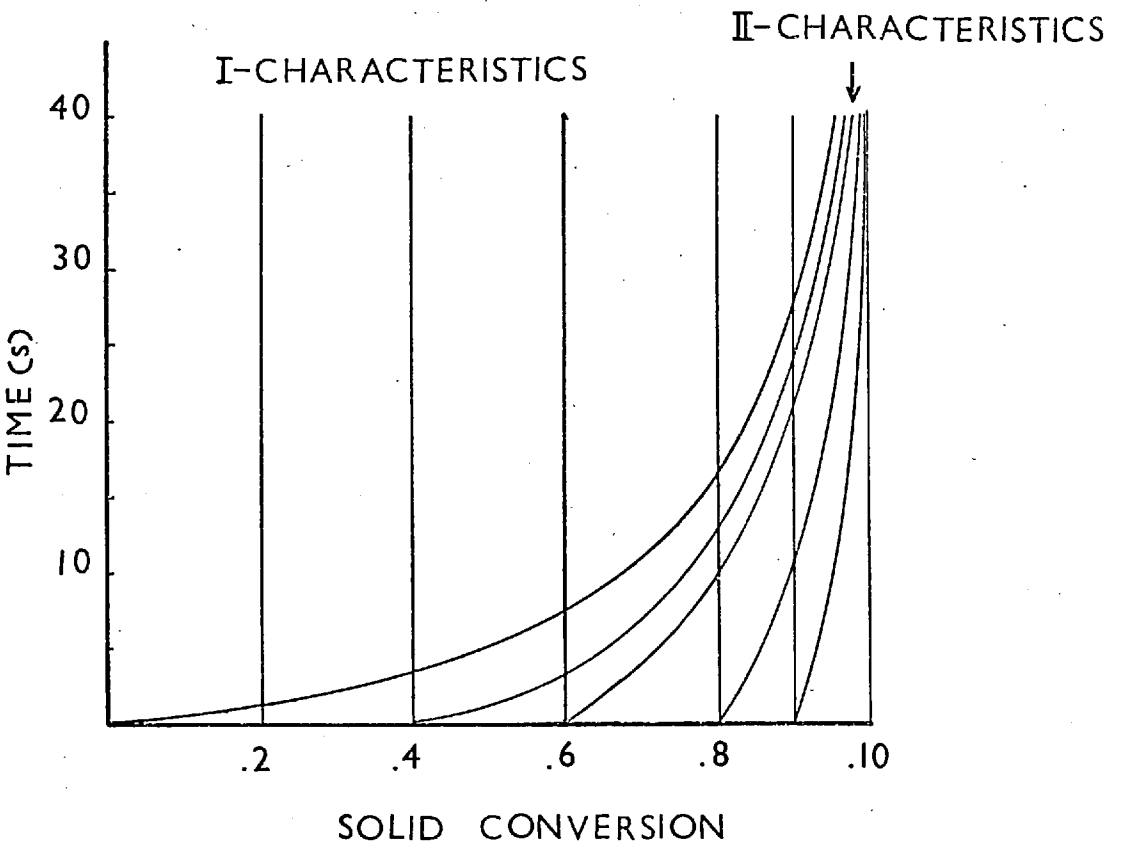

FIGURE 4.1-3 Typical characteristics grid for the case of intraparticle diffusion controlled rate of reaction.

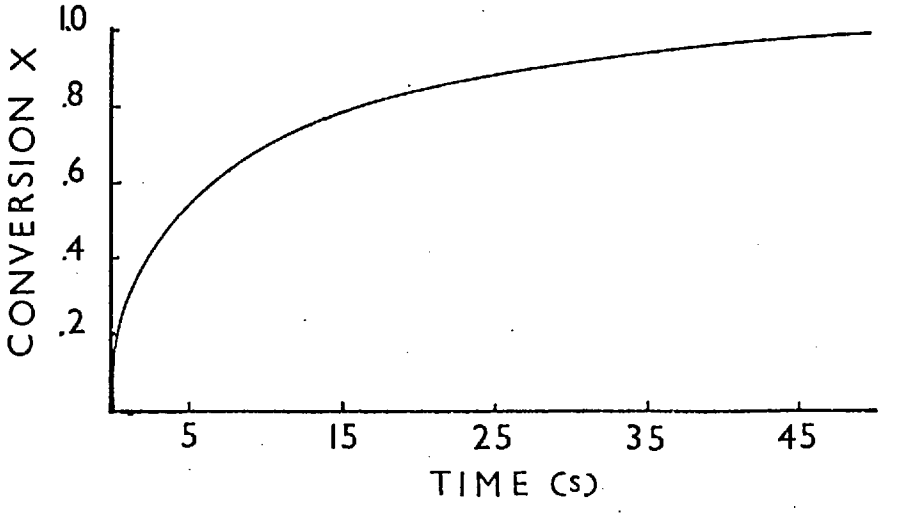

FIGURE 4.1-4 The rate of reaction (dx/dt) as a function of time for fresh solid.

This indicates that steep changes in the composition of both phases occur at the begining of the cycle and then slow down as the cycle proceeds.

To integrate along the II-characteristics, from Equation (4.1.2-3), it follows that

$$\frac{1}{f}\frac{df}{dt} = \frac{1+x^2}{(1-x^2)x}$$

and by integration

$$\ln\frac{f}{f_0} = \ln\frac{x(1-x_0^2)}{x_0(1-x^2)}$$

or

$$f = f_0\frac{x(1-x_0^2)}{x(1-x^2)} \qquad (4.1.2\text{-}8)$$

where f_0 represents the distribution function at time t_0, when the conversion range was given by the x_{0_i}'s.

Since both sets of characteristics are constructed independently, the solution procedure is simplified. It is now only required to integrate forward in time along the II-characteristics. The rate of reaction term R_j can then be evaluated at given points in time (time steps), and with this the liquid composition changes can be found.

The following solution procedure is therefore adopted: For a given initial conversion distribution f_0, and a time step $\Delta t = t_{k-1} - t_k$, the change of solid composition is calculated by Equation (4.1.2-6). In the case of the first time step of the first cycle, the initial x_{0_i}'s, are found from Equation (4.1.2-7). The change in the c.d.f. can then be evaluated from (4.1.2-8). The rate of reaction term R_j can now be computed from the integration of (4.1.2-5). Finally the liquid concentration at the end of the time step is obtained by solving (4.1.2-4).

It is in the integration of (4.1.2-4) where the need for a step-wise procedure arises, since, as seen in Equation (4.1.2-5)

to evaluate R_j the current conversion values and their distribution are needed. The solution of Equation (4.1.2-4) is given by

$$C_j(t) = C_{j-1}(1-e^{-t/\tau}) + C_k e^{-t/\tau} - \frac{1-\epsilon_j}{\epsilon_j} e^{-t/\tau} \int_{t_k}^{t} e^{t'/\tau} R_j(x)\, dt' \quad (4.1.2\text{-}9)$$

where t_k and C_k are the time and the liquid concentration at the begining of the k^{th} time step and t is the time at the end of the step. Due to the curved characteristics an arithmetic average value of the rate R_j over the time step will not be adequate. A weighted average as would be given by a trapezoidal rule integration, would suffice for sufficiently small time steps. For longer time steps other integration procedures will be needed, which will require mid-interval evaluations of R_j. Therefore, in choosing an adequate step, this last aspect of solution procedure must be taken into account with the usual considerations of accuracy on one side, and computing cost on the other. The size of step chosen for the calculation in this work was found by trial and error. For this work, a trapezoidal rule was found to be the most suitable.

Analogously to the film controlled case, a stage-wise procedure was used to calculate the entire column.

Since in this case the same number and size of time steps can be chosen for all stages, the stored values of liquid concentrations will all be given at the same points in time. Therefore, there is neither need for interpolations of liquid concentrations nor additional adjustments for the c.d.f at the end of the forward flow period as was needed in the film controlled case.

Treatment of solid transfer

In this case, since a continous density function is used, Equation (3.2.2-8) is applied to adjust the c.d.f after transfer of solids. However, since only the values of the function at (n+1) conversion values are known, the following expression is used;

$$f_j^{i'} = f_j^{i}(1-d) + f_{j+1}^{i} d \qquad \begin{matrix} i = 1, 2 \ldots n+1 \\ j = 1, 2 \ldots s-1 \end{matrix} \quad (4.1.2\text{-}10)$$

Superscript i represents the conversion values at which f_j is known.

In general, the values of conversions at which f_j is known would not correspond to the values at which f_{j+1} is known. Therefore, a quadratic interpolation procedure is used to evaluate the function values at the required conversion points. Thus for example, if the values of f_j are taken as a base, the values of f_{j+1} are interpolated using three points which enclose the conversion in question, and Equation (4.1.2-10) can then be used.

Treatment of solid feed

In the film controlled case, a discrete approach was taken. There, solids were added to the system at the end of the time step, and during the time step the resin hold up remained constant. In this section a continuous approach to solid feed is more convenient; it is based in the residence time distribution of the solid that is fed during one cycle.

Consider the top stage after a number of cycles. Just at the begining of the forward flow period the solid material present there has a conversion distribution $f_s^o(x,t)$ with conversion in the range $x_f \leq x \leq 1$, where x_f is the feed composition of the resin. After a given time δt, the 'old' resin, which had conversion $x_f \leq x \leq 1$, will have reacted to a certain extent, and will have reached conversions $x_\alpha \leq x \leq 1$. x_α corresponds to the conversion achieved by resin which was previously at x_f. In the meantime, the 'new' resin added during δt, will have reacted in accordance to the time spent in the stage (residence time) and will have a conversion distribution $f_s^N(x,t)$ in the range, $x_f \leq x \leq x_\alpha$. Now the rate of reaction for the stage for resin at all possible conversions is

$$R_s = k_D \bar{c} \int_{x_f}^{1} f_s(x,t) \frac{1-x^2}{x} dx$$

which can also be written

$$R_s = k_D \bar{c} \int_{x_f}^{x_\alpha} f_s^N(x,t) \frac{1-x^2}{x} dx + k_D \bar{c} \int_{x_\alpha}^{1} f_s^0(x,t) \frac{1-x^2}{x} dx \qquad (4.1.2\text{-}11)$$

or

$$R_s = R_s^O + R_s^N \quad . \tag{4.1.2-12}$$

The term R_s^O for the 'old' resin is calculated as was described earlier. For the term R_s^N, a much simpler approach can be taken, based on the residence time of the resin that has been fed since the begining of the cycle at t = 0. The residence times can be easily evaluated as follows.

For a constant resin flow rate, the residence time distribution of the solid feed is simply the constant function:

$$g(t) = \frac{1}{\delta t} \quad \text{for} \quad \delta t \geq t \geq 0 \tag{4.1.2-13}$$

which is depicted in Figure (4.1-5). For a fraction of solids ε', added during δt, the fraction of material with residence times between t and t + dt is

$$g(t)dt = \frac{\varepsilon'}{\delta t}\, dt \quad . \tag{4.1.2-14}$$

The corresponding cumulative distribution function is given by integration of (4.1.2-14).

$$G(t) = \frac{\varepsilon' t}{\delta t}$$

a graph of $G(t) = \varepsilon' t/\delta t$ is given in Figure (4.1-6).

From the equation of the II-characteristics a relation between conversion and the time the solids have spent in the reacting system (residence time) is

$$t = \frac{-1}{2k_D} \ln \frac{1-x^2}{1-x_0^2} \quad .$$

Therefore,

$$G(x) = \frac{-1}{2k_D \delta t} \ln \frac{1-x^2}{1-x_0^2}, \qquad x \leq x_\alpha \tag{4.1.2-16}$$

where

$$x_\alpha = \sqrt{1-(1-x_f)e^{-2k_D \delta t}}$$

which by differentiation gives its corresponding density function.

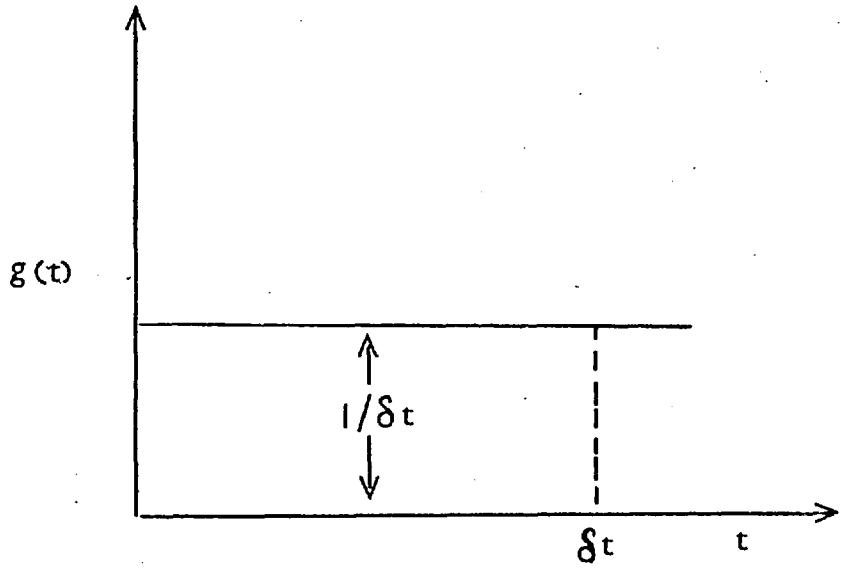

FIGURE 4.1-5 Residence time distribution function of the solids fed in the time interval $[0, \delta t]$.

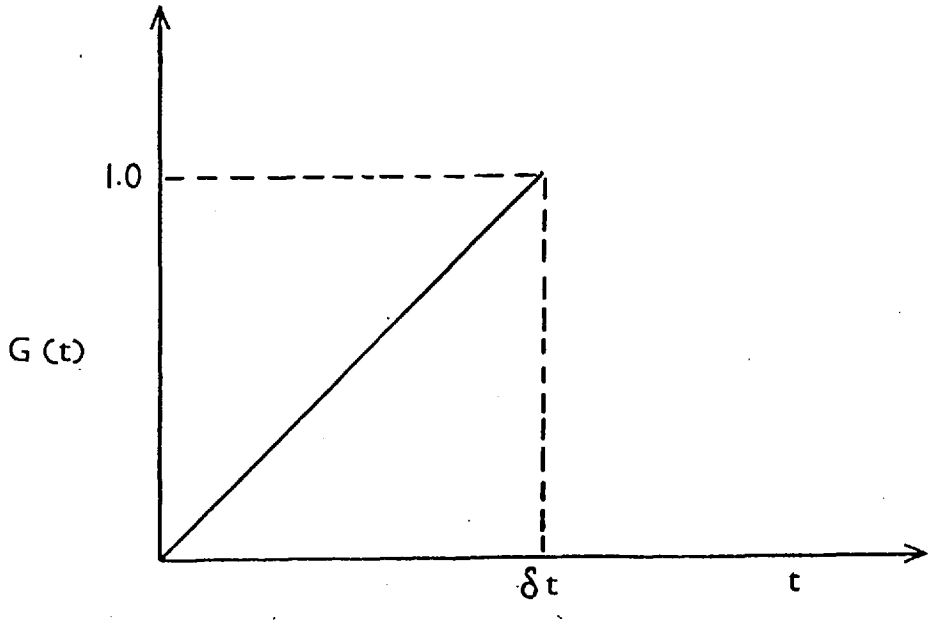

FIGURE 4.1-6 Cumulative residence time distribution of the solids feed.

$$f(x) = \frac{d}{dx} G(x) = \frac{1}{k_D \delta t} \frac{x}{1-x^2} , \quad x \leq x_\alpha \qquad (4.1.2\text{-}17)$$

By integration of (4.1.2-16) between the limits of x_f and x_α an area of unity is found, proving that f(x) is in fact a normalized distribution function.

Using this last result in the definition of R_s^N ,

$$R_s^N = \bar{c} \int_{x_f}^{x_\alpha} \frac{1}{k_D \delta t} \frac{x}{1-x^2} k_D \frac{1-x^2}{x} dx = \bar{c} \frac{(x_\alpha - x_f)}{\delta t} \qquad (4.1.2\text{-}18)$$

This expression for R_s^N can now be used in Equation (3.2.2-9) which after integration, assuming a constant voidage for the time step, gives

$$C_s(t) = C_k e^{-t/\tau} + \left[C_{s-1} - b_1 (x_\alpha - x_f)\right](1-e^{-t/\tau}) - b_2 e^{-t/\tau} \int_{t_k}^{t} e^{t'/\tau} R_s^O(x) dt' \qquad (4.1.2\text{-}19)$$

where C_k is the stage concentration at t_k, that is, at the begining of the time step, t is the time at the end of the k^{th} step, δt the time since the begining of the cycle and the constants b_1 and b_2 are

$$b_1 = \frac{S\bar{c}}{\hat{\varepsilon} V \delta t} \frac{1}{\tau}$$

$$b_2 = \frac{(1-\varepsilon_s(t_F))(1-d)}{\hat{\varepsilon}} ,$$

the average voidage for the time step $\hat{\varepsilon}$ is

$$\hat{\varepsilon} = \frac{1}{2} (\varepsilon_{t_k} + \varepsilon_{t_{k+1}}), \qquad (4.1.2\text{-}20)$$

and ε_{t_k} and $\varepsilon_{t_{k+1}}$ are the voidages at the begining and at the end of the time step respectively.

The main advantage of this continuous approach is that it greatly simplifies the mode of dealing with the solid feed. It permits the treatment of the 'new' resin without interfering with the treatment of the 'old' resin whose conversion change is described by

the path along the II-characteristics. To describe the new solid material composition change in the same way, a new set of characteristics would have to be introduced at each time step. Since a fair number of characteristics are needed to treat the new resin adequately, at the end of the cycle one would be handling many more characteristics than at the begining and this would require a more complex and comparatively more expensive solution algorithm.

In the derivation of Equation (4.1.2-11), $f_s^0(x,t)$ referred to the resin left on the stage after solids transfer and did not include the resin which, as described, is fed during the transfer period. This resin was accounted for in the following manner.

It was earlier assumed (section 3.2.1) that there is no mass transfer between phases during solid transfer; therefore, the volume V_t of resin fed in this period can be considered as to have spent no time in the reactor up to the moment when liquid flow was reinitiated. This resin could be incorporated to either the 'old' or the 'new' resin conversion distributions. However, if put with the distribution for the old resin one would have to deal with a delta function at conversion x_f. Hence incorporation to the 'new' resin conversion distribution is preferred. This can be simply done by assuming that V_t is added during the first time step together with the volume $S.t_1$.

Finally, the density function for all the resin in the top stage at the end of the forward flow period ($t = t_F$), for the entire conversion range $x_f \leq x \leq 1$ can be easily evaluated by a weighted sum of the 'old' and 'new' resin distributions,

$$f_s(x,t_F) = \frac{(1-\varepsilon_s(t_F))(1-d)\ f^0(x,t_F) + S.T\ \ f^N(x,t_F)}{(1-\varepsilon_s(t_F))(1-d) + S.T} \qquad (4.1.2\text{-}21)$$

Note that $f_s^0(x,t)$ and $f_s^N(x,t)$ have only one common conversion point at $x = x_\alpha$. This is so because the resin last fed during the forward flow periods was assumed not to react while the solids transfer took place.

The residence time distribution of the solids can be used as an alternative approach to the conversion distribution model. This is shown in Appendix F.

4.2 Moments of the Distribution

In working with population balance-based models, it is frequently found that the resulting equations are too complex for efficient mathematical or computational treatment and solution. This is especially true when the expression for the density function is coupled with heat, mass or momentum equations through temperature, concentration, or velocity variables. It is also often the case that this type of system characterization contains more information than can be used, or is required in engineering applications. For instance, in crystallization studies, instead of knowing how the whole distribution of crystal sizes changes with time, knowledge of the time dependence of the total concentration of crystals together with the mean and variance of the size distribution would suffice for simulation purposes. Analogously, in the problem being considered in this work one would be content to know the average conversion of particles, its variance and the fraction of exhausted resin, (when applicable). Therefore, simplifications which can give information about the principal characteristics of the distributions can be used.

Working approximations of unimodal density functions, by the use of the leading moments, were introduced by Katz and collaborators in a series of papers (81,82,83). There, they applied the use of moments to the dynamic analysis of continuous crystallizers and polymerization reactors. Studies of the moments of residence time distributions in chemical reactors have been reported by Klinkenberg (59).

The method consists of expressing the system equations in terms of l moments of the density function being used. This reduces the model to a system of ordinary differential equations which can then be readily integrated simultaneously.

4.2.1 Use of the moments approach

From Equation (4.2)

$$\frac{\partial f_j(x,t)}{\partial t} = \frac{-1}{c} \frac{\partial}{\partial x} \left[f_j (x,t)\, r (x,C_j) \right] .$$

By definition, the l^{th} moment of a continuous distribution is

$$\mu_l = \int_{-\infty}^{\infty} x^l f(x,t)\, dx \qquad l = 0, 1, 2 \ldots.$$

Since resin conversion can only take values between zero and unity, in this problem, the moments for the j^{th} stage are

$$\mu_{l,j} = \int_0^1 x^l f(x,t)\, dx. \qquad \begin{matrix} l = 0,1,2 \ldots \\ j = 1,2, \ldots. s \end{matrix} \tag{4.2.1-1}$$

By differentiation

$$\frac{d\mu_{l,j}}{dt} = \frac{d}{dt} \int_0^1 x^l f_j(x,t)\, dx = \int_0^1 x^l \frac{\partial f_j}{\partial t}(x,t)$$

or

$$\frac{\partial \mu_{l,j}}{\partial t} = \frac{-1}{\bar{c}} \int_0^1 x^l \frac{\partial}{\partial x} \left[f_j(x,t)\ r\ (x,C_j) \right] dx$$

which can be integrated by parts to give

$$\frac{d\mu_{l,j}}{dt} = \frac{-1}{\bar{c}} \left[f_j(x,t)\ r\ (x,C_j)\ x^l \right]_0^1 + \frac{l}{\bar{c}} \int_0^1 x^{l-1} f_j(x,t)\ r\ (x,C_j)\, dx \tag{4.2.1-2}$$

For a unimodal distribution, it is required that:
(i) $f(0,t) = 0$; and (ii) $f(1,t) = 0$. The first condition is usually satisfied in the light of the discussion in section 4.1.2. The second condition requires that no solid reaches complete saturation in finite time, and depends on the kinetics of the reaction. If conditions (i) and (ii) are obeyed

$$\frac{d\mu_{l,j}}{dt} = \frac{l}{\bar{c}} \int_0^1 x^{l-1} f(x,t)\ r\ (x,t)\, dx \qquad l = 0,1,2 \ldots. \tag{4.2.1-3}$$

The rate of reaction term, $r(x,C_j)$, can in general be expressed as a polynomial in x and C_j so that the integrand of Equation (4.3.1-3) can be expanded and replaced by moments.

The resulting expression together with Equation (3.2.2-2) form the set of system equations which can be integrated simultaneously.

To illustrate the method, consider a first order rate expression:

$$r(x,C_j) = B(1-x) \qquad (4.2.1\text{-}4)$$

Here, B is, in general, a function of liquid concentration, i.e. $B = B(C_j)$. After substitution in (4.2.1-3), one obtains

$$\frac{d\mu_{l,j}}{dt} = -\frac{B}{\bar{c}}\, l \left[\int_0^1 x^{l-1}\, dx - \int_0^1 dx \right]$$

which, using Equation (4.2.1-1) becomes

$$\frac{d\mu_{l,i}}{dt} = -\frac{B}{\bar{c}}\, l \left[\mu_{l-1,j} - \mu_{l,j} \right] \qquad l = 1,2 \ldots$$

and with Equation (4-1) and Equation (3.2.2-6), i.e.,

$$\frac{dC_j}{dt} = \frac{1}{\tau_j}\,(C_{j-1} - C_j) - \frac{1-\varepsilon_j}{\varepsilon_j} \int_0^1 B(1-x)\, f(x,t)\, dx \qquad (4.2.1\text{-}5)$$

$$\frac{dx}{dt} = \frac{1}{\bar{c}}\, B(1-x)$$

form the system equations. This set of ordinary differential equations can be solved for any value of l which might be required. That is, the system can be closed off at any desired value of l.

For a second order reaction expression $r(x,C_j) = B(1-x)^2$ a similar procedure yields

$$\frac{d\mu_{l,j}}{dt} = \frac{lB}{\bar{c}}\,(\mu_{l-1,j} - 2\mu_{l,j} + \mu_{l+1,j}) \qquad l = 1,2 \ldots \qquad (4.2.1\text{-}6)$$

In this example the system equations can not be closed off at any desired value of l since the higher order moment μ_{l+1} is necessary to evaluate $d\mu_l/dt$. In such cases, a moment closing technique is required in order to solve the equations. Hulbert and Katz (81) have developed a method to deal with these situations. It consists of approximating the density function being used by an expansion in terms of Laguerre polynomials. These polynomials are orthogonal with respect to a gamma distribution weighting function. As usual in function approximations, they can be used to approximate the density function by an infinite series in terms of such polynomials. The coefficients in the series can be given in terms of the moments of the density function being used, and each coefficient requires only one moment of

next higher order than the previous coefficient. Thus, the series can be truncated at the desired accuracy, say, after the first ℓ terms and then the density function and all other moments can be expressed in terms of those ℓ moments. The case of first order kinetics is particularly interesting since as it is demonstrated in Appendix E, in that case only the mean solid conversion is needed for a complete description of the c.d.f.

Treatment of Solid Transfer

In section 3.2.2 the following expression was obtained for fractional transfer adjustment of the density function:

$$f'_j(x,0) = (1-d)\, f_j(x,t_F) + d\, f_{j+1}(x,t_F) \qquad (4.2.1\text{-}7)$$

By multiplying each term by x^{ℓ} and integrating with respect to x, one obtains

$$\int_0^1 x^{\ell} f'_j(x,0) = (1-d) \int_0^1 x^{\ell} f_j(x,t_F)\, dx + d \int_0^1 x^{\ell} f_{j+1}(x,t_F)\, dx$$

and by Equation (4.2.1-1)

$$\mu'_{\ell,j} = (1-d)\, \mu_{\ell,j} + d\mu_{\ell,j+1} \qquad \begin{matrix} j = 1, \ldots s-1 \\ \ell = 1,2, \ldots \end{matrix} \qquad (4.2.1\text{-}8)$$

thus, the moments of the density function at each stage can be easily adjusted after the solids fractional transfer.

Treatment of Solid Feed

The discrete mode is considered here; in it, it is assumed that the solids are added at the end of each time step. Thus, the moments of the density function need to be re-evaluated at each time step.

The density function at the beginning of the $(k+1)^{th}$ time step can be calculated by a simple weighted sum. This sum involves the distribution of the resin already in the stage and that of the resin fed during this time step.

Hence,

$$f_s(x,t_{k+1}) = \frac{V_s(1-\varepsilon_s) f_s(x,t_k) + S\,\Delta t\, f_F(x,t)}{V_s(1-\varepsilon_s) + S.\Delta t}$$

where $\Delta t = (t_{k+1} - t_k)$, ε_s is given by Equation (4.1.1-13) and $f_F(x,t)$ represents the density function of the solids feed.

Multiplying by x^{ℓ} and integrating as before,

$$\mu_{\ell,s}\ (t_{k+1}) = \frac{V_s(1-\varepsilon_s)}{V_s(1-\varepsilon_s) + S\Delta t}\ \mu_{\ell,s}(t_k) + \frac{S\Delta t}{V_s(1-\varepsilon_s) + S\Delta t}\ \mu_{\ell,F} \quad (4.2.1\text{-}9)$$

where $\mu_{\ell,F}$ is the ℓ^{th} moment of the feed density function.

4.2.2 Application to the Film Controlled Case

It was mentioned earlier, that a condition for the application of the moments approach is that the distribution function is unimodal. The expression of the rate of reaction for this case is $r(x,C_j) = k_L a C_j$, which is zero order in solid composition. Therefore, solid can reach complete conversion in a finite time. In this situation, the moments method can only be used if it is assumed that $f(0,t) = f(1,t) = 0$.

Hence,

$$\frac{d\mu_{\ell,j}}{dt} = \frac{k_L a C_j}{\bar{c}}\ k\mu_{\ell-1,j} \qquad \begin{matrix} \ell = 1,2, \ldots \ ; \\ j = 1,2, \ldots s \end{matrix}$$

which with (4.2.2-1)

$$\frac{dC_j}{dt} = \frac{1}{\tau_j}(C_{j-1} - C_j) - \frac{1-\varepsilon_j}{\varepsilon_j} k_L a C_j$$

form the system of equations to be integrated.

It should be stressed that equations (4.2.2-1) can only be used to simulate the contactor when resin exhaustion is negligible, and the above assumption can be considered valid.

It is therefore, possible to apply this method to cases in which relatively low liquid feed concentration is used, and very little resin saturation occurs.

In solving this problem, the Equations (4.2.2-1) can be integrated simultaneously for all stages. This requires the solution of a $(s + \ell.s)$ system of ordinary differential equations. A numerical technique such as Runge-Kutta can be easily applied here. At each time step, the moments for the top stage and its voidage are updated according to Equations (4.2.1-9) and (4.1.1-13). At the end of the cycle, fractional transfer is dealt with by Equation (4.2.1-8).

4.3 Finding the Pseudo-Steady State

It has been mentioned that pseudo-steady state conditions can be obtained by two methods: (i) relaxation or direct simulation method and (ii) boundary condition iteration method.

In the first method, the system equations are integrated forward in time from a set of initial conditions at $t = 0$. Thus, the end state, that is, the value of the state variables at $t = t_F$, $\underline{x}(t_F)$ is evaluated. After performing the state transformations as indicated by Eq(3.1.1-4) a new state $\underline{x}(0)$ is obtained. This is then used as the initial condition in the next iteration. The procedure is then repeated until the pseudo-steady condition stated by Eq(3.1.1-2) is observed.

In the second method an updating technique is used to obtain a better estimate of the initial conditions for next iteration. This updating technique is basically of the Newton-Raphson type and is based on the boundary condition stated by Eq(3.1.1-4). This expression tells how the initial state depends on the conditions at the end of the cycle. By denoting the initial guess of the end state by $\underline{x}^k(t_F)$ the initial condition is then

$$x_i^k(0) = g_i(x_1^k(t_F), x_2^k(t_F), \ldots, x_m^k(t_F)) \qquad i = 1,2 \ldots m \qquad (4.3\text{-}1)$$

Integration of the system equations (3.1.1-1) with these initial conditions gives a new end state $\underline{x}^{k+1}(t_F)$. From the last expression it is clear that for a small variation of this new end state one obtains after neglecting second and higher order terms

$$\Delta x_i^k(0) = \frac{\partial g_1}{\partial x_1(t_F)} \Delta x_1^k(t_F) + \frac{\partial g_1}{\partial x_2(t_F)} \Delta x_2(t_F) + \frac{\partial g_1}{\partial x_m(t_F)} \Delta x_m^k(t_F)$$

$$i = 1,2 \ldots m$$

or in vector notation

$$\underline{\Delta x}^k(0) = \frac{\partial \underline{g}}{\partial \underline{x}(t_F)} \underline{\Delta x}^k(t_F) \qquad (4.3\text{-}2)$$

where $\underline{\Delta x}$ is a column vector and $\partial \underline{g}/\partial \underline{x}(t_F)$ a square matrix.

The effect that a variation of the initial state $\underline{\Delta x}^k(0)$ has on the updating term $\underline{\Delta x}^{k+1}(t_F)$ of the next cycle, can be found from the theory of differential equations (84) or from calculus of variations (54) by linearising Eq.(3.1.1-1). The relation obtained is of the form:

$$\underline{\Delta x}^{k+1}(t_F) = \underline{\Lambda}^{-1}(t_F)\ \underline{\Lambda}(0)\ \underline{\Delta x}^k(0) \qquad (4.3\text{-}3)$$

Here $\underline{\Lambda}(t)$ represents the set of adjoint variables and is an m-dimensional square matrix which satisfies

$$\frac{d\underline{\Lambda}}{dt} = -\underline{\Lambda}(t)\ \frac{\partial \underline{f}}{\partial \underline{x}} \qquad (4.3\text{-}4)$$

and $\partial \underline{f}/\partial \underline{x}$ is the Jacobian matrix of the system of equations (3.1.1-1).

From Equations (4.3-2) and (4.3-3) one obtains

$$\underline{\Delta x}^{k+1}(t_F) = \underline{\Lambda}^{-1}(t_F)\ \underline{\Lambda}(0)\ \frac{\partial \underline{g}}{\partial \underline{x}(t_F)}\ \underline{\Delta x}^k(t_F) \qquad (4.3\text{-}5)$$

The difference between two consecutive end states can be defined as

$$d_i' = x_i^{k+1}(t_F) - x_i^k(t_F) \qquad i = 1,2 \ldots m \qquad (4.3\text{-}6)$$

Now, for pseudo-steady state it is required that

$$x_i^{k+1}(t_F) + \Delta x_i^{k+1}(t_F) - (x_i^k(t_F) + \Delta x_i^k(t_F)) = 0 \quad i = 1,2 \ldots m \qquad (4.3\text{-}7)$$

Therefore, $\underline{\Delta x}^k(t_F)$ is chosen so that (4.3-7) is satisfied. From Equations (4.3-7) and (4.3-6) it follows that

$$\underline{\Delta x}^{k+1}(t_F) = \underline{\Delta x}^k(t_F) - \underline{d}' \quad .$$

Substituting in Eq.(4.3-5) and rearranging an expression for the updating term $\underline{\Delta x}^k(t_F)$ is obtained i.e.

$$\underline{\Delta x}^k(t_F) = -\left(\underline{\Lambda}(0)\frac{\partial \underline{g}}{\partial \underline{x}(t_F)} - \underline{\Lambda}(t_F)\right)^{-1} \underline{\Lambda}(t_F)\ d' \qquad (4.3\text{-}8)$$

The new end state calculated using the updating term $\underline{\Delta}^k\underline{x}(t_F)$, that is $\underline{x}^k(t_F) + \underline{\Delta}^k x(t_F)$, is not the exact pseudo-steady state value

of the end state since second order terms have been neglected. Therefore, if the initially guessed state was sufficiently close to the exact p.s.s. to justify the linear approximation used in Eq.(4.3-2), the updated end state is closer to the exact p.s.s. The whole procedure is then as follows.

From a starting point $\underline{x}^k(t_F)$, which as discussed above, needs to be not too far from the exact p.s.s. to ensure convergence, the initial state $\underline{x}^k(0)$ is calculated using Eq.(4.3-1). Then, the system equations (3.1.1-1) are integrated between $t = 0$ and $t = t_F$. During this step the Jacobian matrix $\partial \underline{f}/\partial \underline{x}$ is evaluated as a function of time. Hence, the adjoint system Equations (4.3-4) can be integrated and the result used to calculate the updating term Eq.(4.3-8). The procedure is then repeated until no further improvement is found.

In the direct simulation method, the attainment of p.s.s. is slow but ensured (provided it exists). In the case of the Newton-Raphson scheme, the convergence to p.s.s. is much faster, however a good initial guess of the end state is necessary to ensure convergence. Therefore, a combination of both methods is generally used. In this procedure, the relaxation method is used to provide the initial guess $\underline{x}^k(t_F)$ for the boundary iteration method.

4.4 Evaluation of the average exit composition

When pseudo-steady state conditions are attained, it is useful to evaluate the average exit liquid concentration for each stage over the cycle. The average composition of the exit stream from the top stage can then be used as a performance criterion for the system. The average composition is defined as

$$\bar{C}_j = \frac{1}{t_F} \int_0^{t_F} C_j(t)\, dt \qquad (4.4\text{-}1)$$

Since the method of characteristics evaluates the liquid concentration C_k at t_k, using variable time steps (section 4.1.1), a standard Simpson rule can not be applied to integrate Eq.(4.4-1). In this work, advantage was taken of a quadratic interpolation routine which upon each call returned the values of the coefficients of the parabola segment determined by the three coordinates (t_k, C_k) under consideration. The area under the segment was easily calculated analytically and the value of the integral in Eq. (4.4-1) was therefore the sum of the areas of all segments.

CHAPTER 5

EXPERIMENTAL

5.1 Experimental Criteria and Description of the Design of Experiments

The objective of the experimental work was to study the behaviour of the contactor over a range of operating conditions and its response to variations in either input or control variables, so that comparison with theoretical predictions could be made. Hence, an experimental plan was devised considering the following aspects and limitations in the operation of the pilot plant.

The contactor can be represented by a set of input, output and control variables. For given solid and liquid residence times, the control variables are: voidage ε, total cycle time T, and fractional transfer d. The inputs to the system are, liquid flow rate, resin flow rate, liquid feed concentration and initial resin distribution function. The output variables are the exit liquid concentration and exit resin distribution function. The controls are all interrelated by a solids mass balance Equation (3.2.1-3b). This relation indicates that for any given modification of the controls, at least two of them must be varied at the same time to achieve a pseudo-steady-state. It also suggests three patterns of variation by keeping one of the control parameters constant and modifying the other two. These patterns are:

a) constant voidage, varying fractional transfer and cycle time;

b) constant fractional transfer, varying cycle time and voidage;

c) constant cycle time, varying voidage and fractional transfer.

From a theoretical point of view case (a) is the most interesting. From Equation (3.2.1-3b), it can be seen that for constant ε, V and S,

$$\frac{T}{d} = \frac{(1-\varepsilon)V}{S} = \text{constant}$$

therefore, liquid and solid residence times remain constant since by definition

$$\tau_L = \frac{\text{liquid hold up}}{\text{liquid feed rate}} = \frac{s\varepsilon V}{L} .$$

Analogously,

$$\tau_S = \frac{s(1-\varepsilon)V}{S}$$

For the limit of very small d and T, the column can be considered a steady-state continuously operated system without interruption of liquid flow or resin overflow. Thus, by increasing the fractional transfer while keeping both residence times constant, the effect of cycling can be examined.

In addition, from the experimental point of view, pattern (a) offered several advantages in its implementation.

It proved to be very difficult to preset accurately either ε or d to any particular value. Their actual values could only be checked after the run had finished and the pseudo-steady state hold ups of resin were measured. These resin hold ups were dependent upon the particular set of operating conditions used and were very difficult to predict. Thus, an experimental plan which did not involve the precise preselection of either ε or d was preferred. Pattern (a) was the most simple and reliable to implement.

By maintaining the inputs to the system constant, it was expected to keep ε constant. Then, a series of runs were carried out varying T (accurately) and adjusting d during the initial part of the run. This adjustment consisted of matching the amount of resin fed during a cycle with that transferred at the end of it. (See section 5.2.3) Results from preliminary experiments showed that, for stable or well behaved runs, the voidage can be kept reasonably constant over a range of fractional transfer values. See, for example, runs 6, 7 and 8 in Table 1 of Appendix C.1.

The ranges of operation for inputs and control variables were selected considering a number of requirements and limitations. Liquid flow rates were chosen to produce a good degree of fluidization (good mixing) without carrying resin over. Resin flow rates were selected to give flexibility to operate either long or short cycles. Cycle duration and fractional transfers are closely interrelated and have their ranges restricted by either one or the other. Bearing in mind that, in the modelling, it was assumed that the transfer of solids was

instantaneous, short cycles which imply low fractional transfers are limited. The limit was considered to be the point where the time required for reversing of flow and repositioning of the magnetic float, became significant when compared with the forward flow time. On the other side of the scale, long cycles and high fractional transfers were restricted to the point where the resin being transferred from stage j to stage j-1 started to by-pass to stage j-2. Therefore, the cycle time range was set to be from 20 to 40 or 45 seconds for the forward flow operation which corresponded to fractional transfers from about 0.4 to 0.9.

Considering all that has been said the following experimental approach was adopted:

Having chosen a set of inputs, runs were carried out varying the cycle time throughout the selected range, and adjusting the fractional transfer as required, keeping liquid and solid residence times constant. This involved runs with forward flow periods from 20 to 40 or 45 seconds. To have an appreciable change in the value of the fractional transfer, the forward flow period was varied by five seconds between runs. Since it was desired to operate at different resin conversions, these sets of runs were repeated using different liquid feed concentrations. This also enabled operation either under conditions where the rate of ion exchange was film diffusion controlled (low liquid concentrations) or intraparticle diffusion controlled (high liquid concentrations).

Note that in the case of the second set of runs in Table (6.1.1-2), the experiments did not follow this pattern since other objectives were pursued there (section 6.1.1).

5.2 Apparatus and Experimental Technique

5.2.1 The Pilot Plant and its Operation

The experimental work was carried out in an existing vertical version of the Cloete-Streat contactor. A diagram of the experimental set up is given in Figure (5.2-1).

The contactor itself (1), was built of standard Q.V.F. glassware. It consisted of a series of vertically arranged stages separated by

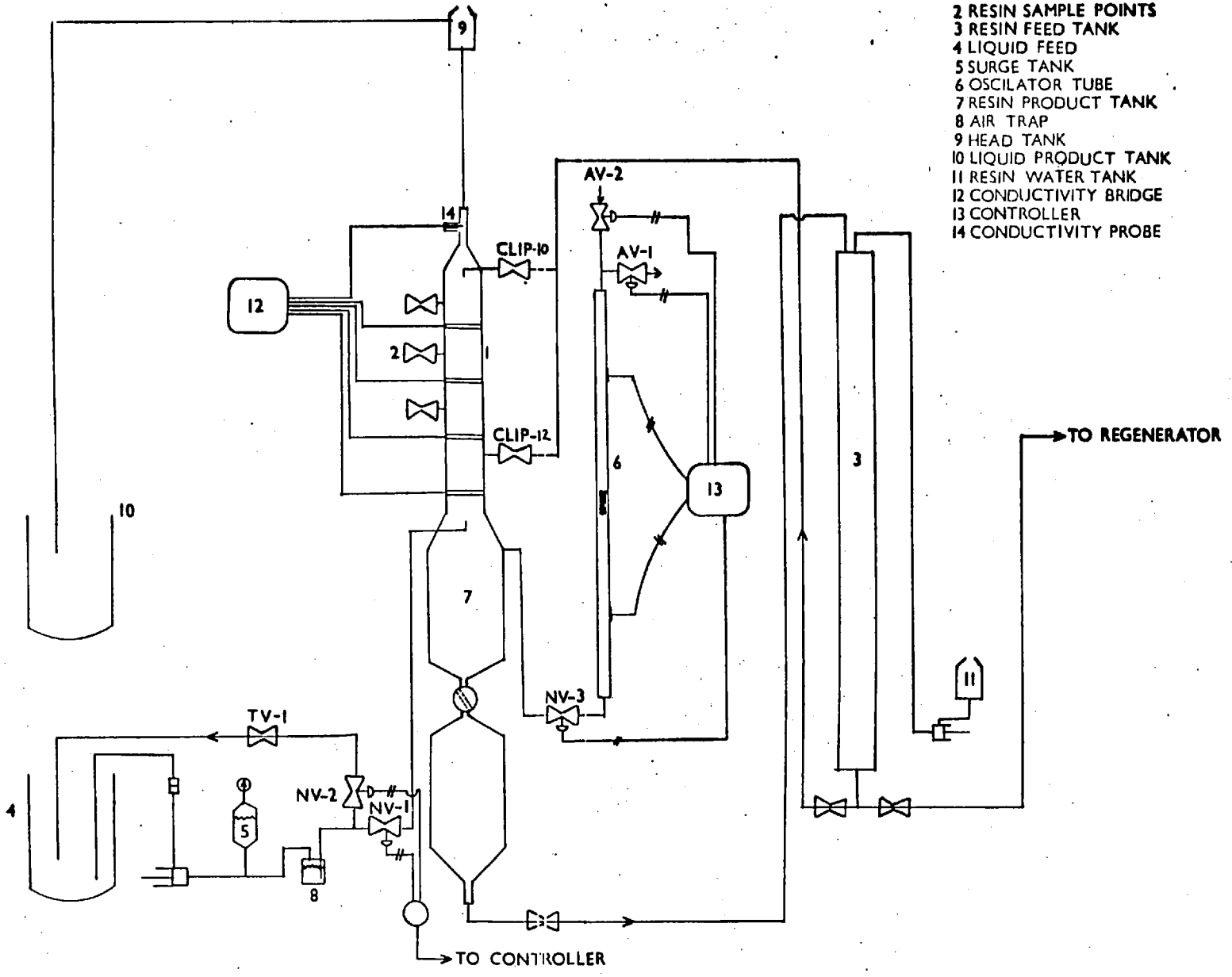

FIGURE 5.2-1 SCHEMATIC DIAGRAM OF THE EXPERIMENTAL SET-UP

specially designed perspex trays. Each stage was a pipe section 5 inches long and 3 inches diameter. The separating tray was made of three plates as shown in Figure (5.2-2). The top plate which acted as a distributor had twelve 3/16 inch holes on a square pitch giving 4.7 per cent free area. The bottom plate contained five 3/16 inch holes which, when all plates were assembled, lay opposite the centre of the square pitch arrangement of the top plate holes. The middle plate acted merely as a spacer to allow the flow of resin between the off-set holes of the top and bottom plates. Its thickness, and the distance between the off-set holes gave an angle of repose of 12.8^{o}. This was such that, under zero liquid flow, the resin could settle down on the top plate without draining downwards. A sample point (2) from which resin could be extracted for analysis was located in the middle of each stage. All stages and trays were assembled by push-fitting them together.

A calibrated 5 inch diameter glass column (3) was used for the resin feed tank. All other parts of the rig were also made of either single or assembled pieces of standard Q.V.F. glassware. Liquid and resin lines were $\frac{1}{2}$ inch polythene tube and screw clips were used to close or open them. Liquid feed and product tanks were 25 or 40 gallon drums lined with polythene. All other containers (head tank, resin feed water tank) were 10 litre polythene bottles.

Liquid feed flow was achieved by a battery of eight positive displacement D.C.L. pumps in parallel. A surge tank (5) was located in the common exit line to dampen pressure fluctuations.

The resin feed was added continuously into the top stage by dense phase flow (74). Water was pumped to the top of resin tank by means of two D.C.L. pumps in parallel. This forced a mixture of resin and water at the bottom. Of this mixture, at least 60 percent was solid material. The resin flow rate was thus controlled by the rate at which water was pumped into the resin tank.

The movement of a magnetic float between reed switches in a vertical tube was used to control the periodic transfer of solids (6). On a signal from a timing device, the liquid feed was diverted by closing valve NV-1 and opening valve NV-3,thus, connecting the oscillator with the column. At the same time, the air vent valve AV-1 was also opened.

FIGURE 5.2-2 PLAN OF PERFORATED PLATES

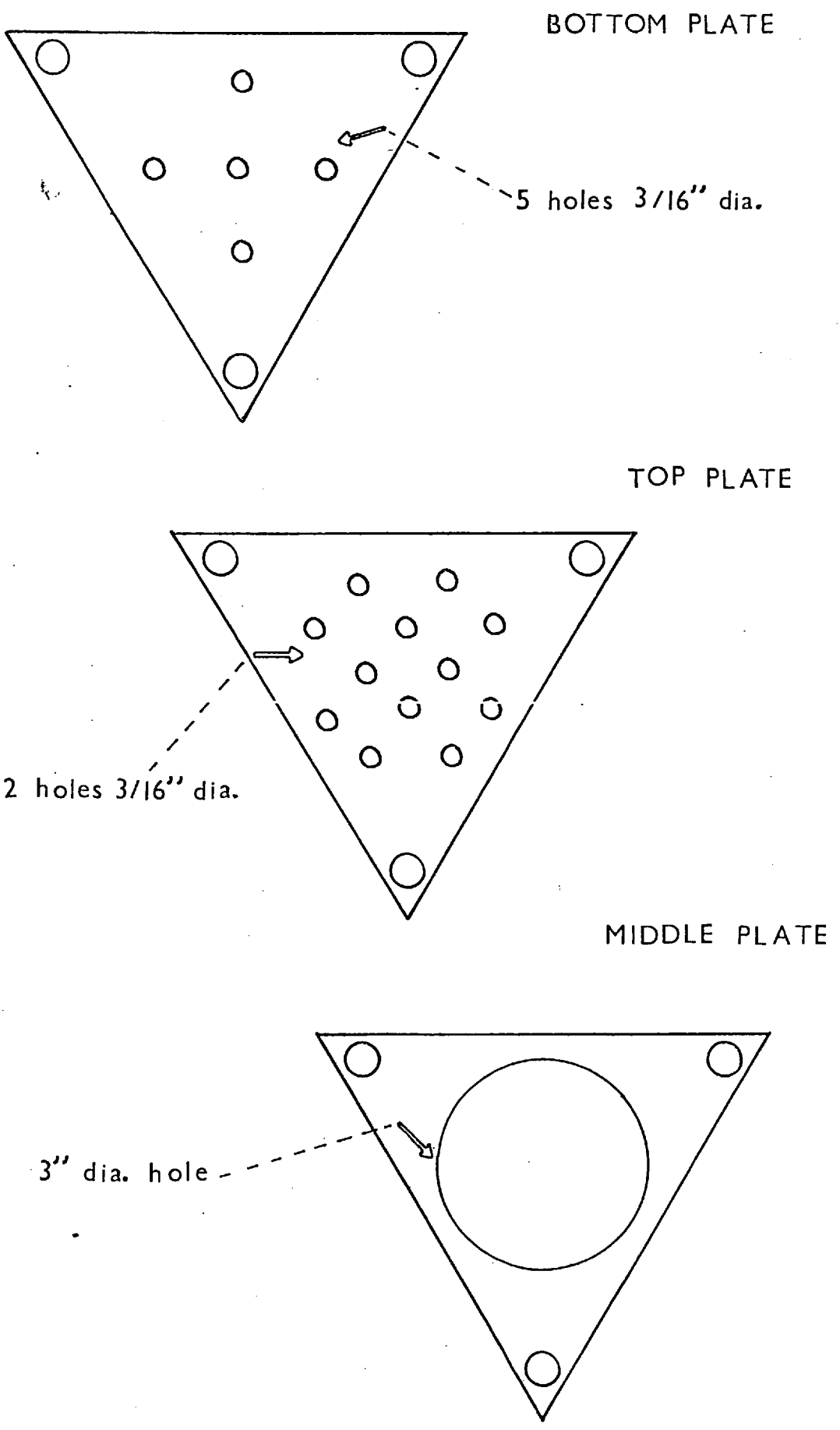

This permitted the head of liquid in the contactor to push the resin downwards between adjacent stages, whilst the float moved upwards in the oscillator tube, carried by the solution from the solids collecting tank (7). When the float reached the upper reed switch a system of relays operated to close the air valve AV-1 and open the compressed air valve AV-2. This forced the float down to the lower reed switch which actuated the system of relays to close off the compressed air, shut valve NV-3 and open NV-1 to resume liquid flow. This sequence was repeated for each cycle to transfer equal volumes of resin. The volume actually transferred and hence the fractional transfer was varied by modifying the separation of the reed switches, thus altering the amplitude of the transfer period.

As mentioned, during the reversal of flow, the liquid feed to the contactor was diverted through a recycle line back to the feed tank, by closing valve NV-1 and opening NV-2. To avoid pressure changes between forward and reversal periods, a throttle valve TV-1, was used to equilibrate the pressure drop across the contactor and the recycle line.

The system was automatically controlled by a timer, a complex system of relays and the magnetic float oscillator which operated a series of pneumatically actuated diaphragm valves.

5.2.2 Modifications Installed

Controlling System

At the beginning of the experimental work it was found that the existing timing device and ancillary circuitry were not working properly, and it was decided to replace it. A new system was then designed and installed.

The main part of the controlling system consisted of an all-purpose Crouset electric clock type 207 and a system of relays together with the magnetic float oscillator. A schematic diagram of the electric circuit is shown in Figure (5.2-3). This system was geared to another set of relays which permitted manual or automatic control over all pumps and air valves.

FIGURE 5.2-3 SCHEMATIC DIAGRAM OF OSCILLATOR AND TIMING CIRCUIT

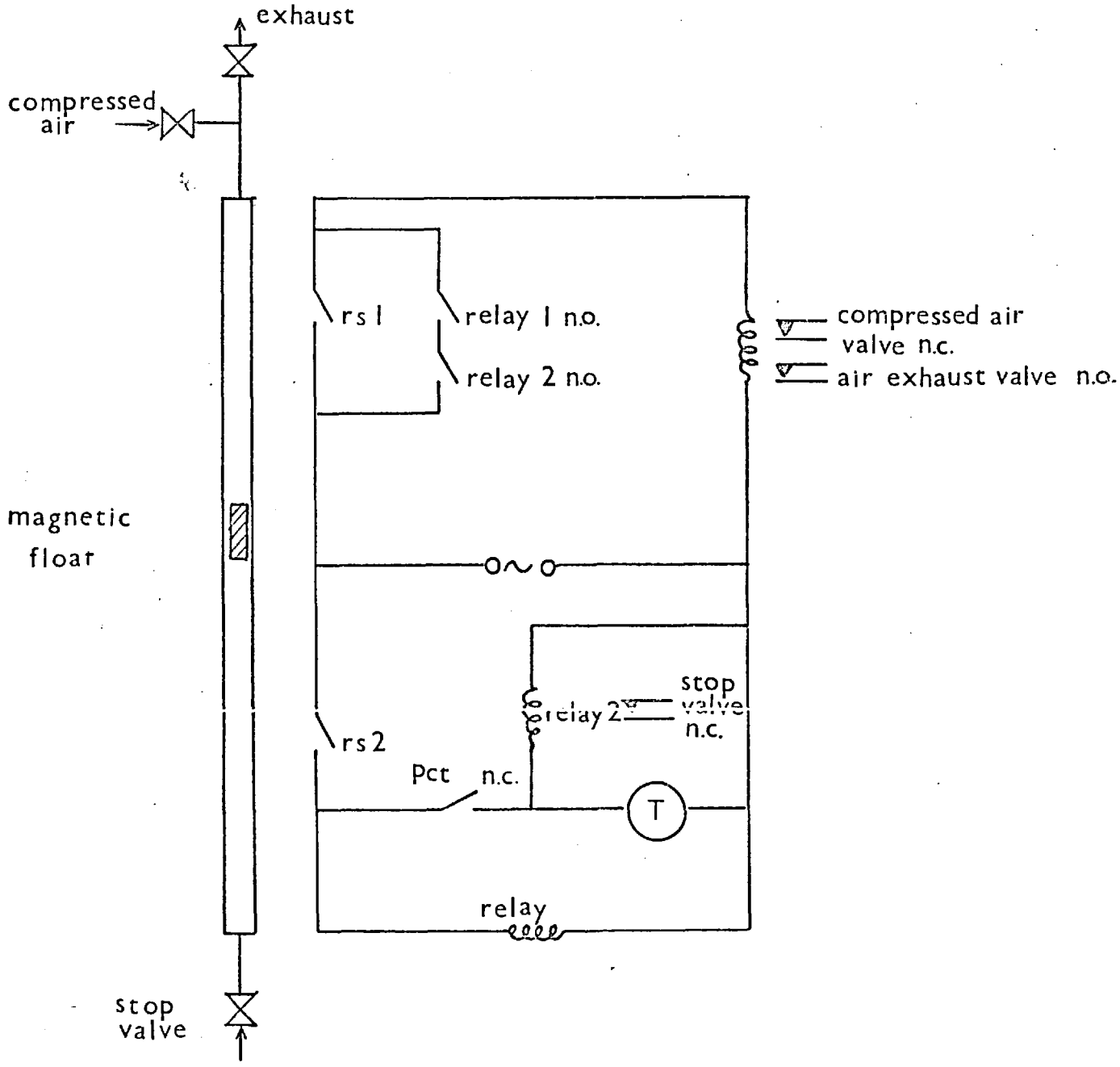

n.o. normally open
n.c. normally closed
rs reed switch
pct passing contact (timer)
T electric clock

Conductivity Probes

In order to be able to examine the dynamic behaviour of the plant during a cycle, it was necessary to measure the concentration changes taking place during the cycle.

Continuous or intermittent sampling of resin was impossible due to the fact that given the typical resin hold ups, drawing an amount of resin sufficient for analysis would affect the behaviour of the system. Therefore, only continuous liquid concentration monitoring was considered.

Conductivity probes were installed in the trays between the stages and at the inlet and outlet of the contactor. For the inter-stage probes, advantage was taken of the separation of top and bottom plates to form a small conductivity cell. Electrodes were embedded in each plate and wired to the outside through a hole drilled horizontally in the plate, see Figure (5.2-4). Although this arrangement of electrodes had the drawback that resin beads could occasionally pass through and affect the reading, it was, in fact, the best point to measure an average liquid composition from the stage, because the small space between the plates acted as a minute mixing tank. Furthermore, by embedding the electrodes in the plates, no hindrance to the flow of the phases was introduced. For the inlet and outlet streams, standard needle conductivity probes were used.

It was later found that small bubbles of air could be trapped between the tray plates and, if near the conductivity cell, could alter its reading. Although during reversal of flow the resin would displace the bubbles, it was decided to install an air trap in the liquid feed line (8) to stop the bubbles reaching the contactor.

5.2.3 Description of a Run

Before carrying out a run, a fair amount of preparation was required. First of all, the loaded resin from the previous run needed to be regenerated to its hydrogen form. Since the regeneration reaction is a much slower process, a long contact time was necessary. Hence, a twelve stage horizontal version of the Cloete-Streat contactor (50) was used. Resin was passed through the contactor at a slow flow rate,

FIGURE 5.2-4 PLAN OF PERFORATED PLATES WITH CONDUCTIVITY PROBES

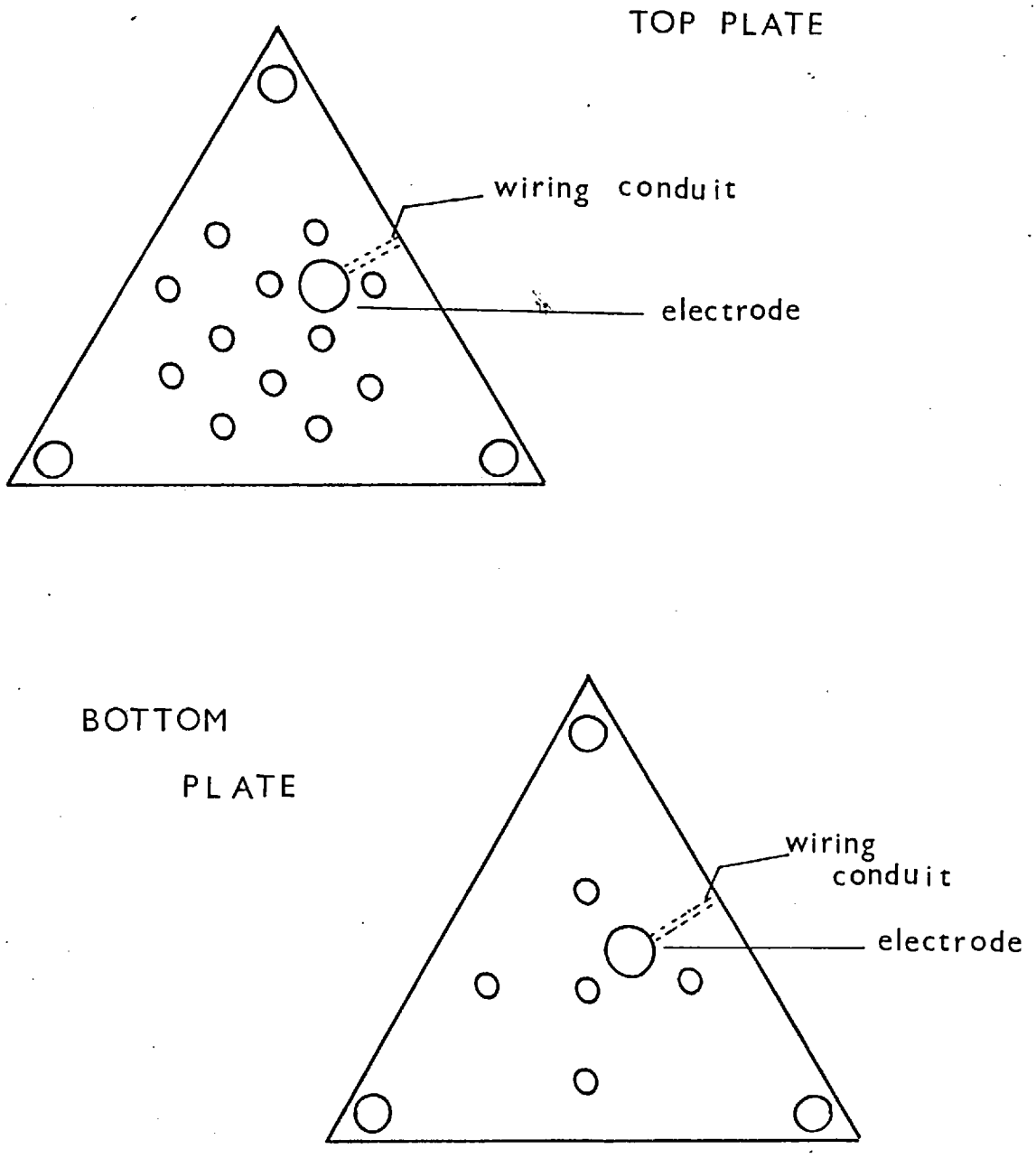

countercurrent to a flow of about 0.12 N nitric acid. Flow rates and other parameters were heuristically selected to give a maximum of resin regeneration after one pass.

From the regenerator, the resin was transferred to the resin tank where it was fluidized with distilled water to remove all traces of acid. Samples of the washing solution were taken from time to time, and the washing continued until a simple (methyl orange) test indicated no acid in the solution. The contactor and feed lines were emptied and washed out with distilled water. For runs in which it was desired to start up with partially filled stages, resin was pumped by dense flow to the bottom stage (closing clip 10 and opening clip 12) and carried upwards to the other stages by fluidizing it up with distilled water through the liquid feed line. Given a flow rate of the fluidizing water, any resin present in excess of a certain amount was carried over to the next stage if sufficient time was allowed for fluidization. Hence, to obtain equal resin hold ups in all stages fluidization was continued for a while after the resin feed was stopped. It was important to have fed the correct amount of resin otherwise too little or too much resin resulted in the top stages.

A volume of the liquid feed solution (usually 200 litres), at the required concentration, was prepared in the feed tank ensuring that it was well mixed. Feed and recycle lines, as well as the surge tank and the air trap were flushed out with the feed solution. The liquid flow rate was adjusted by selecting an appropriate number and the position of the micrometers of the D.C.L. pumps. Similarly, for the resin flow rate, the corresponding D.C.L. pumps were adjusted. To allow the resin to flow into the top stage, clip 12 was closed and clip 10 opened.

The timer was set to the desired forward flow time and the separation of the reed switches was adjusted to give the required volume of transfer. The latter was only an approximation, since the exact position of the reed switches was to be found during the initial part of the run.

A number of initial readings were taken prior to starting the actual run. The capacity of the regenerated resin was measured from

samples taken from the resin feed tank at different heights (see section 5.3.1). The liquid feed and product drum as well as the resin feed water tank were weighed. The resin in the calibrated feed tank was fluidized and its freely settled height taken. Similarly, the resin in the trays was also fluidized and its freely settled height noted. With this, the initial amount of resin in the feed tank and the column resin hold ups were evaluated.

The run was then started. The control system was switched on, the conductivity chart recorder and a stop clock started. For the first cycles, care was taken to ensure that the resin feed rate and the fractional transfer matched exactly. This was done by observing the fluidized height of resin in the top stage just before the reversal of flow. A change of this level gave an indication of whether too little or too much resin was being transferred per cycle. If required, the separation of the reed switches was varied. A confirmation that the matching was correct was obtained from the conductivity reading for the top stage, since for pseudo-steady state operation, it was required that no build up or depletion of resin occurred in the column. The fluidized levels of resin in the other stages were also noted at regular intervals to check constancy. Since only one conductivity reading could be taken at a time, a switch was used to select signal from the desired probe to the conductivity bridge.

Once pseudo-steady state was achieved (constancy in the liquid concentration profiles), readings of conductivities and fluidized heights for all stages were taken. For about five cycles, the effluent from the contactor was diverted to another container. A sample of this liquid, was later titrated to evaluate the average liquid concentration of the effluent stream over a cycle. Towards the end of the run, resin samples were taken from each stage as near as possible to the end of the forward flow period. Care was taken not to withdraw too much resin from the stages, since it would affect the stability of the pseudo-steady state. The run was then stopped by switching off the contactor. The resin in the feed tank and in the contactor was fluidized with distilled water and their settled heights noted. All relevant drums and tanks were weighed again.

In Appendix B.I a typical set of the data obtained and calculations performed for each run are shown.

In some runs, the attaining of the p.s.s. was particularly long or difficult. In those cases, use of the average values of the fractional transfer and solid and liquid flow rates obtained by considering the entire run, would lead to inaccuracies, since the actual values could have varied significantly throughout the run. Therefore, to obtain true p.s.s. values, the run was stopped once p.s.s. was achieved. The resin in the stages was immediately fluidized with distilled water to prevent the reaction from continuing. Then initial readings were again taken and the run reinitiated. No adjustment of the fractional transfer was required and after a few cycles pseudo-steady state was reestablished. From then on the run was treated as described in the previous paragraph.

5.2.4 Grading of Resin and Related Properties

An important parameter in the expression of the rate of reaction in the case of film controlled mechanism, is the surface area per unit volume of resin. Similarly, the porosity or voidage of the settled bed ε_B, and its density ρ_B, that is, the weight of a unit volume of freely settled bed, were required in the calculations. To evaluate these quantities, ten random samples were taken from the total volume of resin and mixed together. From this, two 5 mls. samples were drawn to evaluate ε_B and ρ_B. The rest of the resin was allowed to dry in air until constant weight was achieved.

Evaluation of the resin average size

A portion of the dried resin (approximately 30 gm) was sieved using B.S. mesh sizes 14-36. Bigger and smaller sizes had previously been excluded when the batch of new resin was wet screened before loading it into the system. The mean diameter $\bar{d}_i$ for each range of sieve sizes and the amounts of resin that resulted in each tray were noted.

The average diameter of the beads was calculated using the standard formula

$$\frac{1}{\hat{d}_p} = \sum_{i=1}^{m} \frac{x_i}{\bar{d}_i} \qquad (5.2.4\text{-}1)$$

which gives the surface mean diameter (or Sauter mean). Here, x_i is the weight fraction, m the number of fractions and $\bar{d}_i$ is the average diameter for the fraction (average of mesh opening).

Hence, the surface area per unit volume is simply given by the ratio:

$$a = \frac{\pi \hat{d}_p^{\,2}}{\pi/6\, \hat{d}_p^{\,3}} = \frac{6}{\hat{d}_p} \qquad (5.2.4\text{-}2)$$

Settled bed porosity and density

To evaluate the bed porosity, the freely settled volume or total volume v_T, and the absolute volume of beads v_B were required. The former was found by weighing the equivalent volume of water. The absolute volume, was evaluated with the aid of a specific gravity bottle. The porosity was then calculated from its definition

$$\varepsilon_B = 1 - \frac{v_B}{v_T} \qquad (5.2.4\text{-}3)$$

The amount of resin per unit volume of freely settled bed ε_B, was found by weighing a small amount of resin w_s, which had been previously dried of interstitial water in a Buchner funnel. This resin was then freely settled in a small measuring cylinder and its volume noted. Hence,

$$\rho_B = \frac{w_s}{v_T} \qquad (5.2.4\text{-}4)$$

Actual calculations of these quantities are given in Appendix B.2.

5.3 Methods of Analysis

5.3.1 Treatment of Resin

An important quantity in the study of the performance of the plant is the capacity of the resin. Since all measuremtns referred to the solids were in volumetric units (flow rate, hold ups) the capacity needed to be given in terms of k-eq/m^3 of freely settled resin. However, measurements of small volumes of freely settled resin in a measuring cylinder, are not very accurate. Hence, it was decided to evaluate the capacity in the terms of k-eq/kg of wet resin, and then use the density of the freely settled bed to convert it into volumetric units.

Since for each experimental run up to 25 resin capacity determinations were to be carried out, it was most convenient to choose a simple, quick and reliable analytical method. A volumetric method was chosen for these reasons and consisted of the following procedure.

Resin samples were first throughly washed to remove sorbed ions, and dried of superficial water in a Buchner funnel. A small amount was carefully weighed and then passed to a conical flask. An excess amount of NaCl and 100 mls. of distilled water were added. The following reaction took place:

$$R^{-}H^{+} + Na^{+}Cl \rightarrow R^{-}Na^{+} + H^{+}Cl^{-}$$

A magnetic stirrer was used to mix the NaCl solution. A 0.1 N standard solution of NaOH was used with phenol-phtalein indicator to titrate the free H^{+} ions as Na^{+} was taken up by the solid. The end point of the titration reaction indicated total saturation of the resin. The capacity of the resin was easily calculated from the total volume of NaOH used, since this was equivalent to the amount of Na^{+} taken up by the resin.

It was mentioned that due to the fact that the resin hold ups in stages were usually small (80-100 mls.), resin samples needed to be small in order to minimize the effect of sampling in the behaviour and stability of the contactor. Resin samples from operating stages were of about 5 mls. For evaluating regenerated resin capacities, the

samples were of the same size so the magnitude of the experimental error could be kept constant. Initial tests showed that in titrating amounts of resin less than 0.4 g, too much variability was introduced. This was expected since for small samples the experimental error became significant. Hence, each sample was divided in 5 or 6 sub samples and about 0.7 g of each, was weighed in an analytical balance. The average of the 5 or 6 results gave the value of the resin capacity in the particular point sampled.

An average value for the capacity was all that was needed to examine the performance of the system. However, in the mathematical model set up, a distribution of resin loading or conversion was used. This distribution refers to fractions of resin with capacities in the range from C_{ap}^{o} (fresh resin) to 0.0 (exhausted resin).

An interesting point here, was to try to experimentally determine, if not the form of the distributions, at least evaluate its first and second moments.

Evaluation of the average conversion per bead, even considering that the beads have a certain size distribution is a relatively easy task. All it required, was to evaluate the average number of particles in the 0.7 g samples using the average bead size by accurately weighing a known (200-300) number of beads. Several random 0.7 gm. samples would have given a very good estimate of the population mean. If one denotes $\hat{x}_p$ as the estimate of the population mean conversion given by

$$\hat{x}_p = \frac{\bar{x}}{\bar{L}}$$

where $\bar{x}$ is the average conversion per unit of weight and $\bar{L}$ is the average number of particles per unit weight, then

$$\hat{x}_p = \frac{\Sigma^{L} x_i}{\frac{\Sigma^{M} \ell_j}{M}}$$

Here, L is a random variable denoting the number of beads per unit weight and M the number of unit weight samples, and ℓ_j the number of beads in the j^{th} sample.

It is easy to show that this intuitive estimate $\hat{x}_p$, is in fact an unbiased estimate of the population mean.

By taking the expectation of the right hand side of the last equation

$$E\left(\frac{\frac{\Sigma^{L} x_i}{\Sigma^{M} \ell_j}}{M}\right) = \frac{E\{x_i\}.E\{L\}}{E\{L\}} + O\left(\frac{1}{L}\right) = \frac{E\{x_i\}}{\alpha_c}$$

The correction term α_c is introduced to compensate for the higher order terms $O(\frac{1}{L})$. This correction factor is usually of the form

$$\alpha_c = 1 \pm \frac{1}{L}$$

Since L here is very large α=1 and the estimate $\hat{x}_p$ is in fact an unbiased estimate of the population mean.

Estimation of the population variance was a much more difficult problem. Firstly, since measurements of the composition of individual beads were not possible, the variance had to be estimated from samples of L' beads which gave the average value of the loading, or capacity for that number of beads x_M.

Theoretically the population variance σ_p^2 can be estimated from the variance of the means x_M by

$$s_p^2 = L' s_M^2$$

where s_p^2 and s_M^2 are the variances of the population (estimated) and the means x_M, respectively.

Forgetting for the moment the problem that L' can vary among the samples, a good estimate of s_p^2 requires a good estimate of s_M^2. If one wants to have, say, a 90 percent confidence of evaluating s_M^2 with a precision of 80 percent that is, if it is required that with a 90 percent confidence

$$\ell(I) = \frac{s_M^2}{\chi^2_{\alpha/2}} - \frac{s_M^2}{\chi^2_{1-\alpha/2}} < .2\ \sigma_M$$

where $\ell(I)$ is the length of the confidence interval. It is found in tables of the χ^2/df distribution that more than one hundred samples x_M are needed. Remembering that the sample sizes are limited to a few millilitres and that in each estimation of x_M, samples of at least 0.5 g were needed, it was not possible to estimate the variance of population by the collective analysis of resin beds. The problem was further complicated by variable number of beads and size distribution.

5.3.2 Liquid Analysis

As mentioned in section (5.2.2), the objective of continously measuring the liquid concentration, was to observe the dynamic behaviour of the plant during a cycle.

Apart from the obvious reasons of facility and quickness, the conductivity method was chosen for two important reasons. It did not require sampling from the intermediate stages of the column which could have affected the flow pattern and the stability of the pseudo steady state operation. Secondly, it provided an immediate way of checking the attainment of the pseudo-steady state. This was balanced on the other hand, by the problems of temperature changes which, if large, affect the conductivity readings significantly. However, since the main interest was to observe the concentration changes during the cycle rather than the precise measurement of the liquid concentration, this last point was not a serious obstacle, provided the room and liquid feed temperatures were kept reasonably constant.

A highly accurate Wayne Keir autobalance universal bridge was used to measure the conductance of the passing solution. The bridge could be operated at various degrees of accuracy, that is, readings could be taken with two, three or four significant figures. Preliminary tests in a separate one stage system showed that working at high accuracy (four significant figures), a great deal of noise was introduced in the measurement. The appropriate degree of accuracy was a compromise between sensitivity to concentration changes on the one hand, and introduction of noise on the other. It was observed that except for

the region of very low concentrations (usually occurring on the top stage only), two significant figures gave a good indication of concentration changes. Hence, interstages probes were calibrated using two significative figures, and for the exit (top stage) probe a higher accuracy (three significant figures) was used.

Using these degrees of accuracy, tests were performed to examine the effect of liquid flow rate on the readings. It was observed that changes of up to 30% did not produce significant variations in the measurements.

Near identical calibration curves taken several months apart for concentrations of up to .04 N gave confidence in the results. For higher concentrations the interstage (embeded)probes presented stability problems. However, the exit (needle) probe still gave consistent readings although not as good as in the case of lower concentrations.

The time-average concentration obtained from the area under the chart recorder curve, was compared with the titration of a sample from the collected five cycles of effluent mentioned in section (5.2.3). The average discrepancy between these two values was about 4%.

CHAPTER 6

RESULTS AND DISCUSSION

6.1 Experimental Results

6.1.1 Preliminary Runs

In Tables (1) and (2) in Appendix C.I, preliminary results are presented. They helped to gain insight in the system and experience in the operation of the plant. They also suggested some valuable modifications in the experimental technique and in the set up of the apparatus. Their presentation here is to illustrate some of the problems encountered and their proposed solutions. They also established a point of reference to observe how the experimental technique developed from its early stages, and most important of all, they provide useful data to discuss several interesting aspects of the performance of the plant.

In Table (1) most runs were replicated, mainly to test reproducibility. Variations in the resin flow rate and fractional transfers were observed even though no modifications were made to the mechanisms that control them. These variations which occurred not only between runs but also throughout the run itself, affected the stability of resin hold ups. Therefore, the attainment of the pseudo-steady state was rather difficult.

This problem was caused by pressure changes in the column transmitted from the air trap. During the forward flow operation, tiny bubbles of air accumulated in the air trap, builidng up pressure which was released to the column during the reversal of flow operation. This affected the 'smoothness' of resin flow rate and created a variable time lag between the closing of liquid feed and the actual displacement of the magnetic float in the oscillator tube, which caused a fluctuating (fractional) transfer of solids.

In spite of these instabilities, some interesting aspects can be pointed out about this series of runs.

From runs 3 and 4 which showed good reproducibility, it is seen that although the initial solid capacities and liquid concentrations differ somewhat, the end liquid and solid conversions are very close

to each other. This confirms the 'fact' that the overall rate of ion exchange under these conditions of low liquid concentration and resin conversion, is only a function of the fraction of unexhausted resin available, and not dependent upon resin conversion. Here, resin conversion is related to the initial experimentally measured capacity, that is:

$$X_S = \frac{C_{ap}^o - C_{ap}^f}{C_{ap}^o}$$

Since there is unlikely to be any saturation of resin under these conditions, and the resin hold ups are similar, the overall rates of ion exchange are also similar. Accordingly, the resin and liquid conversions are almost identical.

The chart-recordings from the conductance readings for runs 4 and 5 are presented in Figures (6.1.1-1) and (6.1.1-2) respectively. They illustrate the cyclic behaviour of the liquid concentration profile. In Figure (6.1.1-2) sections of the pseudo-steady state operation for all 4 probes are shown. There, for simplicity, the total cycle time is divided into two parts: the forward flow period and the transfer period, and for a number of cycles, the initial and end points of the forward flow period are marked. It is seen that the exit liquid concentrations of all stages drops to a minimum after transfer and then rises back and stays steady for the rest of the cycle. This illustrates how the periodic additions of fresher resin enhances the performance of the stage. For the top stage, two factors contribute to keep the measured concentration at the lower value for a longer period. These factors are the continuous addition of resin, and the dilution caused by the entrained water fed with the resin. During solids transfer, the volume of this dilution water, builds up, and hence, the conductivity reading for the first few seconds shows a lower value. Later in the cycle, the accumulation of resin is responsible for maintaining the low liquid concentration reading. Note that the noise in the measurement of stage 1, was caused by the occasional passing of resin beads through the cell.

In Figure (6.1.1-1), the recording of almost the entire run is presented. In the initial part, the reading for stage 4 from start up, shows how the pseudo-steady state is approached. Later, readings for all other probes are seen. A similar behaviour to run 5 is observed for all stages.

Table (2) comprises two sets of data. Runs 1, 2 and 3 correspond to the first set, there the reproducibility of flow rates and other parameters was greatly increased. The pseudo-steady state operation was quite stable for most of the run. However, towards the end of the run, the exit of stage 4 liquid concentration profile started to drift in the direction of higher concentration. This coincided with the feeding of the last fraction of resin, which due to classification during washing (see section 2.3), contained most of the finer particles. With smaller particles the fluidized bed voidage ε_b increases. The effect of this, and that of the particle size in the rate of reaction, is seen in the modified expression for the mass transfer coefficient

$$k_L = \frac{.86}{\varepsilon_b} \left(\frac{\rho}{\mu}\right)^{.17} \frac{D^{.67} u^{.5}}{d_p^{.5}} \quad ,$$

here the effect of ε_b would predominate since the exponent of d_p would damp down the effect of its variation. Rescreening of the resin was mandatory. This was done applying the technique of wet screening to a batch of new resin.

When performing the mass balances for this and the previous series, it was noted that in the majority of runs the average rate of mass transfer for the solid phase was above the corresponding value for the liquid phase. Up to then, the resin samples had been drawn for analysis after the end of the run. For some conditions, the resin could continue to react to a certain degree and the resin conversions found would be higher than the actual pseudo-steady state values; this would explain the mass balance errors. It was then decided that the resin samples were to be taken during the course of the run, towards the end of the forward flow period of the cycle. This however, has the draw back that if too big resin samples were withdrawn from the column, the disturbance created could seriously affect the stability of the pseudo-steady state. Tests performed in subsequent runs ,showed differences between 3 and 20 per cent for the two methods of sampling.

Observing runs 2 and 3 which had kept 'constant' residence times, it is seen that by increasing the fractional transfer from 0.5 to about 0.6, the liquid conversion increased from 81% to 89% and resin conversion from 47% to 49%. Further comment on these improvements is deferred to section 6.1.2. The high conversion in run 1 is explained by the unusually

high resin and liquid residence times.

The second set of experiments, runs 4 to 8, were performed to test the hydrodynamic stability of the contactor. A complete study was not intended here. However, it was desired to scrutinize its effects on the attainability and stability of the pseudo-steady state.

The contactor is said to have achieved hydrodynamic stability when the amount of resin in all stages is maintained constant between consecutive cycles. This is checked by observing the fluidized bed heights during a number of cycles.

Pseudo-steady state conditions are reached when the liquid concentration profiles do not differ between cycles.

Two approaches were taken here:

In the first, the system was started up with stages partially filled with fresh resin, as in runs 4, 5 and 6 (for a detailed description of the operation see section 5.2.3). In the second approach, runs 7 and 8 were initiated with no resin at all in the column. Considering that the partial filling up was a laborious and time consuming task, starting up a run with an empty column had obvious advantages. However, the experimental evidence indicated that a larger number of cycles was required to achieve hydrodynamic stability by this method. Figure (6.1.1-3) and (6.1.1-4) and Table (3) show the trajectories followed by the fluidized bed levels towards stability for runs 4 and 7. In the case of run 7 which was started with empty stages, it took 60 cycles to achieve stability whereas the partially filled run 4 only required about 25 cycles. It should be pointed out that in the case of runs started with partially filled stages the actual number of cycles required to reach hydrodynamic stability depended very much on the amount of resin initially present. The bigger the difference between initial and final (steady) values, the more cycles would be needed, as was the case for run 6 where about 40 cycles were required.

Runs 5 and 6 tested the reproducibility of the hydrodynamically stable operation. This was done by starting up the contactor with different initial amounts of resin (see Table (4)). From the results it is seen that the same stable point was obtained. Also, the end resin

FIGURE 6.1.1–1 Conductance readings for run 4 illustrating the cyclic behaviour of the liquid concentration profiles

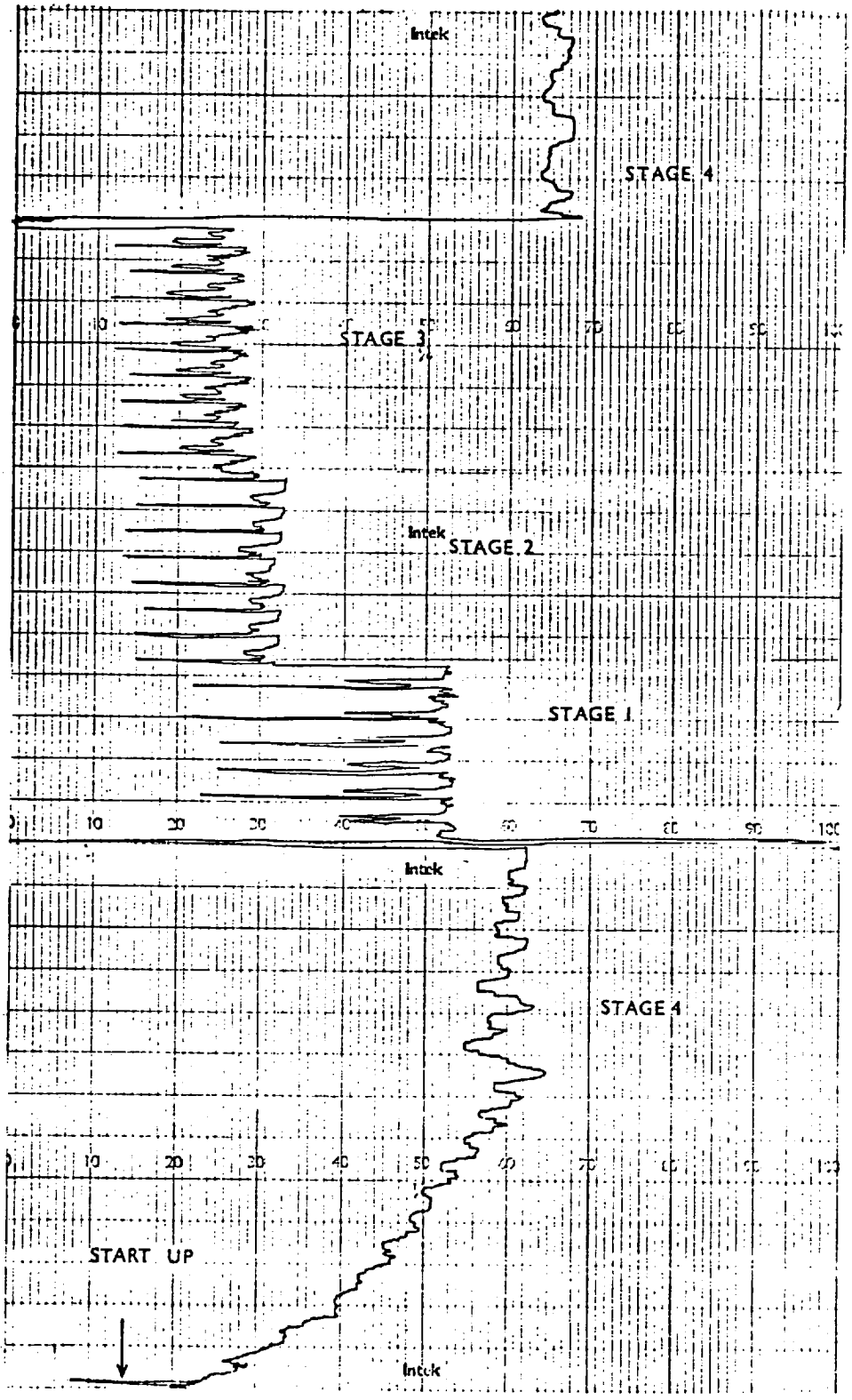

FIGURE 6.1.1—2 Chart recording of pseudo steady state conductance readings for run 5.

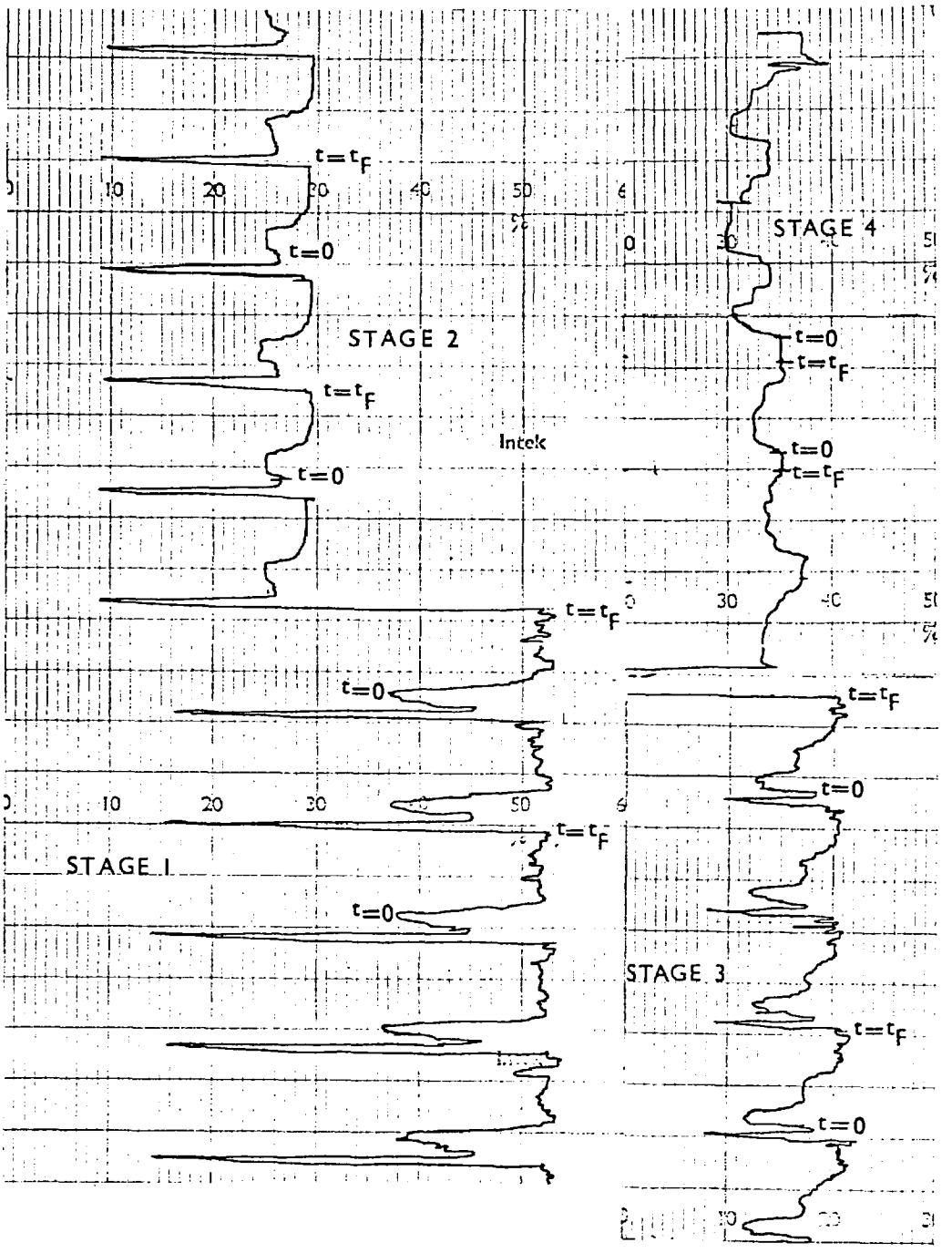

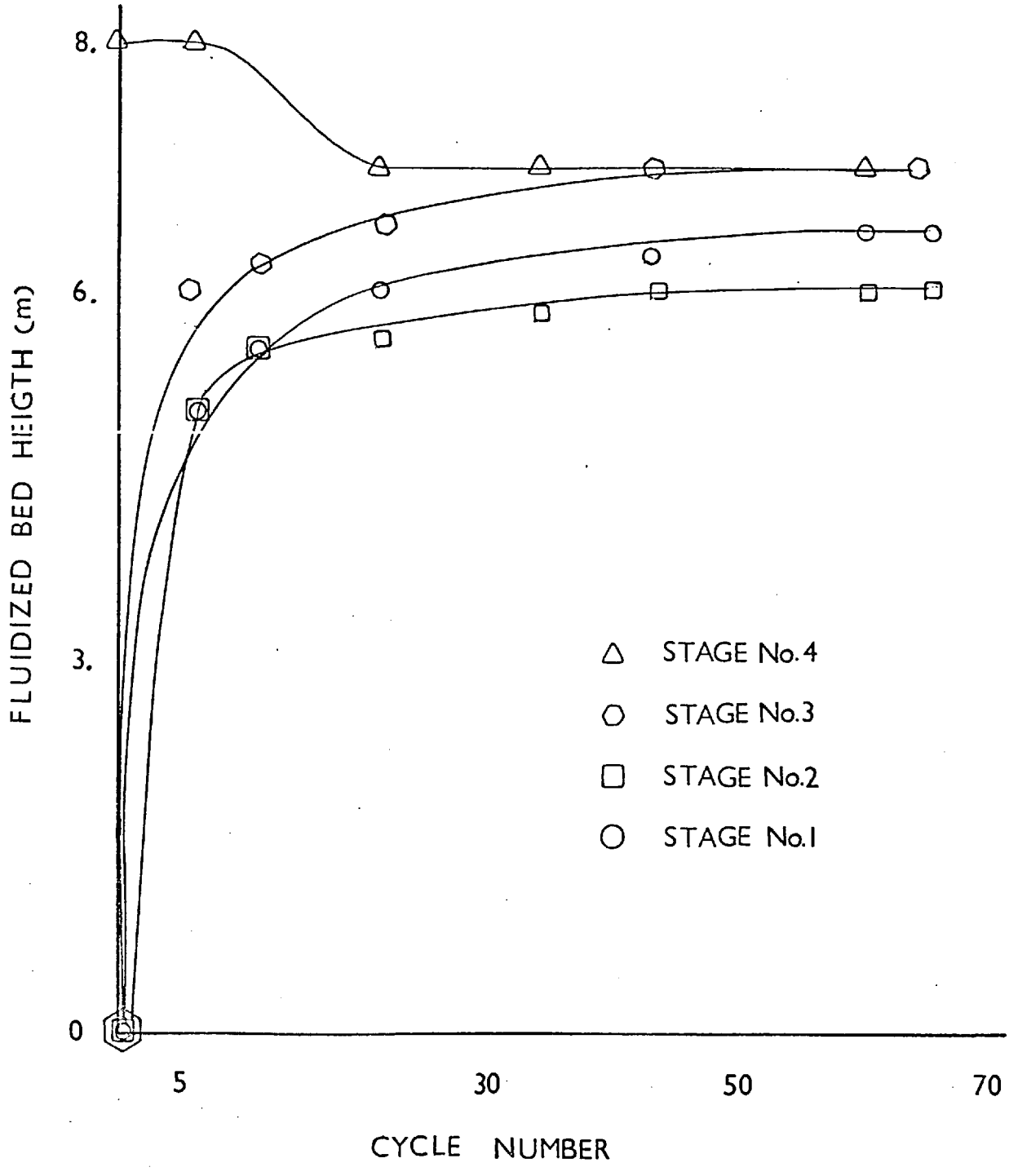

FIGURE 6.1.1-3 Trajectories of the fluidized bed levels for run 7.

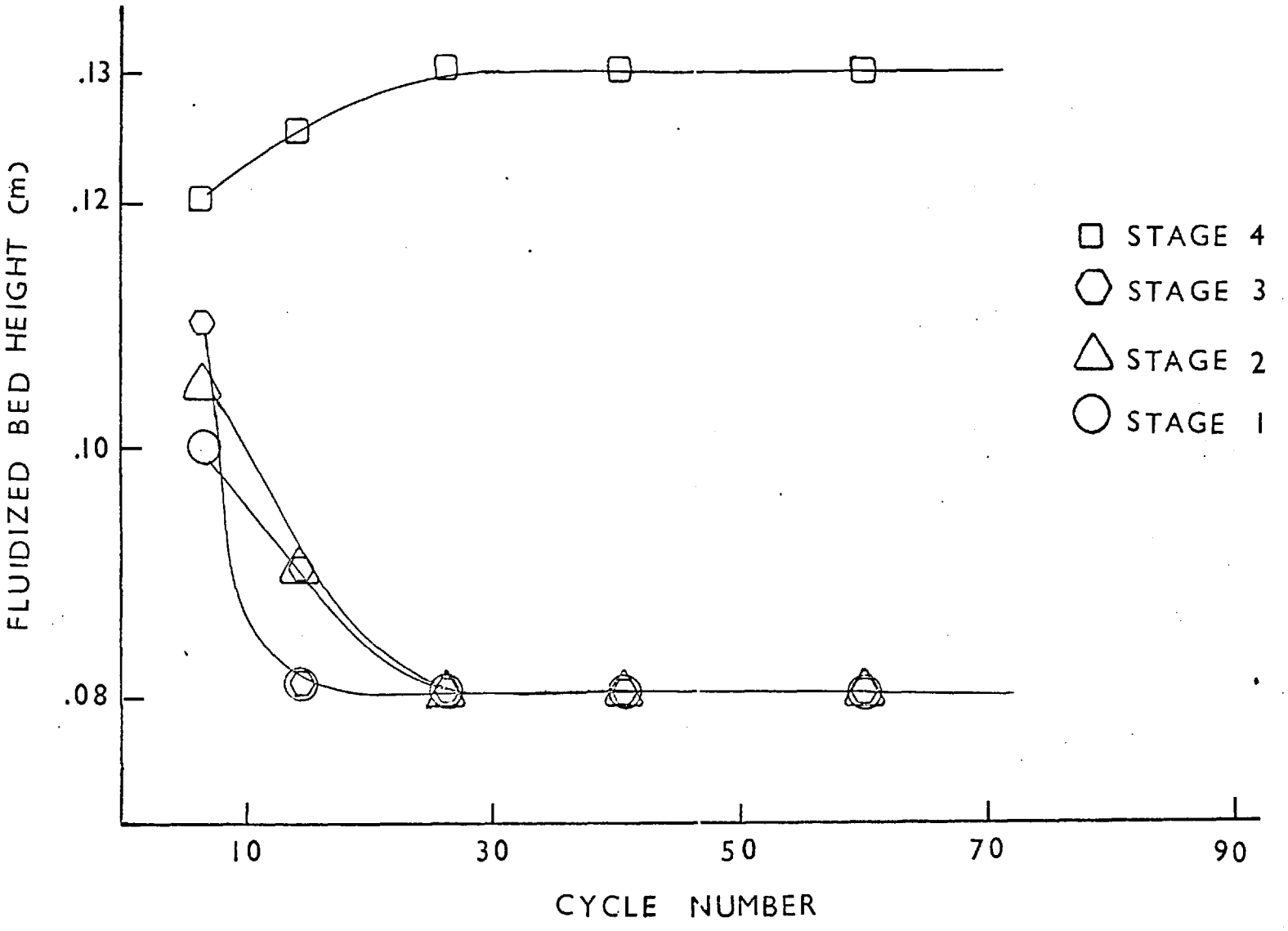

FIGURE 6.11-4 Trajectories of the fluidized bed levels for run 4.

hold ups in all stages are similar, as are the conversions and residence times.

In order to illustrate the effect that the path towards hydrodynamic stability has on the attaining of pseudo-steady state conditions of the liquid concentrations, sections of the conductance chart recording for two typical runs, one for each of the approaches described are given in Figures (6.1.1-5a, 6.1.1-5b and 6.1.1-6).

Figures (6.1.1-5a and 6.1.1-5b) show the results for run 4. The reading corresponds to the top stage probe. It is seen that the concentration profile moves very quickly towards pseudo-steady state which is reached at about cycle 26, where hydrodynamic stability is also achieved. This state is then conserved throughout the rest of the run. Small disturbances will momentarily affect the pseudo-steady state but after a while the system returns to its previous state. This confirms that, at least in a neighbourhood of the pseudo-steady state, the behaviour of the column is self-stabilised, in the sense that the system is capable of returning its pseudo-steady state after small disturbances, provided hydrodynamic stability is maintained.

Results for run 7 are reported in Figure (6.1.1-6). Here, the concentration profile drifts quickly in the early part of the run and after about 40 cycles it changes rather slowly.

Examining Figure (6.1.1-5a) one notes that, after a few cycles from start up, the liquid concentration profiles have already acquired a form which is kept thereafter. All these results suggest that two factors, i.e., the establishing of the solid profiles and the path toward hydrodynamic stability, participate in the attaining of the pseudo-steady state. At the beginning of the run, fresh resin in all stages enhances the liquid concentration changes. However, the solid conversion profiles are quickly set up and cease to have any important effect on the approach to p.s.s. The latter is seen in Figure (6.1.1-6), where, after the rapid initial drift, p.s.s. is approached at the same pace as that of hydrodynamic stability. It therefore appears that, the attainment of the hydrodynamic stability is the controlling factor in the approach to the pseudo-steady state.

FIGURE 6.1.1–5a Effect of the hydrodinamic stability on the attaining of the pseudo-steady state.

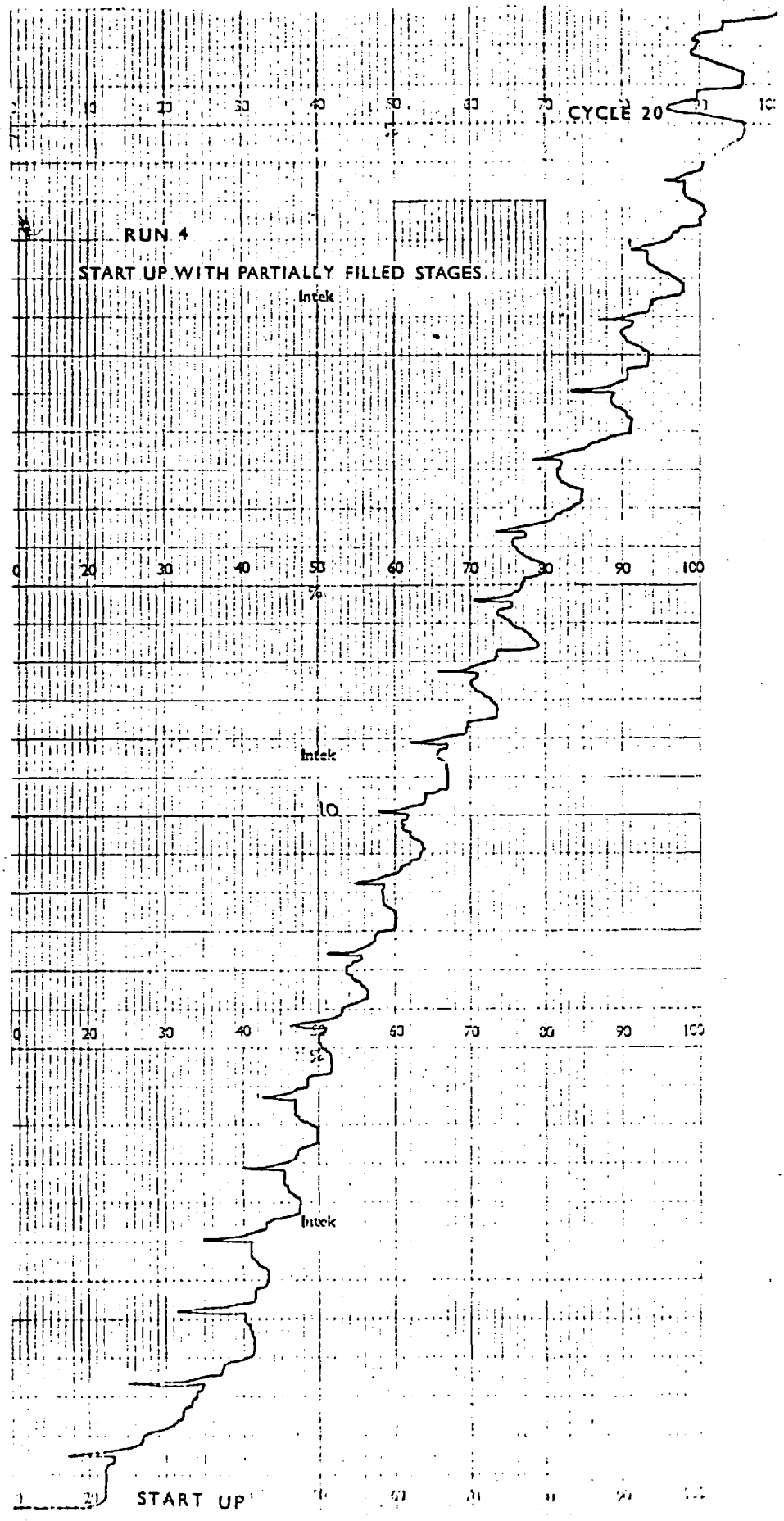

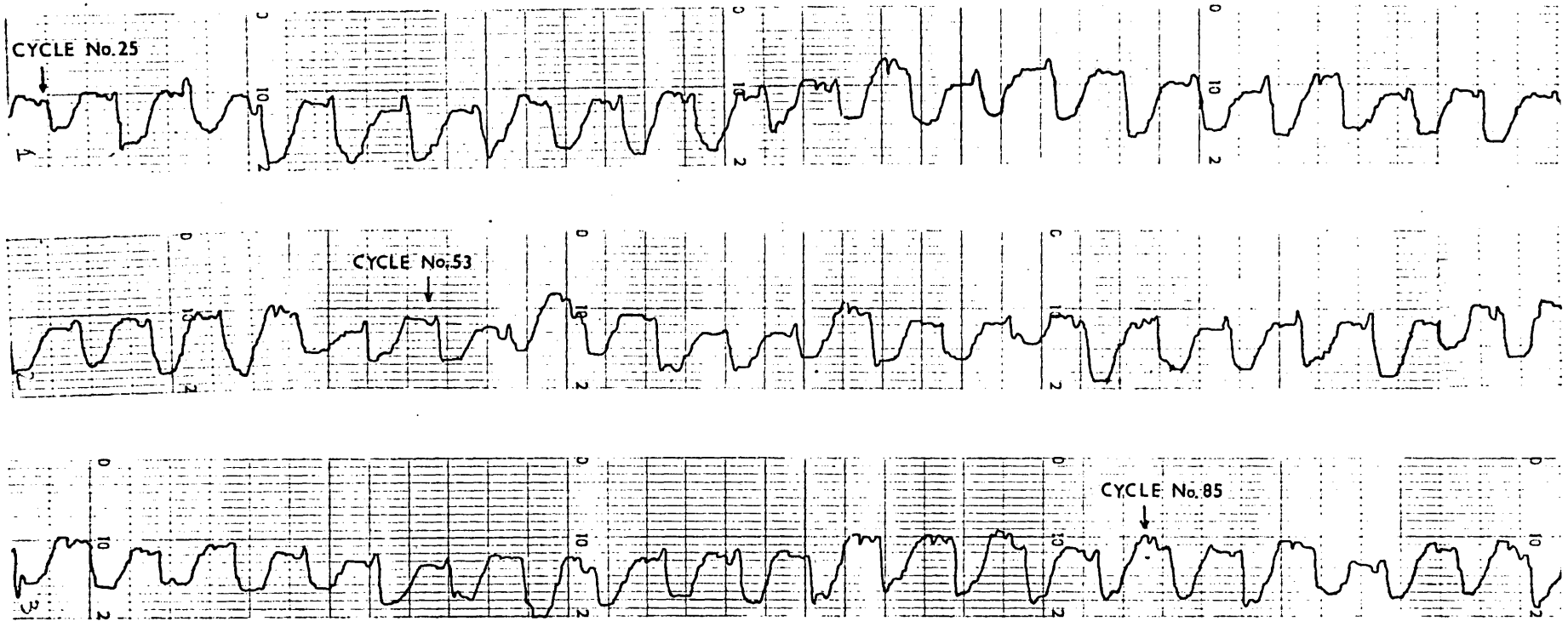

FIGURE 6.1.1–5b Pseudo–steady state liquid profiles for outlet stream illustrating the effect of small disturbances.

FIGURE 6.1.1-6 Effect of the hydrodynamic stability on the attaining of the pseudo-steady state in the case of a run started up with empty stages.

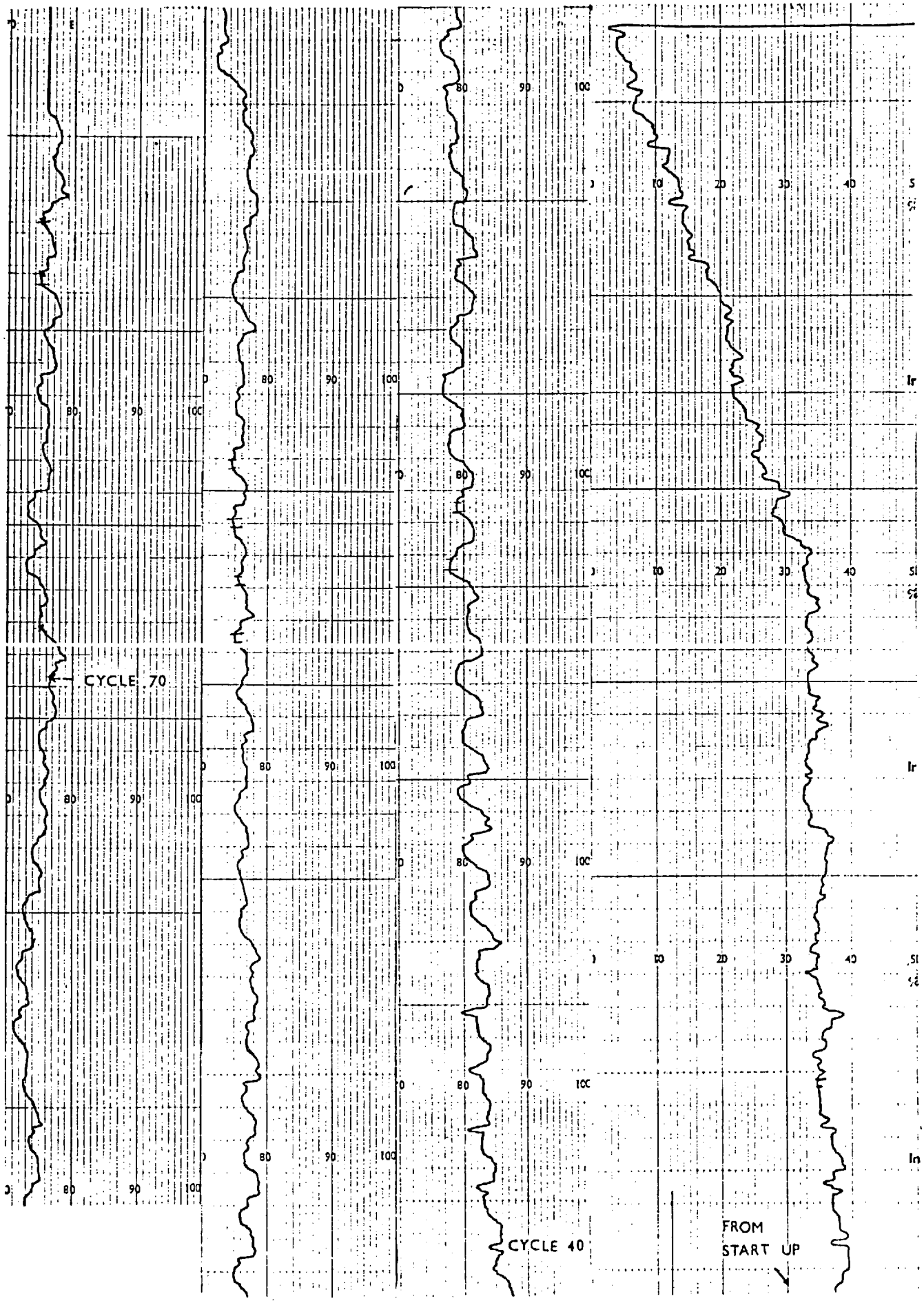

This experimental evidence can be summarized by the following statements:

a) It confirms that the hydrodynamics of the system are inherently stable.
b) Pseudo-steady state operation is also stable and mainly controlled by the hydrodynamic stability of the system.

6.1.2 Low Concentration Experiments

This set of experiments consists of three series of runs, each one at different liquid feed concentrations.

The results for the series using liquid feed concentration of 0.02 N are shown in Table (5). Runs 2, 3 and 5 observed the requirement of constancy in residence times. Liquid and solid conversion for these three runs are plotted in Figure (6.1.2-1). There, it is seen that by varying the resin fractional transfer from 0.504 to 0.9 liquid conversion increased from 79.5% to 82.3% and solid conversion from 38.2% to 43.2%.

Runs 1 and 4 demonstrate the effect of both residence times in the performance of column. Run 1 with a 20% higher solid residence time than the three constant runs shows a high resin conversion not expected at this low value of fractional transfer. On the other hand, in run 4 with less resin hold up and a shorter residence time, a decrease of both conversions is observed.

In Figure (6.1.2-2), the concentration profiles for both phases along the column for runs 2 and 4 are shown. The linearity observed in the case of the resin profiles is expected as long as there is negligible resin saturation. Concave liquid profiles result from typical first order kinetics. Note that the rate law used here for low liquid concentrations is, in fact, first order with respect to liquid concentration. These liquid concentrations refer to the average value calculated over the cycle.

It is of interest to observe in the case of a long cycle run how the liquid concentration profile attains its cyclic steady state. Because the duration of the forward flow period of the cycle is 40 seconds, it is easy to examine the changes in the profile. Figure (6.1.2-3) shows the recording of probe no.4 for the first 8 cycles after start up in the case of run 5. The peaks to the left, are the reversal of flow periods and represent the concentration of solution in the header tank. It is noteworthy to observe the formation of the minimum concentration peak during each cycle; it is non-existent for the first two cycles but at cycle no.4 the minimum is already clearly seen.

In Figure (6.1.2-4), as an illustration of p.s.s. behaviour, the liquid profiles for all 4 stages are shown. In all stages, the concentration falls to a minimum after solid transfer in accordance with the behaviour of previous runs.

For the second series of experiements a liquid feed concentration of 0.03 N was used. Results for six runs performed under these conditions are reported in Table (6).

The improvement in performance by increasing the fractional transfer is seen in Figure (6.1.2-5a). Results for five runs are included there. Solid conversion between runs 1 and 2 show a big improvement, whereas the liquid conversion barely changes. Results for this, and other 20 seconds runs are thought not to be very reliable. It was observed during experiments that the attainability of the cyclic steady-state was more difficult in these runs than in the longer runs. This was probably due to small variations in the volume of the resin periodically transferred since the actual time allowed for transfer, that is discounting the settling time, was very short (around 2 seconds).

Disregarding the first point in the graph a similar pattern to that in the previous series was obtained. The shape of the curve passing through the points suggests that there might be a maximum in the conversion. Unfortunately experiments with higher fractional transfers did not produce reliable results since by passing of resin was clearly seen and therefore this point could not be studied further experimentally.

In Figure (6.1.2-6) liquid and solid conversion profiles for the column are shown. As in the previous experiments, little resin saturation is observed and linear profiles are obtained. Curved liquid profiles are also expected as was discussed earlier.

In Figure (6.1.2-5b) a plot of solid conversion vs. volume of resin transferred per cycle is included. There, it was desired to compare this and Figure (6.1.2-5a) in order to observe how well the fractional transfer value represented the amount of resin actually being transferred, since an average value for d was being used. It is seen that the curves for the solid conversion are satisfactorily similar.

The effect of particle saturation can be seen by comparing the liquid concentration profiles of stage no.1, for runs 5 and 6. Although an overall increase in column performance is obtained, the performance of the bottom stage is in fact lowered. The profiles are depicted in Figure (6.1.2-7). There it is observed that for the first 5 seconds of the forward flow period, the concentration for run 6, falls more steeply than for run 5 due to the larger amount of less reacted resin added during transfer. However, after a few seconds the concentration for run 6 is higher than for run 5. Since the inlet liquid concentration and the resin hold up are the same for both runs, this result can only be attributed to a slower rate of reaction for the stage.

It has been considered that, for this range of liquid concentrations, the rate of reaction is mainly film controlled, and the total rate of reaction is given by Equation (4.1.1-4) as $R_j=k_L aF(x_n,j)C_j$. The term $F(x_n,j)$ denotes the fraction of unsaturated particles. Thus, the rate is decreased if the fraction of saturated particles is increased. In Figure (6.1.2-8), sections of the conductivity readings of all 4 stages for both runs, are shown. There it can be seen that a lowered performance is obtained for stage 1 only. This indicates that most of the saturation takes place precisely at the bottom stage.

It should be pointed out that the concentration readings for the first second or so, are not very reliable. This is so because the liquid in the conductivity cell at the very beginning of the cycle is a mixture of liquid from the stage above (from solids fractional transfer) and the stage liquid at concentration equal to that at the end of the cycle. Thus, this volume of mixed liquid must be replaced by exit solution before the reading becomes reliable.

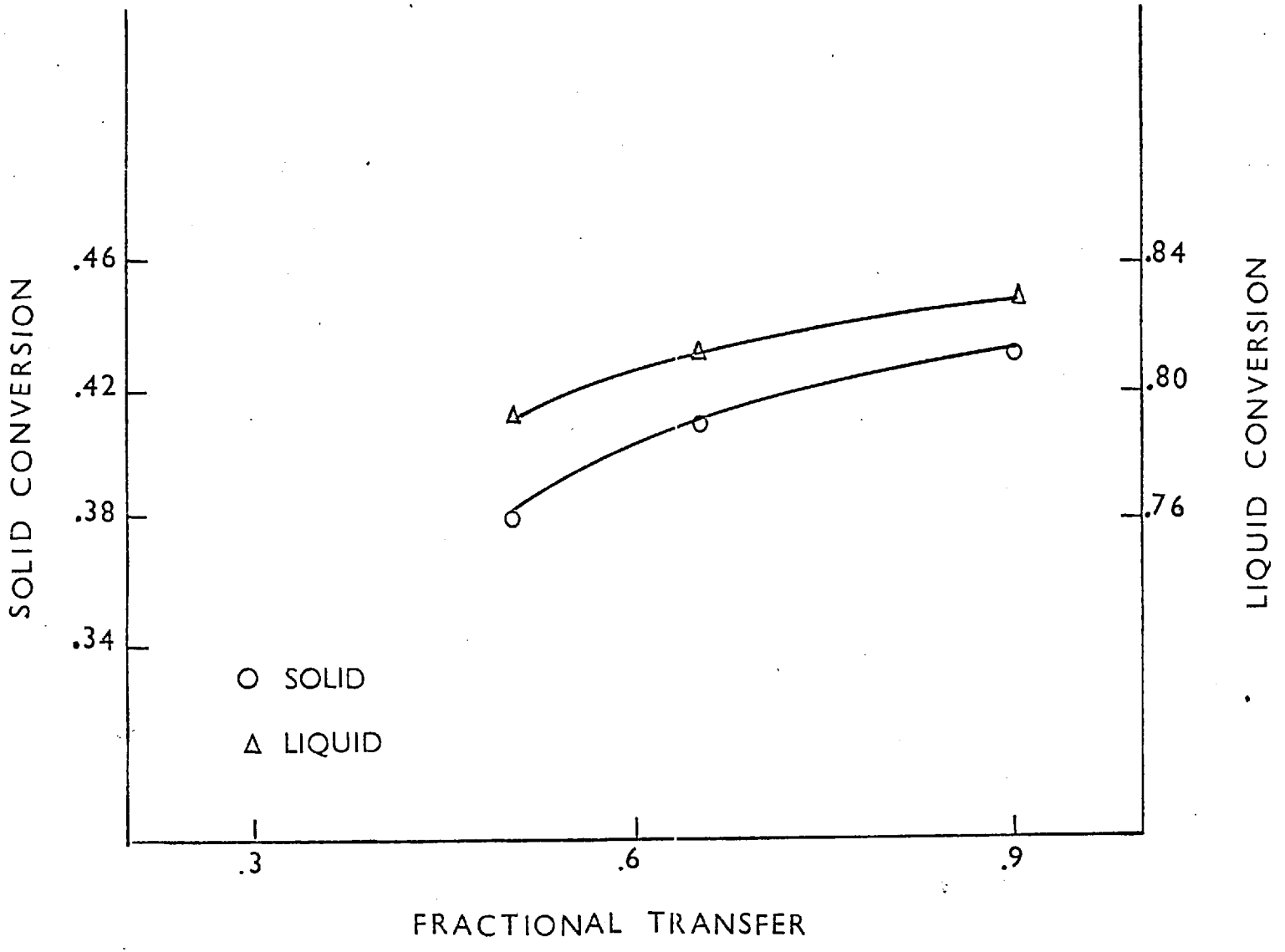

FIGURE 6.1.2-1 The effect of fractional transfer on liquid and solid conversions.

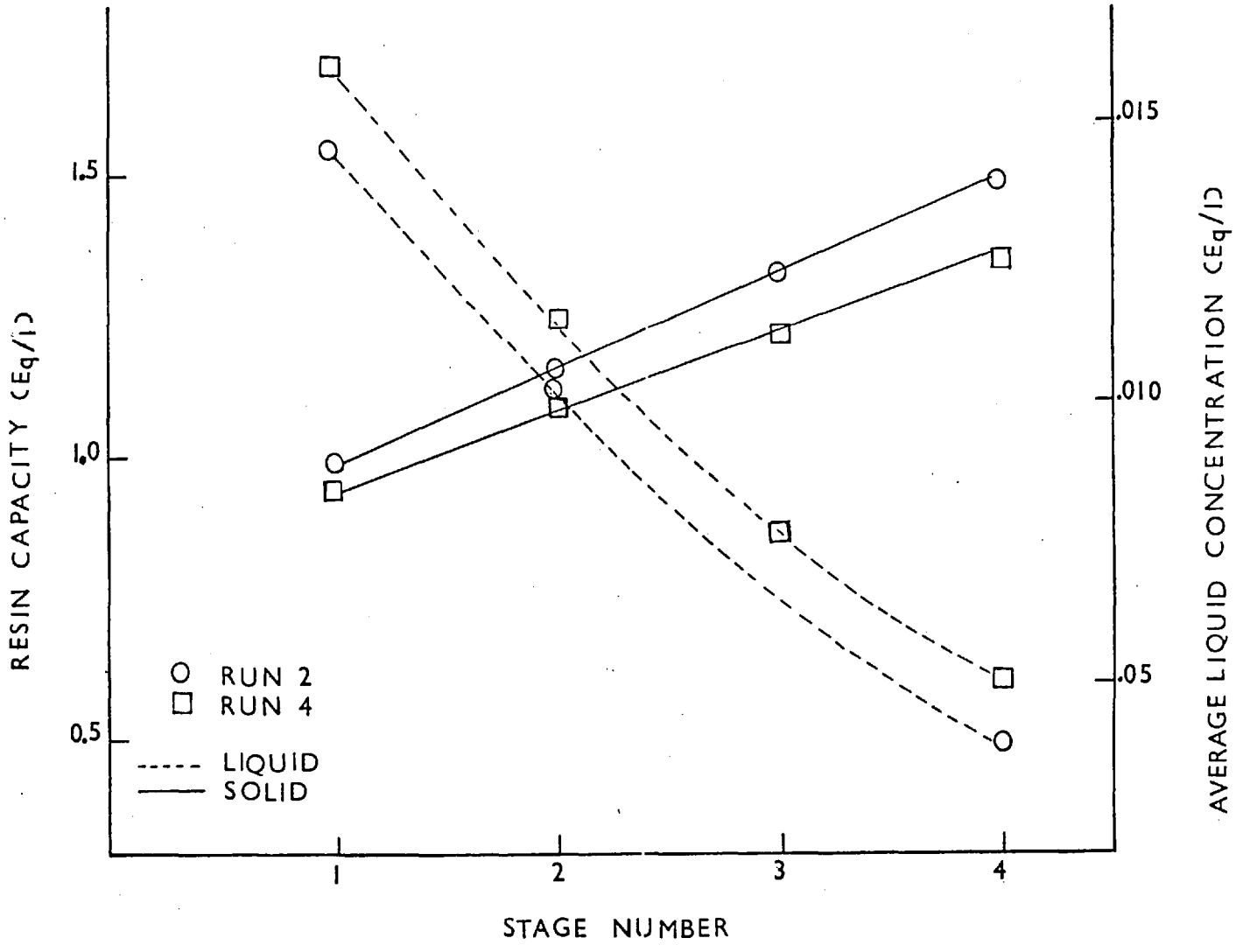

FIGURE 6.1.2-2 Liquid and solid profiles along the column.

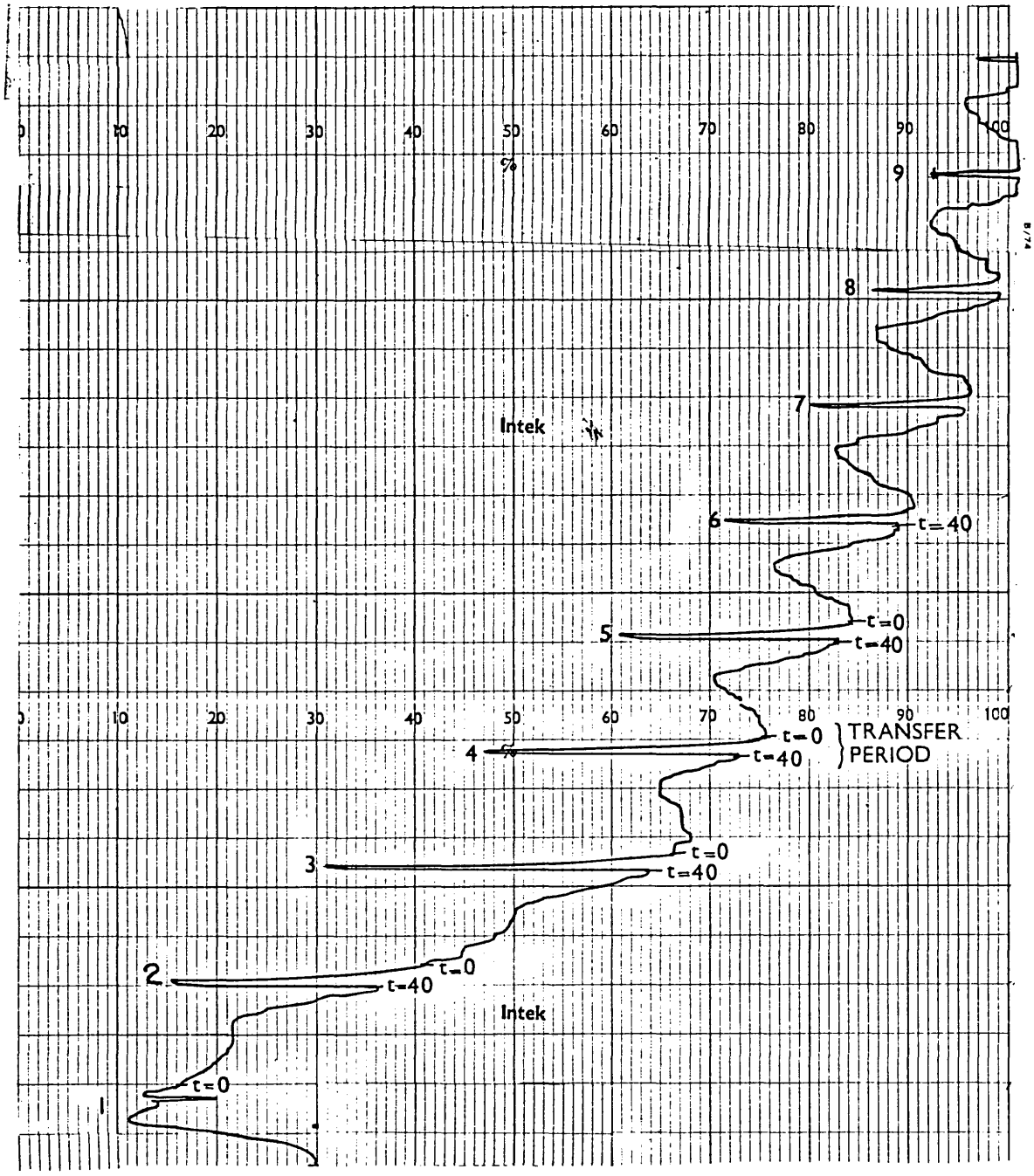

FIGURE 6.1.2-3 Liquid concentration profile for the top stage of run 5 showing the formation of a minimum concentration peak after start up.

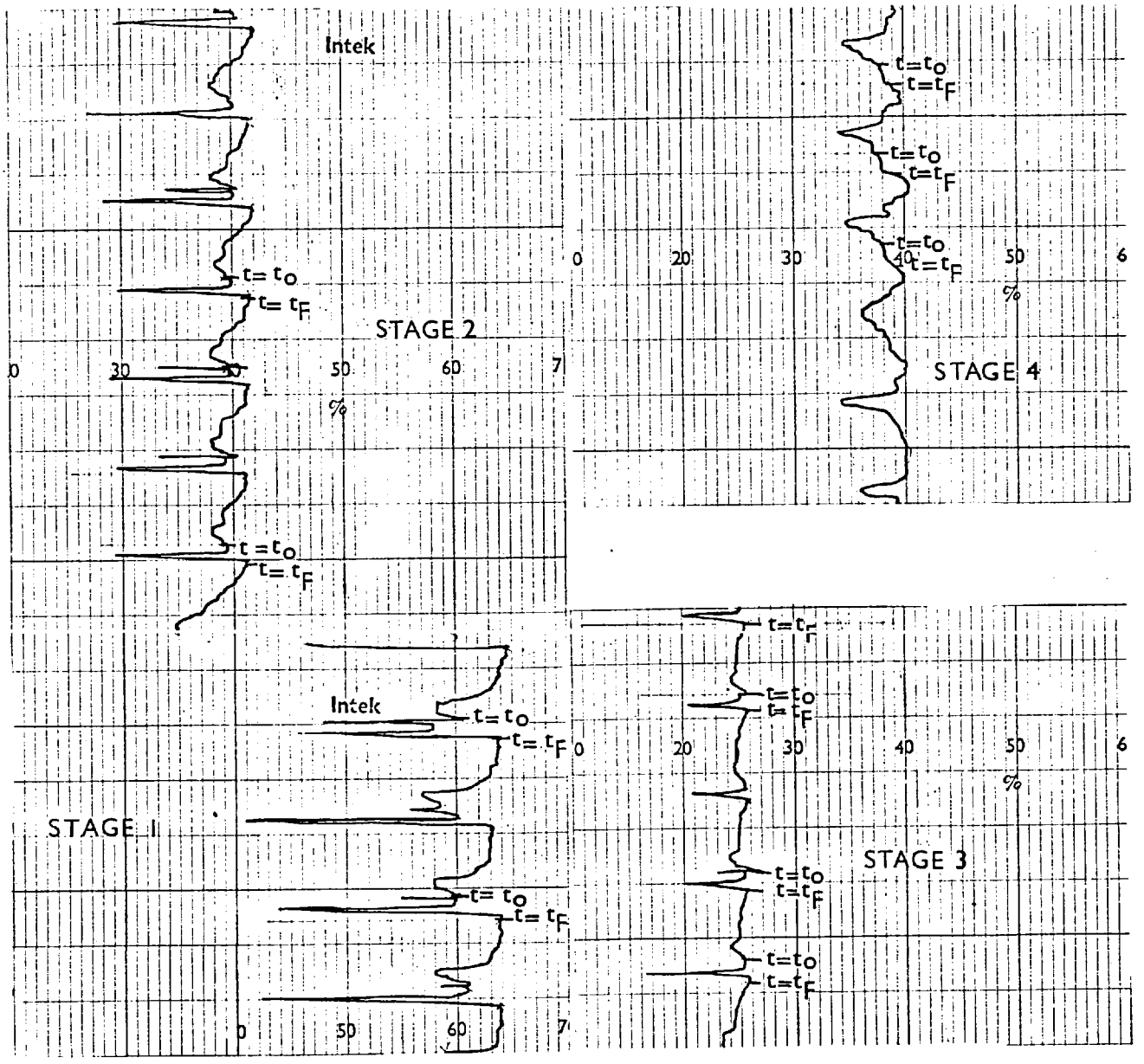

FIGURE 6.1.2—4 Illustration of pseudo-steady state behavior of liquid profiles for all stages of run number 2.

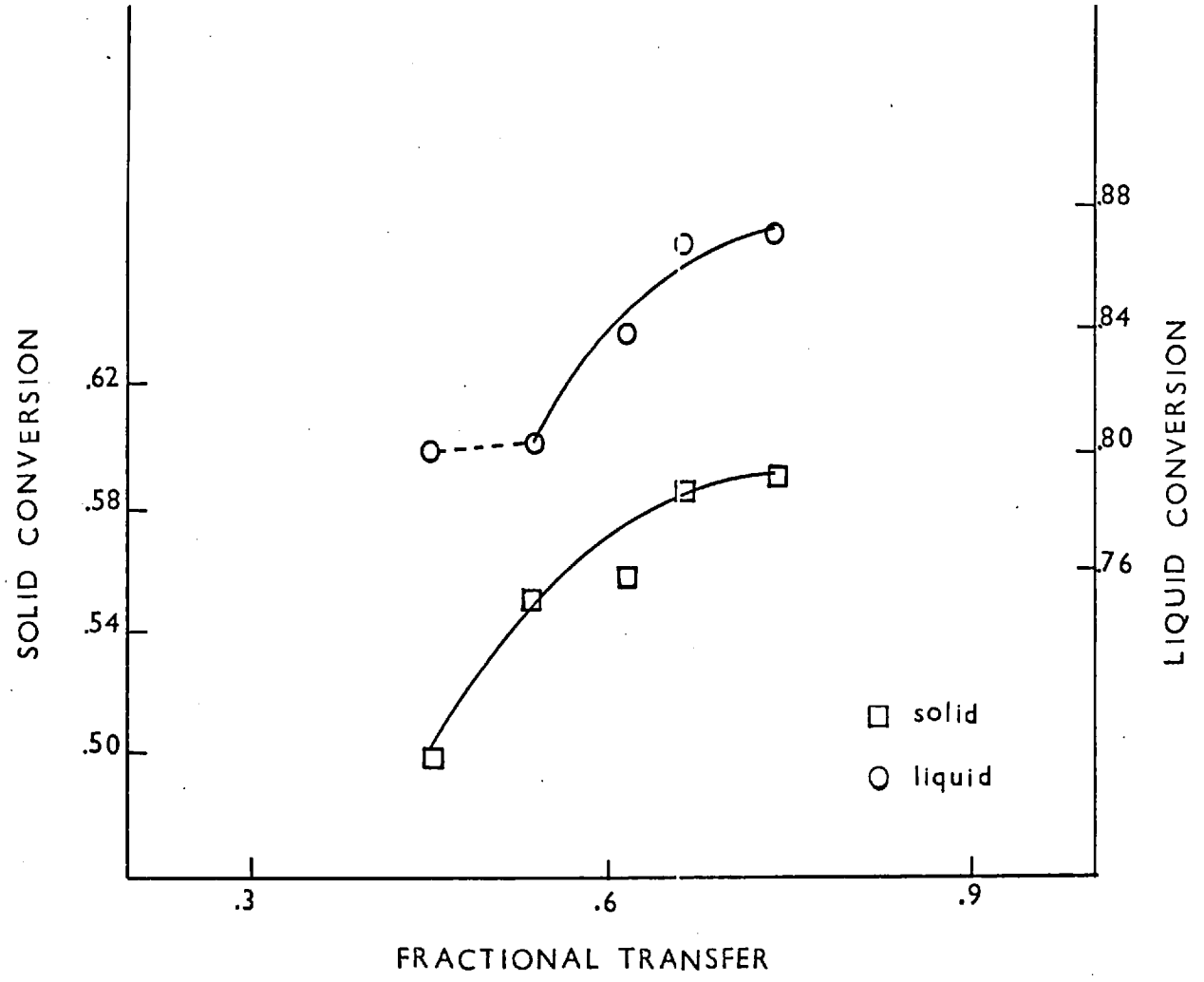

FIGURE 6.1.2-5a The effect of fractional transfer on liquid and solid conversions.

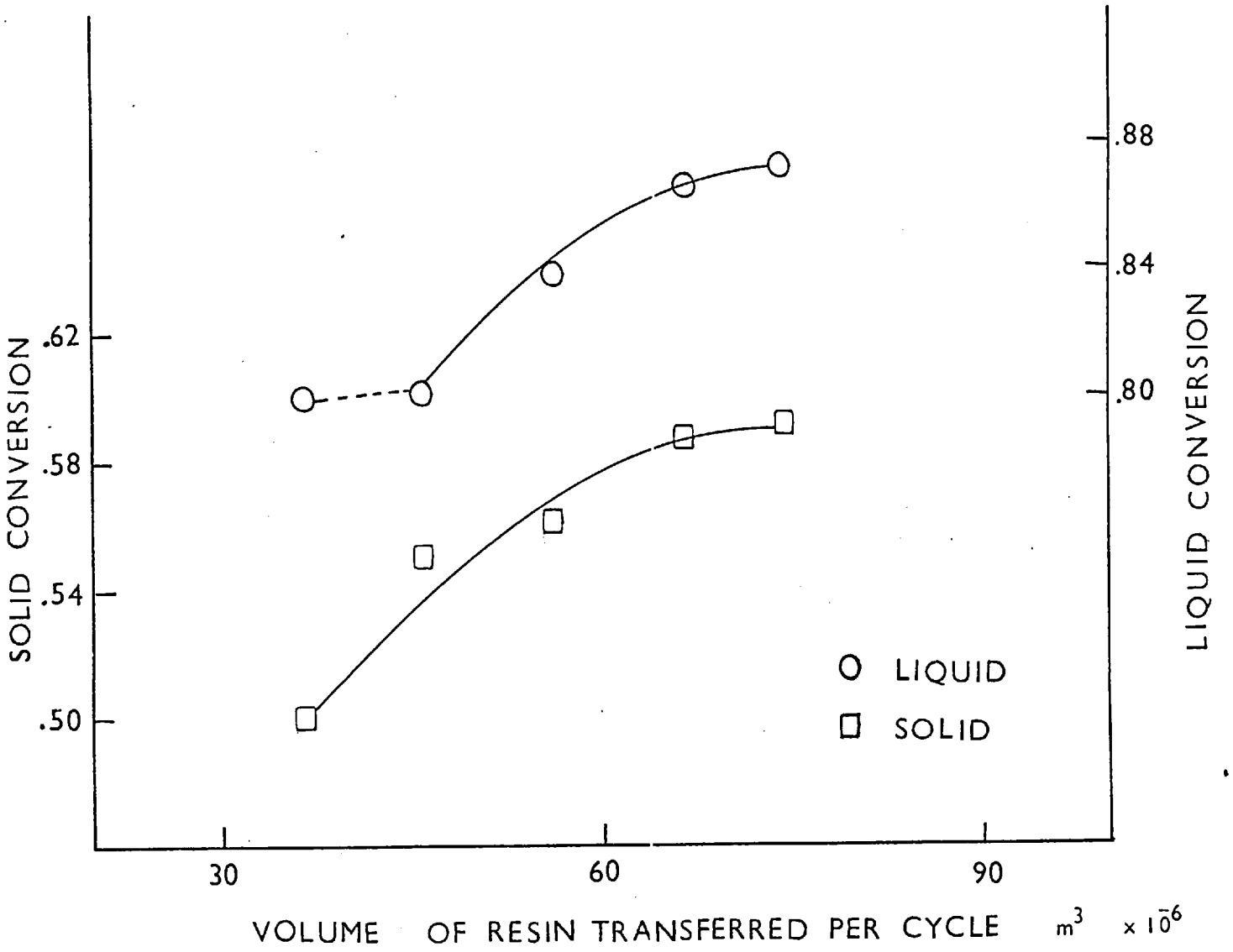

FIGURE 6.1.2-5b The effect of the volume of resin actually transferred on the performance of the column.

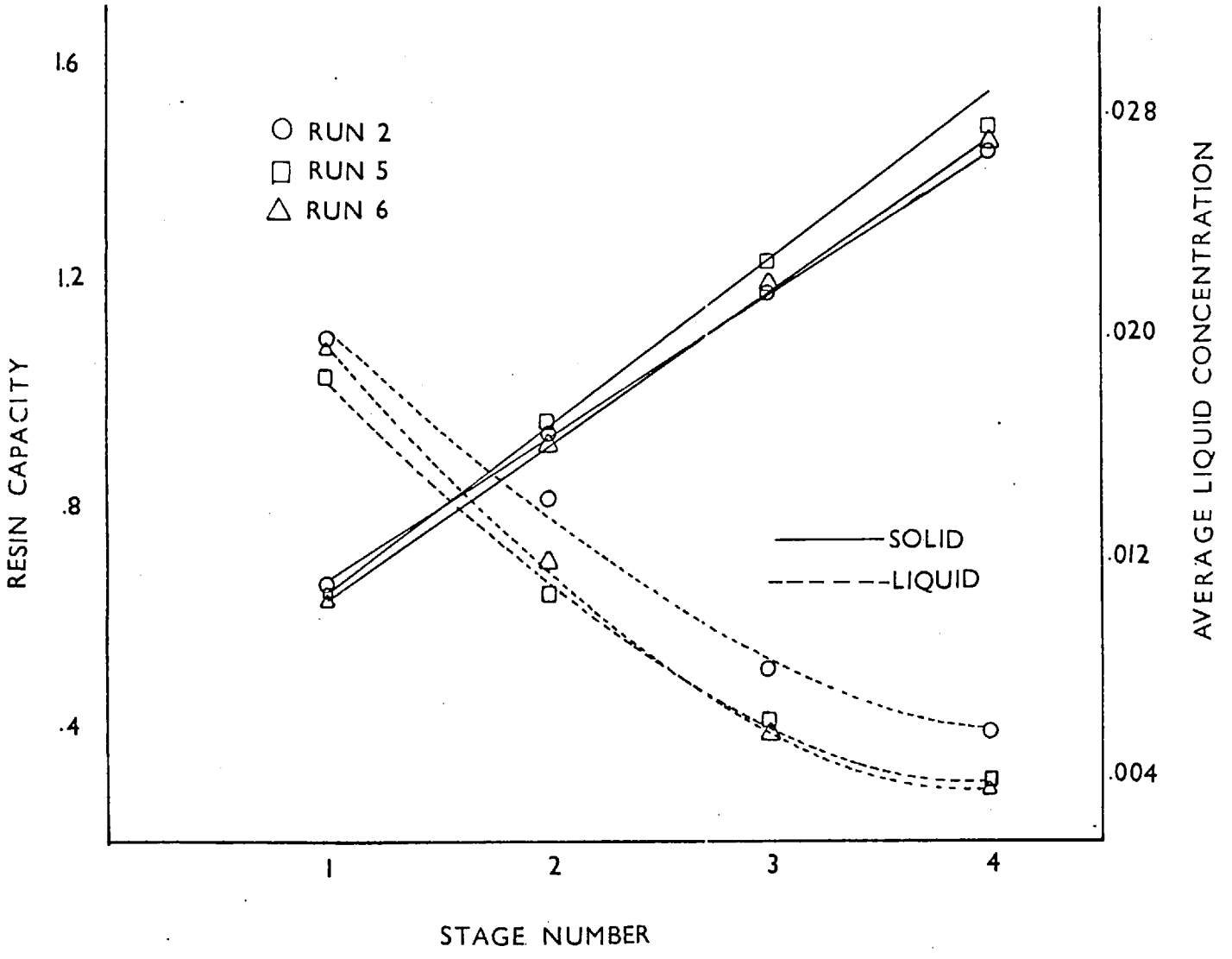

FIGURE 6·1·2–6 Solid and liquid profiles along the column.

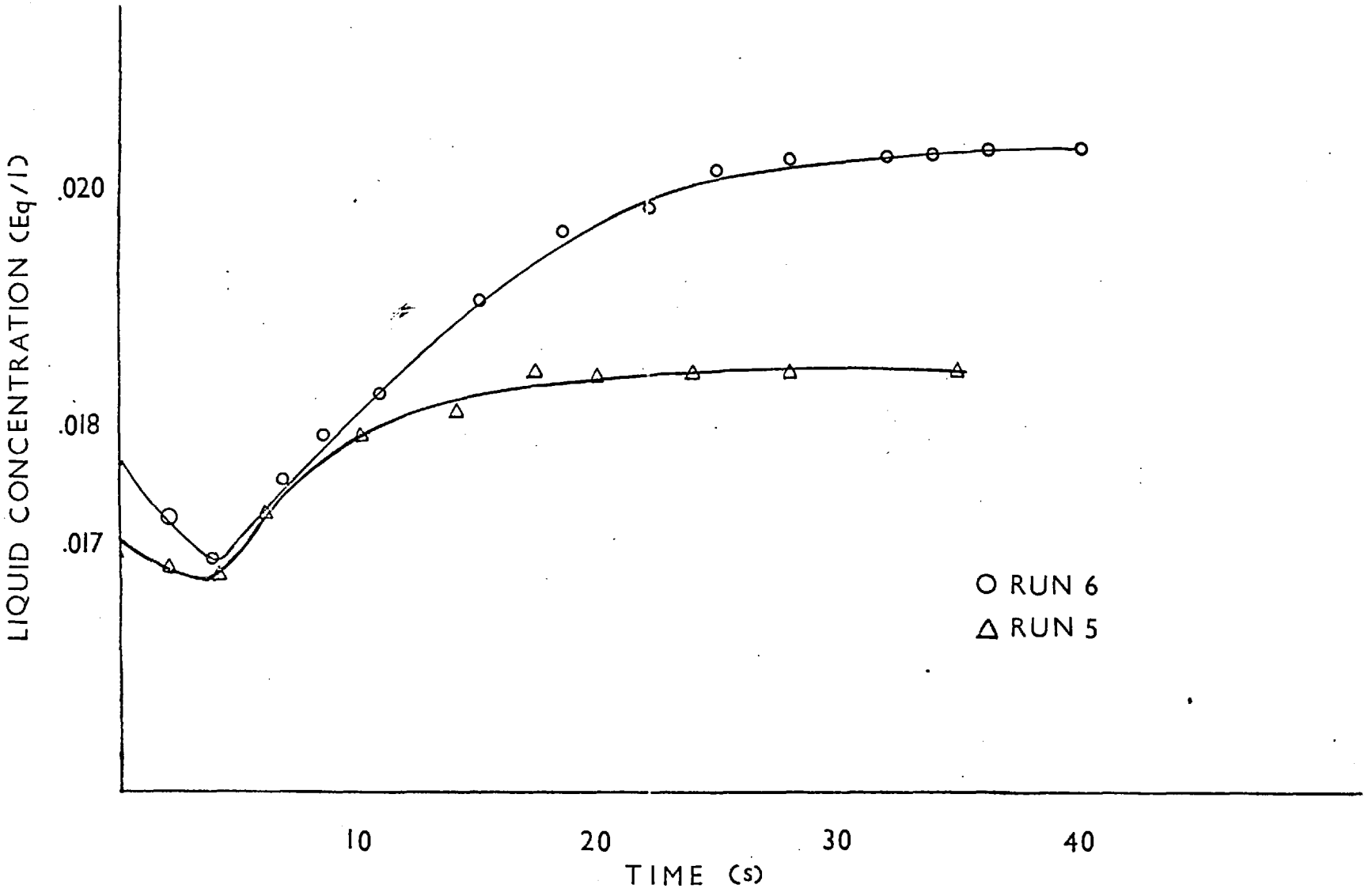

FIGURE 6.1.2-7 Comparison of the liquid concentration profiles for the bottom stage of runs 5 and 6.

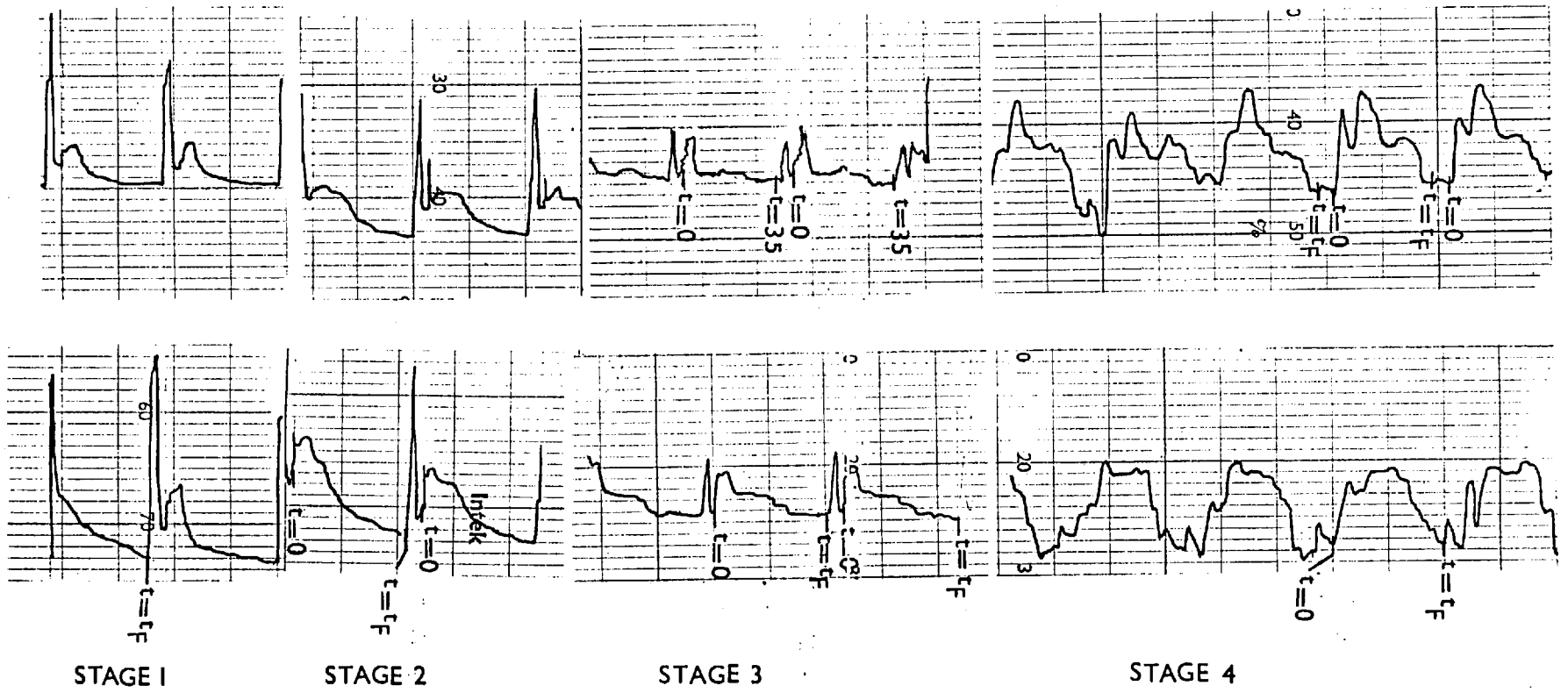

FIGURE 6.1.2-8 Comparison of the performance for all stages between runs 5 and 6 illustrating lowered performance of the bottom stage in the case of run 6

The third set of experiments correspond to an inlet liquid concentration of 0.036 N. Originally, experiments with a 0.04 N feed were tried, but serious stability problems arose due to build up of resin hold up on the bottom stage.

In a number of runs in which the 0.04 N feed concentration and similar input and control variables as before were used, long solid residence times and high conversion (up to 95%) were obtained. It appeared that under a combination of certain fractional transfers and the increased density due to the replacement of the H^+ ion by the much heavier Na^+ ion, the flow of resin through the bottom set of perforated trays was somewhat impeded. Therefore, the amount of resin being transferred out of the stage was less than the amount put into it from above. It should be mentioned that runs of this sort started as a normal stable run for the first 30 or 40 cycles, and even a certain steadiness was achieved. However, once the resin conversion reached a critical point the process of accumulation was initiated.

Figures (6.1.2-9) and (6.1.2-10) show the outlet liquid concentration profiles for two of these unstable runs. It is seen that after an apparent p.s.s. was obtained, drifting towards lower liquid concentration started as the resin hold up is increased. Physically it was possible to observe changes in the resin coloration from a light to dark brown. The effect of the resin density changes were also visible as it became more difficult for the liquid to lift and fluidize the settled resin at the beginning of the forward flow periods.

In an attempt to overcome these difficulties runs were tried with higher resin flow rates (to diminish the residence time) and lower liquid feed concentrations. A liquid concentration of about 0.036 N was found to be adequate with resin flow rate of about 1.63×10^{-6} m^3/s, 10% more than in previous runs.

Results for 6 successful (stable) runs are presented in Table (7) and the conversion results for runs 2, 3, 4, 5 are diagramatically shown in Figure (6.1.2-11).

It is observed that little conversion increment is obtained for the higher fractional transfers probably indicating that a point of maximum conversion was near. Experiments trying to obtain higher transfers again failed, this time due to stability problems caused by building up of resin as described above. Run 6, with a higher solid residence time, showed a decrease of liquid conversion. This is expected since a longer residence time would mean more resin saturation with the consequent decrease of available active solid. In the case of run 1 the results are again thought not to be very reliable although the liquid conversion fits into the pattern of other runs.

Liquid and solid profiles along the contactor for runs 3 and 5 are depicted in Figure (6.1.2-12). It is seen there that the shape of the curves are similar to those of previous runs. Noteworthy to observe is that the resin profiles remain linear, indicating that the reaction is still mainly liquid film controlled.

For the case of run 5, pseudo-steady state sections of the conductivity recordings for all 4 stages are shown in Figure (6.1.2-13). Here again the liquid profiles resemble those of the previous series.

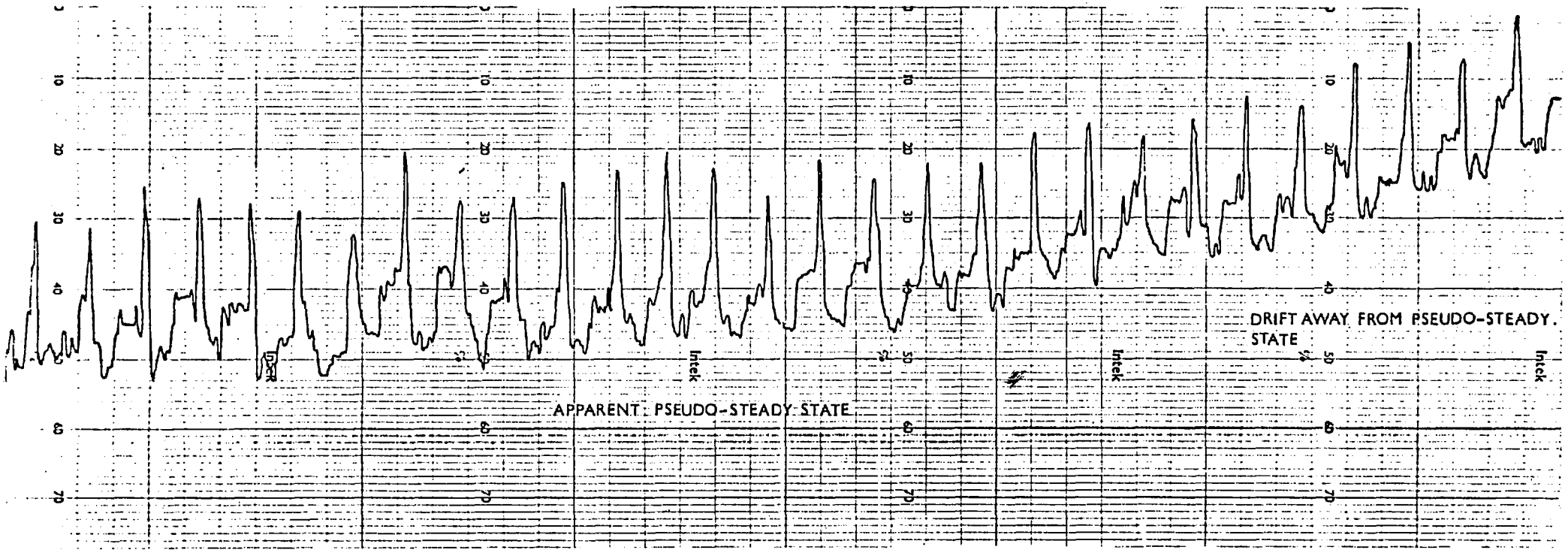

FIGURE 6.1.2-9 Liquid concentration profile of the exit stream showing the drift away from pseudo-steady state conditions with resin build up

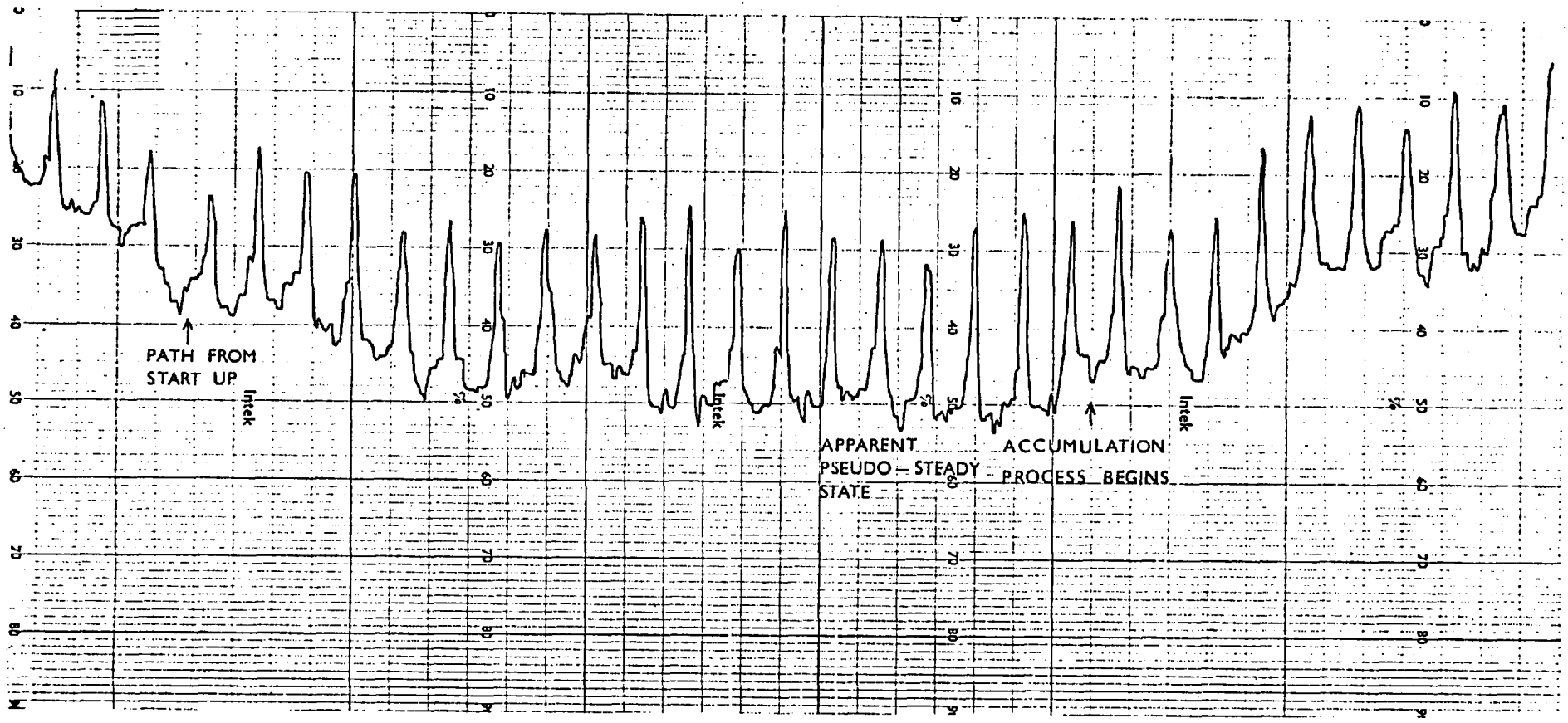

FIGURE 6.1.2–10 Liquid concentration profile for the exit stream illustrating the accumulation of resin effect after apparently achieving stability.

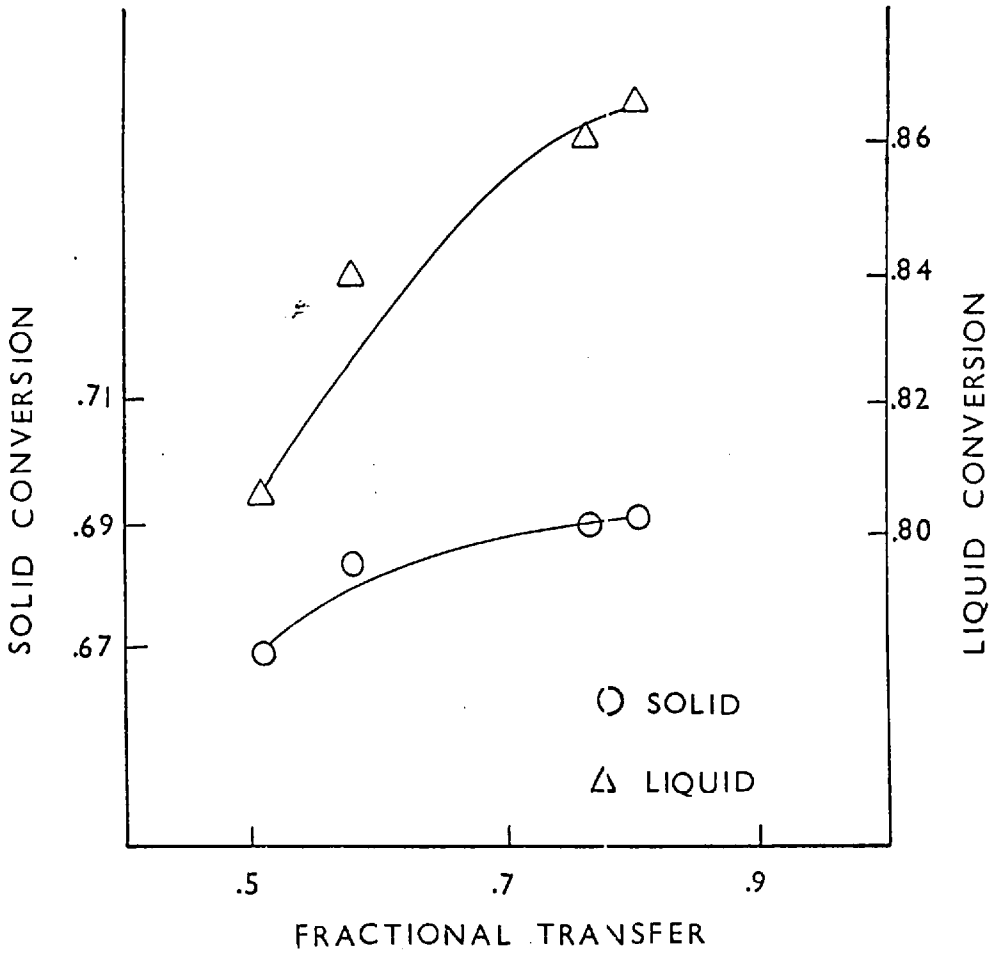

FIGURE 6.1.2-11 The effect of fractional transfer on solid and liquid conversions.

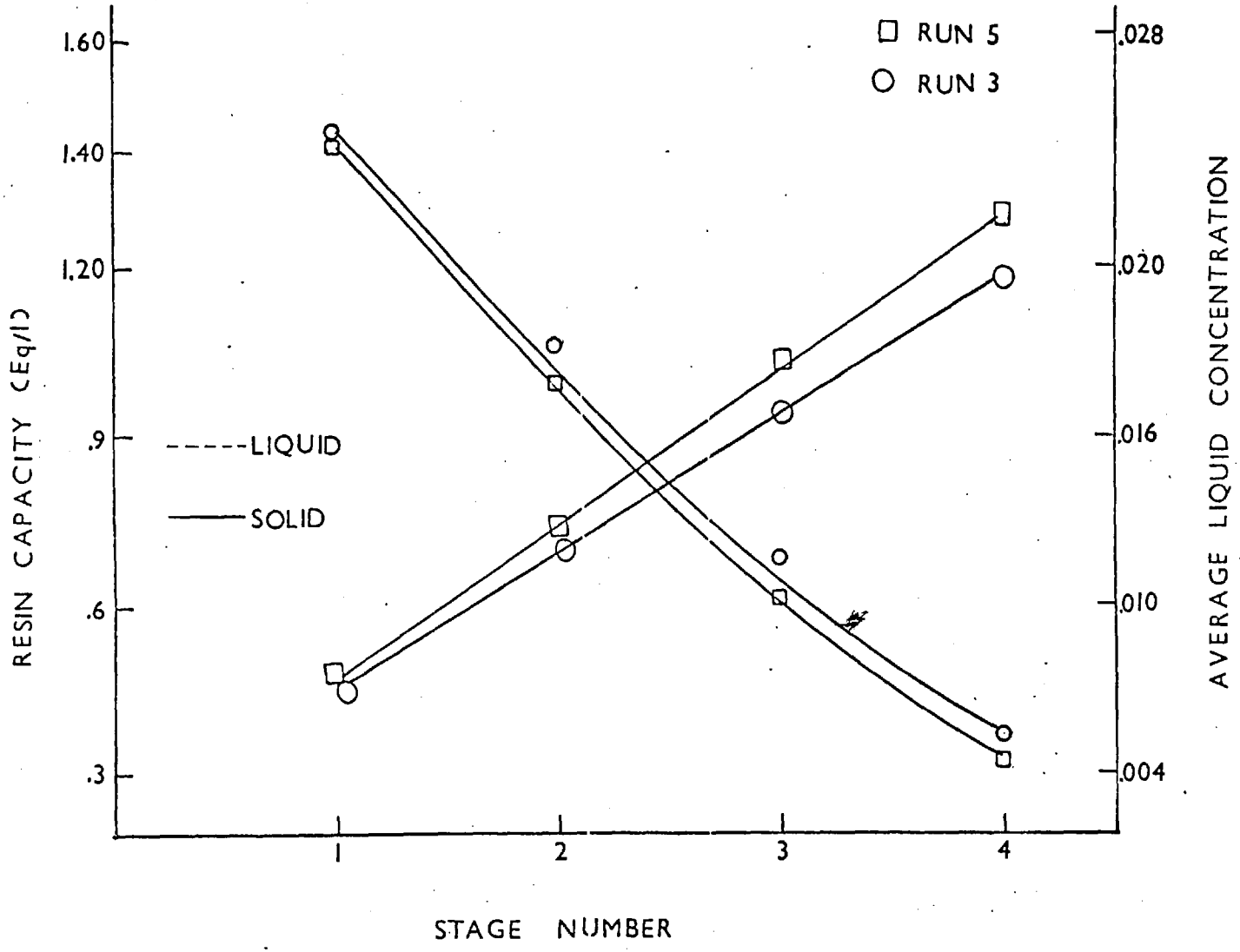

FIGURE 6.1.2-12 Solid capacity and time average liquid concentration profiles along the column.

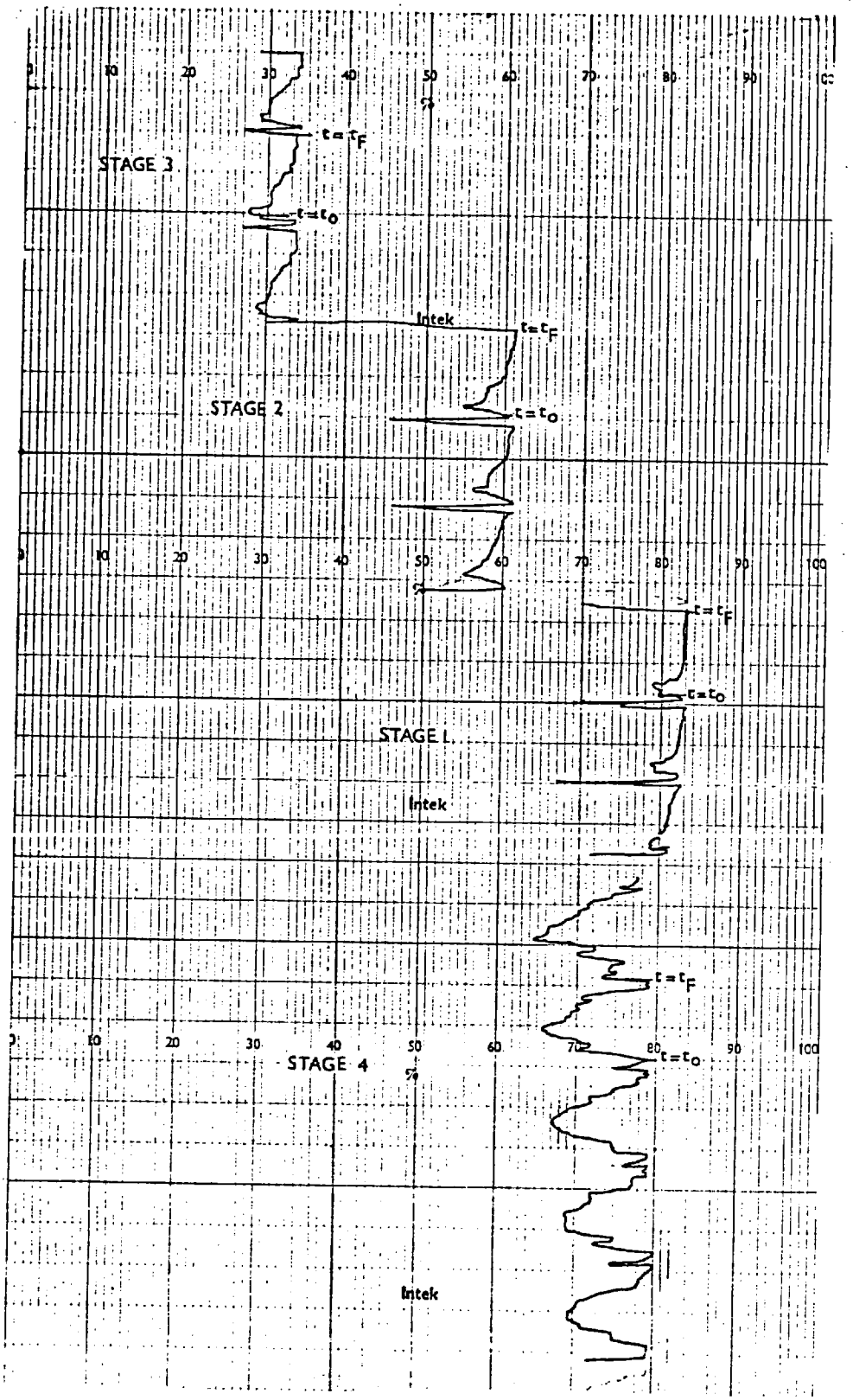

FIGURE 6.1.2-13 Pseudo-steady state liquid concentration profiles for run 5.

6.1.3 High Concentration Experiments

A series of experiments with liquid feed concentrations of 0.1 N were performed in order to obtain data of the operation of contactor under conditions of intra-particle diffusion control of the rate of ion exchange.

In order to avoid total saturation of particles, the column was reduced to a three stage system. Higher resin and liquid flow rates were also required to diminish residence times and reduce the degree of saturation.

Results for five of these runs are shown in Table (8), Appendix C.1. Pseudo-steady state was always obtained although in general more cycles were required when compared with the lower feed concentration runs. Resin concentration profiles along the column are markedly different from those in lower concentrations experiments as shown in Figure (6.1.3-1).

Resin conversion profiles for two typical runs are also shown in Figure (6.1.3-1). There, it is seen that conversion changes between stages 3 and 2 is at least 0.4, whereas the change between 1 and 2 is less than 0.15. This indicates that less reaction has taken place at the bottom stage where the average conversion at the end of the forward flow is around 0.87. This demonstrates that under these conditions of high liquid concentration, the rate of reaction becomes conversion dependent.

In Figure (6.1.3-2) is shown resin capacity and conversion profiles along the column, for run 4. A fictitious '4th' stage, that represents the solids feed, has been added in order to examine the behaviour of stages 2 and 3. These stages operate at resin conversions of 0.7 and 0.4 and can be compared with the results for run 5 of the previous series. There, Figure (6.1.2-12) shows that stage 1 operates at a resin conversion of 0.7 and stages 2 and 3 at conversions 0.53 and 0.35 respectively. It is noteworthy to compare the solid composition profiles of Figures (6.1.2-12) and (6.1.3-2). In the first figure, a linear profile is seen, whereas a curved one is depicted in the second figure. This indicates that although in both cases, the resin conversion levels are similar, the rate of reaction obeys different laws. Note that the inlet liquid concentrations for stages 1 and 2 of run 5 are .036 N and .027 N, whereas for stages 2 and 3 for run 4 of the present series, the concentrations are 0.084 and 0.0640

respectively.

Comparison between runs is difficult since reproducibility in the resin hold ups was not obtained. Furthermore, only cycles of 25 and 30 seconds for forward flow were possible since shorter runs were unstable, and those longer than 30 seconds led to particle saturation. However, a rough comparison of run 5 with all others shows that the 30 seconds run lowers the performance of the column as measured by the average exit liquid conversion.

Comparing runs 4 and 5 one sees that the increase of fractional transfer from 0.66 to 0.75 diminished the liquid conversion from 63.6% to 59.3%. For the case of run 5, the operating resin conversions of the stages are higher than in run 4, thus, a reduction of the rate of reaction can be expected.

Experimental inter stage concentrations for the liquid phase are not shown because the plate conductivity probes readings at high concentration were rather unstable; therefore, the recordings obtained, did not truly represent the concentration changes taking place in the column. However, calculated profiles (from resin data) are plotted in Figure (6.1.3-3) for runs 3 and 4. The convex liquid profiles are expected, since, as discussed above, little reaction takes place at the bottom of the column.

The cyclic behaviour of the column can be seen in Figure (6.1.3.4) where the pseudo-steady liquid profile for stage 3 (exit of column) is shown.

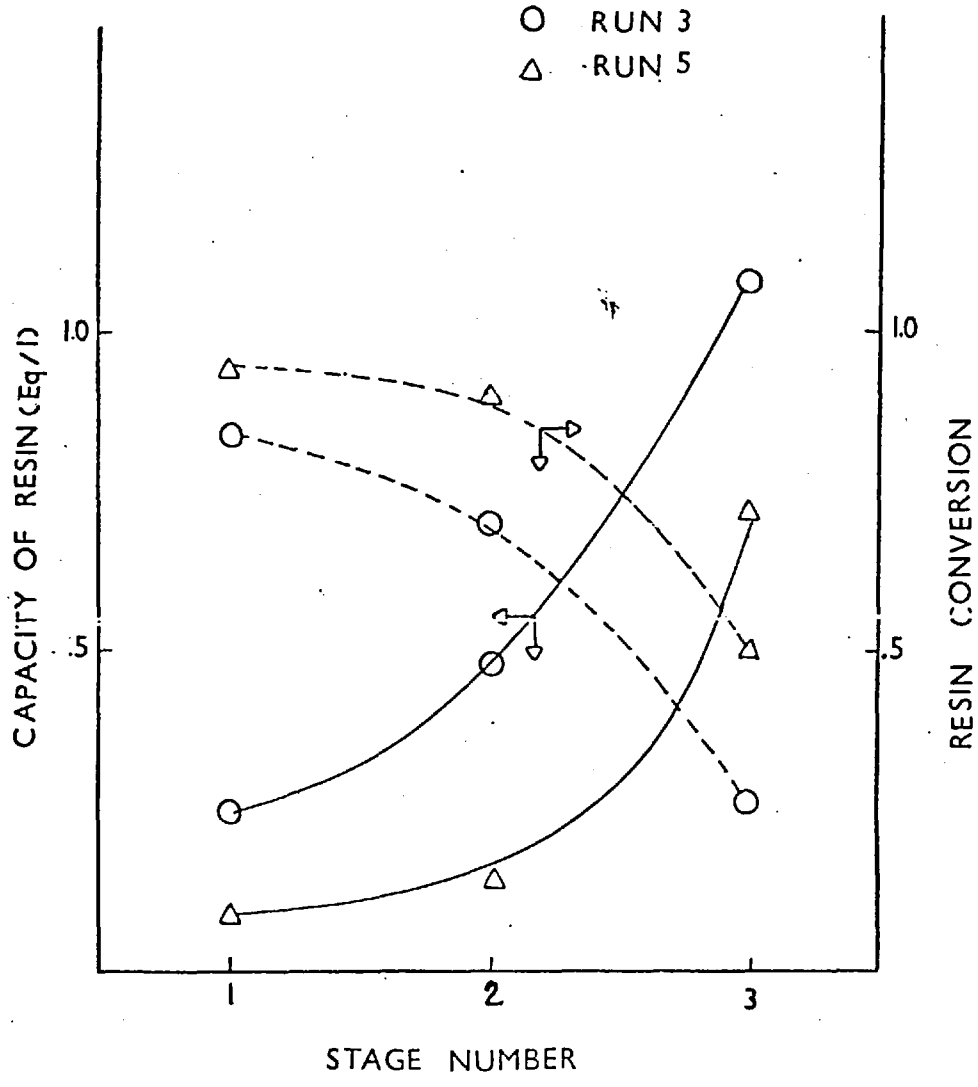

FIGURE 6.1.3-1 Resin conversion and capacity profiles along the column.

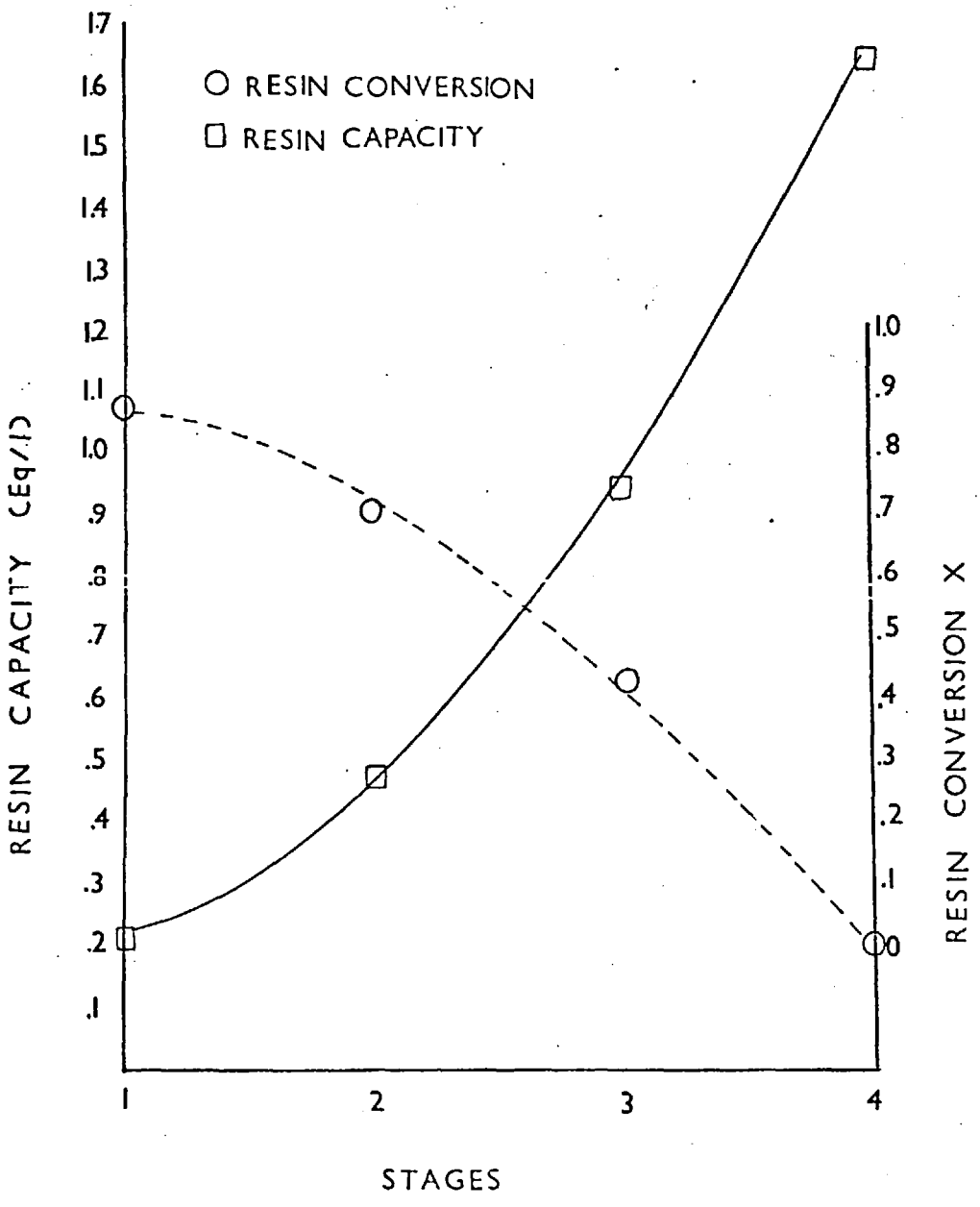

FIGURE 6.1.3-2 Resin capacity and conversion profiles along the column including fictitious 4th stage.

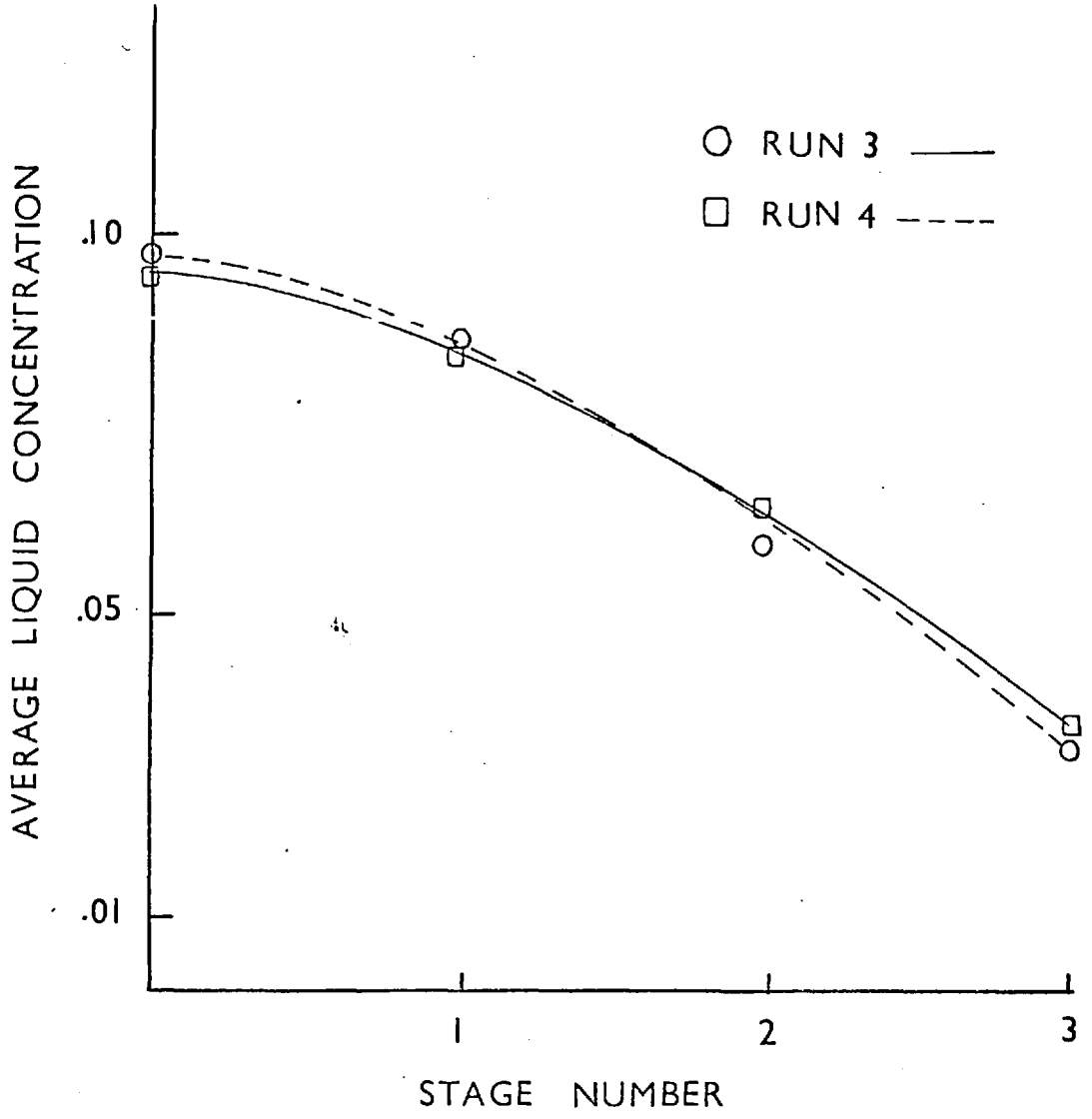

FIGURE 6.1.3-3 Calculated liquid concentration profiles along the column.

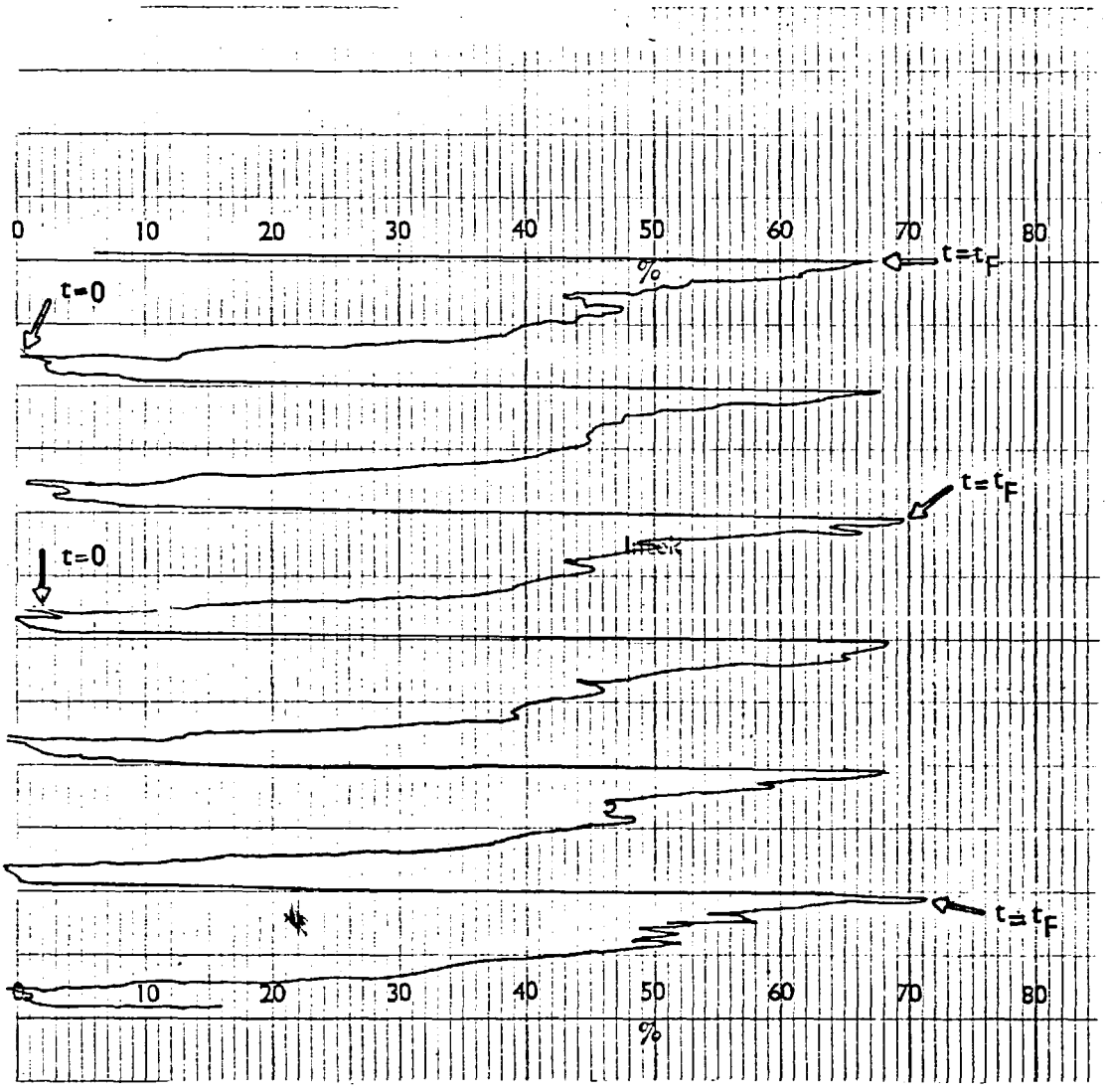

FIGURE 6.1.3—4 Liquid concentration profile of the top stage illustrating the pseudo-steady state operation for run 5.

6.2 Theoretical Results

Several computer programmes were implemented based on the solution algorithms described in Chapter 4. Diagrammatic flow charts of the programmes are given in Appendix D.

In order to test the models over the range of experimental conditions studied, simulation runs were performed for each of the experimental series described in sections 6.1.2 and 6.1.3.

For the film diffusion controlled runs (C_0 = 0.02 N - 0.036 N) the method of characteristics described in section 4.1.1, was applied. The mass transfer coefficients were estimated using Equation (3.3.1-7), with a value for ψ of 0.86 taken from reference (75). The procedure and data used in the calculation of the coefficients are shown in Appendix C.2.

In the case of intraparticle diffusion controlled runs, the parameter k_D of the simplified rate expression given by Equation (3.3.3-3) was obtained from the best linear fit as described in section 3.3.3. The value obtained was k'_D = 1.99. A value for the intraparticle diffusivity for H^+ was taken from reference (73); there, the value of the coefficient for particles of similar size as the ones used here is given as $D_{H+} = 1.07 \times 10^{-9}$ m^2/s.

The method of the moments of the distribution was tested simulating some of the preliminary runs (section 6.1.1) which used low liquid feed concentrations ($C_0 \sim 0.01$ N) and thus, were expected to produce little resin saturation.

6.2.1 Use of the Method of Characteristics

It was known that increasing the number of characteristics improved the accuracy of the method but at the cost of more computing time. Since many simulation runs were to be performed it was therefore important to determine a number of characteristics which would be a compromise between the two extremes of excessive computing time and low degree of accuracy. Hence, simulation runs were performed using typical experimental data (run 3, table 6 of Appendix C.3) varying the number of characteristics between 25 and 350.

The results of the tests are shown in figure (6.2.1-1), where the number of characteristics is plotted versus the average exit liquid concentration. In the same graph, the central processor time required for each run is also shown. There, it is seen that as the number of characteristics increases, the liquid concentration approaches asymptotically to the value of 0.00381 while the computing time rises rapidly. From these results, the use of 100 characteristics for the simulations was chosen, since the difference in the exit composition with the 350 characteristics run is only 0.8 per cent, while the computing time required is one tenth that for 350 characteristics.

For these runs, the relaxation method was used to find the pseudo steady-state. In general, the number of cycles required to attain p.s.s., varied among the different runs, but tended to diminish as the cycle time increased. It was also found that if the initial resin conversion distribution was taken as $f(x,0) = 1/n$ instead of $f(x,0) = 0.0$, fewer iterations were needed, although the difference was only a few cycles.

Low liquid feed concentration runs

Simulation results for the first series of experimental runs ($C_o = 0.02$) are given in Table (1) of Appendix C.3. In Figure (6.2.1-2) a comparison between theoretical and experimental average exit liquid conversions as a function of fractional transfer is shown. A fairly good agreement between predicted and experimental values is observed for this series. Figure (6.2.1-3) depicts the theoretical and experimental liquid concentration profiles along the column for runs 2 and 4 of the present series. Here again a good agreement is found although the predicted values of the average concentration for the lower stages are about 10% lower than the experimental values. Since the model uses average values of fractional transfer, voidage and mass transfer coefficient, these results are expected. For instance, in the case of run 2 the value of the average voidage used is 0.922 but the actual value for the bottom stage is 0.935. This indicates that the model assumes a higher resin hold up in the bottom stage and explains why the predicted value of the average exit composition of stage one is less than the experimental value. It should also be pointed out that, in practice, at high values of fractional transfer, by-passing of resin from stage j to stage j-2, during the transfer of solids period, is more likely; this would also lead to higher differences between theoretical and experimental values.

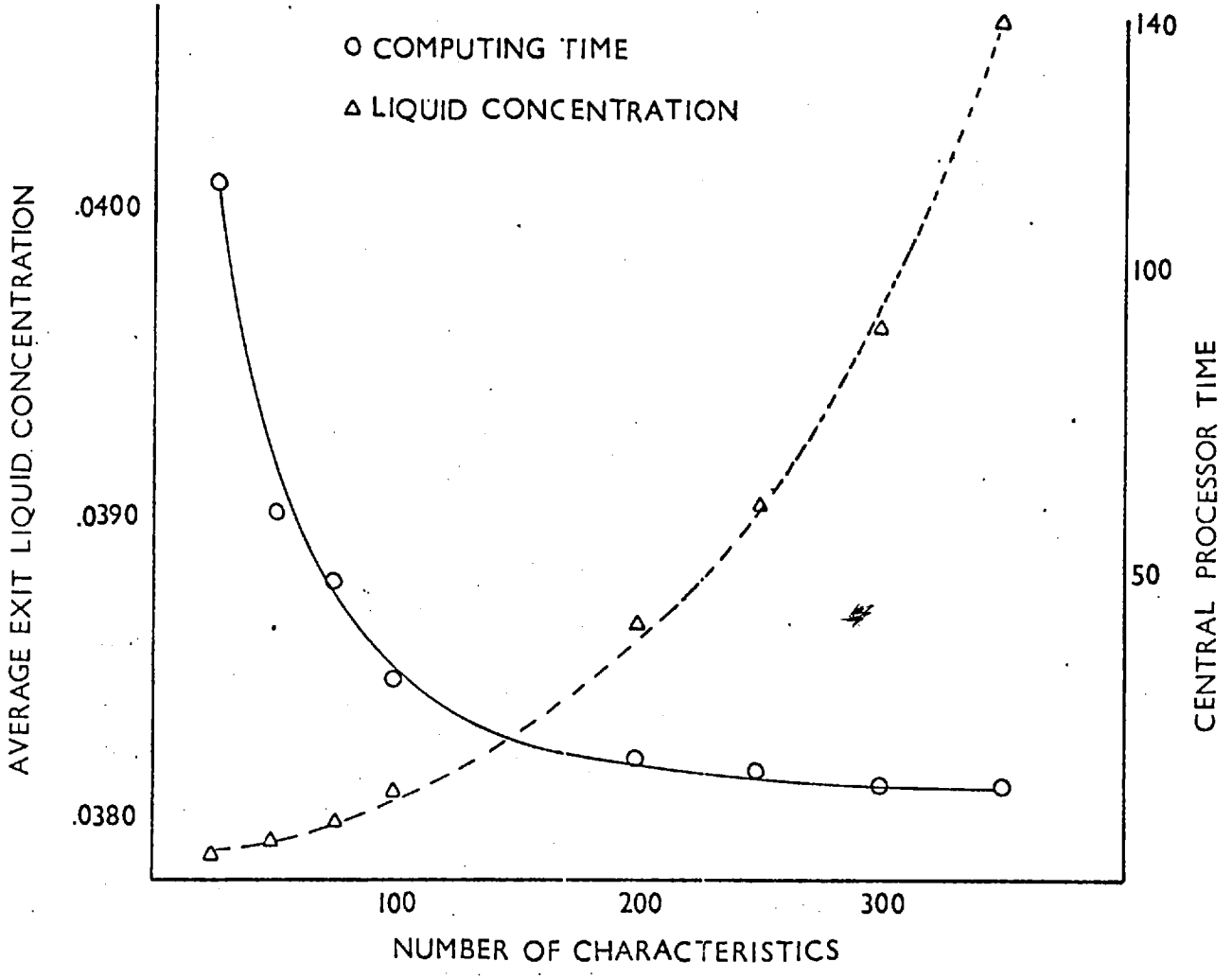

FIGURE 6.2.1-1 The average exit liquid composition and the required computing time as a function of the number of charactics.

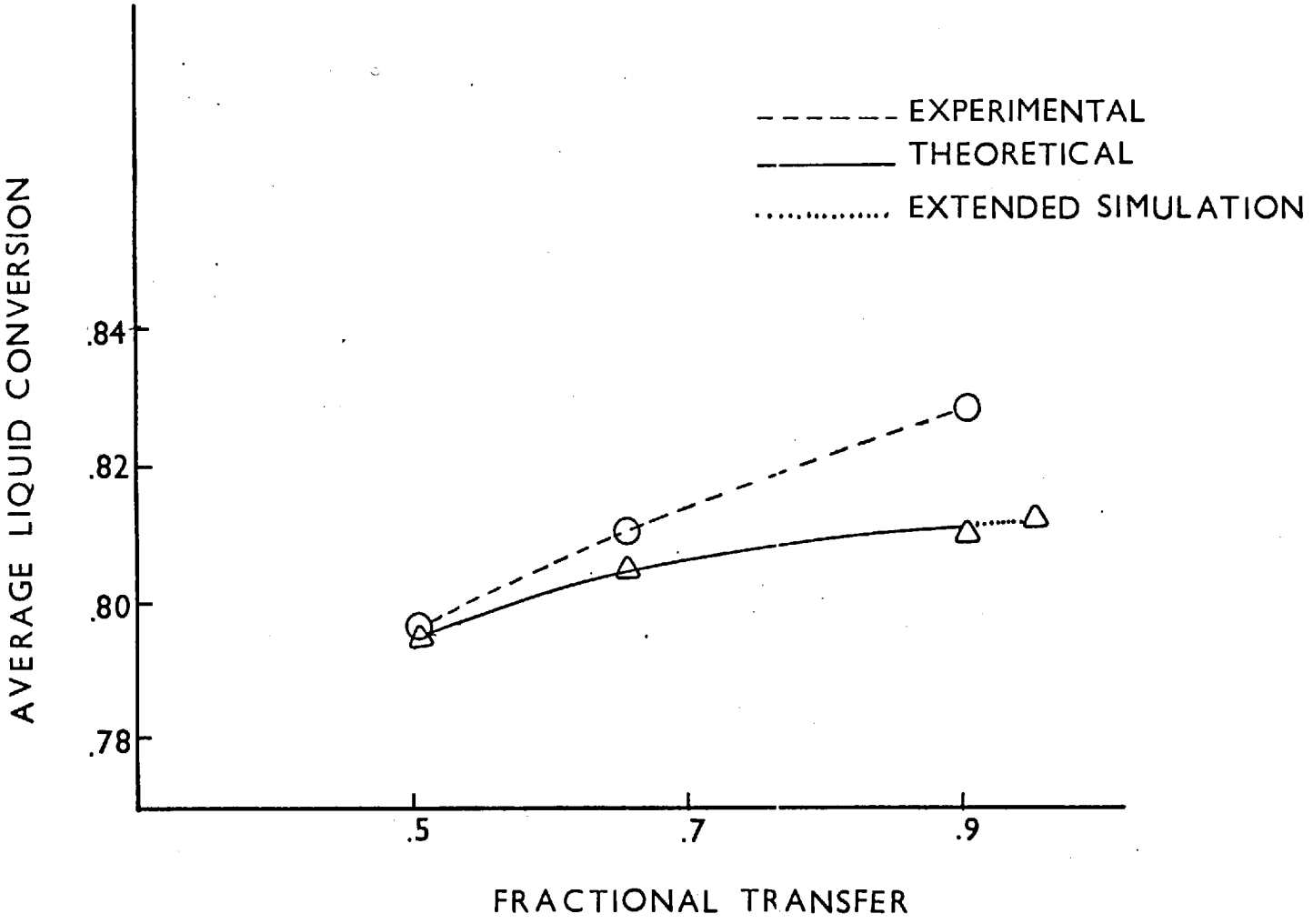

FIGURE 6.2.1-2 Comparison of experimental and theoretical exit liquid conversions as a function of fractional transfer

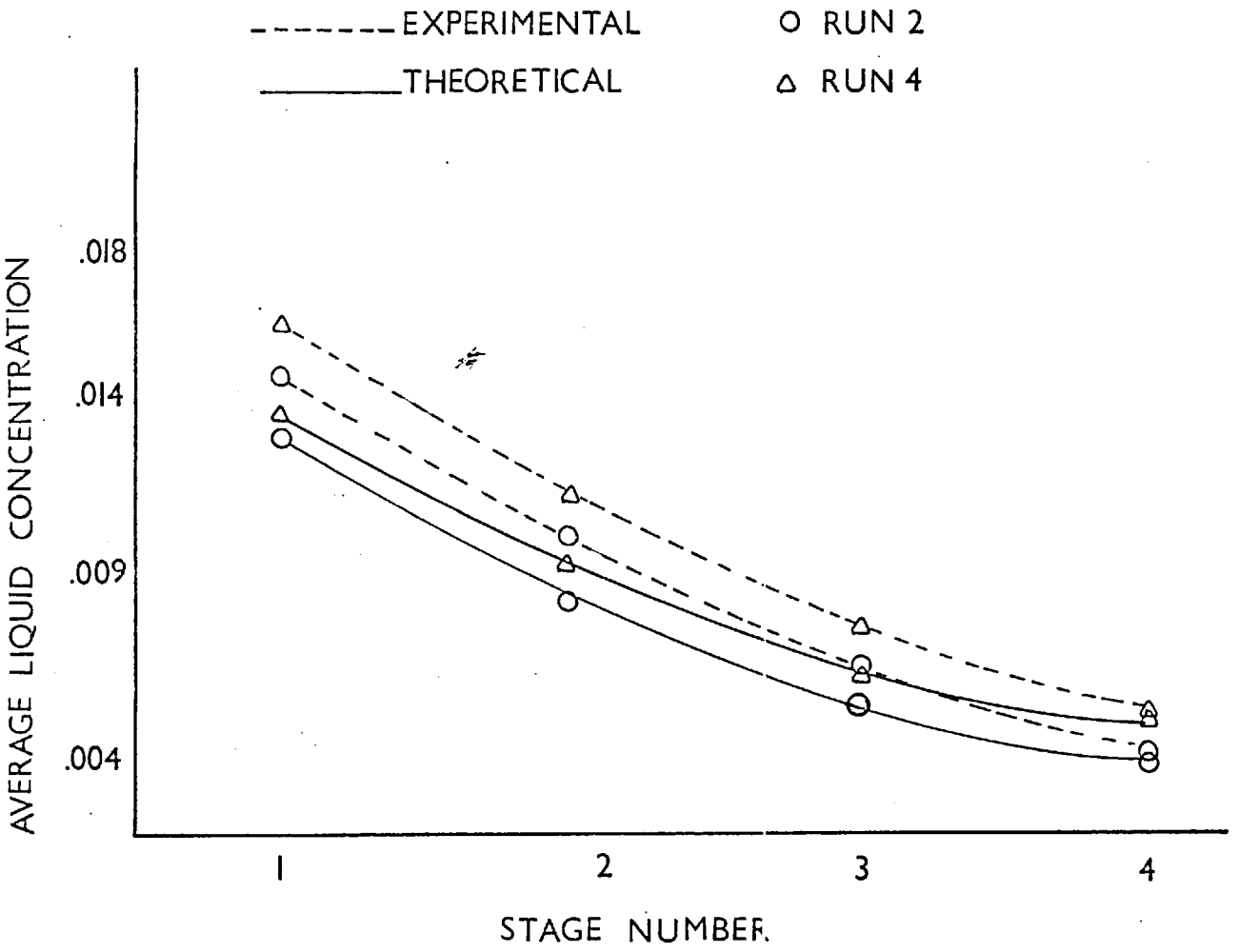

FIGURE 6.2.1–3 Comparison of experimental and theoretical liquid concentration profiles along the column

Figure (6.2.1-4) illustrates the simulated start up and periodic operation for the case of run 6. There it is seen that p.s.s. for the liquid composition is obtained in about 10 cycles. The initial conditions here were resin totally regenerated ($f(x,0) = 0.0$) and $C_0 = 0.0201$. The initial steep drop of concentration results from the contacting of fresh resin with the liquid. Then, the concentration remains at a steady low value while the resin conversion profiles build up. Later the effect of the periodic additions of resin is observed.

For the second series of experiments ($C_0 = 0.03$), the results of the simulation runs are presented in Table (2) of Appendix C.3 and are compared with experimental results in Figures (6.2.1-5) and (6.2.1-6).

In the first figure, the performance of the system versus the fractional transfer is shown. A good agreement between predicted and experimental values was again obtained. The maximum deviation between these two values was about 7 per cent. A comparison of theoretical and experimental average liquid concentration profiles along the contactor, is given in Figure (6.2.1-6). There, it is observed that the model predicted fairly well the concentration changes that take place in the column. It can also be noted that for all cases (stages and runs) the theoretical performance falls short of the experimental. This was indicative that a common factor affected the predicted behaviour of the system. The two more likely aspects of the model which would lead to these results are:

i) a deviation from the assumption of perfectly mixed liquid in all stages and

ii) errors in estimating the mass transfer coefficient.

It should be noted that an important quantity in calculating this coefficient, is the voidage of the fluidized bed. This, in turn, depends upon the height of the fluidized bed which could only be measured with 6 per cent accuracy.

The simulation results for the third series, that is, runs with a liquid feed concentration of 0.036 N are presented in Table (3). Comparisons with the corresponding experimental runs are shown in Figures (6.2.1-7) and (6.2.1-8).

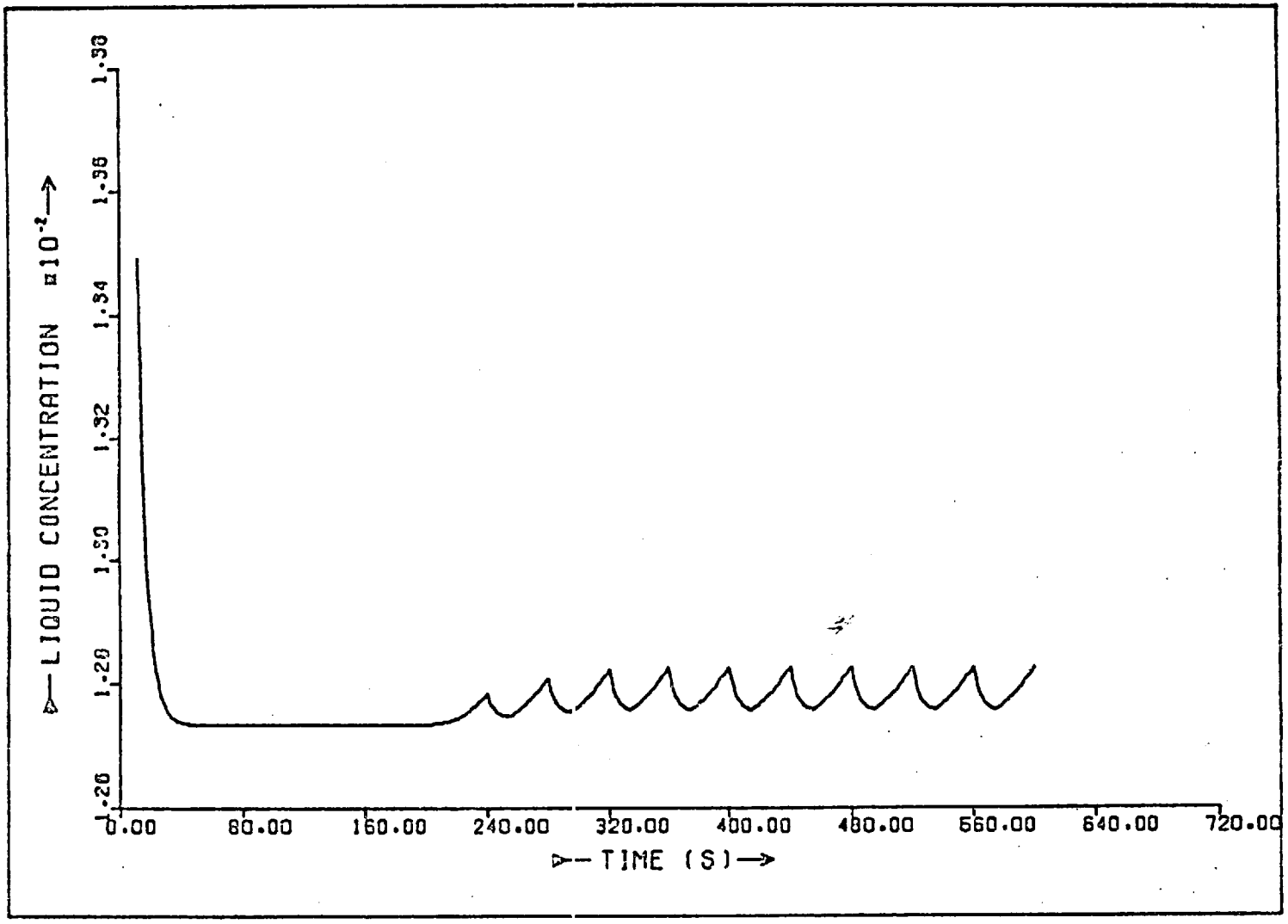

FIGURE 6.2.1-4 SIMULATED START UP AND PERIODIC OPERATION

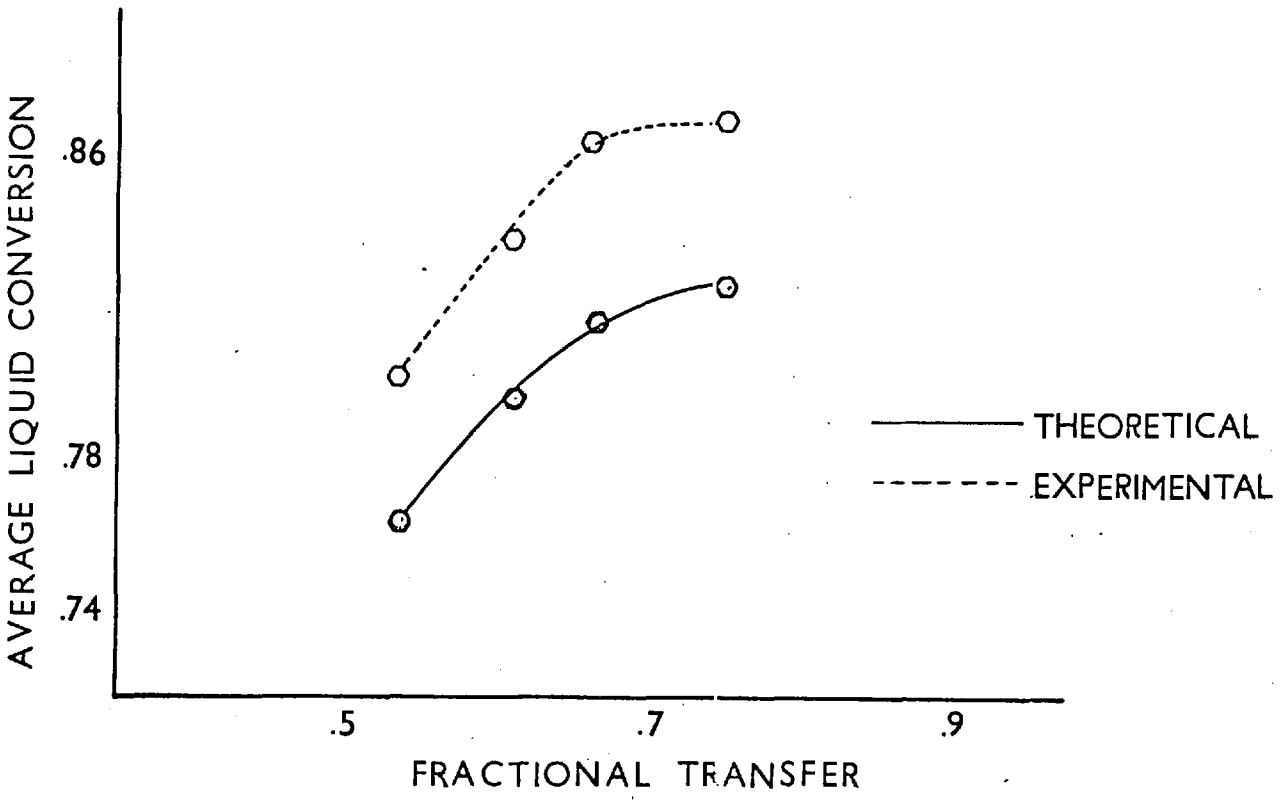

FIGURE 6.2.1-5 Predicted and experimental exit liquid conversions and fractional transfer

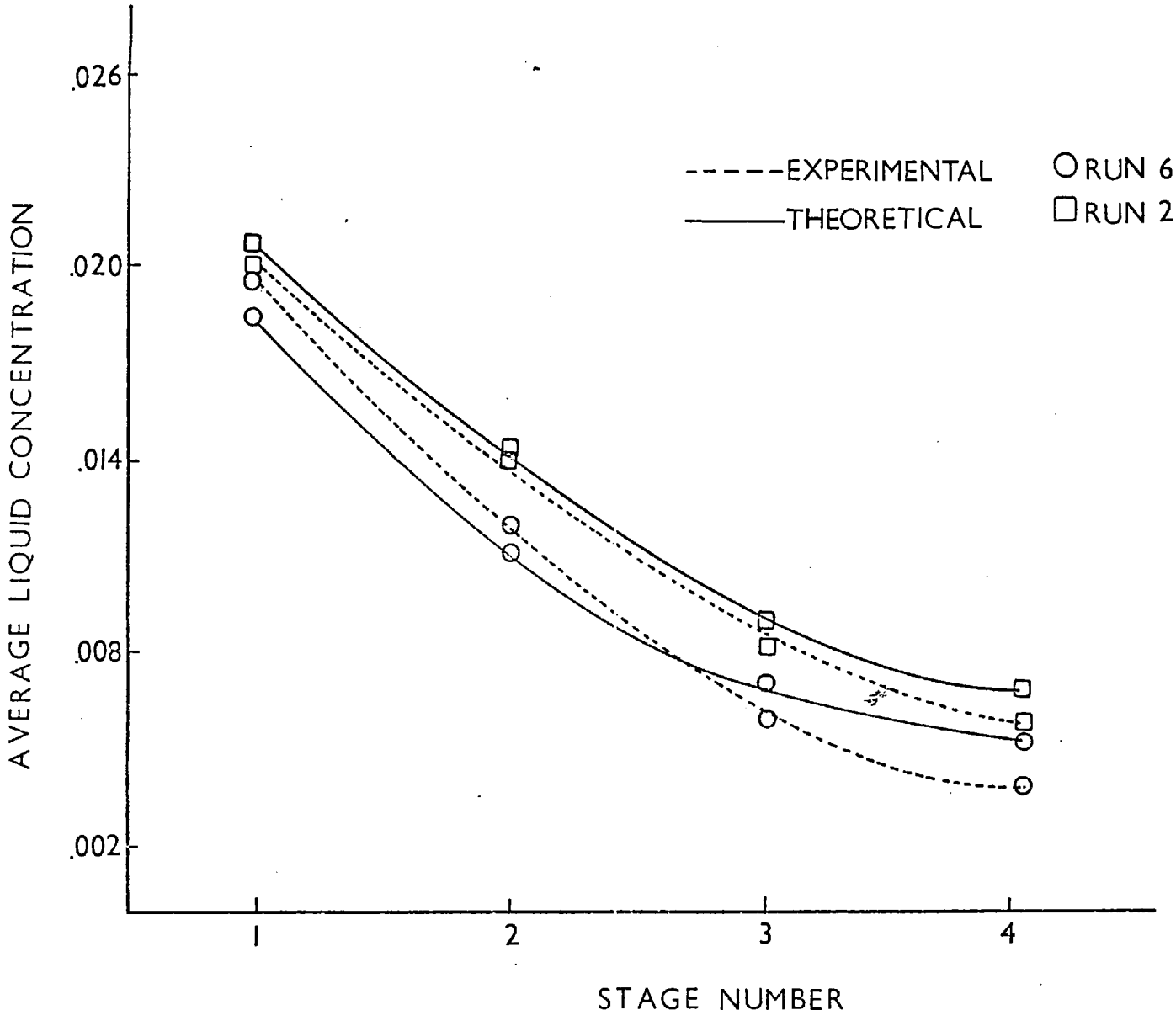

FIGURE 6.2.1-6 Comparison of theoretical and experimental liquid profiles

In Figure (6.2.1-7), predicted and experimental average exit liquid conversions as a function of fractional transfer are compared. The general trend of enhanced performance as the fractional transfer is increased is seen to be adequately predicted by the model. The maximum error between theoretical and experimental values is in this case about 9 per cent, a slight increase over the errors obtained in the previous series. Liquid profiles along the column are shown in Figure (6.2.1-8).

In the discussion of the experimental results for this series, it was mentioned that the resin was more difficult to fluidize than in the lower concentration runs, due to its increased density. This was particularly noticeable for the lower stages of the column. Under these circumstances, the assumption of perfectly mixed liquid and solid is less applicable and greater errors in prediction can be expected. This also explains the increased inaccuracy in the present series of runs.

The transient behaviour of the liquid concentration profiles is illustrated in Figure (6.2.1-9a). There, typical profiles during a cycle at pseudo-steady state conditions are shown for all stages. The corresponding experimental profiles for the same run, are shown in Figure (6.2-1.9b). From these figures, it is seen that the predicted profiles follow the shape of the experimental ones. Exact duplication of these profiles cannot be expected due to initial errors in the conductivity readings caused by the backmix of solution from the stage above. Also, for the top stage, the accumulation of entrained water with the resin feed during solids transfer, affects the reading during the first seconds of the cycle.

The resin distributions for the same run are depicted in Figure (6.2.1-10). There the conversion distributions before and after the solids transfer is shown. This illustrates the effect of the periodic resin transfers on the shape of the distribution.

In the discussion of the experimental results it was also observed that the shape of the curves which illustrated the effect of the fractional transfer on the column performance, tended to level off towards the higher values of d. Due to instabilities or resin by-passing this was not pursued experimentally. Since this was an important aspect of the behaviour of the system, a theoretical study was undertaken.

The study consisted of increasing the fractional transfer beyond the

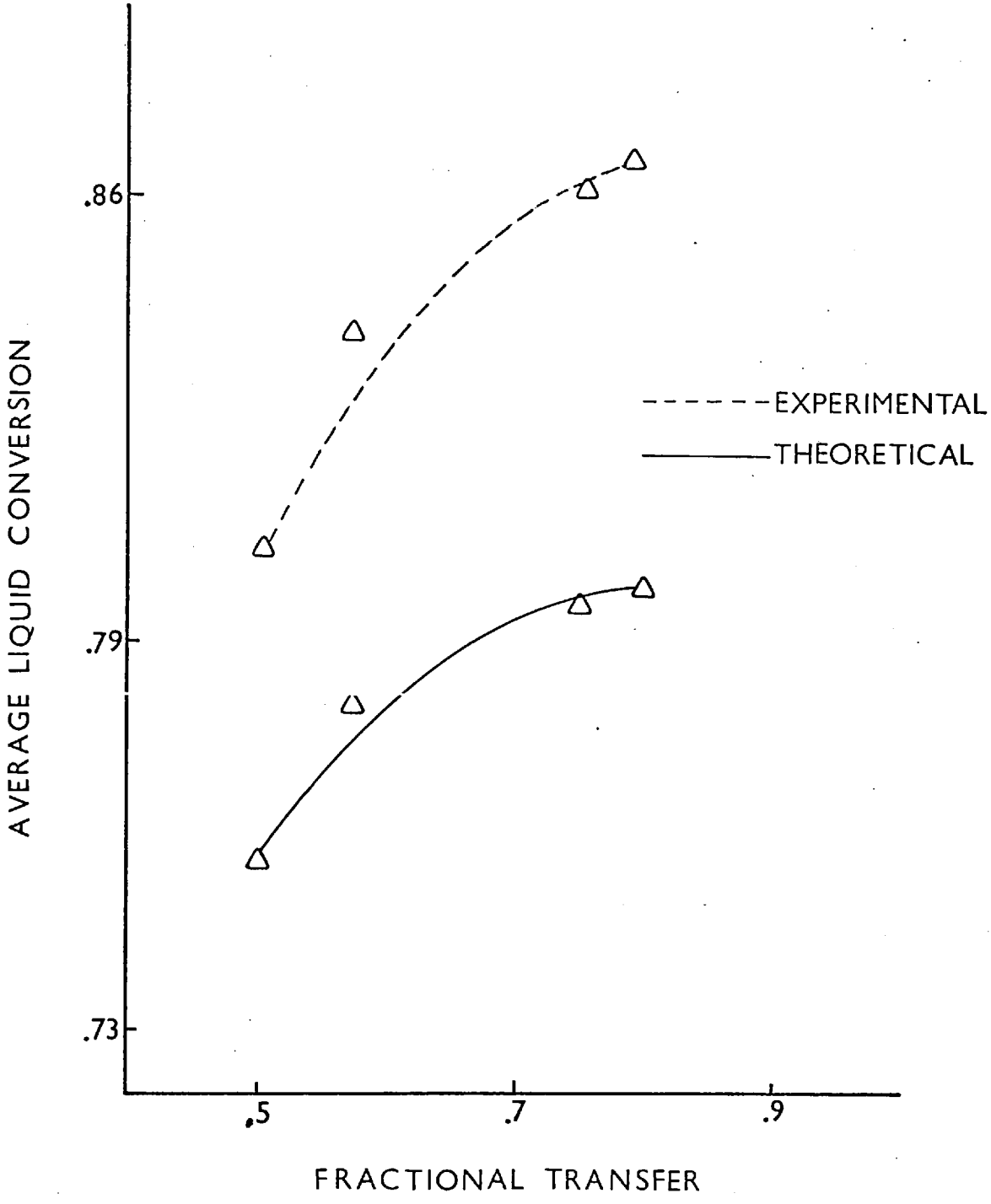

FIGURE 6.2.1-7 Theoretical and experimental liquid conversions as a function of fractional transfer.

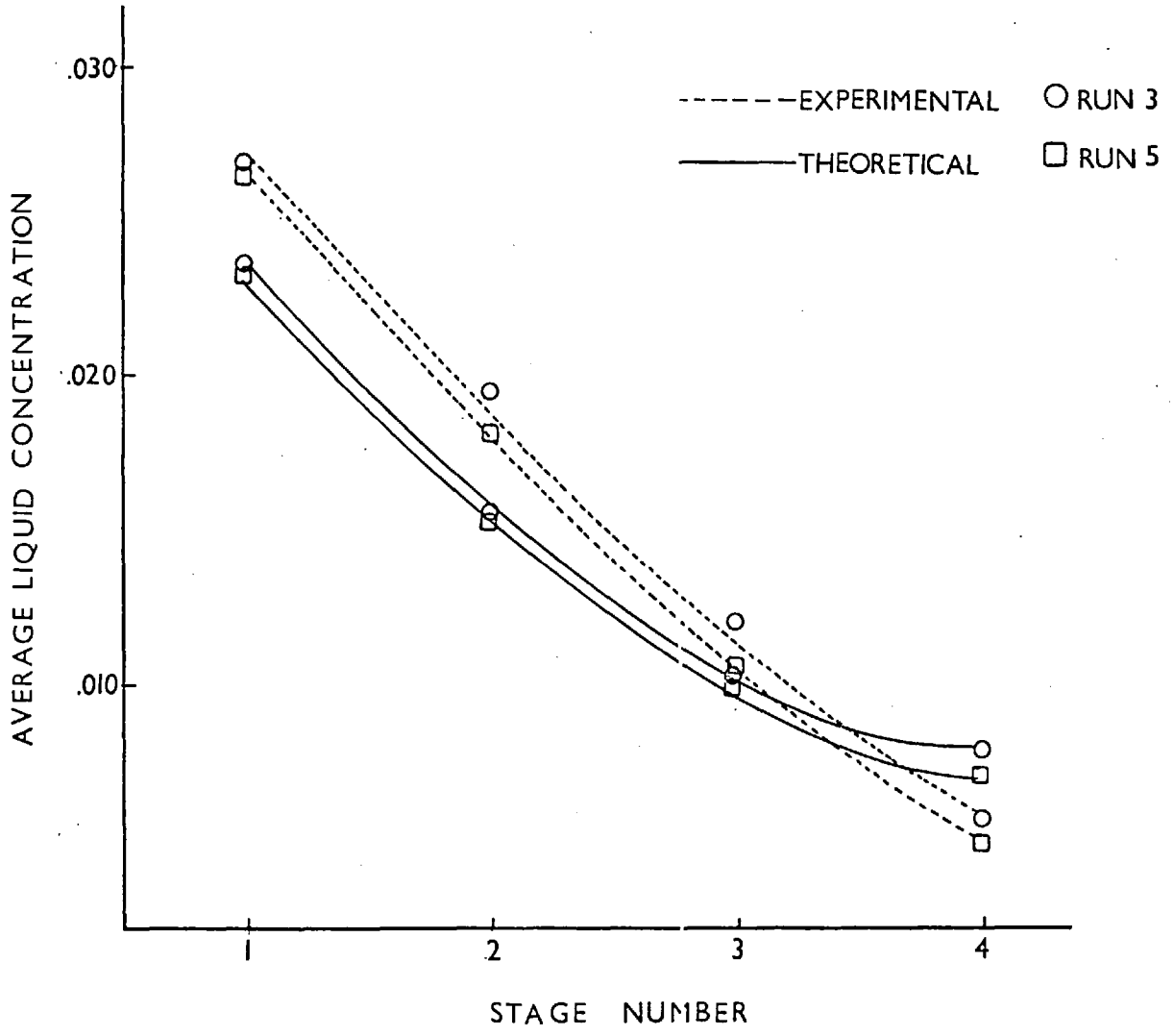

FIGURE 6.2.1-8 Comparison of experimental and theoretical liquid concentration profiles along the column.

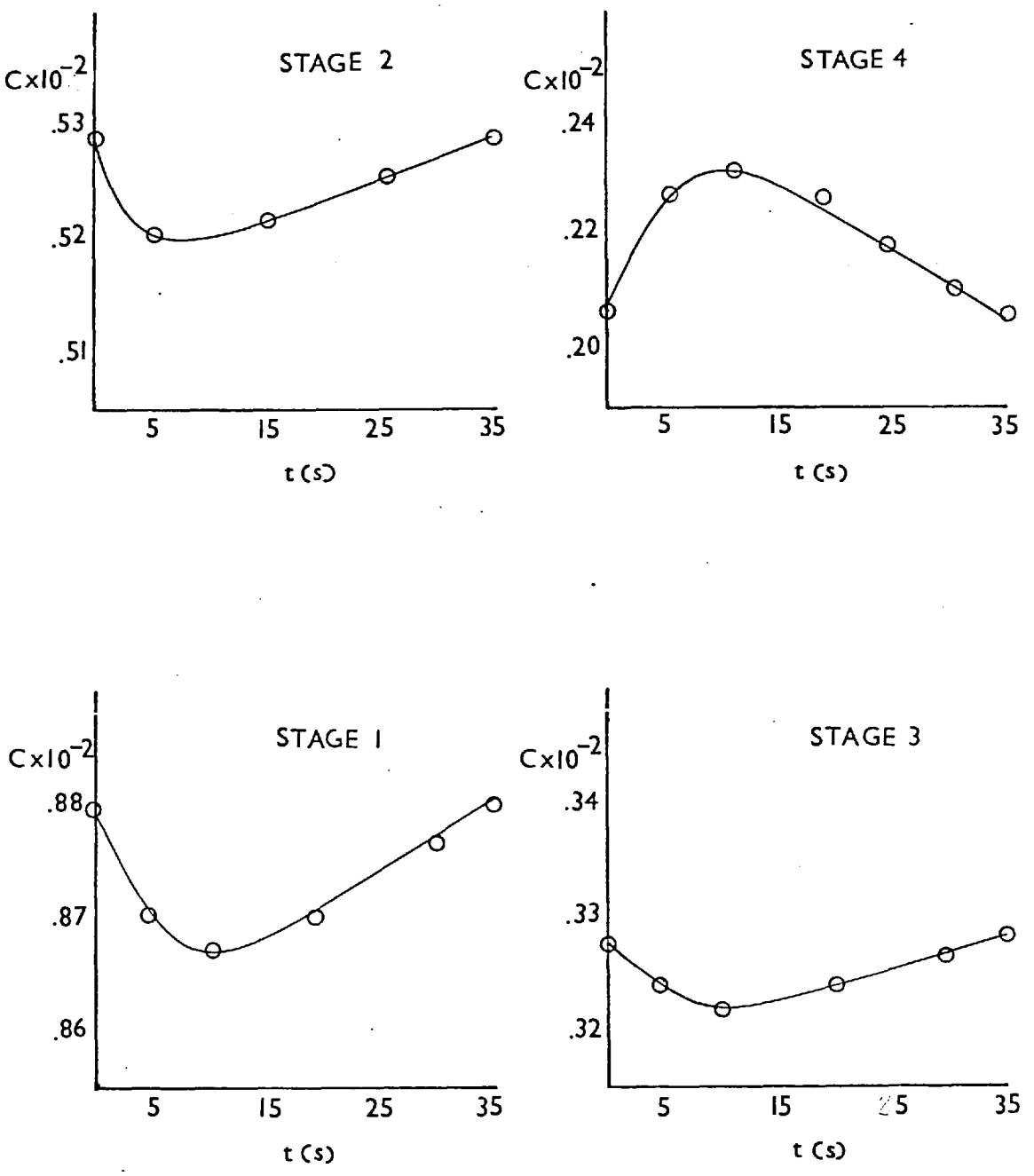

FIGURE 6.2.1-9a Typical transient liquid concentration profiles during a cycle.

FIGURE 6.2.1-9b Experimental transient liquid concentration profiles during a cycle.

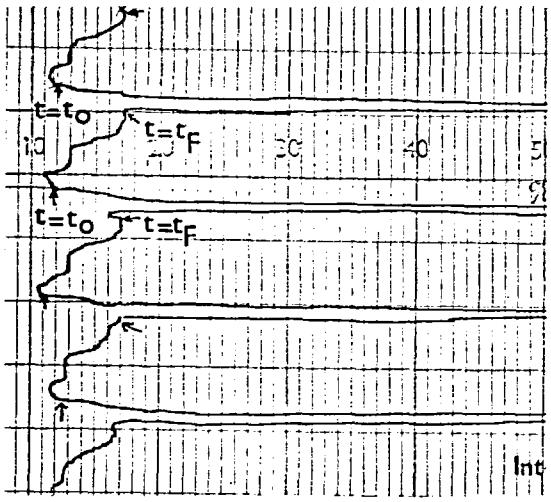

STAGE 3

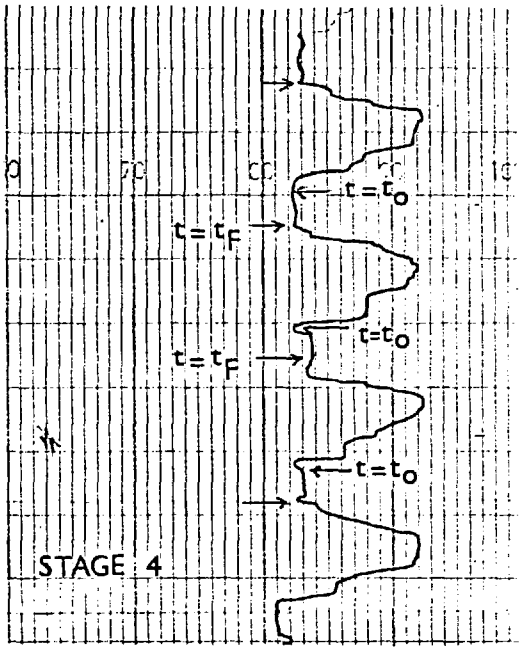

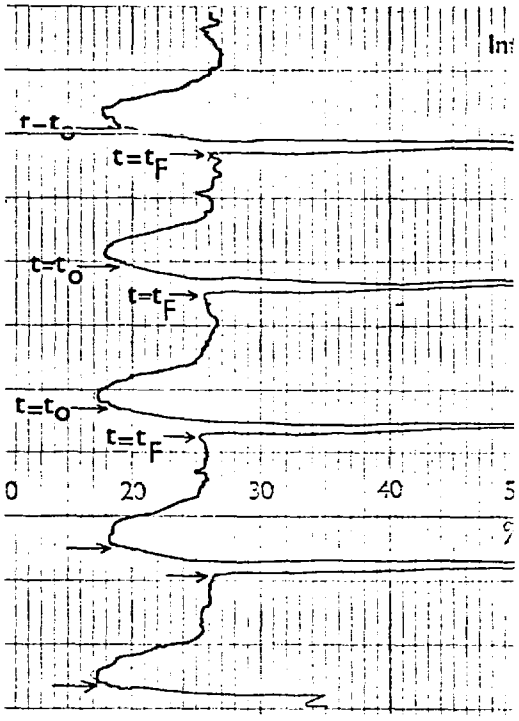

STAGE 2

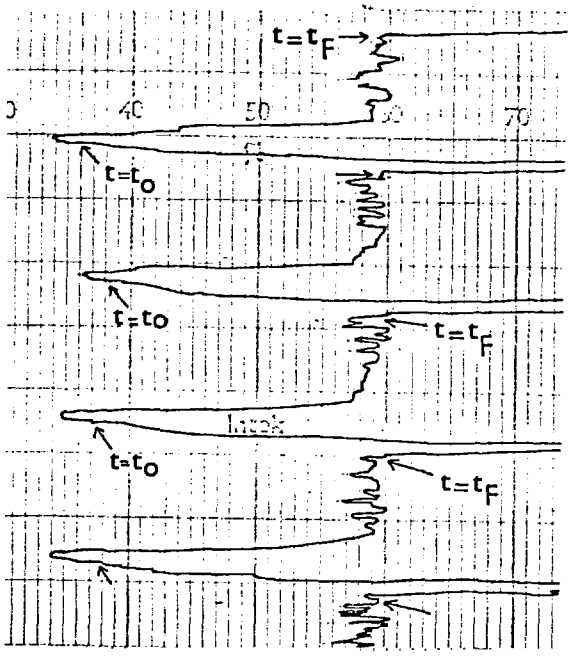

STAGE 1

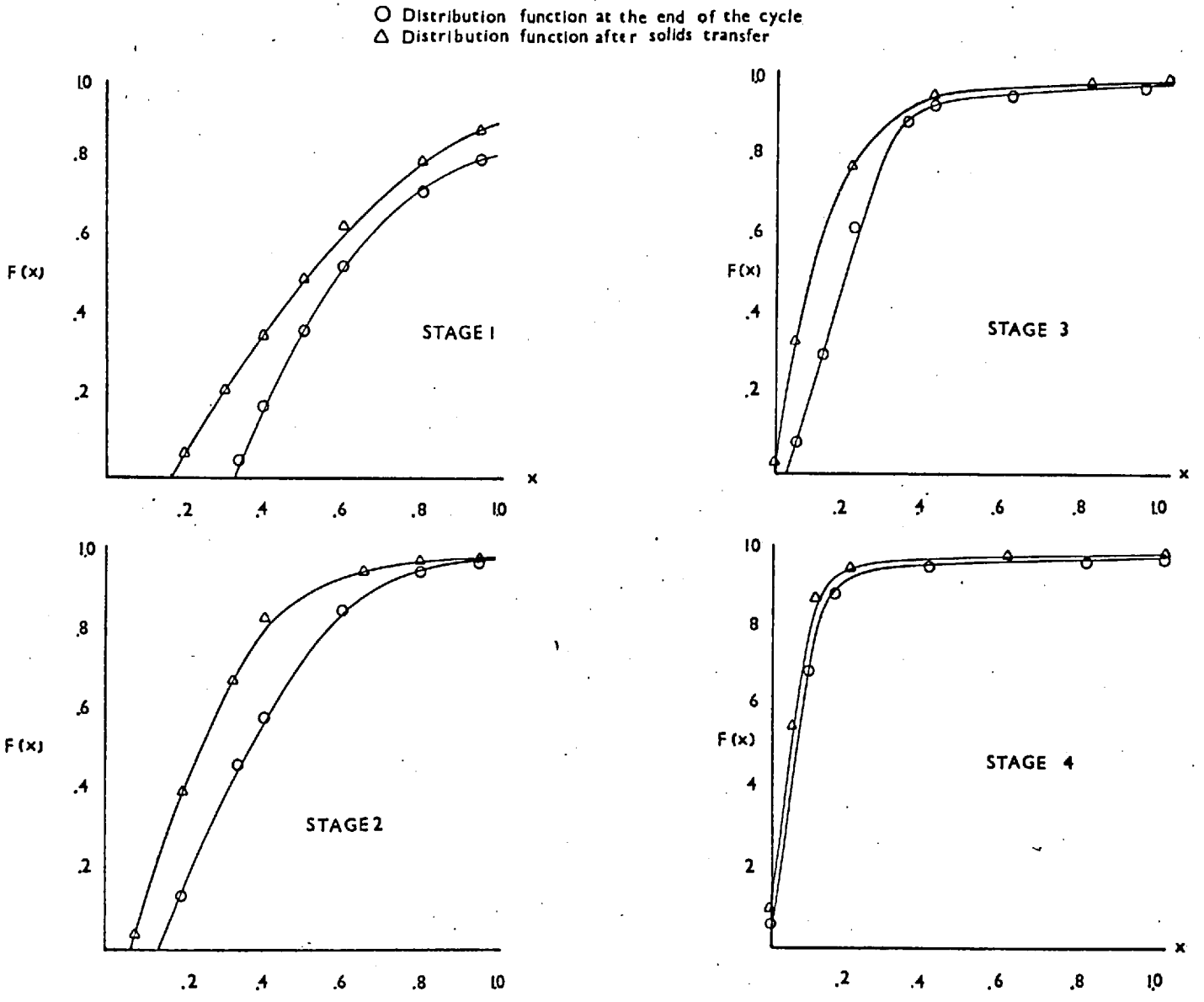

FIGURE 6.2.1-10 Movement of the cumulative conversion distribution function F(x) during a cycle

values reached in the experiments following the same criterion used in the experimental plan (see section 5.1). This criterion required that the controls were varied in such a way that the ratio T/d and all other parameters were kept constant.

The study was first applied to the data of run 5 belonging to the series with C_0 = 0.02 N. Here, the fractional transfer was increased from the experimental value of 0.9 to 0.95; the correspondent cycle time increase gave t_F = 422 . All other parameters were taken equal to those of run 5. The results are included in Table (1) of Appendix (C.3) with the other simulation results for the series. They are also shown in Figure (6.2.1-2) by the dotted line. There it is seen that the same tendency is followed and the liquid conversion is only marginally improved from 81.0% to 81.2%.

A similar study was performed with the second series of runs (C_0 = 0.03 N). In this case, the fractional transfer was increased from the highest experimental value of 0.75 (run 6) up to 0.925. All other parameters and the value of T/d were kept equal to those of run 6. The result from these simulations are given in Table (2) of Appendix (C.3) and depicted in Figure (6.2.1-11). In this graph, the continuous line illustrates the effect of fractional transfer on the system performance. As in the previous case, the curve tended to level off at higher values of fractional transfer.

In examining the reason for this behaviour it was noted that when increasing the value of d, the improvement of the performance obtained for the top stage was out of line with the kind of improvements achieved in the other stages. For instance, considering the runs shown in Figure (6.2.1-11) when increasing the fractional transfer from 0.75 to 0.84, the improvement of the stage performance is around 4.0 per cent for the lower three stages of column, whereas an improvement of only 2.0 per cent registered for the whole column. An explanation for this behaviour can be found by noting that after the solids transfer period, the top stage is in fact depleted of solid during the initial part of the cycle. Hence, the total exchange capacity of the system is somewhat diminished and the enhanced performance of the lower stages is hindered by the top stage initial inefficiency.

For the two cases described, concave downwards curves for conversion versus fractional transfer were obtained; however, it was found that under other conditions convex curves were also possible. Following the same line

of reasoning, the latter indicated that the enhanced performance of the lower stages during the whole of the cycle, together with the performance of the top stage towards the end of the forward flow period, when its resin hold up was restored, compensated for the effect of the initial resin depletion and a higher average conversion was obtained.

Examples of both types of behaviour are shown by the continuous lines in Figure (6.2.1-12). The concave type of curves are obtained at comparatively low values of the resin residence time (T/d) which are obtained at, for instance, high values of voidage (low resin hold up levels). On the other hand, the convex curves result from higher values of T/d i.e. low ε (high resin hold ups).

In order to demonstrate that this sort of behaviour was in effect caused by the periodic depletion of the top stage, it was decided to perform a theoretical study of a system in which the resin feeding was carried out in such a way that depletion of solids at any moment was avoided.

This study consisted of simulating a system similar to what will be referred to as the 'standard' system but instead of the continuous feeding, a 5th dummy stage was used. This stage served to periodically introduce the solids into the system similar to the manner in which the solids move within the column. In other words, at the end of the forward flow period, as the solids from each stage are transferred downwards an equal amount of fresh resin is transferred from this dummy 5th stage into the 4th (real) stage.

Several conditions were used in the simulations in order to cover both cases in which the 'standard' system gave concave or convex results.

In Figure (6.2.1-13) a comparison between the standard and the modified system for the range of d from 0.2 up to 0.98 is shown. Other data used are given in Table (4). There, it is seen that for the modified system, a linear improvement of performance is obtained. Furthermore, it is noteworthy to observe that for the conditions used, the total improvement of the performance when increasing d from 0.2 to 0.98 is 6.0 percent for the modified system and only about 1.5 for the standard system. Other results are included in Figures (6.2.1-11) and (6.2.1-12) where the previously mentioned results from the standard system are compared with

the results obtained using the modified system (broken lines). Exactly the same parameters were used for each pair of runs. It is seen that for all cases the modified version of the system is superior to the standard configuration. In the case in which the standard system gave concave curves of conversion vs. fractional transfer, a linear improvement curve was obtained. For the second case, that of convex curves, the modified system also gave a convex curve since if the standard system was already capable of improving its conversion in that way, the modified configuration would show even better improvements when increasing the fractional transfer.

The results confirm that the depletion of the top stage is responsible for the concave shaped curve of performance vs. fractional transfer. Furthermore, they indicate that a significantly more efficient operation of the column is obtained when no resin depletion is allowed.

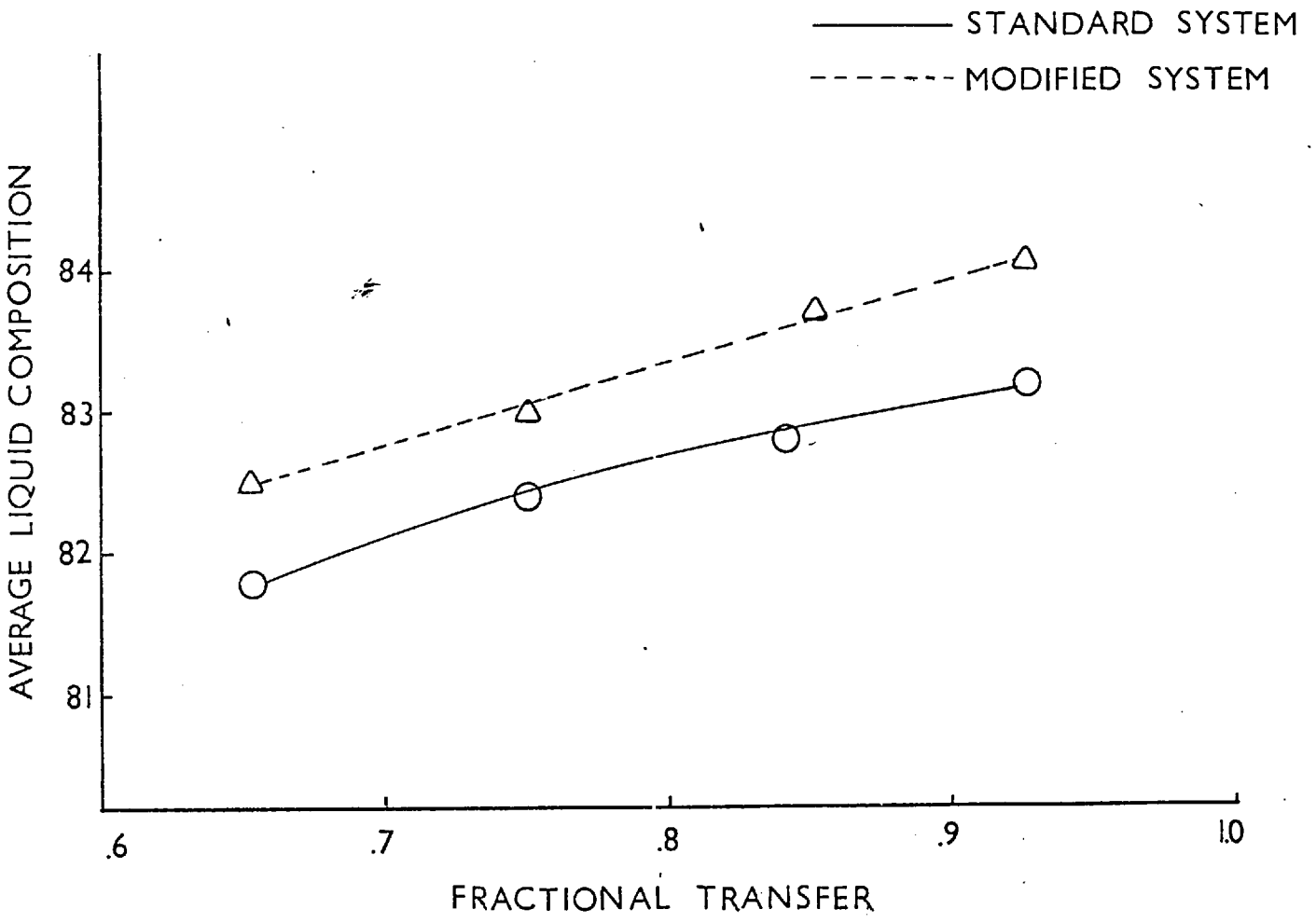

FIGURE 6.2.1–11 Extended simulation results showing the effect of fractional transfer on the column performance.

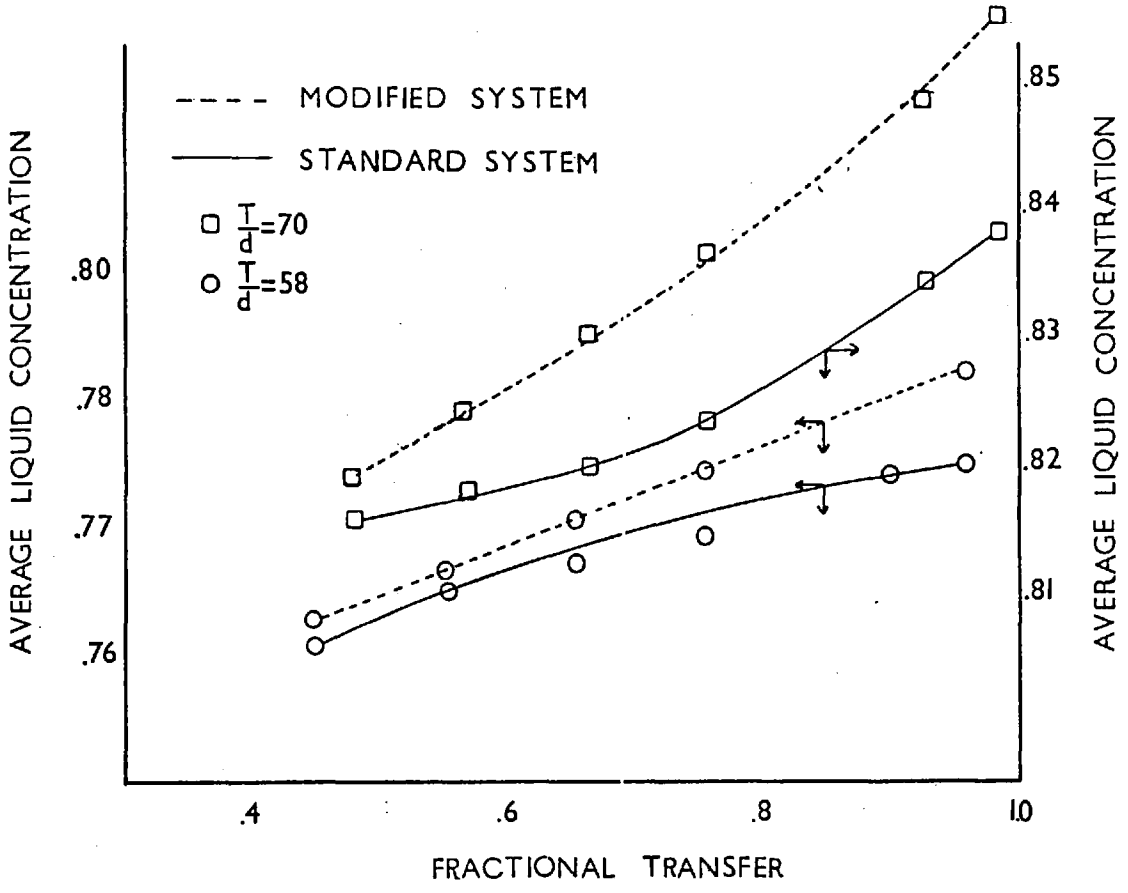

FIGURE 6.2.1-12 Exemplification of the effect of the fractional transfer on the system performance for two different values of T/d and comparison between the standard and modified systems.

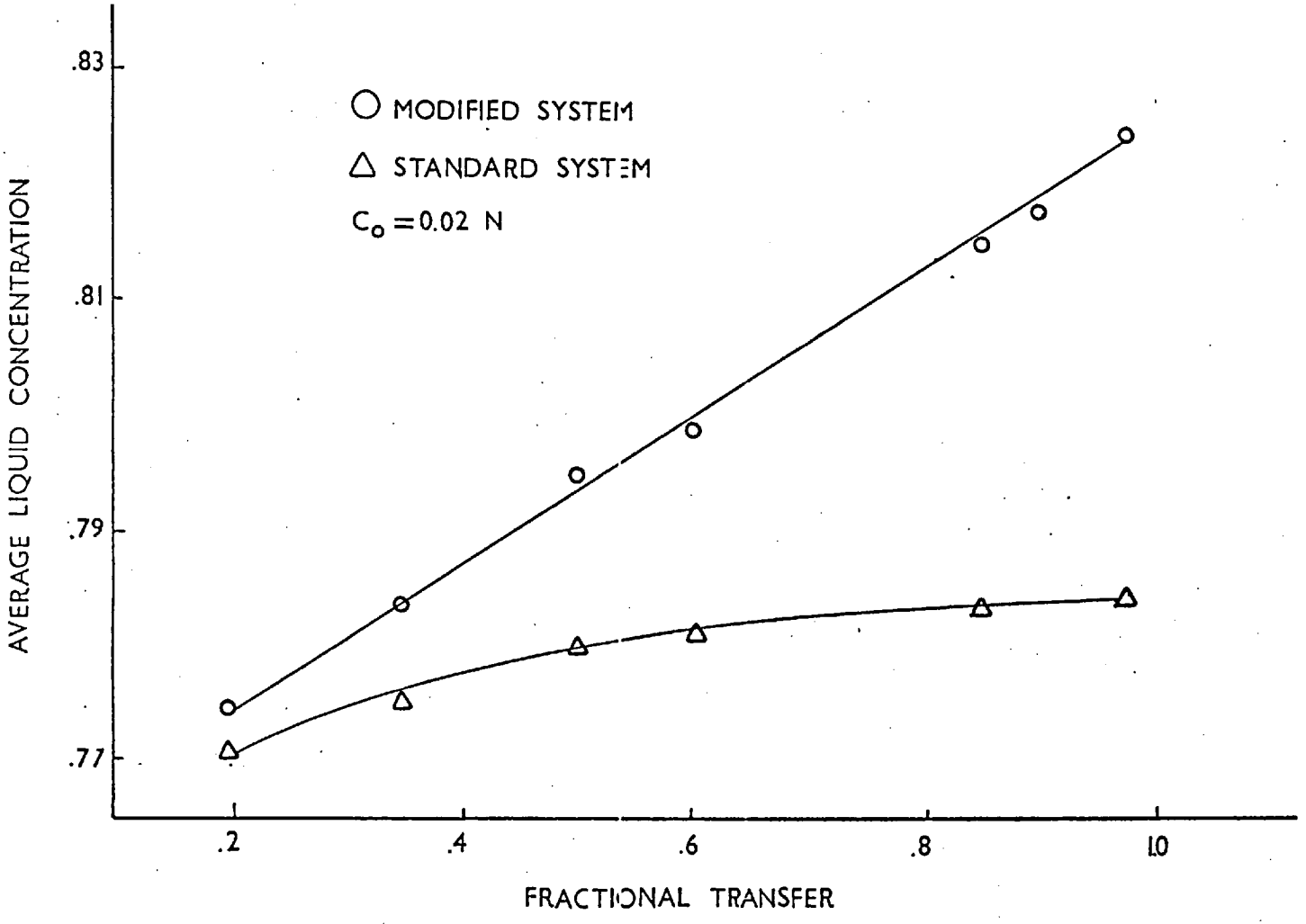

FIGURE 6.2.1-13 Comparison of the average exit liquid conversion as a function of fractional transfer for the case of modified and standard systems.

High Concentration Runs

The method of characteristics for the case of the intraparticle diffusion controlled rate of reaction, was tested simulating runs 3, 4 and 5 of the corresponding experimental runs given in Table 8 of Appendix C.1.

In this case several parameters needed to be estimated. The average resin bead size was evaluated as mentioned in section 5.2.4. The true capacity of the resin $\bar{c}$, was estimated from the experimental values. The ratio of the diffusivities D_{H^+}/D_{Na^+} and the value of the diffusivity D_{H^+} needed to evaluate the constant k_D, were taken from reference (77). There, these quantities were evaluated for the same reacting system though in a small batch reactor. The values used here were: $D_{H^+}/D_{Na^+} = 6.8$ and $D_{H^+} = 1.07 \times 10^{-9}$ m^2/s. These values are only an approximation since the actual values depend on the particular type of resin being used and can vary even between two batches of the same type of resin.

The results of the simulations are given in Table 5 of Appendix C.3 and compared with the experimental results in Figure (6.2.1-14). This figure depicts the experimental and theoretical solid and liquid concentration profiles along the column for the case of run 3. The results in the Table and those in the figure indicate that a good agreement is found between experiment and theory.

When performing these simulations it was found that, in order to adequately treat the solids transfer, a very fine characteristics grid was necessary. This was due to the different conversion ranges at which solid existed in each stage. For example, for run 3, the conversion range in the bottom is $0.96 \leq x \leq 1.0$; the middle tray contains resin in the range $0.86 \leq x \leq 1.0$; and in the top stage, $0.13 \leq x \leq 1.0$. Thus, the conversion intervals $(x_{i+1}-x_i)$ at which the value of the distribution function was known, varied very much from stage to stage. Hence, since in the mixing of the distribution functions after solids transfer, repeated interpolations are needed (section 4.1.2), a fine grid is required to be able to accommodate the resin of the above stage without losing information. This was tested by evaluating the area under the new distribution function which should be unity. At least 150 characteristics were necessary to satisfy these restrictions.

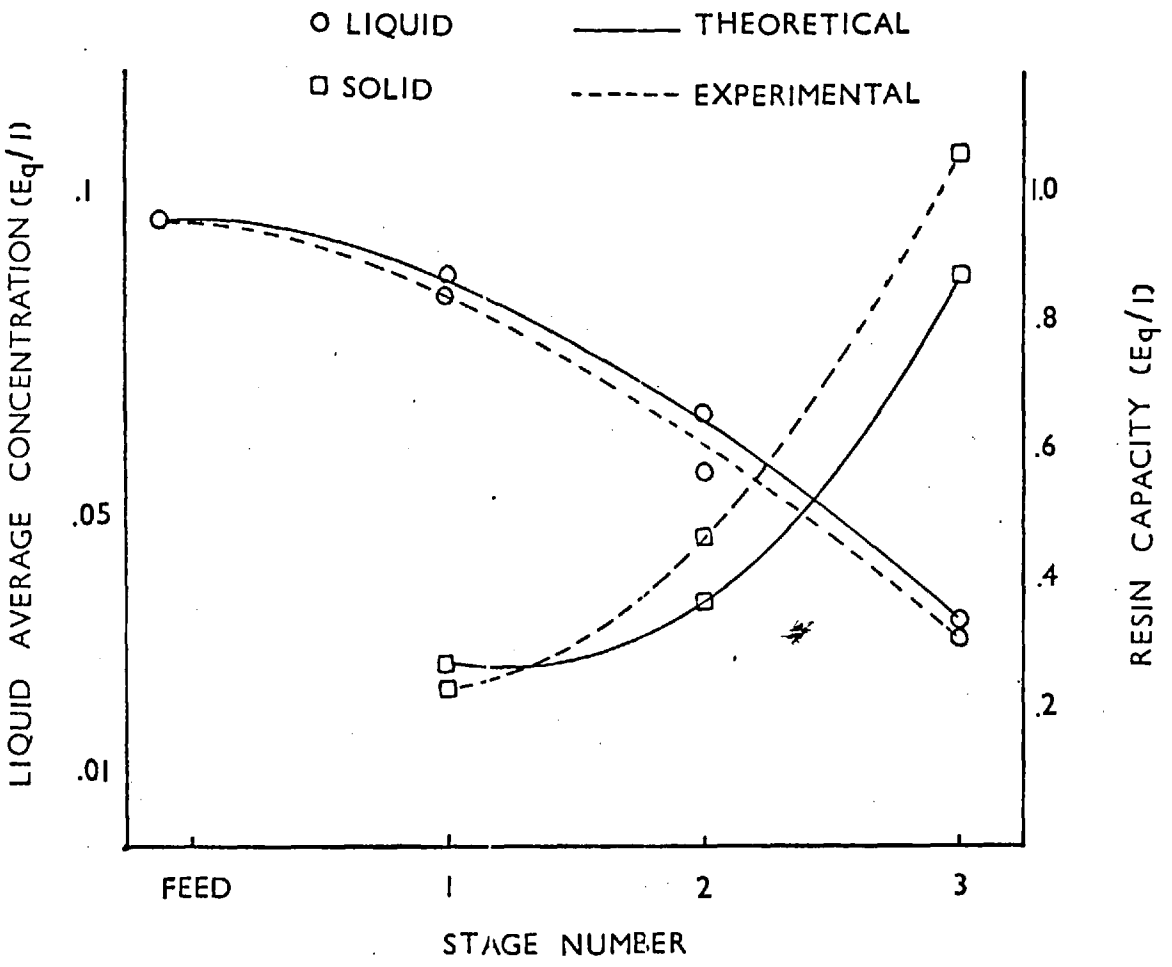

FIGURE 6.2.1-14 Comparison of the theoretical and experimental profiles of both phases along the column for the case of run 3.

Since, here, each characteristic is treated separately an increase in the number of characteristics, increased steeply the computer time required to simulate the behaviour of the system. Also, due to the rapid change of the rate of reaction with conversion (Figure 4.1-4), a time step of 1.0 to 1.5 seconds was needed to accurately evaluate the reaction term of Equation (4.1.2-9). These factors led to a large increase in the computing time (about 120 seconds of central processor time per run).

From the experimental results for this series, the effect of fractional transfer on the system performance was difficult to interpret since total reproducibility of voidages and residence times were not achieved. Also in these cases, the results depend strongly upon the initial conversion of the resin feed which varied slightly in the different experiments. To study the effect of fractional transfer on the system performance under these conditions, a theoretical study was performed for a typical set of data varying T and d as previously described, i.e. T/d = constant. The data used is given in Table (6) of Appendix C.3.

The results for these runs are presented in Table (6.2.1-1) below. There it can be seen that the liquid conversion of the exit stream remains basically unchanged when varying the fractional transfer.

Table 6.2.1-1

t_F	15	20	25	30
d	0.46	0.528	0.66	0.792
X_S	0.968	0.9717	0.976	0.979
X_L	0.6804	0.6801	0.678	0.677

Two factors contribute to this lack of improvement when the fractional transfer is increased. First, due to the kinetics of the particle diffusion controlled rate, most of the reaction takes place during the initial part of the cycle, and since, for the conditions tested, the resin becomes almost saturated, there is little room for an improvement to occur. Secondly, the depletion of the top stage resin, can obscure any improvement of the system performance, as was discussed previously in the low liquid concentration case.

In an attempt to discern the effect of these two factors, a simulation study was undertaken. In this study three cases were considered. In the first case the behaviour of the system was simulated using similar conditions to those used in the previous study except that the liquid and solid flow rates were increased in order to reduce the residence times in the system. In the second case, the system was reduced to a two-staged column to further reduce the solid residence time. The third case consisted of simulating the modified system with dummy feed stage, as previously described.

The results of the first study are shown in Figure (6.2.1-15). These results correspond to a solid residence time of 10 seconds per stage (T/d = 10.0). Other data used are given in Table 7 of Appendix C.3. In this figure, it can be seen that the average exit liquid concentration falls when increasing d, following the same trend as the low concentration series. The concentrations at the end of the cycle are also shown in the figure, where, it is seen that it falls steeply with increased d.

The results for the study of the two-staged system are shown in Figure (6.2.1-16). Here, the same data as in the previous case were used.

In this figure, it is observed that the liquid concentration at the end of the cycle, falls with higher d; however, the average concentration in fact rises with increased fractional transfer. The reason for this behaviour can be found by looking at the transient concentration profiles of the top stage during the cycle. These profiles are given in Figure (6.2.1-17). There it is observed for the cases in which $d > 0.4$ the liquid concentrations first rises and then falls again. This rise is due to the depletion of resin in the top stage and is accentuated as the fractional transfer is increased. It is important to note that in this case, the average exit concentration for the bottom stage reduces from 0.078 N to 0.075 N when increasing from 0.4 to 0.8; which is also indicative that it is the top stage inefficiency which causes the lowering of the performance.

In the simulation of the modified system, the conditions listed in Table 7 were also used with T/d = 10. For this modified configuration an important aspect was that of the conversion distribution of the dummy stage. It was found that in order to accurately mix the conversion

distributions of the dummy and the top stages, a smooth distribution for the dummy stage was required. Here again a fine characteristic grid was required for the reasons explained earlier.

A two parameter gamma distribution normalized between 0 and 1 was used to provide the conversion distribution of the dummy stage.

This distribution is given by the expression:

$$f(x,0) = \frac{(a+1)^{b+1}}{\Gamma(b+1)} \quad (1-x)^a \{\ln \frac{1}{1-x}\}^b$$

where a and b are parameters and Γ denotes the gamma function. It was found that an adequate distribution was obtained with a = 12.0 and b = 0.25, with these parameters, the mean conversion was about 0.1.

The results of these simulations are given in Figure (6.2.1-18). There it is seen that the system performance is increased with higher values of fractional transfer following the same pattern as in the liquid film controlled case.

Due to the kinetics of the particle diffusion controlled rate, in this configuration, the conversion distribution of the dummy stage plays a very important role in determining the sort of improvement that can be obtained. Therefore, in order to fully estimate what kind of improvements can be achieved a realistic conversion distribution of the dummy stage would be necessary. However, as was discussed in section 5.3.1, the experimental determination of the parameters of a distribution, other than the average is a rather difficult task.

6.2.2 Use of the moments of the distribution

The method of the moments was tested simulating the experimental runs no. 1 and 3 of Table 1 given in Appendix C.1. These runs have initial concentrations of 0.01244 N and 0.01328 respectively and are expected to produce negligible saturation of solid. Simulation of these runs using the method of the characteristics showed that in the case of run 1 the fraction of saturated particles is zero for all stages and for run 2 only the bottom stage showed on any saturation (about 1%)

The calculated first and second moments, and the liquid concentration at the end of the cycle for both the method of the moments and the method of characteristics are compared in Table (6.2.2). In Figure (6.2.2-1) the liquid concentration profiles are compared with the experimental case.

The tabulated results and those in figure show that an excellent agreement is found among these two methods and the experimental results. For the case of run 1 with zero saturations the agreement is perfect.

Table (6.2.2)

	Stage	C_f^*	C_f	μ_1^*	μ_1	μ_2^*	μ_2
RUN 1	1	.007047	.007047	.306076	.307971	.115103	.116201
	2	.003992	.003992	.158044	.158030	.003274	.032670
	3	.002661	.002661	.070811	.070932	.007307	.007495
	4	.001355	.001345	.019837	.025241	.000872	.001274
RUN 3	1	.007810	.00780	.34042	.3370	.13944	.1381
	2	.004587	.004581	.18186	.1721	.04197	.03985
	3	.002694	.002691	.08691	.8380	.010611	.009798
	4	.001662	.001627	.02993	.02881	.00184	.001651

the asterisk indicates the case of characteristics

The advantage of the method of the moments can be appreciated by comparing the computing time required for each of the two methods discussed. For 300 characteristics, runs no. 1 and no. 3 required about 60 seconds of computing time in 40 iteration to achieve p.s.s. By contrast, the method of the moments only required about 12 seconds for each simulation and needed about 70 iterations to reach p.s.s. conditions. However, the disadvantage is that its use is restricted to the cases when negligible saturation occurs throughout the column.

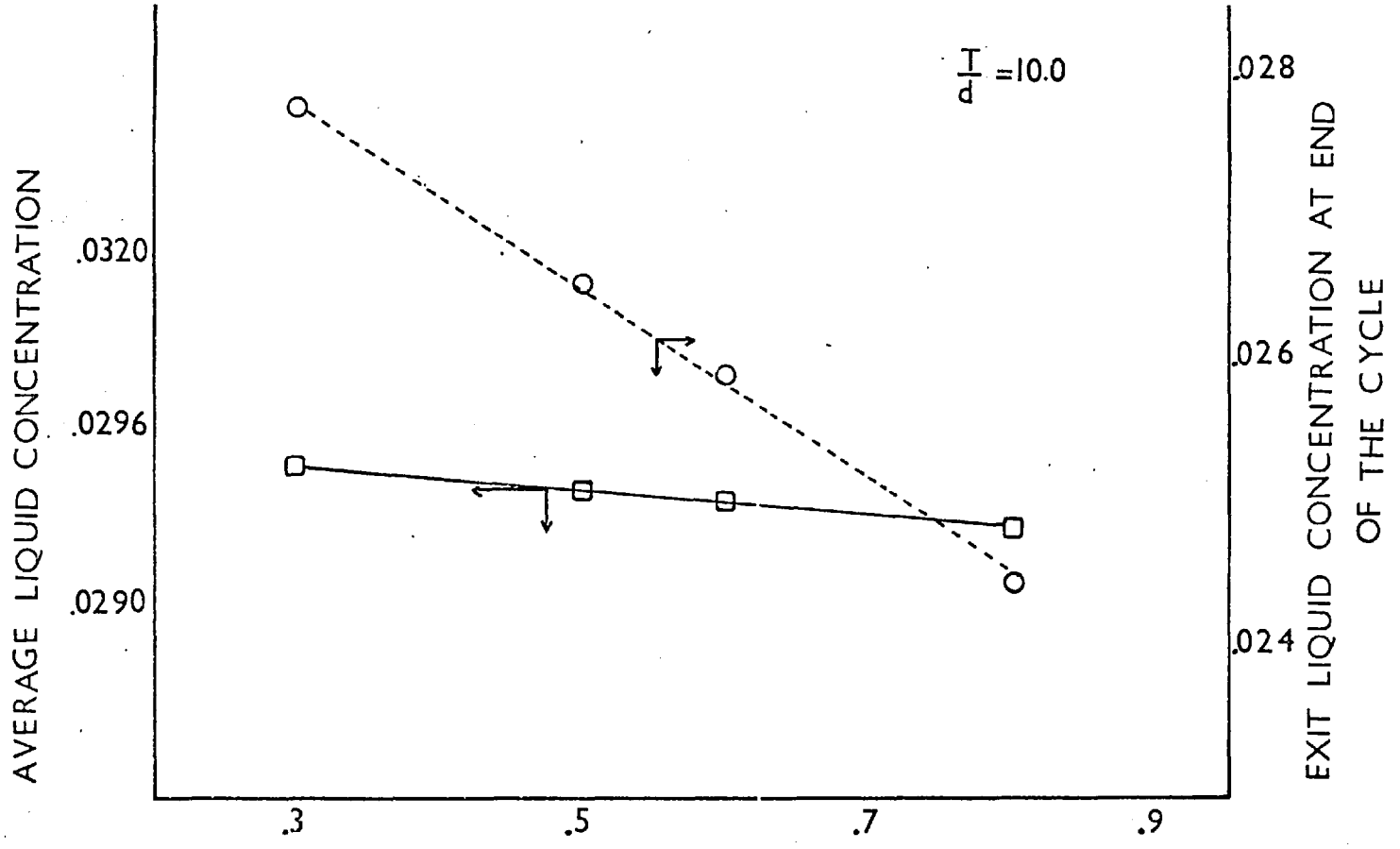

FIGURE 6.2.1-15 The effect of fractional transfer on the system performance for the case of low solid residence time.

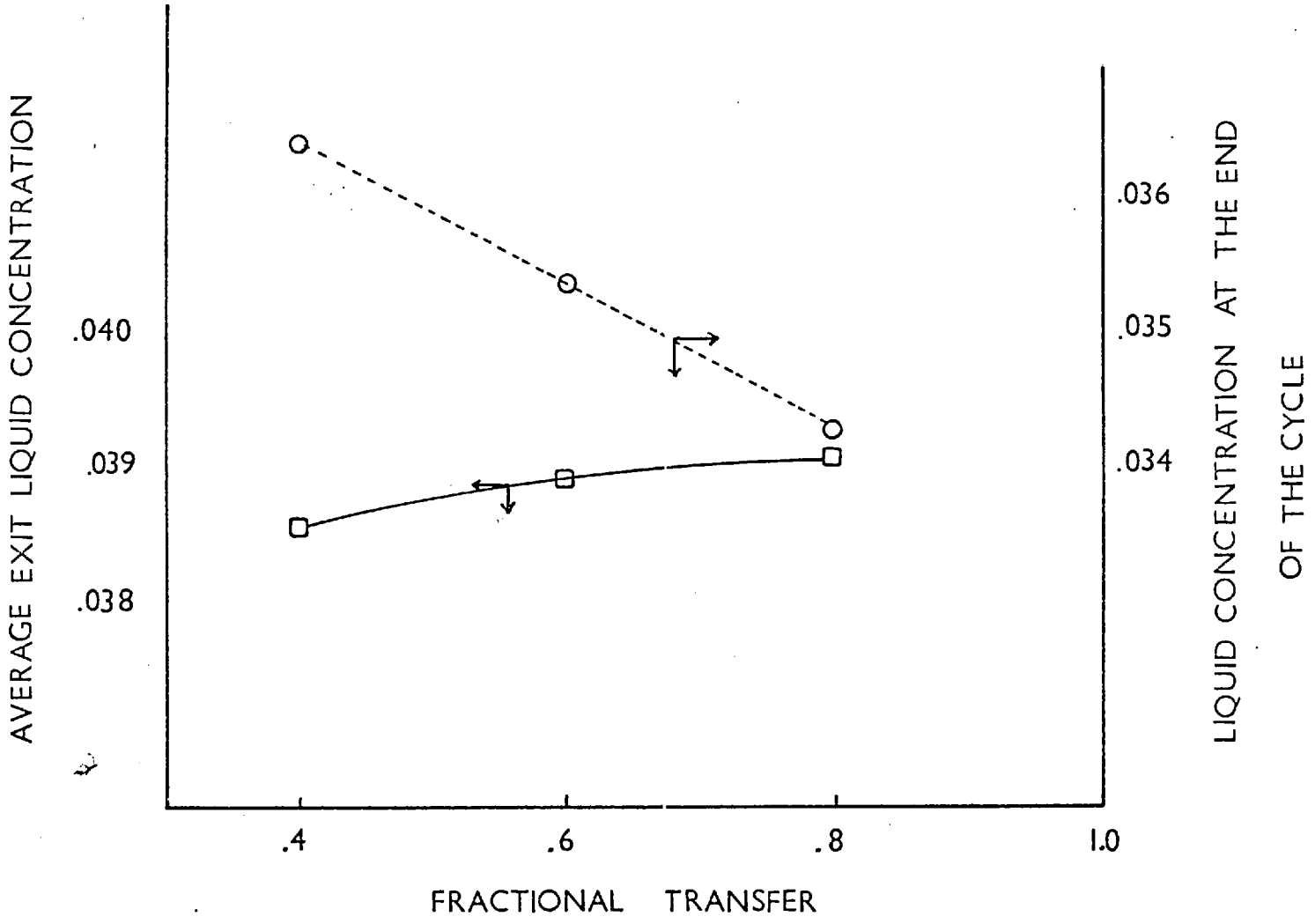

FIGURE 6.2.1-16 The effect of fractional transfer on the performance of the two-staged system.

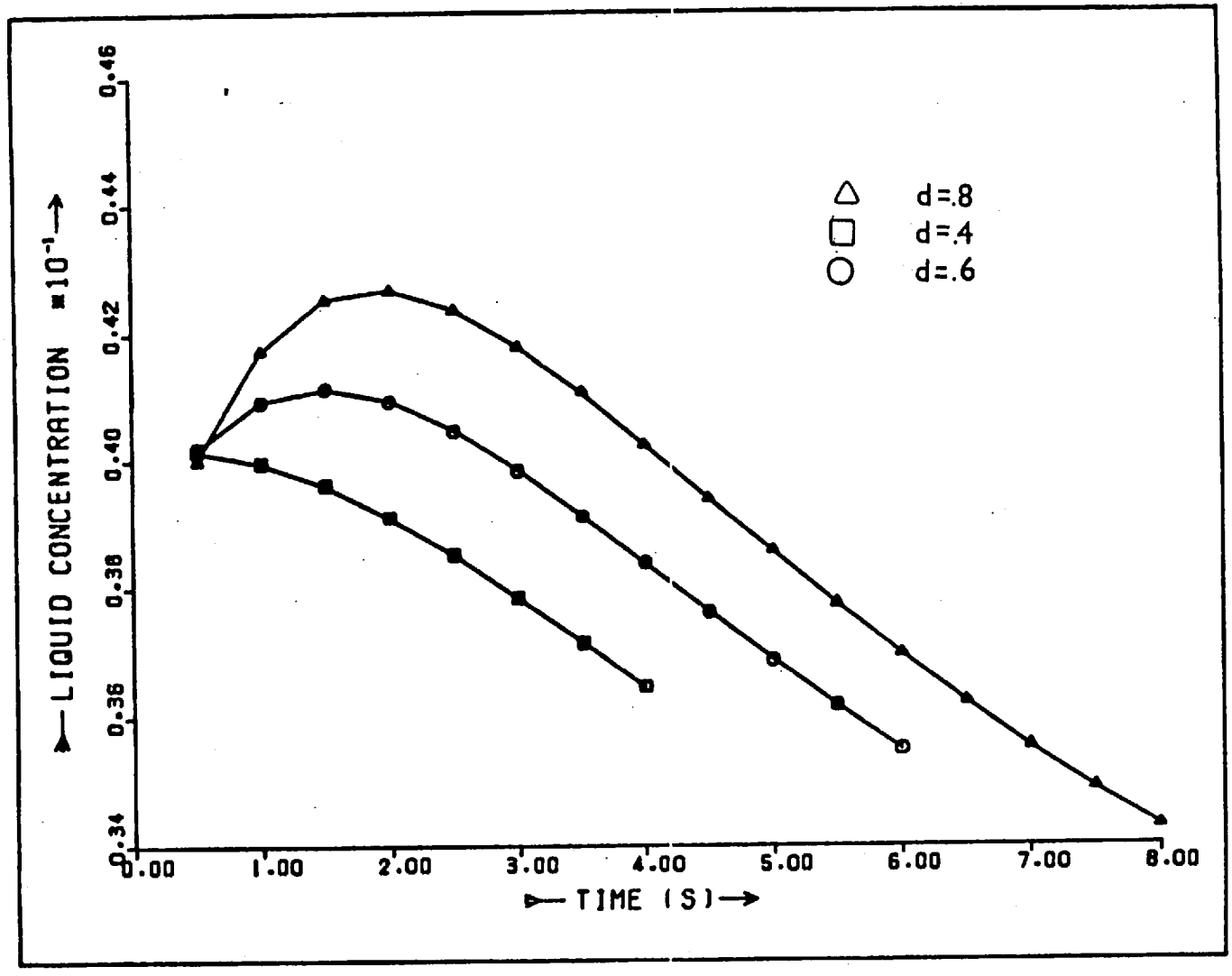

FIGURE 6.2.1-17 TRANSIENT LIQUID CONCENTRATION PROFILES

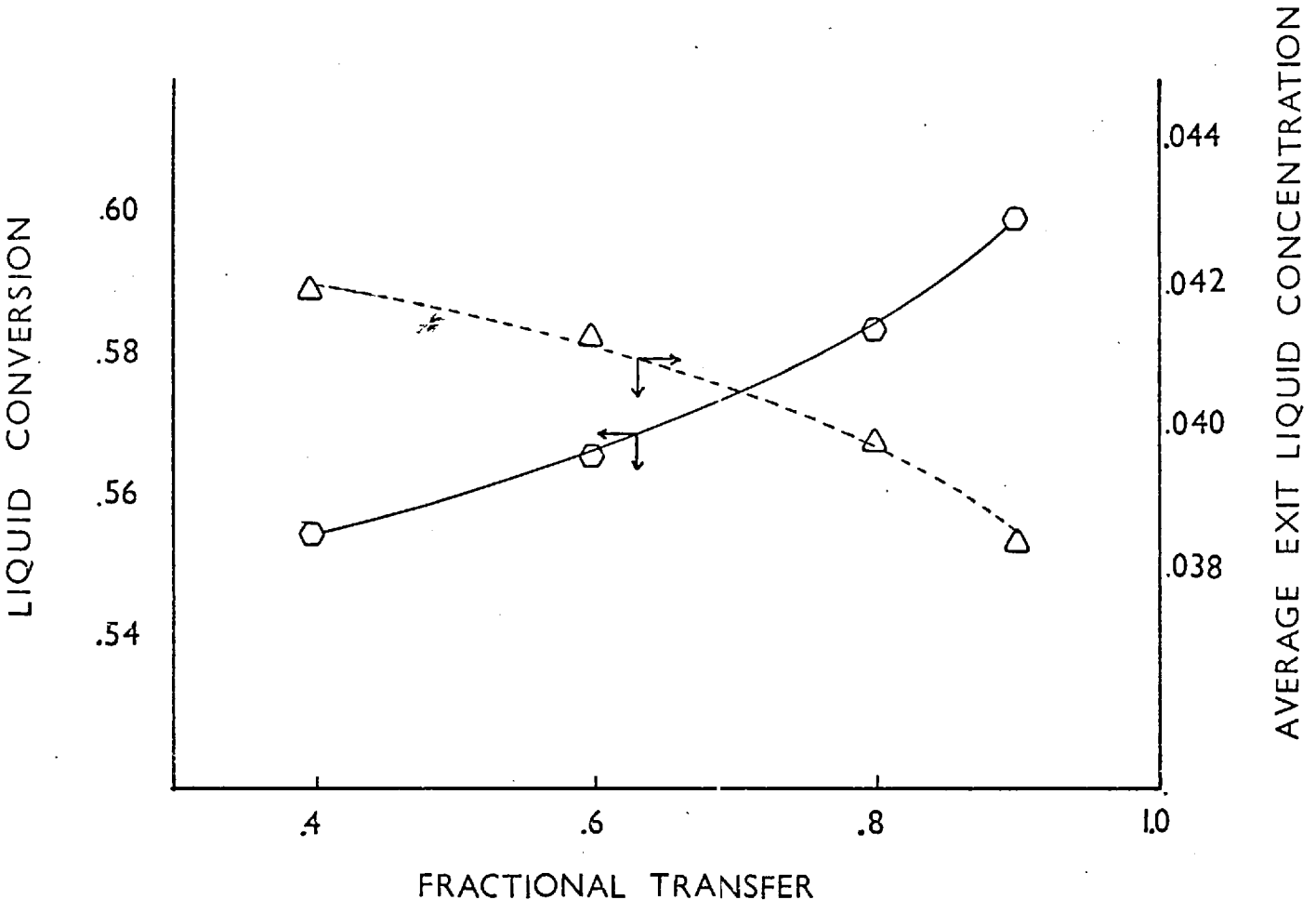

FIGURE 6.2.1-18 The effect of fractional transfer on the modified system performance.

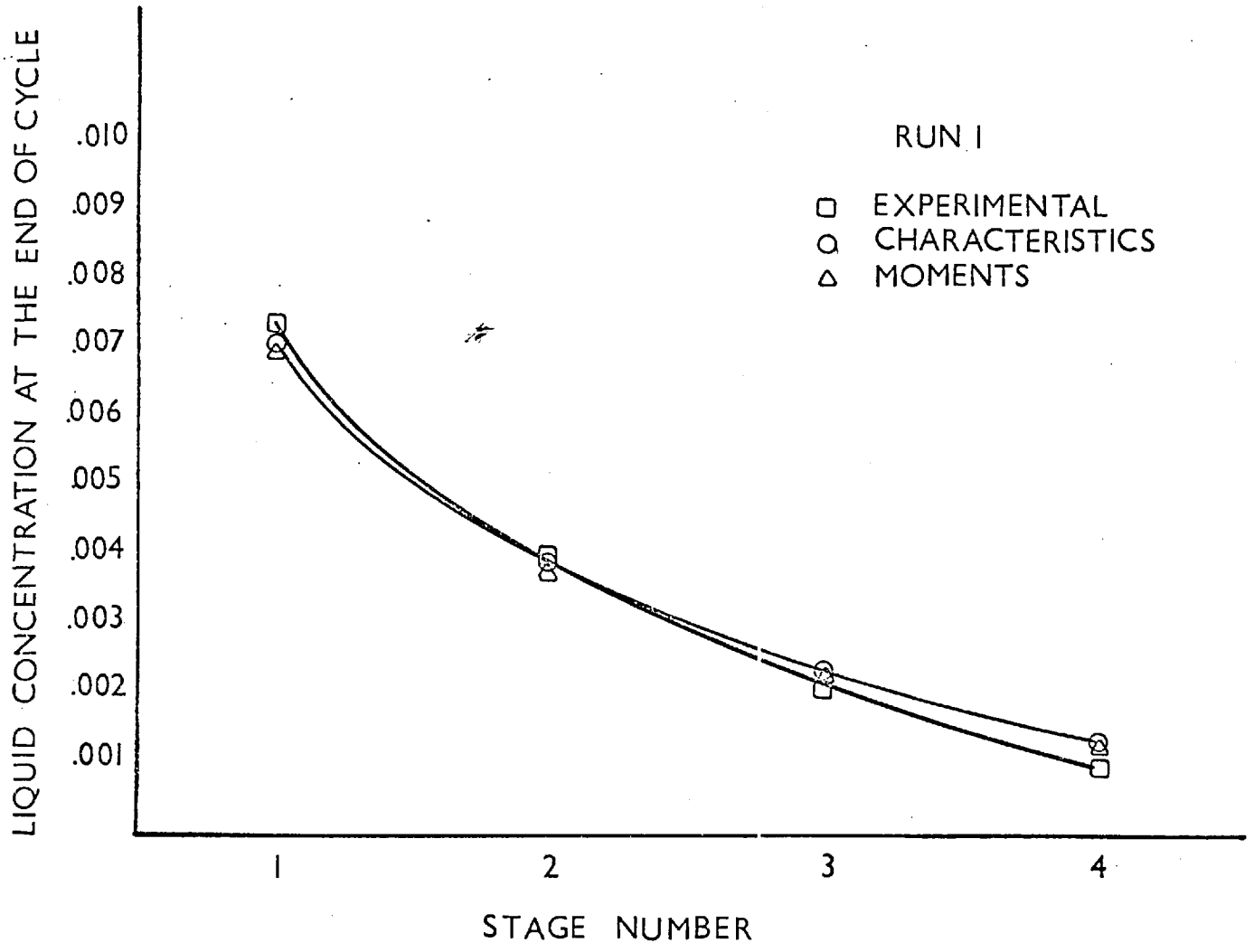

FIGURE 6.2.2-1 Comparison of the liquid concentration profiles along the column between the characteristics and the moments approaches also compared with the experimental results.

CHAPTER 7

CONCLUSIONS AND RECOMMENDATIONS

Conclusions

Two important aspects emerged from the study of the hydrodynamics of the contactor. It was established that the attainment of the pseudo-steady state conditions of the system were mainly controlled by its hydrodynamic stability. From those and all other experiments, it can be concluded that the contactor is hydrodynamically stable over a wide range of operating conditions. The only instabilities observed were in the case of low fractional transfer of highly converted resin, where the flow of solids through the perforated plates was impeded by an initial resistance to flow. It was also found that at least in a neighbourhood of the pseudo-steady state, the system is inherently stable, and that, provided hydrodynamic stability is preserved, the system is capable of returning to the same pseudo-steady state after small disturbances.

A salient conclusion and one which is supported by the experimental results of all experiments at low concentrations is that an increase of the fraction of solids periodically transferred, improves the system performance. These results are similar to the ones obtained in other mass transfer operations such as distillation and liquid-liquid extraction. There, the improved operation when cycling is generally ascribed to a better time average concentration gradient compared to that in conventional steady state operation. For the case of the zeroth order reacting system considered here, the fraction of saturated particles is the important factor. In this case, the periodic transfer of solids serves to replace a fraction of the solids in the stage with less converted solid. Therefore, the conversion distribution after the transfer contains a higher proportion of less reacted solid and the probability of solid becoming totally converted during the cycle, is reduced.

The results of the high liquid concentration runs indicate that the behaviour of the system is basically different from that with low liquid concentrations. These results also show that the rate of reaction becomes solid conversion dependent.

Of all the assumptions made in developing the mathematical model of the contactor, that of perfectly mixed liquid, is the most difficult to justify. Nevertheless, from the comparison between theoretical and experimental results, it can be seen that the model adequately describes the behaviour of the system over the entire range of operating conditions studied, and for both types of kinetics considered. Thus, the assumption can be said to be a valid one. The agreement between theoretical and experimental results for the runs at high concentrations indicate that the implied assumption that the entire contactor operates in the particle diffusion controlled range, is also valid. These results also indicate that the model would be suitable for an optimization technique, such as hill climbing in the function space (54), to be applied to search for the optimum cyclic operating conditions of a more industrially significant reacting system. Such a search was not carried out here since the neutralization of NaOH lacked relevance other than for verification of the model purposes.

The theoretical results support the experimental finding that for all conditions studied, the system performance is improved by increasing the fractional transfer. The results for the case of high liquid feed concentration show that in order to efficiently use the resin inventory in the column, a short residence time of the solids is necessary. This, supports the idea that for the treatment of high concentration streams, semicontinuous contactors would be more advantageous than the conventional batch system.

The results from the simulation of the modified configuration behaviour (no depletion of resin allowed), for both types of kinetics studied, indicate that the capabilities of the system to improve its performance when increasing the fractional transfer cannot be fully appreciated in the standard configuration because the top stage inefficiency hinders the improvement that could have otherwise been attainable.

Recommendations for future work

Having demonstrated that the mathematical formulation of the contactor describes adequately its behaviour, a theoretical search for optimum operating conditions is justified and should be undertaken.

A major field of application of the Cloete-Streat contactor is in the treatment of high concentration streams and in processing unclarified solutions which are typical of hydrometallurgical applications. Therefore,

experimental investigations of the performance of the contactor, operating under the more complex conditions characteristic of those installations, should be carried out.

BIBLIOGRAPHY

1. Nordell C.
   U.S. Pat., 1,608,661, 1926

2. Van Dijck W.J.P.
   U.S. Pat., 2,011,186, 1935

3. Cormack R.H. and Howard J.E.
   Chem.Eng.Prog., 9 (904), 1953

4. Hiester N.K., Russell C., Fields E., Cohen R. and Radding S.
   Ind.Eng.Chem., 45, (2402), 1953

5. Clayton R.C.
   Proc.Int.Conf.on Ion-Exchange in the Process Ind.
   Soc.Chem.Ind., (98), 1969

6. Johnson A.S.W.
   Thesis, University of Cambridge 1966

7. Hiester N.K., Fields E.F., Phillips R.C., Radding S.B.
   Chem.Eng.Prog., 50, (139), 1954

8. Porter R.
   U.S. Pat., 2,973,319, 1955

9. Cloete F.D., Miller A.I. and Streat M.
   Trans.Inst.Chem.Eng., 45, (392), 1967

10. Bouchard J.
    Int.Conf.on Ion-Exchange in the Process Ind.
    Soc.Chem.Ind., (91), 1969

11. Higgins I.R.
    Ind.Eng.Chem., 53, (635), 1961

12. Turner C.R. and Church M.R.
    Trans.Inst. of Chem.Eng., 41, (283), 1963

13. Grimmett E.S. and Brown B.P.
    Ind.Eng.Chem., 54,11, (124), 1962

14. Swinton E.A. and Weiss D.
    Aust.J.of Appl.Sci., 4, (316), 1953

15. Slater M.
    Brit.Pat., 48097/66

16. George D.R., Ross J.R. and Prater J.D.
    Min.Eng.(N.Y.), 73, (1), 1968

17. Javed J.
    Journal of Met., 23, (33), 1971

18. Cloete F.L.D. and Streat M.
    Brit.Pat., 1,070,251

19. Stevenson D.G.
Proc.Int.Conf.on Ion-Exchange in the Process Ind.
Soc.Chem.Ind., (114), 1969

20. Cloete F.L.D., Haines A.K., Tunley T.H.
Colloquium So.Afr.Institute of Mining and Metallurgy,
September 1973

21. Slater M.J.
Bull of the Can.Inst.of Min. and Metall.
67, no.742, (93), 1974

22. Horie M.
Kogaku Kogaku, 29, (420), 1965

23. Cannon M.R.
Oil and Gas J., 51, (268), July 28 1952

24. Cannon M.R.
Ibid, 55, (68), January 23, 1956

25. Cannon M.R.
Ind.Eng.Chem., 53, 81 (639), 1961

26. Gaska R.A. and Cannon M.R.
Ibid, 53, 8, (630), 1961

27. McWhirter J.R. and Cannon M.R.
Ibid, 53, 8, (631), 1961

28. McWhirter J.R. and Lloyd W.A.
Chem.Eng.Prog., 59, 6, (58), 1963

29. Szabo T.T., Lloyd W.A., Cannon M.R. and Speaker S.M.
Ibid, 60, 1, (66), 1964

30. Belter P.A. and Speaker S.M.
Ind.Eng.Chem.Proc.Des. and Dev., 6, (36), 1967

31. Robinson R.G. and Engel A.J.
Ibid, 59, 3, (22), 1967

32. Sommerfeld J.T., Schordt V.N., Parisot P.E. and Chien H.H.
Sep.Sci., 1, 2 & 3, (245), 1966

33. Lewis W.R.
Ind.Eng.Chem., 28, (399), 1936

34. Schrodt U.N., Sommerfeld J.T., Martin D.R., Parisot P.E. and Chien H.H.
Chem.Eng.Sci., 22, (259), 1967

35. Robertson D.C. and Engel A.V.
Ind.Eng.Chem.Process Des. and Dev., 6, (2), 1967

36. Ritter A.B. and Douglas J.M.
Ind.Eng.Chem.Fundam., 9, (21), 1970

37. Di Cicco D.A. and Schoenhels R.J.
J.of Heat Transfer (ASME), 86, (457), 1964

38. Lemlich R.
Chem.Eng.(N.Y.), 68, 10, (171), 1961

39. Baird M.H., Duncan G.J., Smith J.M. and Taylor J.
Chem.Eng.Sci., 21, (199), 1966

40. Krasuk J.H. and Smith J.M.
AICHE J., 10, (259), 1964

41. McKay D.L. and Howard W.G.
Ind.Eng.Chem. Process Des. and Dev., 6, (16), 1967

42. Skarstron C.W.
Ann.N.Y. Acad. of Sci., 72, (75), 1959

43. Kadlec R.H. and Turnock P.H.
AICHE J., 17, (335), 1971

44. Sweed N.H.
Recent Developments in Separation Science
Vol.I. (N.Li. editor) Chemical Rubber Co. Cleveland, 1972

45. Wilhelm R.M., Rice A.W. and Bendelious A.R.
Ind.Eng.Chem.Fundam., 5, (141), 1966

46. Pigford R.L., Biker B. and Blum D.E.
Ibid, 8, (848), 1969

47. Wankat P.C.,
Sep.Sci., 9, 21 (85), 1974

48. Horn F.J.M.
Ind.Eng.Chem.Process Des. and Dev., 6, (30), 1967

49. Dodds R., Hudson P.F., Kershenbaum L. and Streat M.
Chem.Eng.Sci., 28, (1233), 1973

50. Bennett B., Cloete F.L.D. and Streat M.,
Proc.Int.Conf. on Ion-Exchange in the Process Ind.
Soc.Chem.Ind., (173), 1969

51. Douglas J.M. and Rippin D.W.
Chem.Eng.Sci., 21, (305), 1966

52. Douglas J.M.
Ind.Eng.Chem.Process Des. and Dev., 6, (43), 1967

53. Douglas J.M. and Gaitonde N.Y.
Ind.Eng.Chem.Fundam., 6, (265), 1967

54. Horn F.J.M. and Lin R.C.
Ibid, Process Des. and Dev., 6, (21), 1967

55. Bailey J.E., Horn F.J.M. and Lin R.C.
AICHE J., 17, (818), 1971

56. Bailey J.E. and Horn F.J.M.
Chem.Eng.Sci., 27, (1109), 1972

57. Lee C.K. and Bailey J.E.
AICHE J., 20, (1), 1974

58. Lee C.K. and Bailey J.E.
Chem.Eng.Sci., 29, (1157), 1974

59. Klinkenberg A.
Chem.Eng.Sci., 26, (1133), 1971

60. Randolph A.,
Can.J. of Chem.Eng., 42, (280), 1964

61. Ray W.H.,
Ibid, 45, (356), 1967

62. Kershenbaum L.
Personal Communication

63. Ausikaitis L. and Engel A.J.
AICHE J., 20, (256), 1974

64. Bailey J.E.
Chem.Eng.Commun., 1, (111), 1973

65. Boyd G.E., Adamson A.W. and Myers L.S.
J.Am.Chem.Soc., 69, (2836), 1947

66. Helfferich F.
J. of Phys.Chem., 69, (1178), 1965

67. Snowdon C.B. and Turner J.C.R.
Int.Symp.on Fluidization, Eindhoven, The Netherlands,
University Press, 1967

68. Blickenstaff R.A., Wagner J.D. and Dranoff J.S.
J.Phys.Chem. 71, (1655), 1967

69. Turner J.C.R. and Snowdon C.B.
Chem.Eng.Sci., 23, (221), 1968

70. Helfferich F. and Plesset M.S.
J.of Chem.Phys., 28, (418), 1958

71. Plesset M.S., Helfferich F. and Franklin J.N.,
Ibid, 29, (1064), 1958

72. Helfferich F.
Ibid, 38, (1688), 1963

73. Blickenstaff R.A., Wagner J.D. and Dranoff J.S.
J.Phys.Chem., 71, (1670), 1967

74. Bennett B.A., Cloete F.L.D., Miller A.I. and Streat M.
Chem.Eng.(London), C.E.412, No.233, Nov.1969

75. Rahman, K.
Ph.D. Dissertation, University of London, 1973

76. Acrivos, A.
Ind.End.Chem., Vol. 48, (703), 1956

77. Abbot M.B.
An introduction to the Method of Characteristics, Thames and Hudson, London, 1966

78. Ames W.F.
Nonlinear Partial Differential Equations in Engineering
Academic Press, 1965

79. Courant R. and Hilbert D.
Methods in Mathematical Physics Vol.2. Interscience, 1961

80. Himmelblau D.M. and Bischoff, K.B.
Process Analysis and Simulation,
John Wiley, New York, 1968

81. Hulburt H.M. and Katz S.
Chem.Eng.Sci., 19, (555), 1968

82. Katz S. and Saidel G.M.
AICHE J., 13, (319), 1967

83. Sherwin S.B., Shinnar R. and Katz S.
Ibid, 13 (1141), 1967

84. Coddington F.A. and Levinson N.
Theory of differential equations, McGraw Hill, N.Y. 1955

85. Robinson R.A. and Stokes R.H.
Electrolytic solutions, Butterworths, London, 1959

86. Handbook of Chemistry and Physics,
53rd Edition, R.C. Weast, Ed. The Chemical Rubber Company, Cleveland

87. International Critical Tables
E.W. Wasburn, Ed. McGraw Hill, 1926

APPENDIX A.1

Detailed Transformations of the Population Mass Balance Equations

In section 3.2 the following mass balance equation was obtained

$$f(x,t)\,\frac{dx}{dt}\bigg|_{x} - f(x+\Delta x,t)\,\frac{dx}{dt}\bigg|_{x+\Delta x} = \frac{d}{dt}\int_{x}^{x+\Delta x} f(z,t)\,dz \qquad (1)$$

If f(u) is a continuous density function, then, by definition of a cumulative distribution function

$$F(u+\Delta u) = \int_{u}^{u+\Delta u} f(z)\,dz \quad \text{or} \quad f(u) = \frac{d}{du}\,F(u) \qquad (2)$$

hence

$$\frac{d}{dt}\left(\int_{u}^{u+\Delta u} f(z)dz\right) = \frac{d}{dt}\left(F(u+\Delta u) - F(u)\right).$$

Expanding $F(u+\Delta u)$ in a Taylor's series gives for small Δu

$$\frac{d}{dt}\left(F(u+\Delta u) - F(u)\right) = \frac{d}{dt}\left(\frac{d}{du}F(u)\right)_{u}^{\Delta u} = \frac{d}{dt}\left(f(u)\,\Delta u\right)$$

Using this result in the r.h.s. of Equation (1),

$$f(x,t)\,\frac{dx}{dt}\bigg|_{x} - f(x+\Delta x,t)\,\frac{dx}{dt}\bigg|_{x+\Delta x} = \frac{\partial}{\partial t}\left(f(x,t)\right)\Delta x$$

Rearranging and dividing by Δx

$$\frac{-\left(f(x+\Delta x,t)\left(\frac{dx}{dt}\right)\Big|_{x+\Delta x} - f(x,t)\left(\frac{dx}{dt}\right)\Big|_{x}\right)}{\Delta x} = \frac{\partial}{\partial t}\left(f(x,t)\right)$$

Taking the limit as $\Delta x \to 0$ gives

$$\frac{\partial}{\partial t}\,f(x,t) + \frac{\partial}{\partial x}\left\{f(x,t)\,\frac{dx}{dt}\right\} = 0$$

which is Equation (3.2.2-5a).

APPENDIX A.2

Details of the Method for Finding the Characteristic Directions

The procedure for finding the direction of the characteristics and the equations that are integrated along them is described in the given references (70,71,72). For a system of two non-linear partial differential equations of the form:

$$A_1 \frac{\partial z_1}{\partial x} + B_1 \frac{\partial z_1}{\partial t} = R_1 (z_1, z_2)$$

$$A_2 \frac{\partial z_2}{\partial x} + B_2 \frac{\partial z_2}{\partial t} = R_2 (z_1, z_2)$$

The characteristic directions are given by

$$\left.\frac{dx}{dt}\right|_I = \frac{B_1}{A_1} \quad \text{and} \quad \left.\frac{dx}{dt}\right|_{II} = \frac{B_2}{A_2}$$

And along the directions the equations to be integrated are

$$\left.\frac{dz_1}{dx}\right|_I = \frac{R_1}{A_1} \quad \text{and} \quad \left.\frac{dz_2}{dx}\right|_{II} = \frac{R_2}{A_2}$$

From equation (4.1) and (4.2) it is clear that

$$A_1 = 1, \quad B_1 = 0 \quad R_1 = \Phi$$

and

$$A_2 = 1, \quad B_2 = \frac{1}{c} r \quad R_2 = \frac{1}{c} f \frac{\partial r}{\partial x}$$

Therefore,

$$\left.\frac{dx}{dt}\right|_I = 0 \quad \left.\frac{dx}{dt}\right|_{II} = \frac{1}{c} r (x,c)$$

along which it is required to integrate

$$\left.\frac{dc}{dx}\right|_I = \Phi \quad \text{and} \quad \left.\frac{df}{dx}\right|_{II} = \frac{1}{c} f(x,t) \frac{\partial}{\partial x} r(x,c)$$

APPENDIX B.1

Example of Data Gathered in a Typical Run

All data given below correspond to run 1 of table 1 of Appendix C.1.

(1) Capacities determination (keg/m^3)

Sample	Initial	Final
1	1.678	1.098
2	1.634	1.087
3	1.635	1.0101
4	1.613	1.080
Average	1.627	1.092

(2) Weights of drums and tanks (kg)

Tank	Initial	Final	Difference
Liquid feed drum	130.40	38.5	91.9
Liquid product drum	29.100	121.6	92.5
Resin feed tank	10.550	7.65	2.9

(3) Resin fed during run (m^3)

	Initial	Final	Difference
Height of resin in tank (m)	0.829	0.605	0.224

From calibration, a height of 1 m in the resin tank, corresponds to 0.845×10^{-4} m^3 of freely settled resin.

Hence amount of resin fed is $0.224 \times 0.845 \times 10^{-4} = 1.892 \times 10^{-3}$ m^3

(4) Heights of free settled resin in the column (m)

	Stage 1	Stage 2	Stage 3	Stage 4
Initial	0.034	0.033	0.0325	0.035
Final	0.032	0.033	0.0335	0.033
Average	0.033	0.033	0.033	0.034

(5) Fluidized bed heights (m) and voidages

	Stage 1	Stage 2	Stage 3	Stage 4
h_f	0.107	0.108	0.01075	0.125

By definition of fluidized bed porosity:

$$\varepsilon_b = 1 - \frac{\text{absolute volume of beds}}{\text{volume of bed}}$$

Similiarly, stage porosity

$$\varepsilon = 1 - \frac{\text{absolute volume of beds}}{\text{volume of stage}}$$

Volume of stage = Cross sectional area x height = 0.00456 x 0.13
= 593.28 x 10^{-6} m^3

	Stage 1	Stage 2	Stage 3	Stage 4	Average
ε_b	0.838	0.840	0.839	0.858	0.845
ε	0.867	0.867	0.867	0.864	0.866

(6) Other data and calculations

Temperature of liquid feed	24.95°C
Concentration of liquid feed	0.01244 Eq/l
Cycle time t_F	25 s
Total run time	1473 s
Number of cycles	47

Resin flow rate $S' = \frac{1.891 \times 10^{-3}}{1473} = 1.284 \times 10^{-6}\ m^3/s$

Resin flow rate in terms of absolute volume of resin

$1.284 \times (1-\varepsilon_B) = 1.284\ (1-0.476) = 0.673 \times 10^{-6}\ m^3/s$

Liquid forward flow rate

$$L = \frac{91.9}{25 \times 47 + 90^*} = 0.07264 \times 10^{-3}\ m^3/s$$

Average liquid flow rate

$$L_{av} = \frac{91.9}{1563} = 0.0585 \times 10^{-3}\ m^3/s$$

(7) Calculation of Fractional Transfer

Amount of resin transferred per cycle $= \frac{\text{total amount transferred during run}}{\text{number of cycles}}$

$$= \frac{1.892 \times 10^{-3}}{47} = 40.03 \times 10^{-6}\ m^3$$

hence average fractional transfer

$$= 40.03/0.0333\,m \times 0.00456\ m^2$$
$$= 0.266$$

(8) Mass balances

a) on sodium ion:

Liquid $(0.01244 - 0.00091^{**}) \times 0.0000585 = 0.674 \times 10^{-6}$ k.Eq/s

Solid $(1.627 - 1.092) \times 1.284 \times 10^{-6} = 0.686 \times 10^{-6}$ k.Eq/s

b) Total solids mass balance

total cycle time

$$\frac{1483}{47} = 31.55\ s$$

Hence

$S'T\ (1-\varepsilon_B) = 1.284 \times 10^{-6} \times 31.55 \times 0.524 = 21.2 \times 10^{-6}\ m^3$

$(1-\varepsilon)\ Vd = (1-0.866) \times (0.0005928 \times 0.266) = 21.12 \times 10^{-6} m^3$

* In this run, the resin flow rate was started 90 seconds after the liquid flow rate

** The average exit composition is calculated in two ways.

a) from the area under the curve generated by the conductance chart recordings

b) titration from the collected exit stream over a short number of cycles.

In this case the conductance reading gave

$$C'_f = 0.000888.$$

and from the sample titrated

$$C'_f = 0.000872$$

and averaging these two values after correcting for the dilution due to the water feed with the resin.

$$C'_f = 0.000880 \times 1.034 = 0.00091$$

The dilution factor is found by mass balance as follows:

$$0.0726 \quad C_f = \left[(.0726 + \frac{(2.9 + 1.89 \times 0.524)}{1563} \right] C'_f$$

Therefore,

$$C_f = 1.034 \; C'_f$$

APPENDIX B.2

Evaluation of resin related quantities

(1) Surface mean diameter

The results from dry-sieving a resin sample are shown in the following table:

B.S. Mesh (range)	Mean diameter $\bar{d}_i \times 10^{-6}$ m	Weight fraction x_i	$\frac{x_i}{\bar{d}_i}$
14 - 16	1100	0.0013	1.182
16 - 18	925	0.059	63.784
18 - 22	780	0.1150	147.436
22 - 25	655	0.2966	452.82
25 - 30	500	0.489	889.101
30 - 36	460	0.039	84.783
36 - 44	388	0.0001	0.2577

From Equation (5.2.4-1)

$$\frac{1}{\hat{d}_p} = \sum_{i=1}^{m} \frac{x_i}{\bar{d}_i} = 1639.35$$

hence $\hat{d}_p = 610 \times 10^{-6}$ m

(2) Settled bed porosity

As mentioned, this quantity was evaluated by accurately weighing a specific gravity bottle (S.G.) in the following procedure:

Weight of S.G. bottle	w_1 gm
Weight of S.G. bottle + resin beads	w_2 gm
Weight of S.G. bottle + water	w_3 gm
Weight of S.G. bottle + water beads	w_4 gm

Let v = volume of water in bottle (ml) v_B = absolute volume of beads (ml) and ρ = density of water (gm/ml)

then,

$$w_4 = w_2 + v.\rho$$

Hence,

$$w_4 = w_2 \left(\frac{w_3 - w_1}{\rho} - v_B\right) \rho$$

since in this case $\rho = 1.0$

$$v_B = w_1 + w_2 - w_3 - w_4$$

For the experiment

$$v_B = 2.6472$$

To evaluate the total volume of freely settled resin, two methods were used. In the first, a small measuring cylinder was dried and weighed. A quantity of wet resin was freely settled into the cylinder and its level marked in the glass. Then, the resin was emptied and the cylinder filled up to the mark with water. The volumne of resin was then calculated by weight difference.

The second method consisted of freely settling a volume of wet resin into an accurate measuring tube (a 50 ml burette was used), partially filled with resin. The volume of free settled resin (total volume) was evaluated by simply reading the volume difference of resin in the tube. With some practice, it was possible to get these two values to agree.

In the experiment, for the amount of resin used to obtain v_B

$$v_T = 5.05 \text{ (ml)}$$

therefore,

$$\varepsilon_B = 1 - \frac{2.6472}{5.05} = 0.4758$$

(3) Density of the freely settled bed

Here, an amount of resin was dried of interstitial water and weighed. The total volume of settled resin was evaluated as described above.

From Equation (5.2.4-4) i.e.

$$\rho_B = \frac{w_S}{v_T}$$

And for the experiment $\rho_B = \frac{3.7193}{4.5} = 0.8265$

APPENDIX C.1

Tables of Experimental Results

TABLE 1

Run No.

	1	2	3	4	5	6	7	8
t_F	25	25	30	30	35	35	40	45
C_0	0.01244	0.01320	0.01328	0.01286	0.01228	0.01356	0.01281	0.01130
Cap^o	1.627	1.8433	1.5208	1.606	1.546	1.608	1.609	1.723
L	0.0726	0.0722	0.0720	0.0711	0.0705	0.0653	0.069	0.075×10^{-3}
S'	1.284	1.422	1.255	1.250	1.090	1.357	1.496	1.306×10^{-6}
C_f	0.00091	0.00118	0.00153	0.00150	0.00652	0.00230	0.00287	0.00128
Cap^f	1.092	0.9197	0.986	1.0205	0.822	0.970	1.098	0.814
X_S	32.89	50.1	35.47	36.45	46.83	39.67	31.75	50.60
X_L	96.68	91.06	89.5	88.33	93.81	83.0	77.6	88.7
τ_S	472.3	396.0	442.7	461.4	644.4	442	371.7	401.9
τ_L	28.3	28.7	28.9	29.1	25.8	32.0	30.1	25.7
$\bar{\varepsilon}_b$	0.842	0.848	0.848	0.831	0.766	0.856	0.847	0.847
$\bar{\varepsilon}$	0.866	0.875	0.877	0.873	0.845	0.881	0.877	0.884
$\bar{d}$	0.266	0.315	0.351	0.330	0.273	0.446	0.530	0.580
$\bar{L}$	0.0584	0.0555	0.0557	0.057	0.0564	0.054	0.0565	0.059×10^{-3}
H	317.8	296.3	291.5	302.2	367.9	282.9	291.5	274.8×10^{-6}
S.ΔCap	0.686	1.314	0.6753	0.732	0.789	0.865	0.764	1.139×10^{-6}
$\bar{L}$.ΔC	0.673	0.667	0.6622	0.648	0.655	0.608	0.560	0.663×10^{-6}
E	1.84	49.2	1.94	11.47	16.90	29.7	26.7	

TABLE 2

	Run No. 1	2	3	4	5	6	7	8
t_F	25	30	35	30	30	30	30	30
C_0	0.0212	0.01930	0.02019	0.0200	0.020	0.020	0.01956	0.01913
C_{ap}^{o}	1.5906	1.578	1.4013	1.6079	1.368	1.453	1.4936	1.5389
L	0.0725	0.0727	0.0734	0.0713	0.072	0.0725	0.0631	0.0626×10^{-3}
S'	1.445	1.416	1.418	1.495	1.61	1.61	1.5106	1.405×10^{-6}
C_f	0.00110	0.00374	0.00231	0.00624	0.00265	0.00270	0.00205	0.00241
C_{ap}^{f}	0.639	0.823	0.711	1.099	0.713	0.762	0.9242	0.9546
X_S	59.82	47.8	49.33	31.64	47.8	47.6	38.13	37.96
X_L	94.81	80.62	88.56	68.80	86.75	86.5	89.53	87.4
τ_S	454.1	286.3	287.4	384.4	246.4	255.1	286.8	218.7
τ_L	27.9	29.4	29.1	29.0	29.9	29.0	34.0	34.6
$\bar{\varepsilon}_b$	0.831	0.857	0.874	0.809	0.856	0.848	0.805	0.845
$\bar{\varepsilon}$	0.854	0.900	0.901	0.873	0.910	0.888	0.906	0.914
$\bar{d}$	0.29	0.50	0.584	0.381	0.583	0.562	0.513	0.514
$\bar{L}$	0.0569	0.0575	0.056	0.055	0.056	0.056	0.053	0.0529
H	344.0	212.0	210.2	301.1	207.9	215.0	222.0	203.1×10^{-6}
S.ΔCap	1.375	1.069	0.9802	0.761	1.054	1.112	0.860	0.820×10^{-6}
$\bar{L}$.ΔC	1.145	0.894	0.983	0.757	0.972	0.969	0.928	0.875×10^{-6}
E	16.7	16.4	0.31	0.50	7.6	12.99	7.3	6.17

TABLE 3

Fluidized Bed Heights (x 10^{-2}m)

Cycle Number	Stage No. 1	2	3	4
6	10.0	10.5	11.0	11.5
14	9.0	9.0	8.1	12.5
26	8.0	8.0	8.0	13.0
37	8.0	8.0	8.0	13.0
47	8.0	8.0	8.0	12.8
57	8.0	7.9	8.0	13.0
67	8.0	8.0	8.0	13.0
80	8.0	8.0	8.0	13.1
⋮				
128	8.0	8.0	8.0	13.0

Run No. 4

Fluidized Bed Heights (x 10^{-2}m)

Cycle Number	1	2	3	4
1	0.0	0.0	0.0	8.0
6	5.0	5.0	6.0	8.0
11	5.5	5.5	6.2	8.0
21	6.0	5.6	6.5	7.0
34	-	5.8	6.0	7.0
43	6.3	6.0	7.0	7.0
60	6.5	6.0	7.0	7.0
69	6.5	6.0	7.0	7.0
78	6.5	6.0	7.0	7.0
⋮				
160	6.5	6.0	7.0	7.0

Run No. 7

TABLE 4

Run No. 4						
Initial	settled bed height	2.9	2.8	2.8	2.8	x 10^{-2}m
Final(p.s.s.)	settled bed height	3.0	3.0	3.0	3.6	x 10^{-2}m
Run No. 5						
Initial	settled bed height	2.6	2.5	2.6	2.8	x 10^{-2}m
Final(p.s.s.)	settled bed height	2.2	2.0	2.0	2.5	x 10^{-2}m
Run No. 6						
Initial	settled bed height	3.0	3.0	3.0	4.6	x 10^{-2}m
Final(p.s.s.)	settled bed height	2.2	2.0	2.1	2.7	x 10^{-2}m

TABLE 5

Run No.

	1	2	3	4	5
t_F	20	25	30	35	40
X_S	45.45	38.16	41.0	36.5	43.16
X_L	78.50	79.6	81.0	74.4	87.78
τ_S	302.5	256.7	239.8	190.4	242.8
τ_L	34.9	33.9	33.7	33.1	33.5
$\bar{\varepsilon}$	.926	.922	.920	.935	.919
$\bar{d}$	.325	.504	.654	.887	.90
H	175.5	189.0	189.6	155.3	192.0×10^{-6}
S.ΔCap	.807	.836	.922	.834	$.951 \times 10^{-6}$
$\bar{L}\Delta C$	.839	.827	.891	.812	$.912 \times 10^{-6}$

TABLE 6

	Run no. 1	2	3	4	5	6
t_F	20	25	25	30	35	40
X_S	49.8	55.09	48.15	56.17	58.67	59.1
X_L	80	80.41	71.66	83.95	86.55	87.1
τ_S	229.2	232.3	192.2	236.2	266.1	266.1
τ_L	34.2	34.1	33.2	34.5	33.86	34.3
$\bar{\varepsilon}$	0.924	0.923	0.935	0.915	0.907	0.907
$\bar{d}$	0.448	0.533	0.535	0.609	0.66	0.749
H	180.2	182.6	153	196	220.5	220.5×10^{-6}
S.ΔCap	1.17	1.18	1.09	1.32	1.502	1.501×10^{-6}
$\bar{L}\Delta C$	1.237	1.26	1.16	1.357	1.401	1.422×10^{-6}

TABLE 7

Run No.

	1	2	3	4	5	6
t_F	20	25	30	35	40	40
X_S	69.92	67.3	68.4	69.0	69.1	72.3
X_L	79.50	80.5	83.9	86.03	86.6	84.96
τ_S	241.0	214.9	245.5	244.3	242.7	237.8
τ_L	33.24	33.56	32.76	33.8	33.3	35.7
$\bar{\varepsilon}$	0.914	0.923	0.912	0.912	0.913	0.918
$\bar{d}$	0.434	0.506	0.576	0.758	0.795	0.726
H	703.9	182.6	208.7	208.7	206.3	194.4×10^{-6}
S.ΔCap	1.74	1.80	1.62	1.73	1.70	1.74×10^{-6}
$\bar{L}\Delta C$	1.57	1.75	1.61	1.70	1.66	1.65×10^{-6}

TABLE 8

	Run No. 1	2	3	4	5
t_F	25	25	25	25	30
X_S	86.99	91.96	83.4	87.0	94.2
X_L	59.50	71.45	66.51	63.6	59.3
τ_S	161.8	252.5	156.4	184.3	219.4
τ_L	18.24	18.62	20.37	21.26	20.70
$\bar{\epsilon}$	.890	.817	.897	.899	.879
$\bar{d}$	.854	.554	.890	.66	.75
H	195.9	324.0	183.0	179.2	215.0×10^{-6}
S.ΔCap	3.199	3.935	3.63	3.54	3.384×10^{-6}
$\bar{L}\Delta C$	3.36	4.173	3.67	3.49	3.39×10^{-6}

APPENDIX C.2

Evaluation of the mass transfer coefficients

Equation (3.3.1-7) was used to evaluate the mass transfer coefficients k_L. The value of $\phi = 0.86$ was chosen because in the reference from which it was taken (75), the reacting system studied there, was the same as the one considered in this work. Viscosity and density data for the NaOH solution were obtained from standard references (86,87). Ionic diffusivities were calculated from ionic mobilities by the Nernst-Eistein relation: $D_i = RT\lambda_i/F$ where λ is the ionic mobility, T the absolute temperature, R the gas constant and F the Faraday constant. The mobility data was obtained from reference (85). The effective diffusivity for the pair H^+, OH^- was evaluated from equation (3.3.1-3).

For exemplification, consider the data given in Appendix B.1
From (3.3.1-7)

$$k_L = \frac{0.86}{\varepsilon_b}\left\{\frac{\rho}{\mu}\right\}^{.17}\frac{D^{.67}\,u^{.5}}{d_p^{.5}}$$

$T = 24.95^{\circ}C$

$C_0 = 0.01244$

$\rho = 0.998 \times 10^3$ kg/m^3

$\mu = 0.96 \times 10^{-3}$ kg/ms

$u = 15.9 \times 10^{-3}$ m/s

$\lambda_{OH^-} = 19.52$ m^2/kq-eq-ohm

$\lambda_{H^+} = 4.99$ m^2/kq-eq-ohm

$D = 2.110 \times 10^{-9}$ m^2/s

$d_p = 0.650 \times 10^{-3}$ m

$\bar{\rho}_b = 0.845$

Therefore, $k_L = 7.5 \times 10^{-5}$ m/s

APPENDIX C.3

Tables of Theoretical Results

Table 1

Run No.	1	2	3	4	5	Extended Simulation
t_F	20.0	25.0	30.0	35.0	40.0	42.19
$\bar{d}$	0.325	0.504	0.654	0.887	0.90	0.95
ϵ	0.926	0.922	0.920	0.935	0.919	0.919
k_L	6.97	7.50	7.65	7.72	7.90	7.90×10^{-5}
X_S	43.7	34.5	36.2	34.7	37.1	37.2
X_L	77.4	79.5	80.5	72.8	81.0	81.3
Iterations for p.s.s.	43	29	21	20	20	20

Average Initial Capacity for these runs: 1.531 keq/m^3

Average Liquid Forward Flowrate L = 6.45×10^{-5} m^3/s

Average Resin Flowrate S = 0.75×10^{-6} m^3/s

External Surface Area a = 9836 1/m

Table 2

Run No.	1	2	4	5	6	Extended Simulation	
t_F	20.0	25.0	30.0	35.0	40.0		
$\bar{d}$	0.448	0.533	0.609	0.660	0.749	0.8393	0.924
ε	0.924	0.923	0.915	0.907	0.907	0.907	0.907
k_L	7.16	7.16	7.080	7.18	7.38	7.38	7.38×10^{-5}
X_S	49.1	53.1	49.4	51.8	53.2	53.4	54.1
X_L	78.3	76.6	79.8	81.9	82.4	82.8	83.3

Average Inital Capacity for this set of runs: 1.53 . keq/m^3

Average Liquid Forward Flowrate L = 0.0641×10^{-3} m^3/s

Average Resin Flowrate S = 0.8128×10^{-6} m^3/s

External Surface Area a = 9836.0

Table 3

Run No.	1	2	3	4	5
t_F	20.0	25.0	30.0	35.0	40.0
$\bar{d}$	0.434	0.506	0.576	0.758	0.79
ε	0.914	0.923	0.912	0.912	0.913
k_L	7.38	7.20	7.20	7.55	7.65×10^{-5}
X_S	54.0	61.7	60.6	60.9	61.1
X_L	79.0	75.6	78.0	79.6	79.8

For this set of runs:

Average Initial Capacity 1.534 keq/m^3

Average Forward Liquid Flowrate L = 0.0656×10^{-3} m^3/s

Average Resin Flowrate S = 0.85×10^{-6} m^3/s

External Surface Area a = 9055.0 1/m

Table 4

Initial Capacity	=	1.50	keq/m^3
k_L	=	7.50×10^{-5}	1/s
a	=	9836.0	1/m
C_0	=	0.02 N	
L	=	0.0645×10^{-3}	m^3/s
V	=	597.8×10^{-6}	m^3
S	=	0.8×10^{-6}	m^3/s
ε	=	0.919	
h	=	100	
$T/\bar{d}$	=	60.02	

Table 5

	Run No. 3	4	5
t_F	25.0	25.0	30.0
d	0.897	0.66	0.688
ε	0.8975	0.899	0.879
C_0	0.0975	0.0953	0.09593
x_f	0.134	0.03	0.146
L	0.0783	0.0752	0.07551×10^{-3}
S	1.562	1.31	1.30×10^{-6}
X_S	0.8359	0.951	0.844
X_L	0.656	0.605	0.551

$k'_D = 1.99$

$D_{H^+} = 1.07 \times 10^{-9}$ m^2/s

$\bar{c}_n = 1.635$ keq/m^3

$n = 150$

Table 6

Time Step 1.0 s

$\bar{c}$	=	1.635	keq/m^3
D_{H^+}	=	0.9×10^{-9}	m^2/s
d_p	=	620×10^{-6}	m
L	=	0.0752×10^{-3}	m^3/s
S	=	1.58×10^{-6}	
n	=	150	
C_0	=	0.0953	
x_f	=	0.01	
ε	=	0.899	
k'_D	=	1.99	

Table 7

Time Step 0.5 s

$\bar{c}$	=	1.635	keq/m^3
D_{H^+}	=	1.07×10^{-9}	m^2/s
d_p	=	310×10^{-6}	m
L	=	0.23×10^{-3}	m^3/s
S	=	5.987×10^{-6}	m^3/s
n	=	160	
C_0	=	0.0953	
x_f	=	0.01	
ε	=	0.899	
k'_D	=	1.99	

PROGRAM A

This program simulates the column solving the system equation by the method of characteristics for the case of the liquid film controlled case.

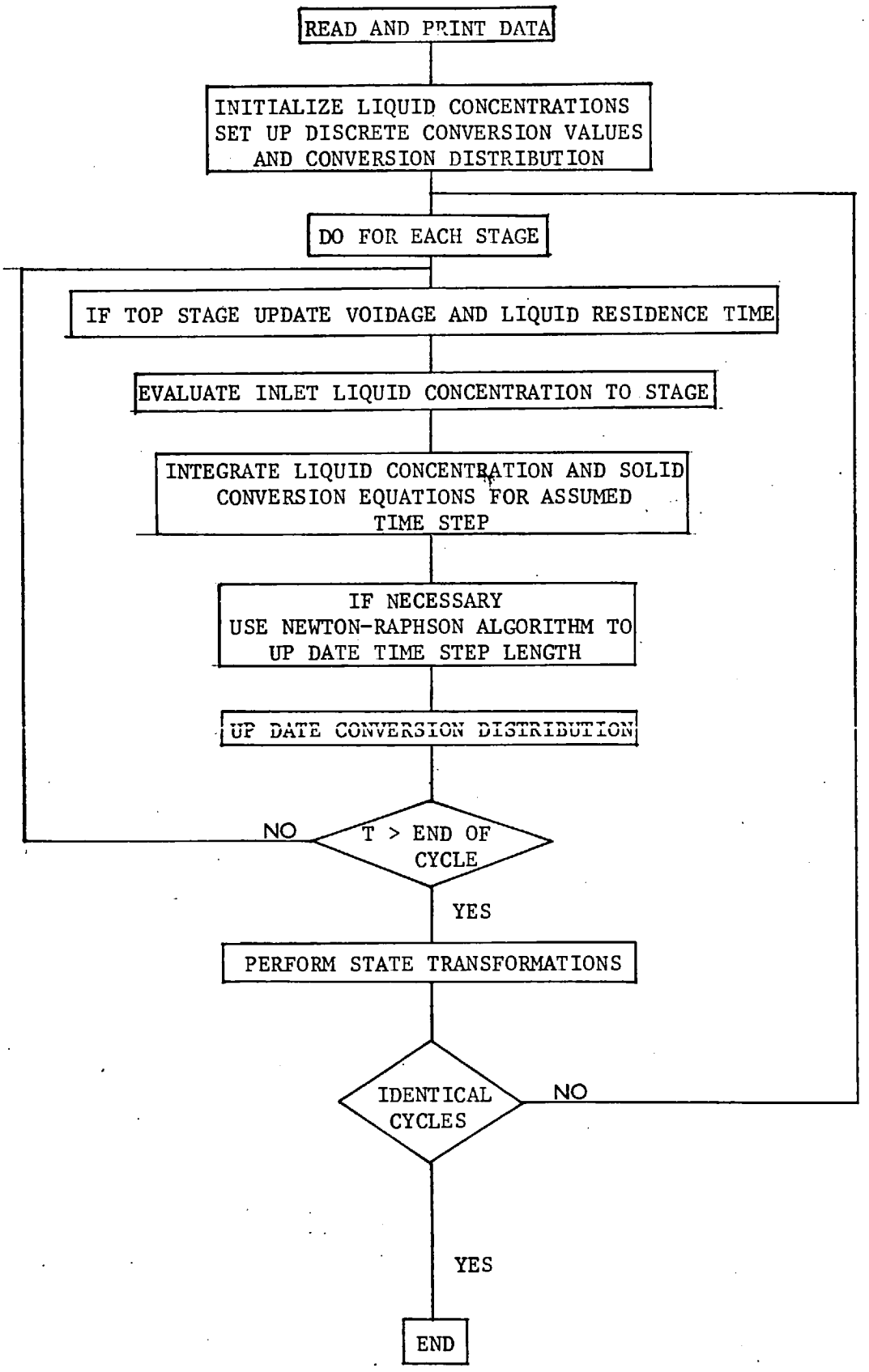

PROGRAM B

This program simulates the system behaviour in the case of intraparticle diffusion controlled case.

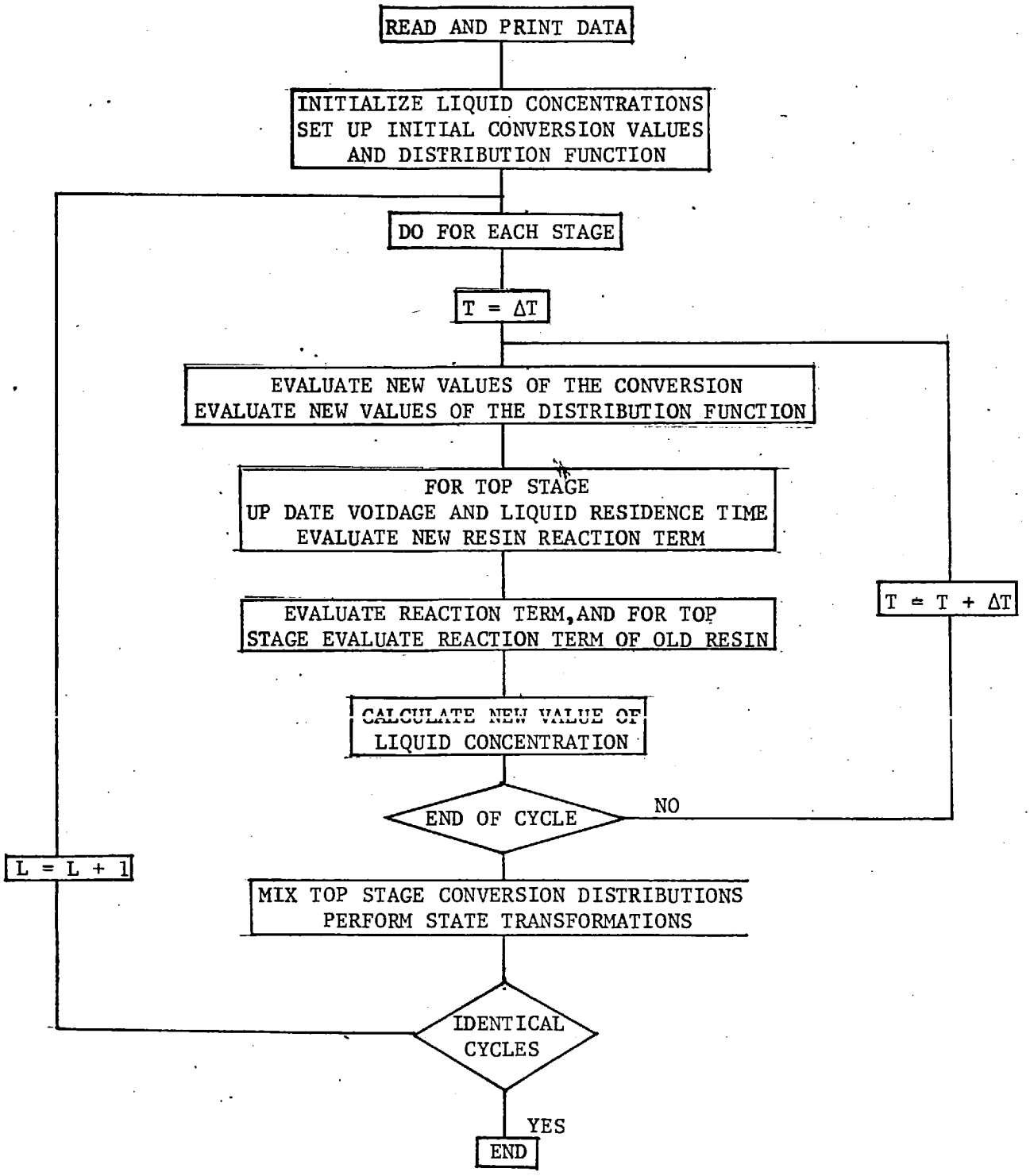

PROGRAM C

This program simulates the column solving the equations by the method of the moments.

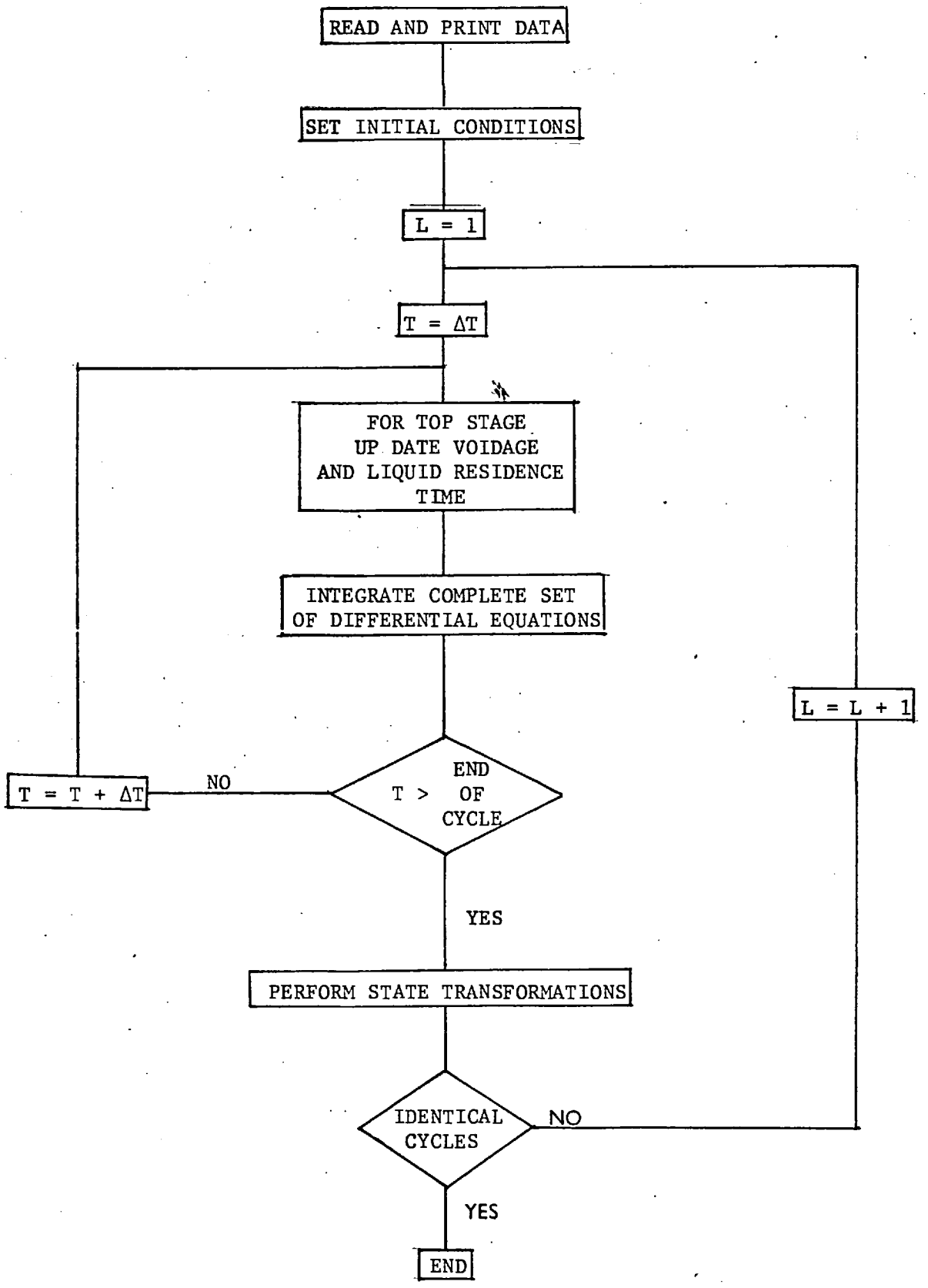

APPENDIX E

Simplification of the conversion density function for first order kinetics

In residence time studies, it is simple to demonstrate that for first order kinetics, the use of the population distribution function can be dispensed with, and only the mean residence time is necessary in the mathematical description of the system in consideration (80).

Similarly, in using conversion distribution functions, for the case of first order kinetics the entire population can be lumped into a mean conversion value.

Consider the mass balance equation for the j^{th} stage in the Cloete-Streat contactor (Equation 3.2.2-2)

$$\frac{dC_j}{dt} = \frac{1}{\tau_j}(C_{j-1}-C_j) - \frac{1-\varepsilon_j}{\varepsilon_j}\int_0^1 r(x,C_j)\, f(x,t)\, dx ,$$

and a rate expression such as

$$\frac{dx}{dt} = \frac{B}{c}(1-x)^n , \qquad n = 1,2,3 \ldots .$$

Expanding the term $(1-x)^n$ by the binomial theorem for integer values of n it is possible to write

$$\frac{dC_j}{dt} = \frac{1}{\tau_j}(C_j-C_{j-1}) - \frac{1-\varepsilon_j}{\varepsilon_j}\,\frac{1}{c}\int_0^1 B\left[\sum_{k=0}^{n}(-1)^k\binom{n}{k}\, x^k f\,(x,t)\right] dx$$

For B independent of C (that is, a zeroth order reaction with respect to the liquid composition) and recalling the definition of the moments of a distribution (section 4.2).

$$\frac{dC_j}{dt} = \frac{1}{\tau_j}(C_j-C_{j-1}) - \frac{1-\varepsilon_j}{\varepsilon_j}\,\frac{B}{c}\left[\sum_{k=0}^{n}(-1)^k\binom{n}{k}\,\mu_k\right] \qquad (1)$$

Therefore, for a first order reaction (n=1)

$$\frac{dC_j}{dt} = \frac{1}{\tau_j}(C_j - C_{j-1}) - \frac{1-\varepsilon_j}{\varepsilon_j}\frac{B}{c}(\mu_0 - \mu_1) = \frac{1}{\tau_j}(C_j - C_{j-1}) - \frac{1-\varepsilon_j}{\varepsilon_j}\frac{B}{c}(1-\bar{x})$$

which shows that for the calculation of the liquid concentration change, only the mean solid conversion is required.

Also in section 4.2.1, the equations for the change of the moments with respect to time were derived. There it is shown that for first order kinetics

$$\frac{d\mu_1}{dt} = \frac{-B}{c}(\mu_0 - \mu_1)$$

or

$$\frac{d\bar{x}}{dt} = -\frac{B}{c}(1-\bar{x}) \qquad (2)$$

This last equation completes the demonstration that for first order kinetics with respect to solid composition only the average value of the conversion is required.

From equation (1) it is seen that for any integer $n > 1$, to calculate the reaction term, the evaluation of higher moments is necessary.

APPENDIX F

Comparison of residence time and conversion distribution models

An alternative model to the one developed in section 2.2 which tells how the conversion distribution function (CDF) changes with time, is one which will consider how the residence time distribution (RTD), evolves with time.

Kershenbaum (62), has developed a model for a one stage, perfectly mixed contactor without resin feed. Assuming an exponential initial residence time distribution, $f(\theta) = k\, e^{-k\theta}$, and using an expression for the rate of reaction as function of time similar to the one given in section 3.2.2, he has analytically solved Equation (2.2.2). There the term R(t), which is the rate of reaction between the liquid and solids with residence time θ, in the range $(0,\infty)$, is used instead of R(x) (0,1).

The rate of reaction for all solids is given as

$$R(t) = \int_0^\infty r(\theta)\, f(\theta,t)\, d\theta \qquad (1)$$

where $r(\theta)$ is the rate expression derived in section 3.3.3:

$$r(\theta) = \frac{dx}{d\theta} \cong \frac{\sqrt{a}}{2}\, \bar{\theta}^{\frac{1}{2}}\, e^{-b\theta}$$

Integration of equation (1) gives

$$R(t) = \bar{c}\, \frac{\sqrt{a}}{2} \sqrt{\frac{\pi}{k+b}}\, e^{kt}\, \mathrm{erfc}\sqrt{(k+b)t}$$

This last expression is then used in the solution of the mass balance equation (Eq. 3.2.2-2). An analytical integration has been performed in the given reference (51) using Laplace transforms. The final expression of this integration is given as

$$C(t) = C(0)e^{-t/\tau} + C_0(1-e^{-t/\tau}) - \frac{1-\varepsilon}{\varepsilon}\, \bar{c}\, \frac{k}{2}\, \frac{\pi a}{k+b}\, e^{-t/\tau} \int_0^t e^{(k+\frac{1}{\tau})\lambda}\, \mathrm{erfc}\sqrt{k+b\ \lambda}\, d\lambda$$

A comparison of these two methods, RTD and CDF, was performed assuming an arbitrary initial RTD of particles. The corresponding initial resin distribution was obtained as mentioned in section 4.1.2, using

the cumulative distribution $G(\theta) = 1-e^{-k\theta}$. Both models are solved for a one stage system with data taken from Table (6) for the case of run 5.

Figure (F.1) shows the liquid concentration profiles for the initial solid conversion distribution:

$f(x) = 4x(1-x^2)$ which is equivalent to $f(\theta) = 0.0836\ e^{-0.0836\theta}$ for values of the rate expression parameters:

$a = 0.0418 \qquad b = 0.0314$

There it is seen that an excellent agreement is obtained.

The RTD method was also used to study the behaviour of the stage assuming that the entire solid population can be lumped into its mean conversion value.

For the rate expression given by Eq. (3.3.3-3) the change of the mean conversion $\bar{x}$ with time can be evaluated by integrating it, i.e.

$$\int_{\bar{x}(0)}^{\bar{x}(\theta)} \frac{\bar{x}(\theta)d\bar{x}(\theta)}{(1-\bar{x}^2(\theta))} = k_D\theta$$

Hence

$$\bar{x} = \sqrt{1 - (1-\bar{x}(0)^2)\ e^{-2k_D\theta}}$$

The liquid concentration change is now given by

$$C(\theta) = C(0)e^{-\theta/\tau} + C_f(1-e^{-\theta/\tau}) - \frac{1-\varepsilon}{\varepsilon}\cdot\bar{c}\ \ k_D e^{-\theta/\tau}(1-\bar{x}(0)^2)\int_0^{\theta_e}\frac{(1/\tau - 2k_D)\lambda_{d\lambda}}{\sqrt{1-(1-\bar{x}(0)^2)e^{-2k_D\lambda}}}$$

The liquid concentration profile obtained using this last equation is also shown in the figure, where it is seen that this approximation is less satisfactory with an average error of about 4 per cent.

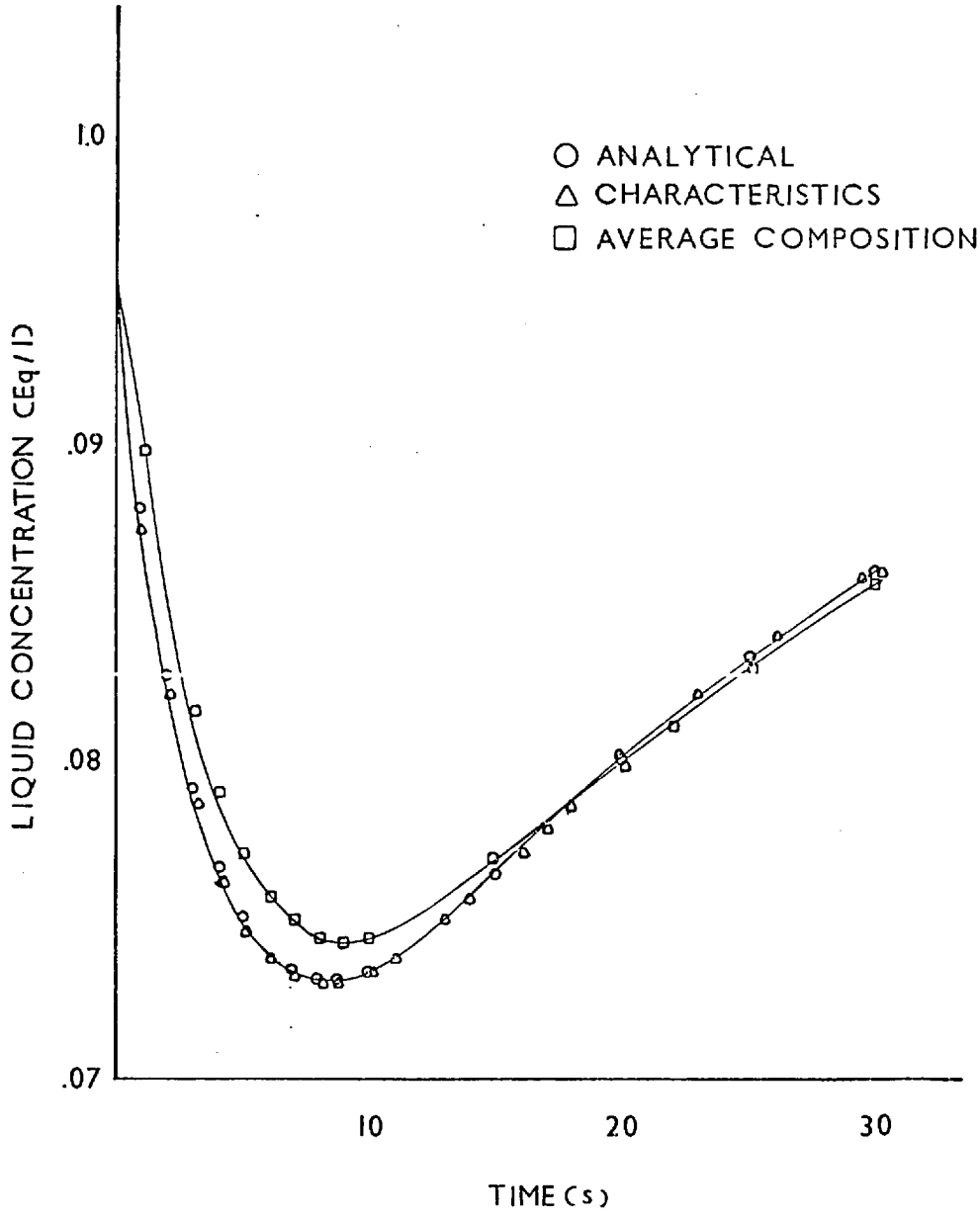

FIGURE F.1 Comparison of residence time distribution and conversion distribution function approaches.